ALSO PLEASE LET ME KNOW THAT EVERYTHING HAS ARRIVED

HOPE YOU ARE SATISFIED I HAVE NOT RE-READ COULD BE SPELLING MISTAKES

QUERIES AND NOTES PLEASE BRING THIS BACK SO WE CAN CHECK AND DISCUSS TOGETHER.

Note new method $\frac{r}{B}$, $\frac{l}{u}$ on 3rd page (Chapter 5)

Complete missing symbols $\frac{2700\ r\ S}{T}$ on same page

extraplotted (one word) ?

Last page Chapter 5 Cannot read pencil overwriting, please complete. Also complete various missing symbols.

Chapter 6 2nd paragraph in General. Is analagous spelt correctly.

Chapter 7.3.3 Forcing spelt FORCEING Please correct in 2nd paragraph.

Chapter 7.5 Is Muti-pump correct?

Chapter 7.5.1 Is cusecs correct?
6 inch, should it be 6 inches? 3rd paragraph

Chapter 7.5.2 3rd Paragraph MONOMETER or MANOMETER ?

Chapter 9.2 4th Paragraph(Word missed out, space left.
(Have typed ease instead of easy
(Have typed overhauls not overalls

Chapter 9.3 Last paragraph. Next to last line is STATOR Correct ?

Chapter 10.2 First paragraph. Is ESTUORINE correct ?

ARE ALL 36'↘ THIS TO MEAN FEET ? HAVE WRITTEN FEET IN SERVERAL PLACE WHERE ' IS SHOWN.

Chapter 10.12 AQUIDUDE is this correct ? 2nd paragraph. There appears to be a word missing last line 10.12.

Chapter 11.4 4th paragraph. Have typed be not by (next to word logarithmically)

Chapter 11.7.1 2nd paragraph part 6. 3rd line from bottom the word 'the' sounds to be wrong. Beginning of next paragraph also sounds wrong.

In Situ Hydraulic Parameters in Jointed Rock – Their Measurement and Interpretation.

by Y.N.T.Maini BSc, ACGI, DIC, AMICE.

A thesis submitted to the University of London
(Imperial College of Science and Technology)
for the degree of Doctor of Philosophy
in the Faculty of Engineering.

ACKNOWLEDGMENTS

The author would like to thank all members of the Rock Mechanics Department for their help, in particular:

Prof. E. Hoek	For creating an atmosphere where free debate and individual initiative was encouraged.
Dr. H. Kutter	For his constant help during the entire period of the research project and also for his critical comments on the manuscript.
Mr. D. Pentz Dr. J. Sharp	Without whom the author would have never strayed into rock mechanics.
Dr. J. Bray	For his help and stimulating discussions.
Mr. J. Sullivan and his merry workshop.	For all the laboratory and field equipment.
Mr. R. Sidey	For his immense help in creating everything electronic.
Mr. D. Hinds	For his organisation and muscle work during the field trip.
Mr. L. Wilson	For almost everything.
Miss A. Rawlings Miss H. Kerr Miss R. Duffy	For typing the manuscript so quickly.
Mr. B. Holt Mr. P. Huckle	For production of the thesis.
Miss M. Rathbone	For some of the better diagrams and photographs.
Mr. C. Louis Mr. C. St.John	For their helpful criticism of the research.
Mr. J. Boyd Mr. T. Harper	For making Geology so complicated.
Mr. S. Tilburn	For his very hard work during the fieldtrip.

The Rio Tinto Zinc Corporation Ltd., for generous support both for laboratory and field studies, on behalf of Anglo American International (U.K.) Ltd., Bougainville Copper Pty. Ltd., Consolidated Gold Fields Ltd., English China Clays Ltd., Iranian Selection Trust Ltd., National Coal Board Opencast Executive, Palabora Mining Co. Ltd., Rio Tinto Espanola, S.A., Roan Selection Trust Ltd., and seven member companies of the Australian Mineral Industries Research Association Ltd.

Finally the author wishes to thank his wife and family for their constant support and cheerfulness.

ABSTRACT

This thesis is part of a research project on slope stability which is at present being carried out at the Imperial College. This work forms the logical extension to the general theory of fluid flow through a fissured media. The theory and in particular the computer model presented are compared with hydraulic models to test their validity. No amount of theoretical sophistication is useful unless it is possible to obtain meaningful data from the field. In view of the importance of such data the author critically examined existing methods of field evaluation and presents theory which should make the interpretation more reliable. Special equipment was designed, built and tests carried out in the field to measure permeability in the context of the very wide range of fissure spacings and orientations that may exist in realistic problems.

Part 1 presents the theory of fluid flow through single and multiple non-deformable fissure systems. Computer stimulations are made of flow through a discontinuum and the results are compared with those from physical flow models. The problem of the influence of stress on the permeability of a jointed rock mass is considered for a particular case. The numerical analysis takes account of the influence of fluid pressure on joint aperture.

Part 2 considers the theory of fluid flow either from or towards a cylindrical cavity in a fissure system. Where possible analytical solutions are presented. Alternatively use is made of a parametric study involving computer simulation. Laboratory tests are carried out for idealized models in order to test the theory.

In view of the importance of the fissures in a discontinuum concept of permeability, field tests were carried out to measure in-situ hydraulic parameters. The data consists of a structural evaluation and the results from Pumping-in tests. Special equipment had to be designed and built for the field investigation. Using this equipment it was possible to study the influence of scale on a test and to assess the degree of non-linearity between pressure and flowrate.

Part 4 presents the theory of tracing in fissured rocks. Several methods are available for tracing a dye in order to determine the seepage velocity or permeability. Fluorometric techniques are discussed in detail prior to the description of the Fluorometer which was designed and built at Imperial College.

PART 1.

CHAPTER 1.	Flow through a fissured media.	1
1.1.0	Review	
1.2.0	The structure of the rock mass.	
CHAPTER 2.	Fluid flow through a single fissure.	11
	Synopsis	
2.1.0	Introduction	
2.1.1	Experimental verification of a non-linear flow for the case of fluid in a single fissure.	
	Conclusions.	
CHAPTER 3.	Flow through multiple fissure systems.	18
	Synopsis.	
3.1.0	Introduction.	
3.1.1	Fissure intersection model.	
3.1.2	Experimental details.	
3.1.3	Dynamic similitude.	
3.1.4	Experimental results.	
3.1.5	Conclusions.	
3.2.0	Introduction to flow in multiple isotropic fissure systems.	
3.2.1	Hydraulic model.	
3.2.2	Experimental details.	
3.2.3	Experimental results.	
3.2.4	Numerical analysis.	
3.3.0	Introduction to flow in an anisotropic multiple fissure system.	
3.3.1	Details of the hydraulic model.	
3.3.2	Scale of the model.	
3.3.3	Model single fissure characteristics.	
3.3.4	Multiple fissure characteristics	
3.3.5	Numerical analysis of fluid flow through anisotropic multiple fissure system.	
	Conclusions.	

CHAPTER 4. Interaction between stress and permeability in jointed rock. 62

Synopsis.

4.1.0 Introduction.

4.2.0 Interaction model.

4.2.1 Structural analysis of the rock mass.

4.2.2 Fluid flow analysis.

4.2.3 Linkage of the two numerical schemes.

4.2.4 Details of the rock slope model.

4.2.5 Results of analysis.

4.3.0 Experiment to observe change in permeability with shear displacement.

4.3.1 Test set up.

4.3.2 Results.

Conclusions.

PART 2.

CHAPTER 1.	Pressure testing in rock	73
	Introduction	
	Synopsis	
1.1.0	Field of application.	
1.2.0	Historical development.	
1.3.0	Current practice.	
1.4.0	Recent research.	
CHAPTER 2.	Equations of motion of a fluid.	81
	Synopsis	
2.1.0	Axisymmetric seepage.	
2.1.1	Influence of fissure frequency in direction orthogonal to borehole.	
2.1.2	Effect of inertia in a linear system.	
2.1.3	Use of non-linear pressure-flow law.	
2.1.4	Use of inertia term in the non-linear pressure flow relationship.	
2.1.5	Aquifer of infinite radius - implications.	
2.1.6	Anisotropic flow in the horizontal plane.	
2.1.7	Influence of secondary fissures.	
2.1.8	Influence of fluid stresses during a pumping test.	
2.2.0	Two and three dimensional flow from a cavity.	
2.2.1	End effects in a gravity system.	
	Conclusions.	
CHAPTER 3.	Motion of a fluid towards or from a cavity - numerical solutions.	103
	Synopsis	
3.1.0	Introduction.	
3.1.1	Flow from a vertical cavity into a two dimensional anisotropic fissure in the horizontal plane.	
3.1.2	Numerical model	
3.1.3	Method of solution.	
3.1.4	Numerical analysis	

3.1.5	Determination of principal permeability ratio: approximate method.	
3.2.1	Two and three dimensional flow systems.	
3.2.2	Details of the numerical model.	
3.2.3	Numerical analysis.	
3.3.1	End effects in a pressure test.	
3.3.2	Determination of anisotropy ratio in a two dimensional fissure system.	
3.3.3	A simple one hole method to estimate the degree of anisotropy in a two dimensional system.	
3.3.4	Influence of test cavity size on permeability value.	
3.3.5	Influence of boundary conditions on the test.	
	Conclusions.	
CHAPTER 4.	Laboratory evaluation of pumping tests.	133
	Synopsis	
4.1.0	Introduction.	
4.1.1	Pressure test in a fissure under a natural flow field.	
4.1.2	Test Results.	
4.2.1	Pressure test in a model fissure.	
4.2.2	Test results.	
	Conclusions.	
CHAPTER 5.	Non steady state flow-axisymmetric case.	151
	Synopsis.	
5.1.0	Field of application.	
5.1.1	Falling head test: Cased hole below G.W.T.	
5.1.2	Falling head test carried out when test section is below the groundwater table.	
5.2.0	Equations for a falling head test in an unsaturated fissured media.	
5.3.0	Laboratory tests.	
5.3.1	Laboratory tests.	
	Conclusions.	

PART 3.

CHAPTER 1.	Field evaluation.	165
	Synopsis	
	Introduction	
1.1.0	Instrumentation	
1.2.0	Details of the apparatus used in the field	
1.2.1	Packers.	
1.2.2	Measurement of fluid pressure	
1.2.3	Flow measurement	
1.2.4	Valves.	
1.2.5	Pump.	
1.3.0	Assembly.	
1.3.1	Controls.	
	Conclusions.	
CHAPTER 2.	Alltwen Quarry.	184
	Synopsis	
2.1.0	General	
2.2.0	Regional geology	
2.2.1	The geology of Alltwen Quarry.	
2.2.2	Orientation.	
2.2.3	Determination of fracture frequency.	
2.2.4	Anisotropy.	
	Conclusions.	
CHAPTER 3.	Determination of in-situ hydraulic parameters.	214
	Synopsis	
3.1.0	Linear pressure-flow relationship.	
3.1.1	Non-linear pressure-flow relationship.	
3.1.2	Test to demonstrate fracture breathing.	
3.2.0	Changing geometry of the test section.	
3.2.1	Introduction.	
3.2.2	Influence of "end effects" in a water test.	

3.3.0 Triple packer probe.
3.3.1 Introduction
3.3.2 Field test.
3.4.0 Scale effect in a test.
3.4.1 Field results on the influence of fracture frequency on the value of permeability.
3.4.2 Correlation of frequency of fissures and water absorption.
3.5.0 Influence of borehole orientation on permeability values.
3.6.0 Anisotropy of the fissure system.
3.6.1 Approximate determination of principal permeabilities from tests in one hole.
3.6.2 Ratio of principal permeabilities as obtained from water tests in orthogonal directions.
Conclusions.

CHAPTER 4. Unsteady state tests to determine permeability. 256
Synopsis
4.1.0 Test set up.
4.2.0 Determination of permeability using the falling head test
4.2.1 Calculation of permeability from the H-t curve.
4.2.2 Practical advantages of the falling head test.
Conclusions.

PART 4.

CHAPTER 1.	Groundwater tracing.	*260*
	Introduction.	
CHAPTER 2.	Transit time tracing.	*262*
	Snopsis	
2.1.0	Transit time tracing	
2.2.0	Single well test.	
2.2.1	Laboratory evaluation.	
2.3.0	Two well-tracer test in fractured rock.	
2.3.1	Case study of a two well tracer test.	
	Conclusions.	
CHAPTER 3.	The dilution method.	*272*
	Synopsis.	
3.1.0	Dilution method: Theory of the proposed method.	
3.1.1	Mathematical derivation of seepage velocity in terms of the decay of the salt solution.	
3.2.0	Experimental verification of the mathematical derivation of seepage velocity.	
3.2.1	Model.	
3.2.2	Verification of the "Pinching Effect" of the borehole.	
3.2.3	Diffusion and mixing of the tracer.	
3.3.0	Determination of seepage velocity using the dilution method.	
3.4.0	Field equipment.	
	Conclusions.	
CHAPTER 4.	Geochemical analysis.	*295*
	Synopsis	
4.1.0	Introduction	
4.1.1	Schoeller's graphical method.	

4.2.0 Case studies.
4.2.1 Gortdrum mine.
4.2.2 Scammonden dam.
Conclusions.

CHAPTER 5. Fluorometry. 302
Synopsis.
5.1.0 Introduction.
5.1.1 What is fluorescence.
5.1.2 Commonly available dyes.
5.2.0 Borehole fluorometer.
5.2.1 Essential concept of the borehole fluorometer.
5.2.2 Operation of the borehole fluorometer.
5.2.3 Laboratory tests.
5.3.0 Field trials.

PART 1

FLOW THROUGH FISSURED MEDIA

1.1.0 REVIEW

A vast amount of literature exists on fluid flow through fissured media. It is not proposed to review the relevant research work in a chronological order, but to briefly describe areas of research which are considered essential in understanding fluid flow through fissured media.

Early work assuming an isotropic porous media with relatively high permeability resulted in predictions of pressure distributions and flowrate so wide off the mark that it lead Terzaghi (58) to comment that "the most unpredictable factor determining slope stability is the hydrostatic pressure in the water flowing out of a reservoir or a leaking pressure tunnel through the joints towards a slope, etc". Snow (7) formulated the concept that a fissured rock mass could be considered as a system consisting of intersecting planar conductors arbitrarily orientated in space. Assuming Darcy's law holds, Snow has demonstrated how a tensor form of Darcy's law adequately describes the motion of fluids in such a medium. In such an analysis two factors cause anisotropy of the system. The first one is the variation in aperture of the fissures and the second is the variation in fissure frequency in different directions. Later work by Snow (43) has incorporated the use of sophisticated statistical analysis into the above system. The above method can, given data of water tests in various holes at different depths, predict the pressure and flowrate distributions in a fissured rock mass. The approach to the problem is essentially a phenomenonlogical one, ie. a model is built on the basis of observation together with certain assumptions on the medium being a continuum and homogenious, a given flow law and finally the structure conforming to a certain system. Obviously, such a method is very powerful since it does not involve the detail and quantitative description of the structural geology. However, application of the method must be made subject to the initial assumptions being justified. The first one of the medium being a continuum must be proved prior to using such a method. Snow has considered the problem theoretically and described a few field examples. It is felt that this is such an important assumption that it needs further detailed work to justify it. In order to consider a medium as a continuum one has to take account of the interaction between the permeability of the individual fissures, the spacing of the fissures, the different number of fissure sets and the size of the structure, ie. a dam or rock slope. Until such a criteria has been established by considering a large number of idealised cases and building numerical or physical models it is virtually impossible to assess the validity of the method. The second assumption made by Snow

is that the relationship between pressure and flowrate is linear. While this may be true for low gradients recent evidence points to a large class of problems where this relationship is nonlinear (8, 9, 10, 19, 12). Further, the data from the water test must be such that it reflects the 'pressure-flowrate' relationship at the correct pressure field and also must be free of any side effects due to the nature of the test (see Part II). Finally there are a large number of problems where the parallel plate analogy of a fissure breaks down due to preferential channels within the plane of the fracture (59). The above assumptions should be studied in greater depth to be able to apply the methods proposed by Snow with a greater degree of confidence. Louis (8) has considered the problem of fluid flow through a fissured media on the basis of a discontinuum model. This is one of the earliest studies which considers the flow laws within a fissure in great detail and subsequently integrates the flow through a discrete number of conductors to give pressure distributions in a fissure system. For the linear case, the integration is very similar to the electrical network system when for n elements which constitute the model, n different equations are written between potential and flowrate which are then solved by matrix inversion. In such a system it is possible to have any anisotropy ratio, impermeable seams and area or points of recharge. In order to establish 'flow-pressure'relationship Louis carried out extensive tests on large planar models with different roughness surfaces. For different ratios of particles size to effective opening Louis has derived friction factors for different Reynolds numbers. In this way it is possible to define permeability precisely in terms of opening and roughness both in the linear and non linear regime. Louis has further shown the difference on a fundamental level between flow in porous and fissured media. This is achieved by considering a large number of stability calculations on rock slopes and dam foundations for a variety of cases. The flowrate pressure relationship although very fundamental and probably representing a large number of problems does not really represent the case where flow is taking place in a fissure which is very much more tortuitious and also one in which certain areas of the fissures are either in contact or within the plane of the fissure there exist solution cavities, eg. Karstic limenstones. The method of integrating a large number of elemental flows so that they satisfy certain boundary conditions is excellent except that the demands of the method are very much more extensive, in that it is important to know the geometrical structure of the fissure skeleton and the permeability characteristics within it. Sharp (9) carried out tests on a porphyry fissure to determine the relationship between pressure and flowrate for a wide variety of effective openings. His results showed that after an initial linear regime the relationship became nonlinear. This nonlinearity has been attributed by Sharp to the irregular flow path in terms of changing

effective opening of the fissures and the direction of the streamlines. A large part of Sharp's work is the steady state solution to boundary value problems with varying ratios of permeability and with either impermeable zones or areas of recharge. Solutions to these problems are either carried out on an electrical analogue or by numerical techniques. The numerical techniques are powerful in that they can deal with a large number of elements of varying properties in two and three dimensions. Solutions are also given for phreatic surfaces although the numerical method is not tested either for a known analytic solution or a physical model. A field problem is discussed on the basis of the methods described for the case of fluid flow through a fissured media. Sharp's work is essential in understanding of a certain class of problems, eg. drainage of slopes but it does not give an indication of the effect of fracture frequency and spacing on the drainage phenomenon. As in the case of Louis the methods presented by Sharp are versatile but they need very sophisticated and quantified information from the field.

An enormous amount of material exists in the Petroleum literature on fluid flow through naturally fractured reservoirs. Perhaps the most extensive work is that of Warren & Root (41), Kazemi (27), Odeh (42) and Pollard (40). In general these studies are computer simulations of Well performances in a heterogeneous porous media. The geometry of the fractured system, permeabilities involved, and pore volumes of each rock type constitute systems which are so complex that they need to be solved not only by numerical techniques but also by probabilistic models. These methods are outlined in Part II which deals with fluid flow from a borehole into a fissure system. Huitt (50) carried out tests on simulated fractures which consisted of small sand particles stuck on steel plates and found that fluid flow obeyed Darcy's law for low Reynolds number. In general the petroleum approach is not very practical for mining or civil engineering problems because the mathematical models take into account the compressibility of the fluid and at high stress levels unsteady flow conditions are obtained due to the change in volume of fluid in a confined reservoir.

A recent publication by Wilson and Witherspoon (61) is an investigation of laminar flow in fractures porous media. Finite element techniques are used to describe fluid flow through a fissured rock mass. Flow can take place either in the rock matrix and fissures simultaneously or through fissures alone. The fractures in the system can have any spacing, orientation and aperture. Similarly the porous media may be anisotropic and vary from block to block.

Two particular cases are considered in detail. The first is a dam on a fissured formation and the second is a tunnel in a fissured rock mass. For different ratios of anisotropy the behaviour of the jointed rock mass is compared to that of a porous media. Here it is shown that the fracture aperture is the most sensitive parameter in governing the volumetric flow-rates. Also if the aperture of one set of fracture is very much higher than the others little pressure drop occurs in that set. A consequence of this could be that the area of recharge can be at a considerable distance from the area of investigation. Wilson and Witherspoon have shown by numerical methods that fracture orientation plays little part in the amount of fluid that flows beneath a dam; but it does significantly alter the pressure distribution. For a given fracture system and size of dam the authors illustrate how the probability of occurrence of a given flowrate can be made without knowing the actual apertures of the fissures. The only input required in the model is a random estimate of the apertures. The study on the flow into a tunnel proves that the total inflow is linearly related to the ratio of tunnel diameter d to fracture spacing l provided d/l is greater than 1.5. This study is a step further from the work of Louis and Sharp in that it relates the size of structure to the mean fracture spacing. Since this study is enumerative it too relies on detailed field evaluation for meaningful results.

There is a whole new field of study, ie. fluid flow through Karstic formations. The problem here is as severe as flow in fissured rock masses with the added unknown solution cavities which can exist almost anywhere and can be of any size. For those interested in the topic papers (62, 63) will provide an adequate introduction to the subject.

The author is not aware of any field tests where the medium is considered as a discontinuum for the purpose of permeability evaluation or for that matter where the geometry of the fissure skeleton is taken into account when determining in-situ hydraulic parameters.

1.2.0 THE STRUCTURE OF THE ROCK MASS

It is obviously beyond the scope of this work to consider the different types of fracture systems in terms of their genesis, continuity and importance to fluid flow. However, a little background must be given to be able to appreciate the reasons for the mathematical formulation of the equations in subsequent parts of this thesis. It is also proposed to stress the importance of quantifying the intensity of jointing and the degree of heterogeneity so that future research work in fluid flow through rock masses will take these factors into account.

It is generally assumed that as far as the macrostructure is concerned that fractures occur in sets so that a rock mass can be subdivided into blocks. These blocks may be of any size (indicating spatial heterogeneity) and shape. Further within such a mass it is possible that there can be areas which are impermeable or alternatively sources of water supply, ie. recharge boundaries. At the same level fractures can exist for a considerable areal extent covering many miles (64). The reader interested in measurements in complex environments is recommended to read Ramsay (50). Estimate of the effective fissure opening or aperture is very much more difficult since there is so much variation even within one single fissure (9). Attempts have been made to photograph these directly by Bianchi (65) who showed that the aperture can be characterised by a log-normal distribution. Measurement of fissure frequency is a very much more difficult problem and is not widely reported in the literature. Snow (7) has inferred it indirectly from water tests while Zemanek et al (51) have measured it directly in a borehole with a televiewer. Fookes and Denness (66) have made a very large number of surface measurements and propose an interesting classification system based on the measure of the number of fissures per unit volume, ie. count the number of fissures and divide by the volume in which they are found. The following table describes their classification system.

Intensity Type	Area of Fissures per unit volume sq.m/cu.m	Average size of intact block
Low	3-10	0.027 - 1 cu.m
Moderate	10-30	0.001 - 0.027 cu.m
High	30-100	27 - 1000 cu.m
Very High	100-300	1 - 27 cu.m
Excessive	300	1 cu.m

Such a simple system could be the basis of an initial field examination of a problem so that information from the field is readily transmitted from the geologist to the engineer. The transition from the statistical approach of Snow and Kochina to the enumerative approach of Louis, Sharp and Wilson is a very difficult problem. It is precisely in the transition zone that a majority of mining and civil engineering problems lie. Until a large number of problems are studied in the field with all the

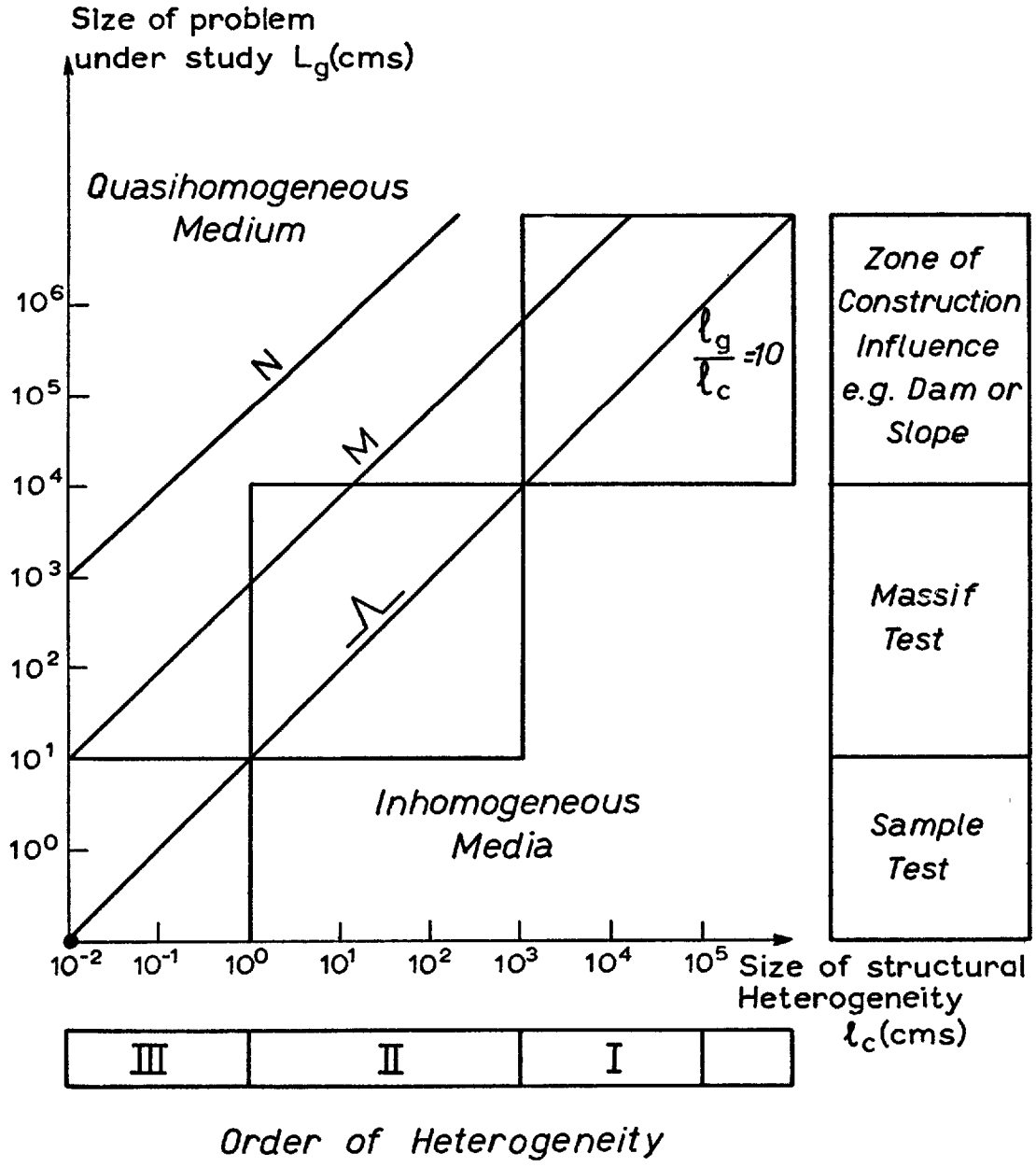

Size of problem
under study L_g(cms)
Quasihomogeneous
Medium
N
M
Λ
$\frac{l_g}{l_c}$ =10
Inhomogeneous
Media
Zone of
Construction
Influence
e.g. Dam or
Slope
Massif
Test
Sample
Test
10^6
10^5
10^4
10^3
10^2
10^1
10^0
10^{-2} 10^{-1} 10^0 10^1 10^2 10^3 10^4 10^5
Size of structural
Heterogeneity
l_c(cms)
III
II
I
Order of Heterogeneity

FIG. 1·1.

above points in mind it is difficult to generalise on the various aspects of flow through a fissured rock mass. It is suggested that the hypothesis of Rats and Chernyashov (67) is used in the meantime to display the importance of spatial heterogeneity in a fissured rock mass. The authors suggest the following heterogeneity subdivision, a summary of which is:

(a) 3rd Order Heterogeneity

Form difference, grain size difference, pore distribution, presence of microjoints etc.

(b) 2nd Order Heterogeneity

Heterogeneity of structure and composition of the rocks within the limits of one bench rhythm, interstratification of the rocks of different composition, macrojointing, small tectonic and non tectonic dislocation. On account of this heterogeneity, no two tests will yield the same results.

(c) 1st Order Heterogeneity

Heterogeneity of the rock massif, magma intrusion, different degree of lithification, tectonic faults, zones of hydrothermal action - in general it is the scale at which geohydrological investigation is carried out.

Fig. 1.1 illustrates the above points graphically. The vertical axis is the size of problem under investigation, for example, a core sample for permeability testing in the laboratory, a pumping test in the field or the zone of influence surrounding a dam. The horizontal axis is the order of heterogeneity, eg. distance between fissures. The diagonal differentiates the homogenious area above from the heterogeneous area below the line. As can be seen the same area can be homogeneous as well as heterogenious. It all depends on the size of the problem. For example, a pumping test in a given medium can be classed as "heterogenious problem" while on the same foundation, a large dam would behave (as far as the potential distribution is concerned) as if it were on a homogeneous media. The cross hatching is the area of dispersion of the results. Field testing which was carried out by the author in Altwen will be discussed in the context of this concept in Part II.

FLUID FLOW THROUGH A SINGLE FISSURE

SYNOPSIS

Fluid flow through a single fissure is considered in this chapter especially in view of the nonlinear pressure-flowrate law which has been reported by several workers recently (8, 9, 10). In order to understand why this nonlinearity exists, the author carried out flow tests on transparent fissure replicas made from liquid araldite which sets at room temperature. By using coloured dyes and the method of flow visualisation, it was possible to follow the streamlines and also find out areas within the fissure plane where no flow occurred. Equations are presented which describe this phenomenon, together with experimental data from laboratory tests.

2.0 INTRODUCTION

Louis (8) has demonstrated how at a high Reynolds number flow becomes turbulent in a fissure. The basis of his analysis was similar to that of pipe flow in that a fissure could be represented by two parallel plates with some form of roughness superimposed on it. In this way it is also possible to give an idea of the friction factor at a given Reynolds number provided the ratio K/D_h is known where K is the absolute roughness and D_h is the hydraulic diameter. Louis concluded that the transition from laminar to turbulent flow began at a Reynolds number equivalent to 2000. While this method may be useful for the case where the fissure aperture is very narrow and the surface is planar it does not consider the cases where the fissures have a very rough surface and may also be in contact at several places within the plane of the fissure where stress transfer is taking place.

Sharp (9) carried out tests on an actual fissure in the laboratory and found that nonlinear flow could take place at fairly low flowrates, ie. 0.1 cu.secs (Fig. 2.2) when the mean opening of the fissure was 270 microns. Fig. 2.1 shows the profile of the opening of the fissure on which the tests were carried out. A Reynolds number criteria was not used by Sharp for the following reasons (summary);

(a) Wide variation in fissure geometry, therefore geometrical similitude not possible.

(b) Difficulty in determining a representative hydraulic length parameter.

(c) Use of friction factor for highly tortuous flow is doubtful.

Sharp's empirical equation for nonlinear flow for this particular fissure is:

$$Q = 0.00046J - 0.00013\ (J-0.25)^{1.3}$$

where Q is the flowrate and J the hydraulic gradient.

2.1 EXPERIMENTAL VERIFICATION OF A NON-LINEAR FLOW LAW FOR THE CASE OF FLUID FLOW IN A SINGLE FISSURE

Since nonlinearity in the 'pressure-flowrate' law has been observed it would be very interesting to have an understanding of the nature of the nonlinearity. For this purpose, it was proposed that the method of flow visualisation would be used. This method was used early this century by Osborne Reynolds to

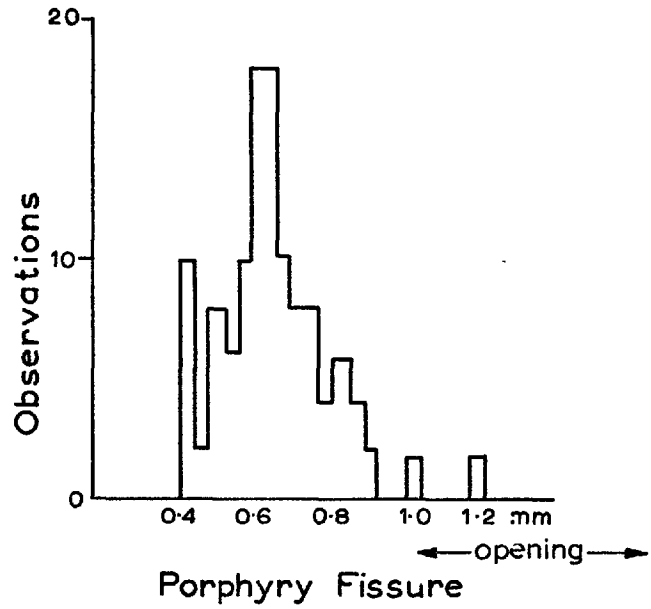

20
10
0
Observations
0·4
0·6
0·8
1·0
1·2 mm
opening
Porphyry Fissure

FIG. 2.1.

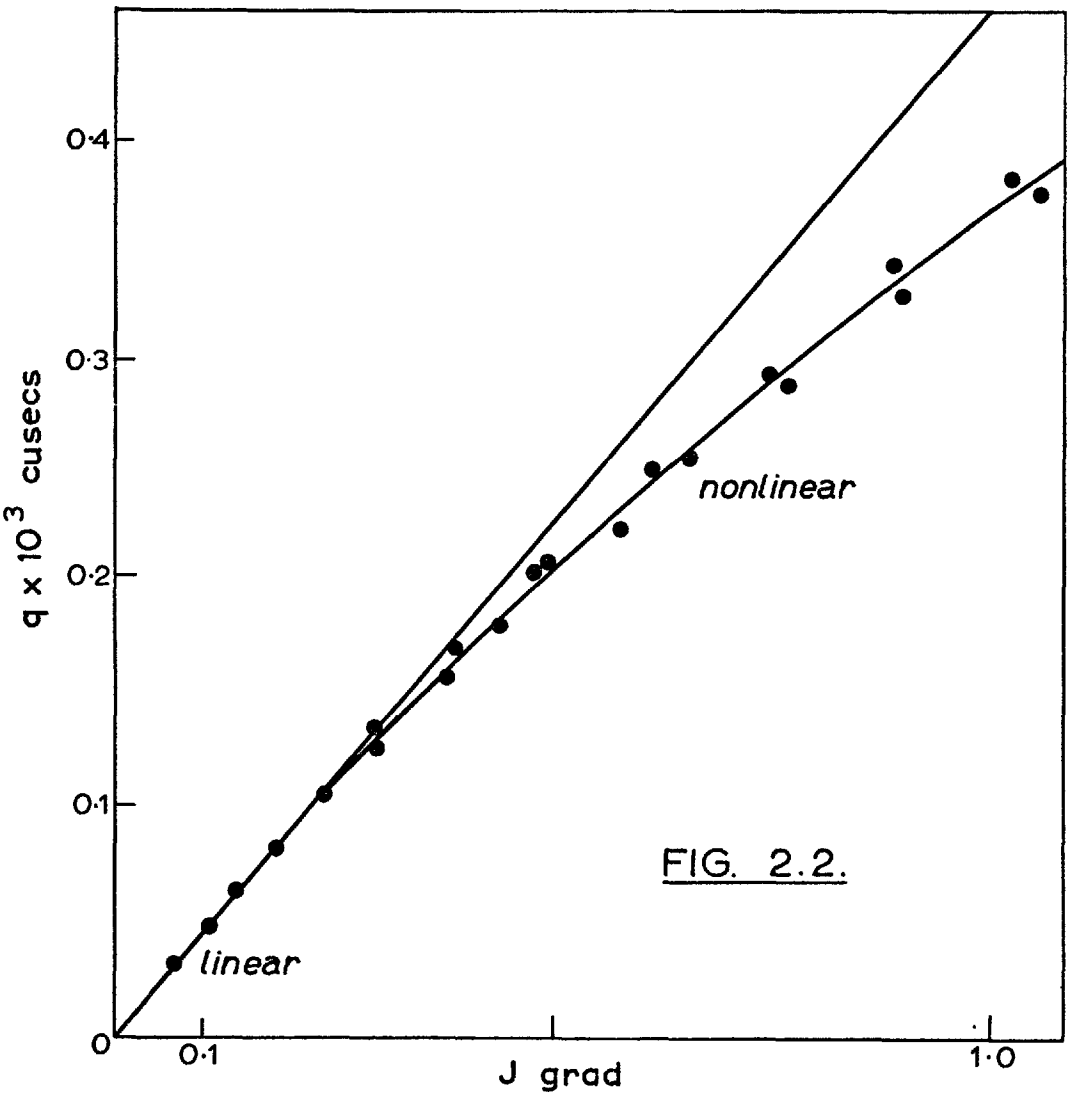

0·4
0·3
0·2
0·1
0
q x 10³ cusecs
linear
nonlinear
0·1
1·0
J grad

FIG. 2.2.

find out why the resistance to flow in a given size pipe changed with increasing velocity. Coloured dyes were injected by Reynolds into a transparent pipe and the streamline patterns were observed for different flowrates. As the velocity of flow was increased, it was observed that vortices were formed and that the flow changed from a laminar to a turbulent condition at a particular velocity. This criterion is now called the Reynolds number and is given by:

$$\text{Reynolds number} = \frac{ud}{v}$$

u mean velocity
d hydraulic radius
v kinematic viscosity

It was decided that the flow visualisation technique would give an insight into the mechanics of flow within a fissure. Liquid araldite when poured into a mould takes up the exact shape of the mould, sets hard at room temperature and, subsequently can be peeled off without damaging the surface. The first cast was made in this way by using the surface of a fissure in the laboratory. Another replica was then made from the araldite impression so that two identical but mirror image surfaces would adequately represent a fissure through which flow could take place. Fig. 2.3 illustrates the model together with the system for injecting a coloured dye. Fig. 2.4 indicates the degree of roughness of the fissure as can be seen from transverse and longitudinal sections of the model. The mean opening of the fissure was of the order of 1/10 mm.

It is proposed that the following law is used to describe the nonlinear pressure flowrate phenomenon in a single fissure:

$$(V_m)^n = CJ \qquad (2.1)$$

V_m = mean velocity

J = hydraulic gradient

C = a constant depending on the fissure opening, viscosities and velocity; nonlinear permeability function (N.P.F.)

n = Degree of nonlinearity, variable depending on the applied gradient.

The mean velocity in the above law is defined as the ratio of flowrate to the cross-section area of flow. Owing to the variation in the effective opening of the fissure this value is difficult to define. Therefore for unit width of fissure the

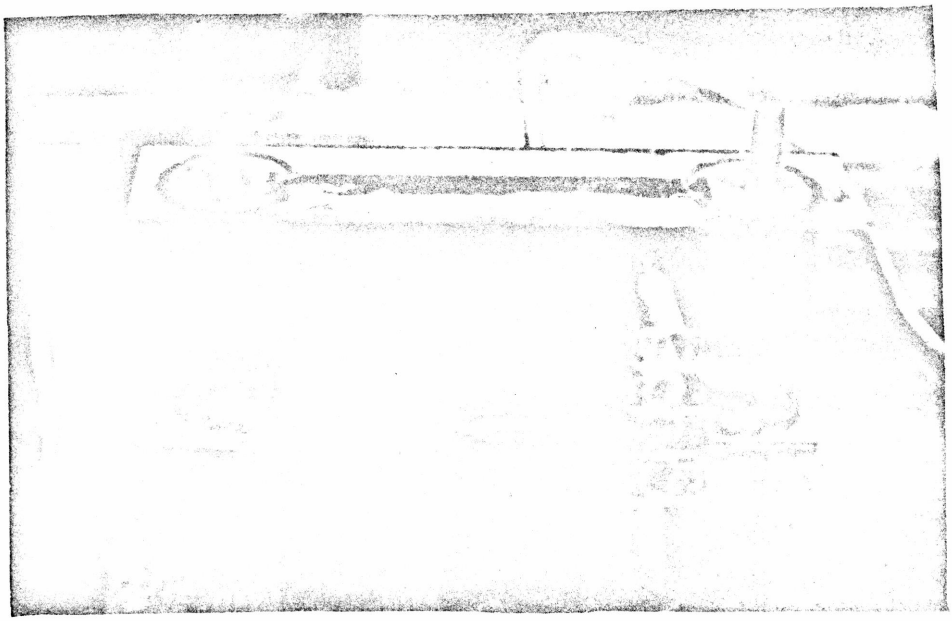


FIG. 2.3. Artificial Fissure Model

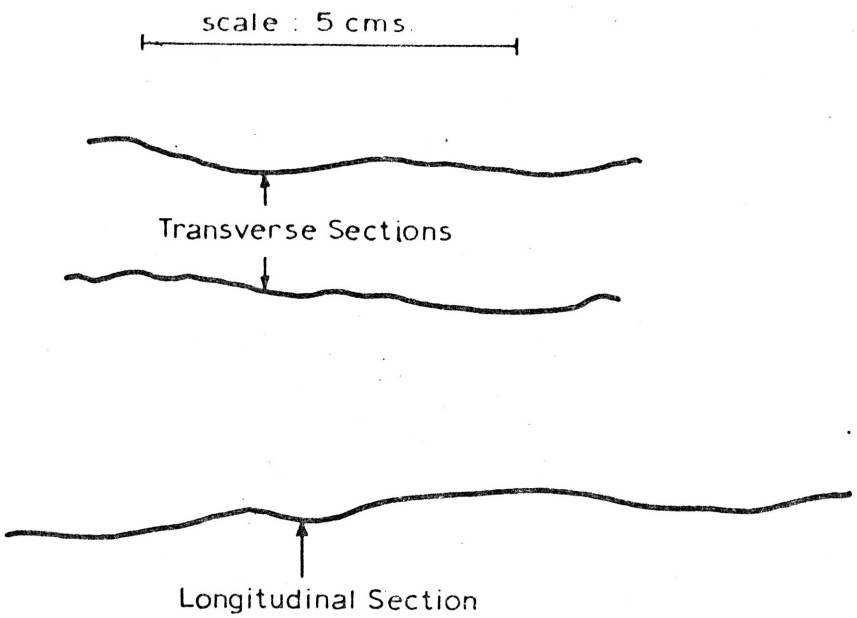


FIG. 2.4. Fissure Profile

above equation becomes:

$$Q^n = e^{nCJ} \qquad (2.2)$$

For a particular fissure, applied gradient and viscosity the value of:

$$e^nC = \text{constant.}$$

Therefore the effective opening or permeability of a fissure is only meaningful in the context of a pressure field J.

Water is supplied to the input of the model from a constant head device so that the pressure and flowrate can be controlled. A large number of tests were carried out with different applied gradients and the dye was introduced in two different ways each time. The first dye injection is such that the entire input of water is contaminated. This is done to distinguish deadwater areasϕ within the flow model. It was noticed that the deadwater area decreased with increased applied gradient. (Fig. 2.5 and 2.6). This obviously suggests that the contact area of flow changes, thus altering the frictional resistance and this could lead to nonlinearity in the 'pressure-flowrate' relationship. The deadwater areas are parts of the fissure where the fluid cannot enter because the height of the boundary layer is greater than the aperture. However, if the applied gradient is increased, the velocity of the fluid increases and the boundary thickness decreases (68). In this way the fluid penetrates the smaller apertures which it could not at lower gradients. This hypothesis is analagous in some respects to fluid flow through unsaturated porous media. The permeability of an unsaturated media depends on the moisture content and can thus vary by orders of magnitude. The relationship between permeability, degree of saturation and applied hydraulic gradient is an extremely complex one and is discussed by Childs (12). More detailed work is required to establish the relationship between permeability, deadwater area and applied hydraulic gradient for the case of steady flow through fissures. Further, it is yet to be established if the history of wetting has any effect on the above relationship.

The second injection of the dye was carried out near the input end, through equally spaced fine holes orthogonal to the direction of flow. This method was chosen so that the behaviour of the streamlines could be studied. For plane laminar flow the streamline should be parallel to the direction of the applied gradient.

ϕ Deadwater area is one in which no flow takes place



FIG. 2.5. Dead Water Area - Low Gradient

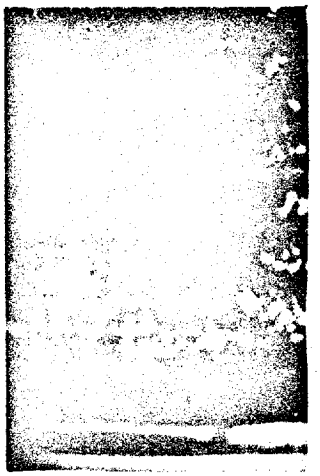


FIG. 2.6. Dead Water Area - High Gradient

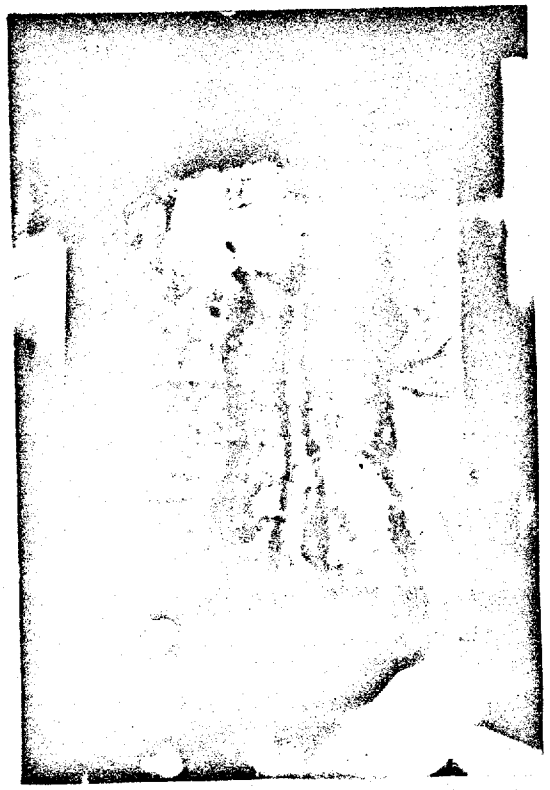


FIG 2.7 Stream Lines at Low Gradient

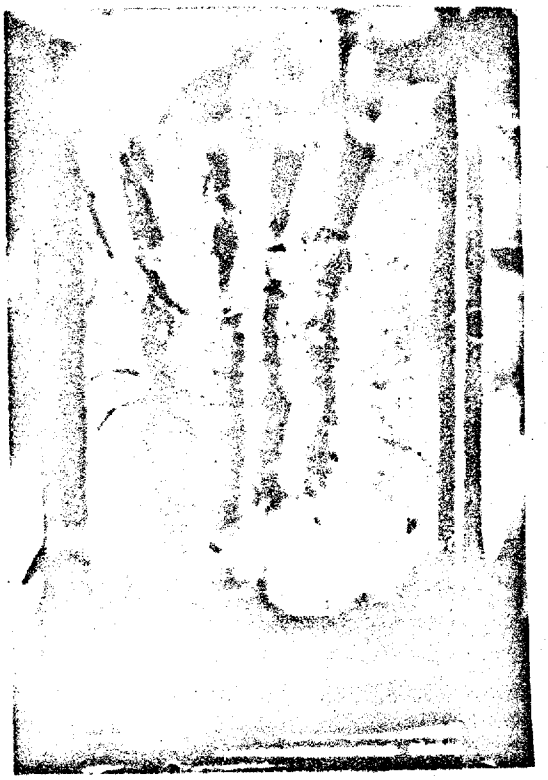


FIG 2.8 Stream Lines at High Gradient

Fig. 2.7 however, shows that the streamlines follow a tortuous path and even divide when they meet an obstacle. If in the direction of flow two streamlines converge it means that the fluid is accelerating (68) and when they diverge the fluid undergoes decceleration. This type of behaviour, together with the constantly changing flow direction, leads to non linearity in the 'pressure-flowrate' relationship. As the flowrate is increased the above process must become more violent thus generating local eddies. These eddies disperse the dye making it rather diffused and faint as can be seen in Fig. 2.8. Finally, at very high flowrates it is virtually impossible to see the dye because it mixes rapidly with the flow and becomes indistinguisable.

CONCLUSIONS

With the help of transparent fissure models it has been possible to see the mechanism that lead to a nonlinear pressure-flowrate law, from the qualitative studies carried out so far it seems that the two main reaons for such a phenomenon are the variation in 'deadwater volumes' with gradient and the tortuousity of flowlines. The results of the quantitative tests by Louis (8) and Sharp (9) together with the flow visualisation tests are encouraging enough to study the problem in much more depth so that the above factors can be assessed for a wide variety of fissures to see if any generalised form of laws can be established as in the case of pipe flow. Clearly the engineering importance of such a nonlinearity is important because it alters the approach to complex boundary value problems and it might provide a closer agreement between theory and practice than has already been achieved.

FLOW THROUGH MULTIPLE FISSURE SYSTEMS

SYNOPSIS

In the discontinuum concept of a fissured rock, the medium consists of planar conductors with prescribed dimensions and 'pressure-flowrate' properties. One of the essential differences between such a rock mass and an equivalent porous medium is that there exists a large number of intersections of fissures in the discontinuum model. It is therefore important to assess the role of such intersections in the model and also have some idea of the pressure losses that may occur because a large number of such intersections may prove to have an important bearing on the overall potential distribution. The behaviour of one such intersection is examined and the loss quantified in terms of the equivalent pressure drop along the length of the fissure. Subsequently an idealised condition of flow through a multiple fissure system is examined in a perpex model. Computer simulation is then made of the model so that results of the numerical model can be compared with those obtained from a physical or viscuous model. Finally the case of fluid flow through an anisotropic media consisting of a pile of rough impermeable bricks is considered and comparison of potential distribution is made with numerical techniques. If subject to the above tests it can be proved that numerical techniques agree reasonably well with simple model tests, complex boundary value problems can be attempted with much greater confidence.

3.1.0 INTRODUCTION

Numerous computer simulations of fluid through porous media exist (12, 16, 17, 18) which are essentially solutions to Laplace's Equation. However, it was Louis (8) and later Sharp (9) who applied these techniques for the case of fluid flow through discontinua in civil engineering and mining problems. Neither of the above authors provided a check for the numerical technique in terms of a physical model or a known analytic solution. In this chapter it is proposed to carry out this check and prior to that to examine the case of frictional losses at an intersection to see if these are significant enough to be included in the final model. A recent publication by Wilson (61) has come to the attention of the author (at the time of writing) where the intersection experiment has been carried out to determine the magnitude of the losses involved. Although the experiments carried out by Wilson were on circular pipes for Reynolds number < 1000 as opposed to the parallel plate model used by the author for Reynolds number > 800 there is good agreement in the answers where the Reynolds numbers overlap. As a result, the two experiments cover the entire range from laminar to turbulent flow.

3.1.1 FISSURE INTERSECTION MODEL

At the time of carrying out the intersection experiment (1967) the author was not aware of any work that had been carried out to determine the hydraulic pressure losses at an intersection. Louis (8) reported that an intersection could be considered as if it were a curved pipe and that the losses were given by Kozeny's equation.

$$H_t = \frac{v^2 k}{2g}$$

H_t = loss at intersection
v = mean seepage velocity
g = gravitational constant.
k = constant

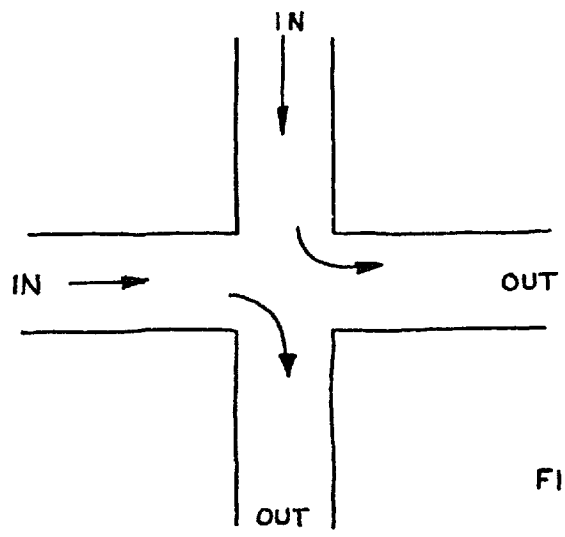


FIG 3.1

Fig. 3.1 illustrates how flow at an intersection divides without interfering and that the loss is given in terms of Equation 3.1. Similar work on the energy losses in pipe intersections is reported by Blaisdell (69). Unfortunately, this type of work is not applicable because the flow instead of mixing from two inputs branches off from one pipe as in Fig. 3.2. It is suggested that neither Fig. 3.1 or Fig. 3.2 represents the case of a fissure intersection where two flows meet, interfere and divide as in Fig. 3.3.

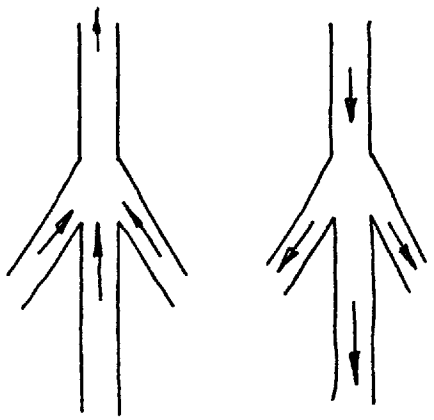


FIG 3.2

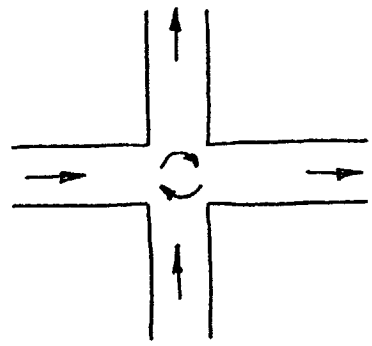


FIG 3.3

3.1.2 EXPERIMENTAL DETAILS

The dimensions of the model are given in Fig. 3.4 and it is made of a perspex block with two 1 mm aperture orthogonal slits. The two inputs are supplied with water from the constant head apparatus and the water leaves via stilling basins (to maintain constant back pressure). For a large number of input pressures or flowrates the pressure distribution was measured within the model and the volume of output measured with a measuring cylinder and stopwatch.

3.1.3 DYNAMIC SIMILITUDE

It is possible to compare the hydraulic characteristics of two fluid conductors of similar geometrical configuration but different sizes by using a dimensionless group of variables (68). For viscuous flow, this dimensionless group is called Reynolds number and it is given by:

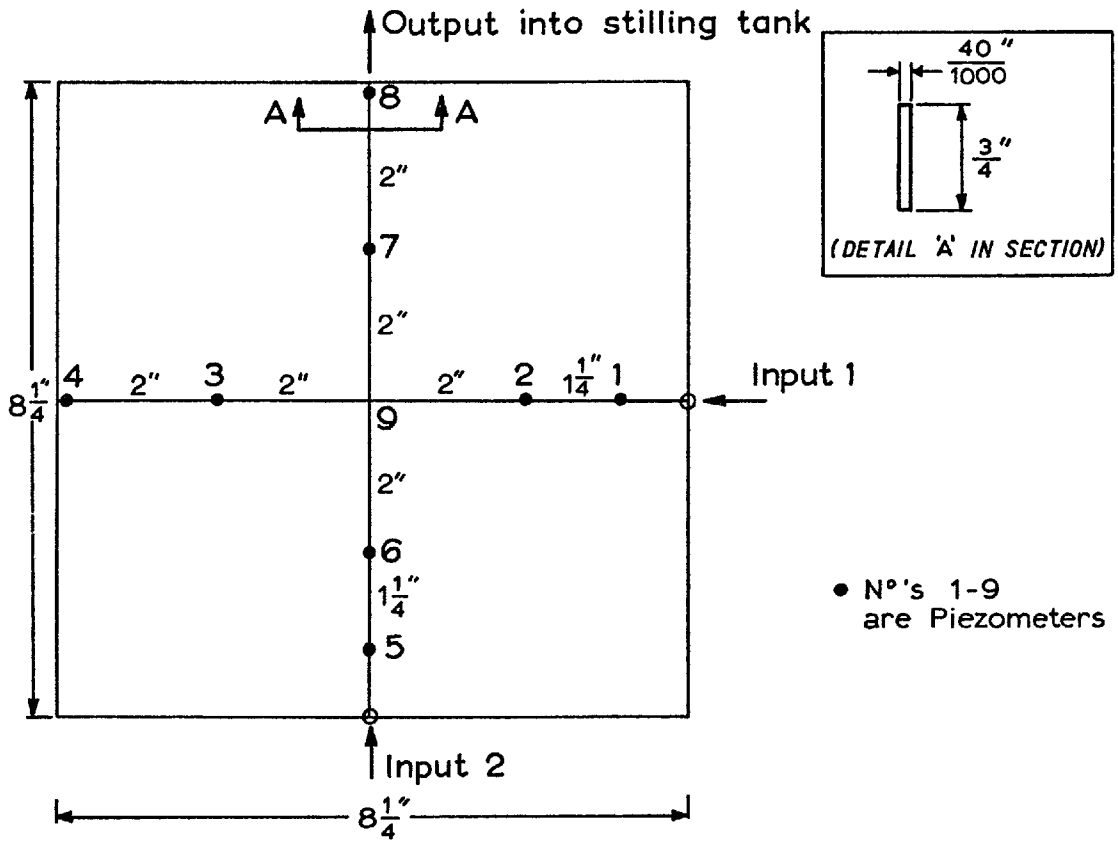
$$R_n = \frac{ud}{v}$$

u = mean velocity

d = hydraulic mean radius = $\frac{\text{Area}}{\text{Perimeter}}$

v = kinematic viscosity

MODEL DETAILS :



PLAN

FIG. 3.4.

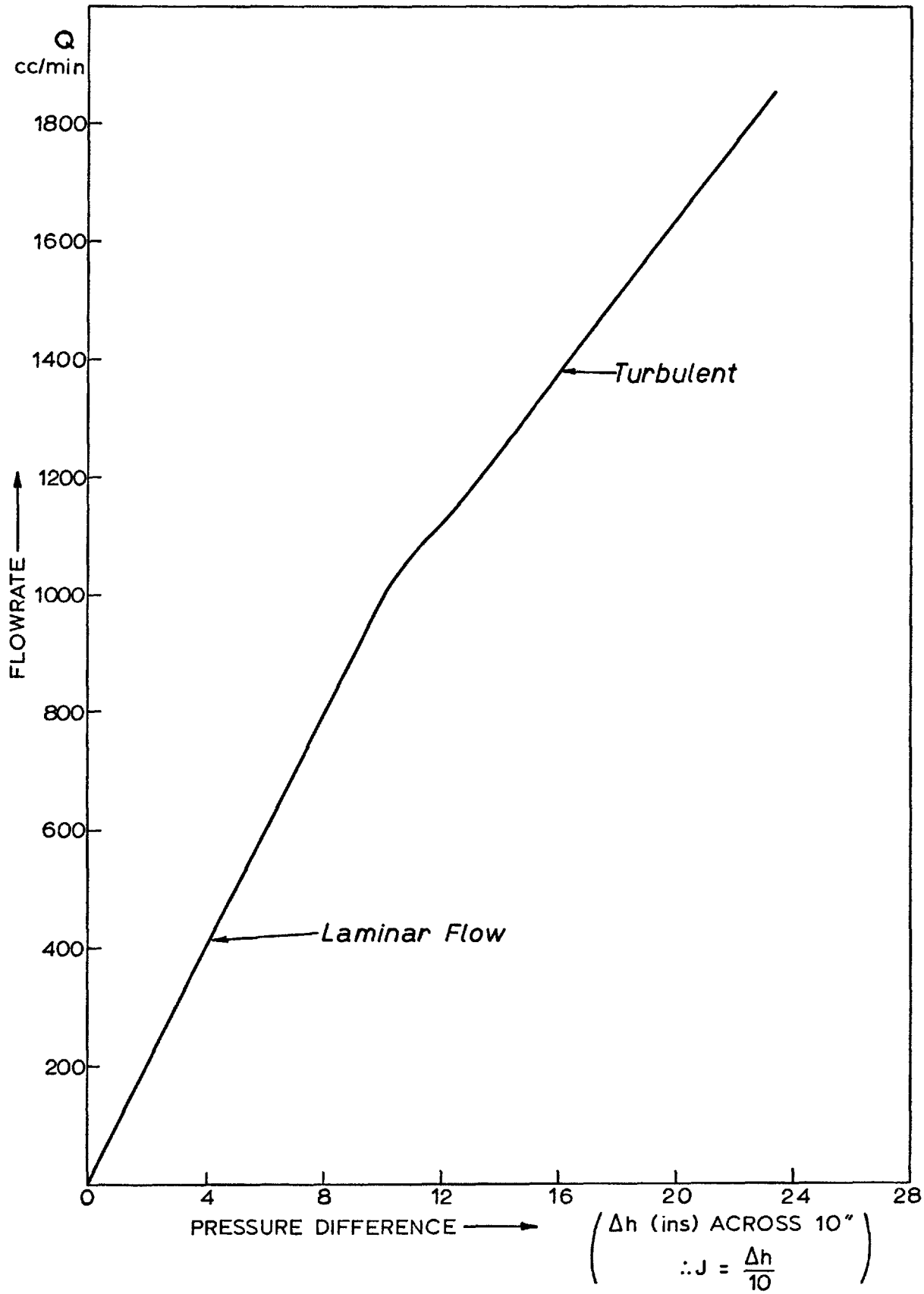

Q
cc/min
1800
1600
1400
1200
1000
800
600
400
200
FLOWRATE
Turbulent
Laminar Flow
0
4
8
12
16
20
24
28
PRESSURE DIFFERENCE
Δh (ins) ACROSS 10"
∴J = Δh/10

FIG. 3.5. (A)

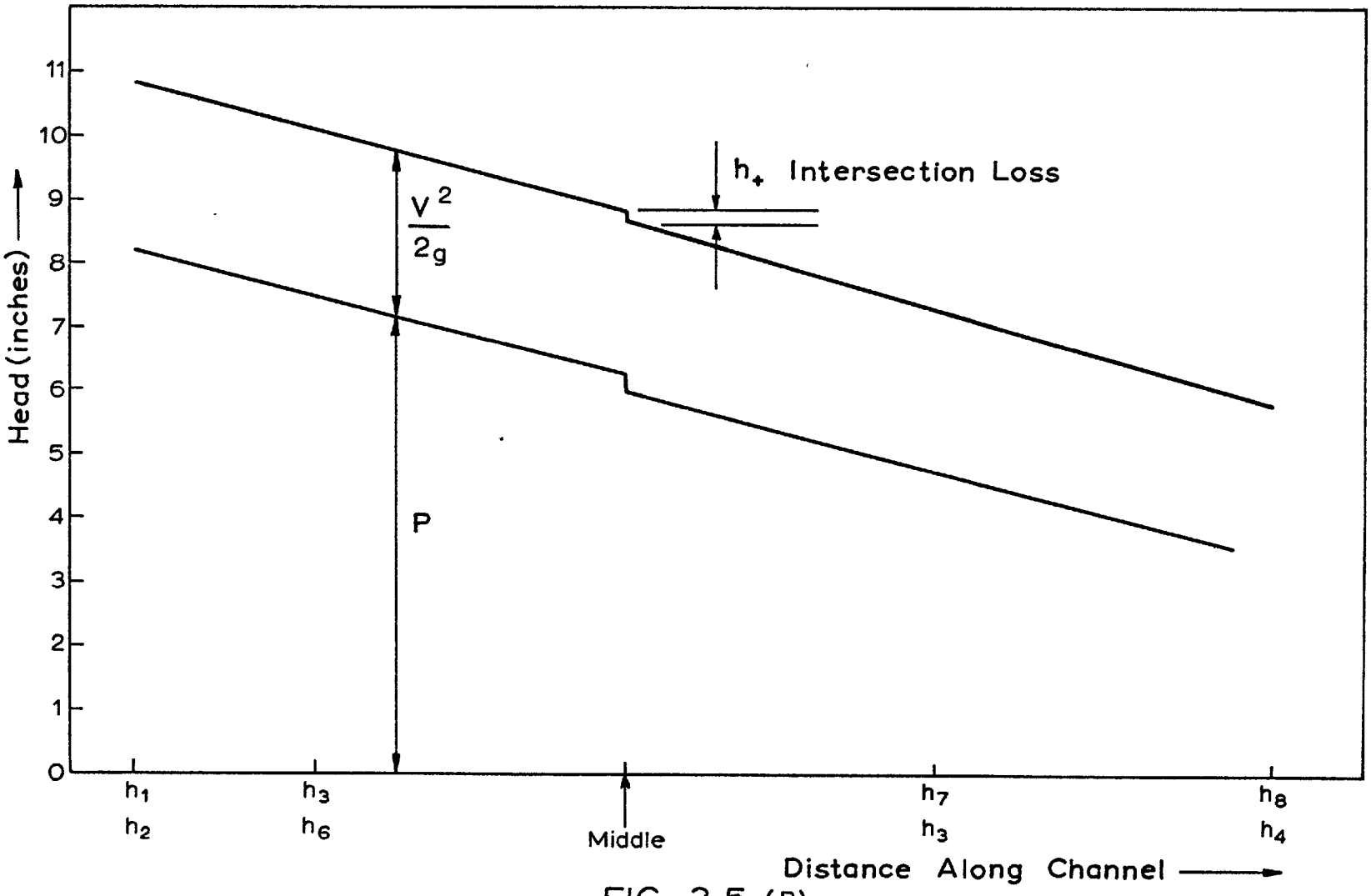

Head (inches)
11
10
9
8
7
6
5
4
3
2
1
0
$\frac{V^2}{2g}$
h_+ Intersection Loss
P
h_1
h_2
h_3
h_6
Middle
h_7
h_3
h_8
h_4
Distance Along Channel

FIG. 3.5. (B)

If, for example, the intersection losses in this experiment are given for different Reynolds numbers it is then possible to use the experimental results for field problems by invoking such a dimensionless group.

3.1.4 EXPERIMENTAL RESULTS

Initial tests were carried out by blocking one exit at a time, to assess the hydraulic characteristics of each individual channel. The permeability value of both the rectangular slits was found to be identical as in Fig. 3.5(A) which is the curve of flowrate vs pressure difference across two given points 10 inches apart. The transition from laminar to turbulent flow begins at a Reynolds number of about 2000 as predicted by Louis (8), Francis (68) and many others who have carried out hydraulic tests on rectangular pipes of different sizes.

In order to understand clearly what is meant by an intersection loss, it is best to refer to Fig. 3.5(B) which shows the pressure distribution along either channel. From the input to the output end of the model there is a decrease in pressure. If there was no abrupt change in direction of flow in either channel this pressure drop would be continuous in which case it would reflect the frictional drop in the pipe. However, a finite change, as in Fig. 3.5(B) indicates the energy loss which could be due to turbulence.

Louis (8) suggests the use of the Kozeny formula for intersection losses, ie.

$$H_t = K\frac{v^2}{2g}$$

$K = 1 \rightarrow 1.2$

H_t = intersection loss in inches

v = velocity

g = gravity

This concept accounts for a sudden change of direction but not mixing as would be the case of flow in a bent pipe. Fig. 3.6 illustrates the Kozeny concept graphically together with experimental results from the model test. For low flowrates, the curve is nonlinear, but then becomes almost parallel to the Kozeny line. This representation of the intersection loss is not general enough because it deals with the intersection loss as a function of one one variable, ie. v_1. This however, is not really the case, since the intersection loss depends on the magnitude of the two input velocities.

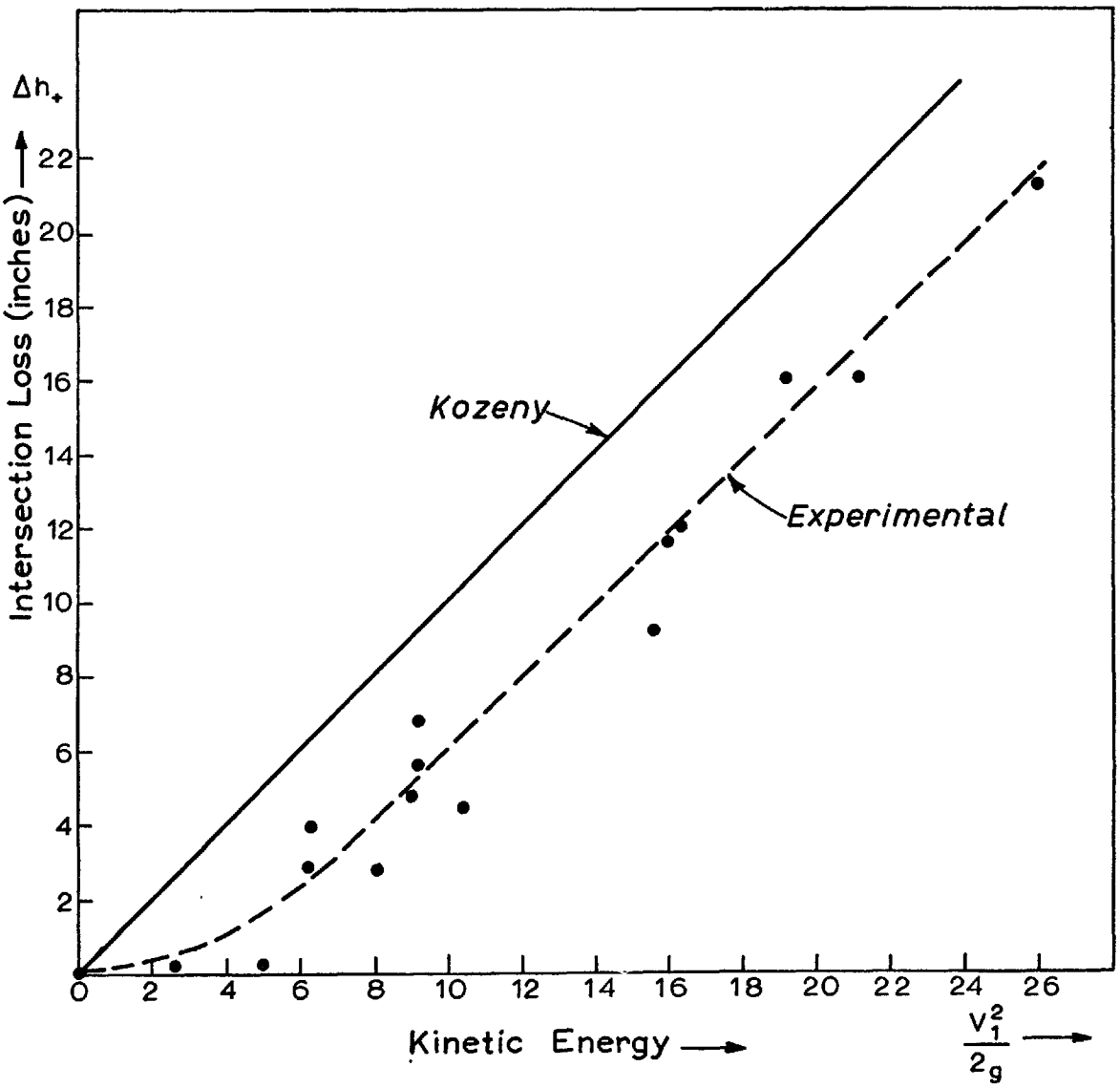

Δh+
Intersection Loss (inches)
22
20
18
16
14
12
10
8
6
4
2
0
2
4
6
8
10
12
14
16
18
20
22
24
26
Kozeny
Experimental
Kinetic Energy
V1²/2g

FIG. 3.6.

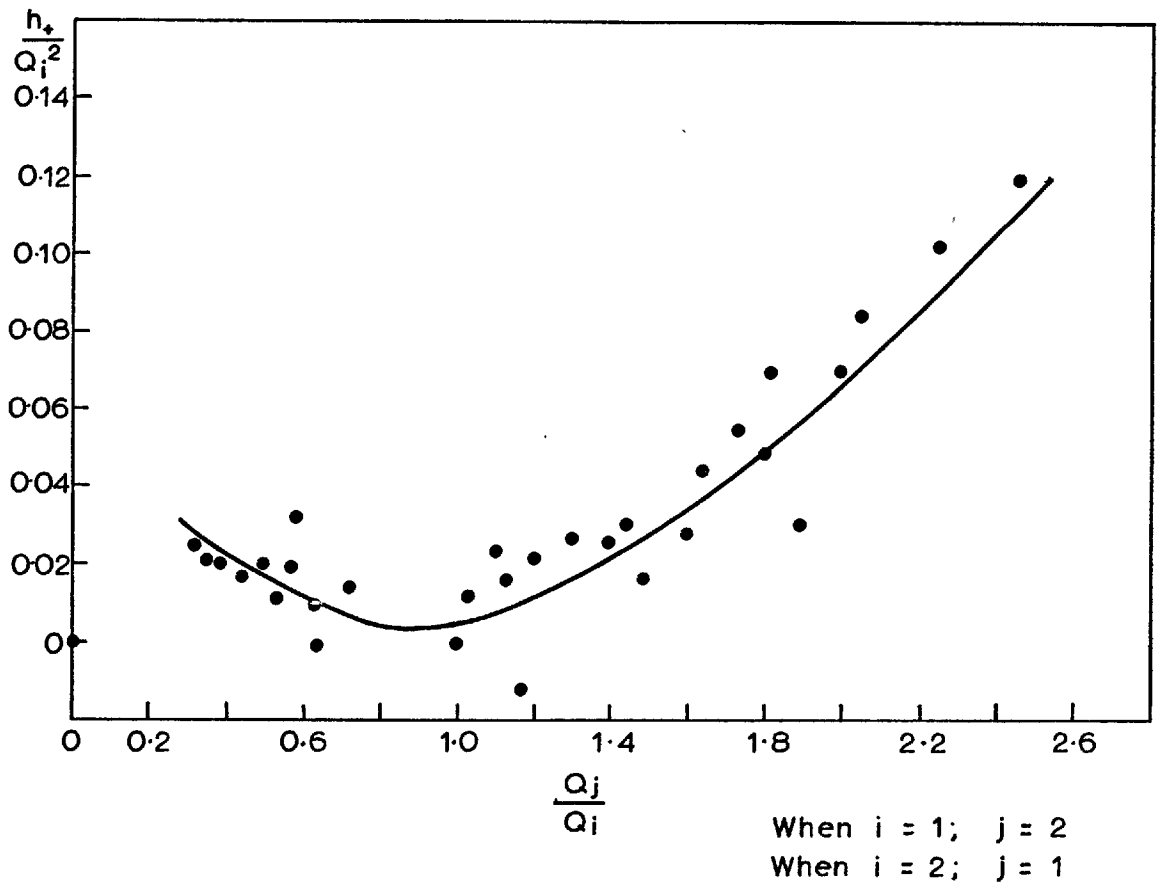

$\frac{h_+}{Q_i^2}$
0·14
0·12
0·10
0·08
0·06
0·04
0·02
0
0
0·2
0·6
1·0
1·4
1·8
2·2
2·6
$\frac{Q_j}{Q_i}$
When i = 1; j = 2
When i = 2; j = 1

FIG. 3.7.

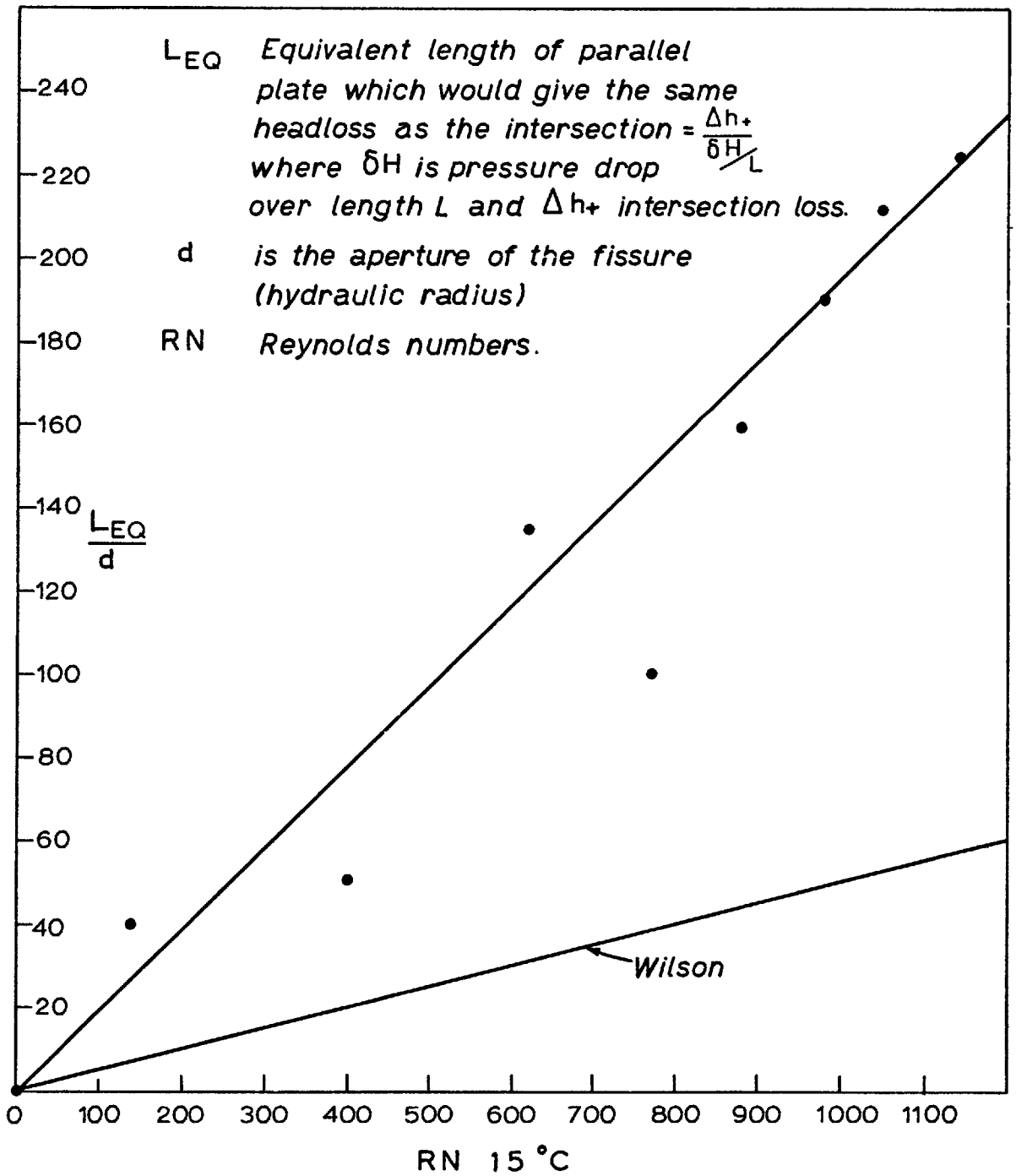

L_{EQ} Equivalent length of parallel plate which would give the same headloss as the intersection = $\frac{\Delta h_+}{\delta H/L}$ where δH is pressure drop over length L and Δh_+ intersection loss.
d is the aperture of the fissure (hydraulic radius)
RN Reynolds numbers.
$\frac{L_{EQ}}{d}$
240
220
200
180
160
140
120
100
80
60
40
20
Wilson
0
100
200
300
400
500
600
700
800
900
1000
1100
RN 15 °C

FIG. 3.8.

Fig. 3.7 demonstrates the above concept where i, j refer to the channel numbers, ie. when i = 1 j = 2 and if j = 1, i = 2. In the latter case for example the ratio Q_j/Q_i means the ratio of the flowrate in channel one to channel 2. The intersection loss is a minimum when the two input velocities are equal, suggesting perhaps that when the flows are unequal in addition to mixing losses there is a change in direction of some of the flowlines especially the slower ones, since they have less momentum than the other input.

Intersection losses have been normalised in terms of equivalent length of straight conductor of the same shape which would be necessary to create a similar headloss to (a) generalise the result in terms of Reynolds number; (b) to compare results of a similar experiment carried out by Wilson (61). Fig. 3.8 is a dimensionless plot of intersection losses expressed in terms of equivalent length of a parallel plate model vs Reynolds number. Only two experimental points are available at low Reynolds numbers, but since at higher Reynolds numbers a straight line fits the data well, the line is back extrapolated to the origin. Wilson's intersection experiment was carried out using circular tubing with an internal diameter of 0.186 inches as opposed to the author's intersection model which consisted of parallel plates 0.04 inches in aperture. It is suggested that the difference in headlosses at the intersection is due to the early onset of turbulence at the intersection in the case of the parallel plate model. In Wilson's model the corners at the intersection are very much smoother than in the parallel plate model and also the larger diameter of the circular tube allows a certain amount of flow to turn through a bend without mixing with the input from the other channel. In the parallel plate the small area of the intersection encourages mixing to occur of almost all the flow from the two inputs, see Fig. 3.9.

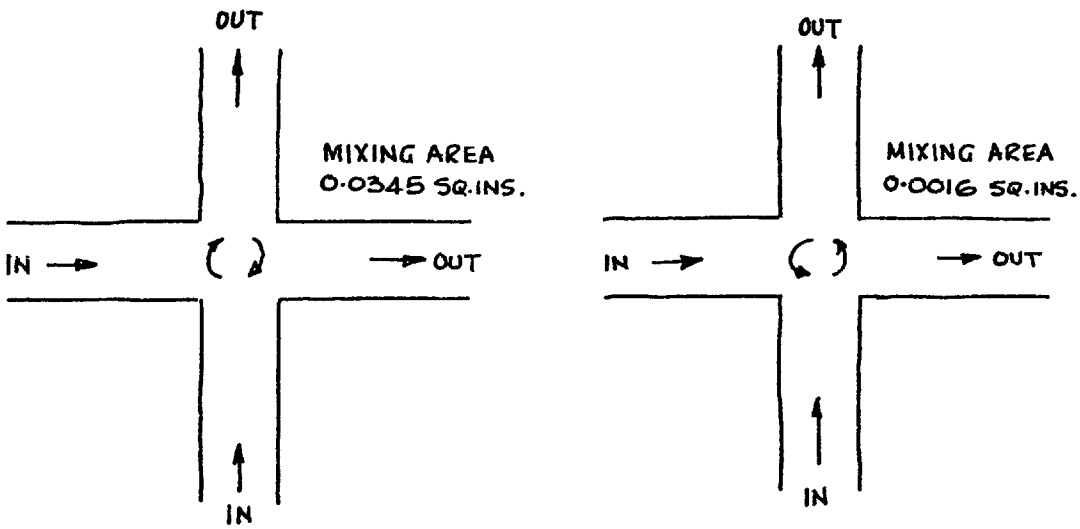


FIG 3.9

The two results in Fig. 3.8 indicate that the intersection loss expressed in terms of equivalent length of fissure increases linearly with Reynolds number. For low Reynolds number the results of the two experiments are not significantly different and since a large number of problems occur where Reynolds number is low the error involved in ignoring the intersection losses is not too great. For example, let us consider a fissure system with a mean aperture of 0.01 cms with flow at Reynolds number of 100 from Fig. 3.8,

$L_{eq} = 20 \times 0.01 = 0.2$ cms

If the intersections occurred every 10 cms for example, the error in ignoring the intersection effect would be 2%. However, at high Reynolds number, ie. flow within the vicinity of a tunnel for example, assuming the same conditions as before,

$L_{eq} = 200 \times 0.01 = 2$ cms

For the same fracture frequency, the error in omitting intersection losses would be 20%.

Intersection losses can be important when calculating the potential distribution in areas where the Reynolds number is high. Further, it can possibly be one of the reasons for non-linearity in the pressure-flowrate relationship since the onset of turbulence is very much earlier in a system where flows interfere as opposed to conditions of uninterupted flow.

3.1.5 CONCLUSIONS

The experiments carried out by the author and by Wilson have attempted to quantify the losses that occur at intersections for two different geometries. The results indicate that the losses are small when Reynolds number is less than 100, but as the Reynolds number increases, the losses become more significant. A great deal more must be done to study the influence of different geometries and angles of incidence of the two input flows. For cases where the Reynolds number is likely to be large, the intersection loss curve can be easily incorporated into the numerical model as part of the frictional resistance (permeability) of each element.

3.2.0 INTRODUCTION TO FLOW IN MULTIPLE ISOTROPIC FISSURE SYSTEM

Numerical techniques exist which provide solutions to the boundary value problems in porous media (12, 16, 17, 18). Louis (8) has considered the case of fluid flow through a discontinua with different permeability ratios, orientation of fissures. The solutions are however, for cases where all the boundary potentials are known, ie. no phreatic surface is involved. Sharp (9) has considered a vast number of problems with and without a free surface. Neither of the above simulations of fluid flow through a discontinua compare the methods with a physical method or with known analytic solutions. Obtaining a free surface involves certain assumptions whether the method of solution is an analogue or a digital computer. It is proposed to test a very simple case of flow through a multiple fissure system before applying numerical methods to more complex problems. A recent publication by Wittke (70) compares the finite element solution of a drainage problem to a hydraulic model. This publication was not available at the time of carrying out the model work, but it does, however, confirm that numerical techniques whether Finite Element or Finite Difference are successful in solving boundary value problems where conditions on one boundary are unknown and have to be arrived at iteratively.

3.2.1. HYDRAULIC MODEL

The hydraulic model consists of a large perspex block 1 inch thick with an orthogonal fissure system as in Fig. 3.10. The fissures are carefully machined with an aperture of 1 mm $\pm$ 5%. The block is firmly held between two perspex plates which form a tank and water is supplied into the input end from a constant head tank. Care was taken not to introduce air bubbles into the model by having a very fine gauze wire screen. The output is maintained at a steady pressure by the stilling basin within the model. The fissure frequency is identical in the orthogonal directions and the spacing is $\frac{3}{4}$". Twenty-one pressure points are provided to get some idea of the internal pressure distribution. By using a coloured dye it is possible to locate the channels where flow is occurring and also the exact location of the free of phreatic surface. The model during the tests was regularly washed out with a detergent to reduce the surface tension within the models to a minimim and also to release trapped air bubbles.

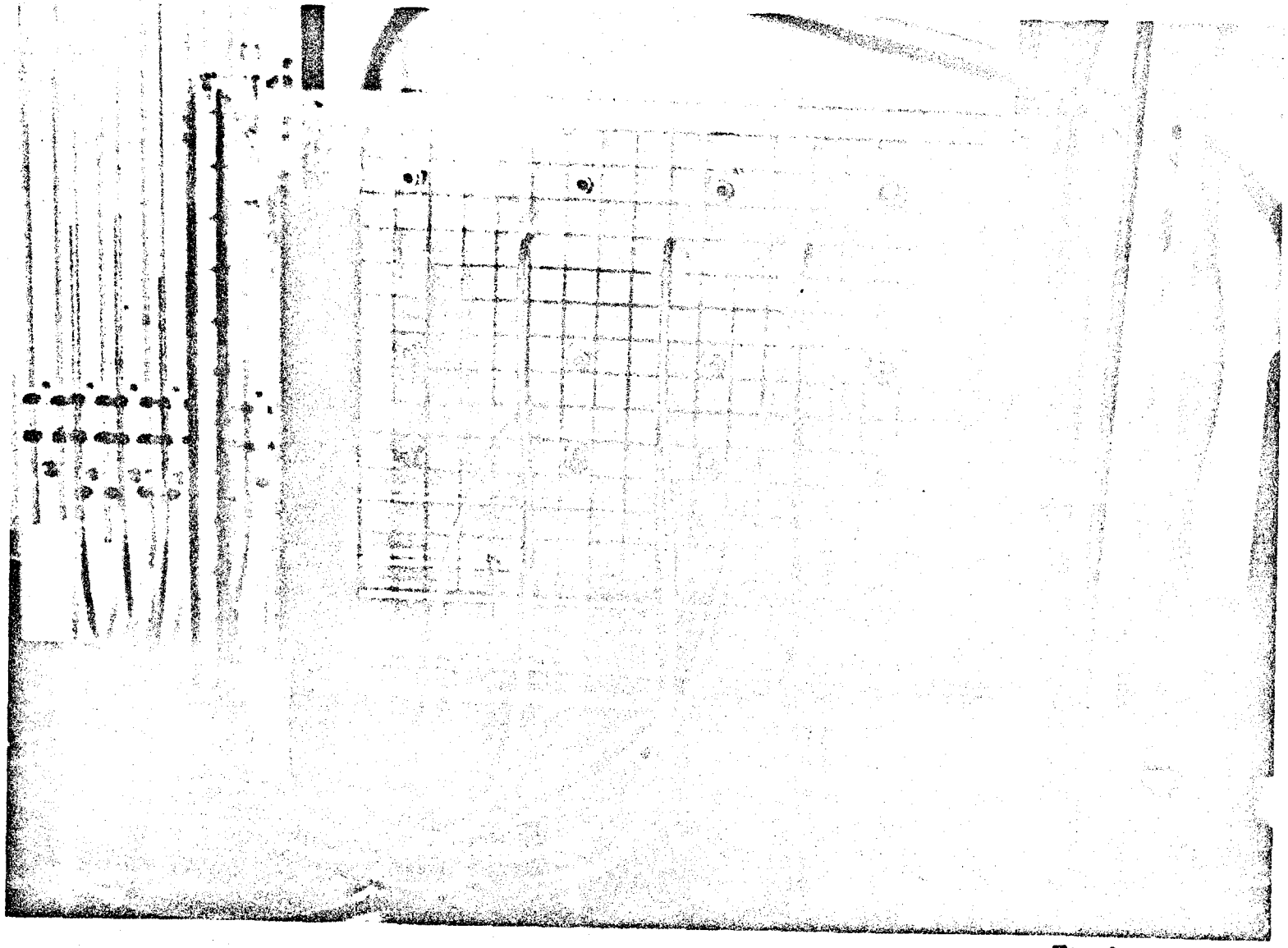


Fig 3.10

A Summary of the Physical Parameters

(a) Distance between fractures = d = 1.9 cms

(b) Area of small block = 3.61 cm^2

(c) Fissure Aperture = e = 1 mm

(d) Porosity = $\frac{e}{d} = \frac{0.1}{1.9} = 5\%$

(e) System permeability = $K_s = \frac{e^3 g}{12Vd} = \frac{10^{-3} \times 980}{12 \times 10^{-2} \times 1.3 \times 1.9} = 3.3$ cm/sec

(f) Fissure conductivity = $K_J = \frac{e^2 g}{12V} = \frac{10^{-2} \times 980}{12 \times 1.3 \times 10^{-2}} = 63.3$ cm/sec

3.2.3 EXPERIMENTAL DETAILS

Flow tests were carried out with different applied upstream and downstream boundary conditions. Once steady state was reached, pressure readings were taken from the model via the manometers so as to obtain an idea of the pressure distribution and also the dominant direction of flow. By contaminating the entire input reservoir with a coloured dye it was possible to see (a) the phreatic surface; (b) the channels in which there was flow. By taking photographs of each steady state it is possible to keep an accurate record of the phreatic surface.

3.2.3 EXPERIMENTAL RESULTS

Fig. 3.11 illustrates a typical potential distribution in the perspex model. The hydraulic gradient within the model is J = 0.06 .

It is interesting to note that there is very little pressure drop in the vertical direction indicating that the majority of flow is in the horizontal direction. This was further observed when a dye was introduced upstream. The dye front moved almost exclusively in the horizontal direction. The measured output for the boundary conditions in Fig. 3.11 is 700 cc/min. A very simplified calculation is carried out to see how accurate an estimate of total quantity of flow can be made by applying Darcy's law to the medium and considering it as a unit block with a certain system permeability. This calculation is very crude and only possible if the water table or phreatic surface is shallow.

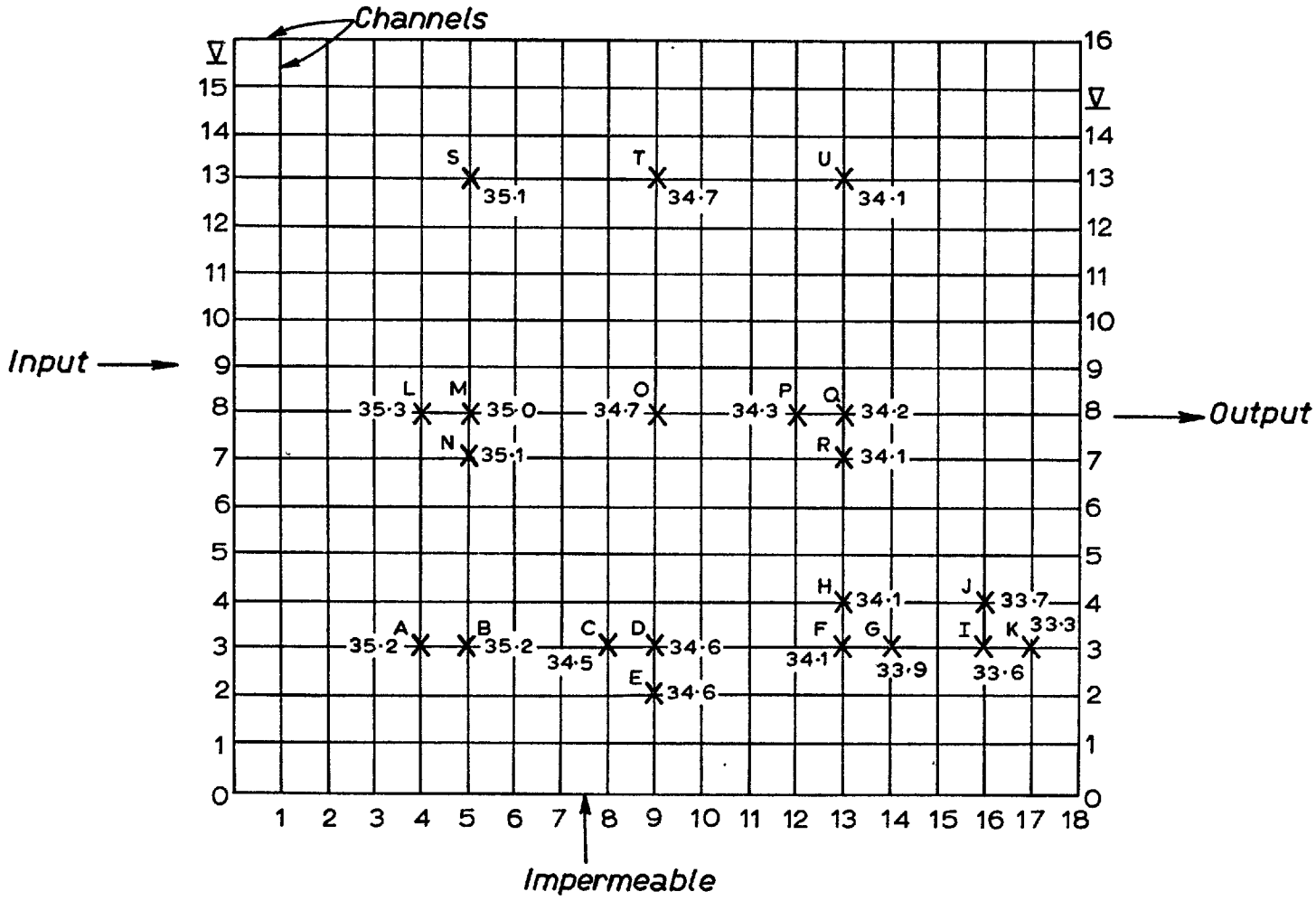

Channels
Input
Output
Impermeable
S
35·1
T
34·7
U
34·1
L
35·3
M
35·0
O
34·7
P
34·3
Q
34·2
N
35·1
R
34·1
H
34·1
J
33·7
A
35·2
B
35·2
C
34·5
D
34·6
E
34·6
F
34·1
G
33·9
I
33·6
K
33·3

FIG. 3.11.

System permeability from section 3.2.2 K_s = 3.3 cm/sec

Hydraulic gradient J = 0.06

Approximate area of flow = 15 x 1.9 x 1.9 = 54 cm^2

Darcy's law for equivalent porous media

$Q = AK_sJ$ A cross section area
K_s system permeability
J hydraulic gradient

$= 54 \times 3.3 \times 0.06$

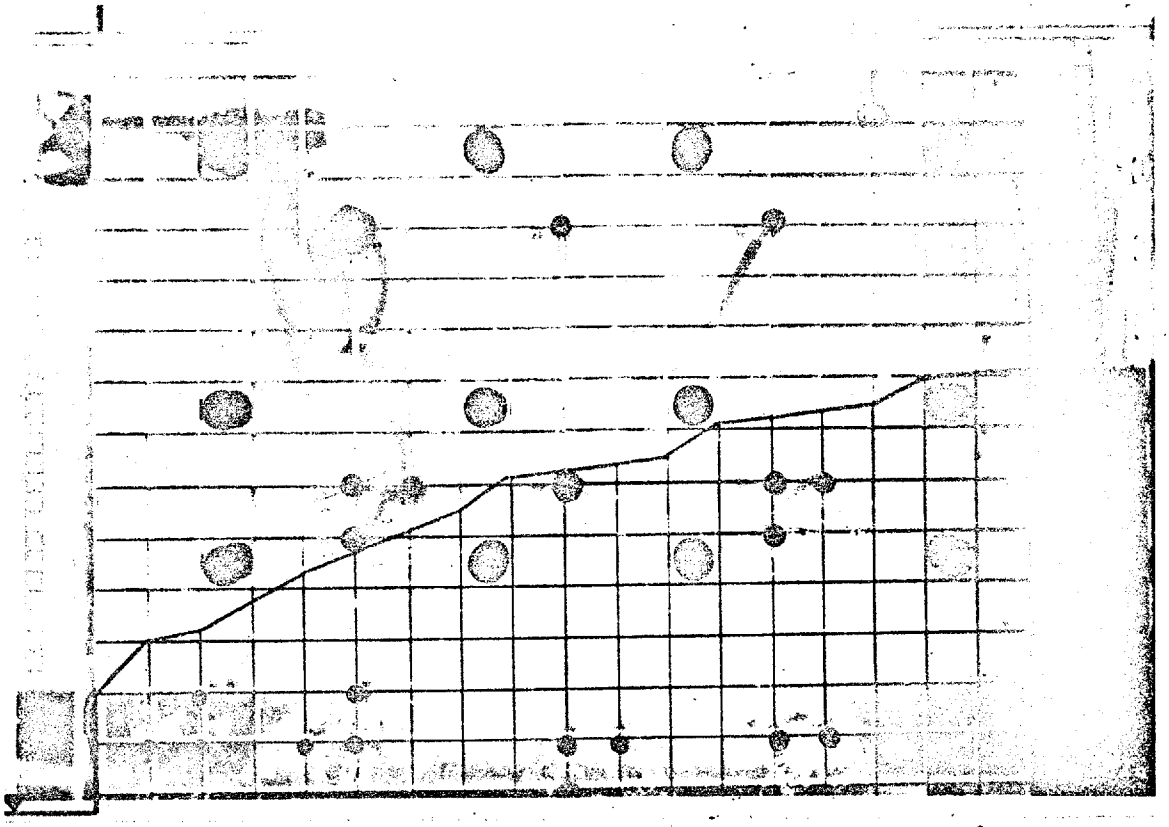
$= 10.8\ cm^3/sec$

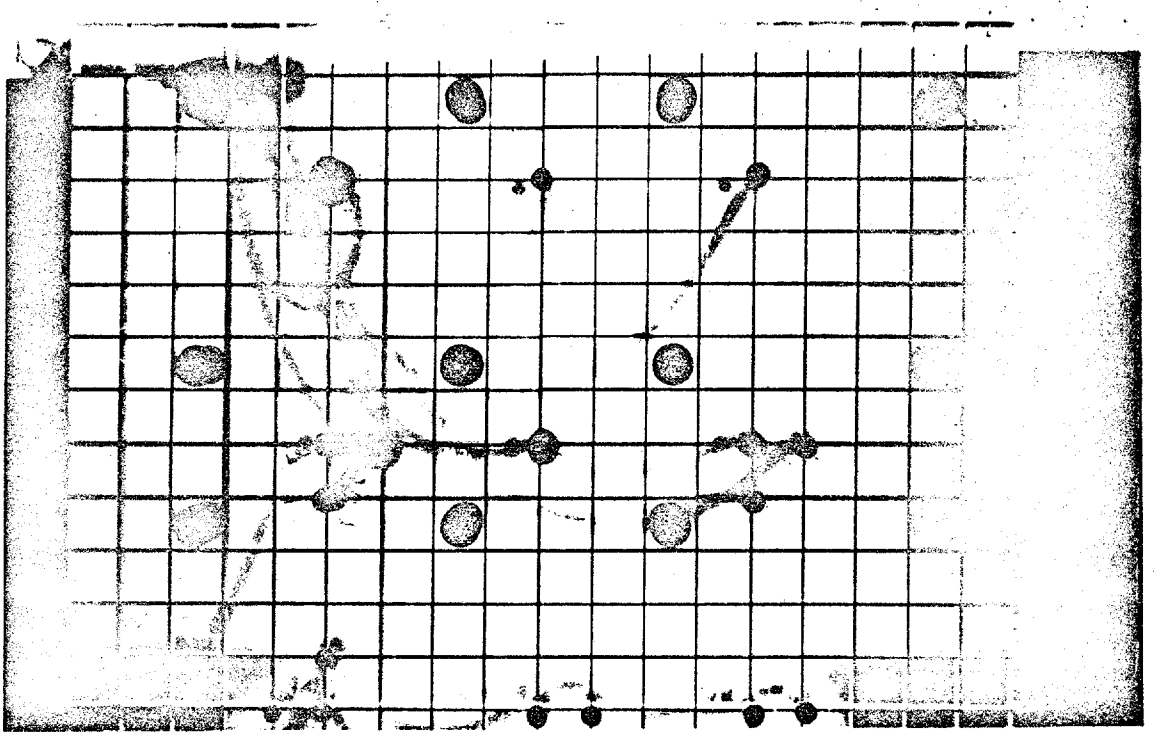
$Q = 650\ cm^3/min$

The measured value of $Q_m = 700\ cm^3/min$

This calculation shows that it is reasonable to use the above approximation when estimating very crudely, the total flowrate provided the gradient is small (less than J = 0.06).

Fig. 3.12 is a typical phreatic surface which stands out clearly because a dye has been introduced into the input reservoir. The phreatic surface is normally defined (6, 12) as the boundary in a flow system where the fluid pressure is equal to atmospheric pressure and consequently, no flow can occur across it. In a porous media where the size of the pores is not very much different to the size of the particles there is no ambiguity in the above definition. However, it can be seen in Fig. 3.12 that there are two ways of defining the phreatic surface - it can either be the level to which water rises in the vertical channels in which case the phreatic surface is the line joining these highest points or alternatively, the phreatic surface can be approximated to the uppermost boundary of flow, ie. the line joining the uppermost horizontal channel where there is flow. In the latter case the phreatic surface takes up a stepped appearance.This matter will be further dealt with in the next section on numerical solutions to boundary value problems with a phreatic surface. An interesting experiment was carried out to see if the boundary conditions at the downstream end made any difference to the phreatic surface, ie. the first experiment was made with the output from the tank flowing out so rapidly that water level at the output end of the model could not build up to the level of the highest horizontal fissure which has flow in it. With the same input boundary, water was subsequently allowed to rise to the level of the fissure with flow. This condition amounts to examining the head loss due to the kinetic energy of the discharge.





It was found that for small gradients no appreciable difference could be detected. For the maximum gradient the difference in the phreatic surface was of the order of 10%. This experiment confirms the assumptions made by Sharp (9) and Polubarinova Kochina (6). In this experiment the Reynolds number rarely exceeded 100 and therefore the intersection losses are ignored.

3.2.4 NUMERICAL ANALYSIS

A problem such as this is not amenable to any analytical solution (8, 12) and therefore it is suggested that the unknown boundary and the potential distribution are calculated by a numerical technique. Numerous methods exist which can be applied to such a problem such as the Finite Element (18, 61) technique and the Finite Difference method (16, 17, 9, 12). For reasons of clarity, computer storage, computer execution time etc, the Finite Difference method (9) is chosen; details of which are included in the Appendix. Typical boundary conditions required for the numerical method are shown in Fig. 3.13.

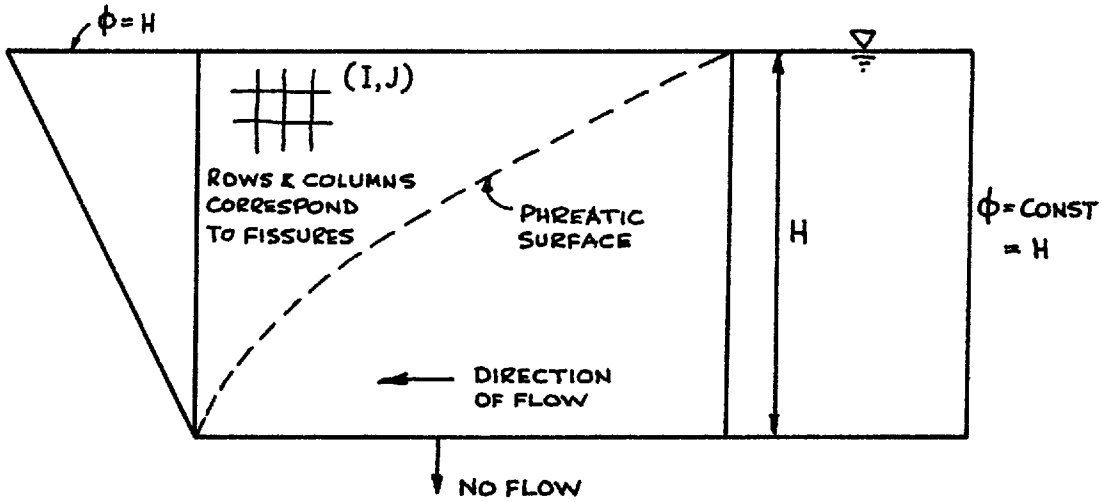


FIG 3.13

Potential is defined as $\phi = \frac{P}{\rho} + Z$

P = pressure

ρ = density

Z = elevation above a given datum.

If in the above model on the upstream size water is to the top of the model, at any elevation.

$$\phi = \text{constant} = H + \frac{P}{\rho} \text{ cm of water.}$$

On the downstream side if water is at the bottom of the model.

ϕ = Z and if the datum begins at the base of the model, the potential increases linearly with elevation.

Point X(I, J) is given by the intersection of the i^{th} column with the J^{th} row.

The position of the phreatic surface is unknown and has to be calculated using a numerical method. By assuming that the fissures in the model correspond to the rows and columns in the numerical model a Finite Difference model is set up of the physical model. Solutions to Laplcus Equation in a finite difference form are discussed in detail in Sharp (9) and Childs (12) and therefore they will not be repeated here.

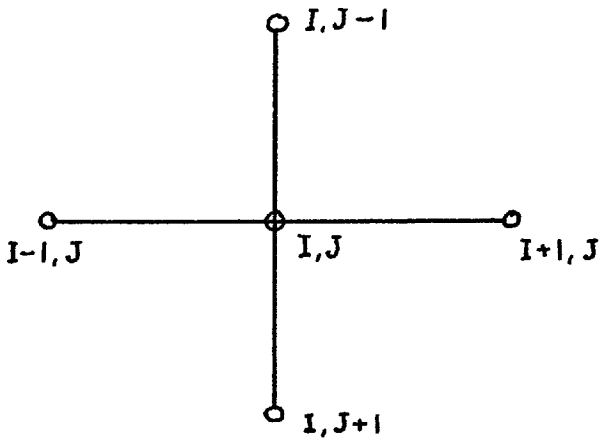


FIG 3.14

Having established the boundary conditions as in Fig. 3.13, arbitrary but realistic values of potential are fed into the internal nodes of the mesh. Each nodal point, eg. (I, J) refers to the intersection if the Ith column with the Jth row. A linear flow law is used for this problem and the potential distribution within the model is obtained for the given boundary conditions. Since this numerical model cannot simulate gravity the position of the phreatic surface cannot be established without trial and error.

Procedure for Obtaining Phreatic Surface

As a result of the first cycle of calculations the values of potential are examined beginning with the top left hand corner and looking at one row at a time. If at any node, the value of total potential $\emptyset$ is equal to the elevation potential H the node defines the upper limit of the free surface. This exact relationship very rarely exists and therefore the following criteria is used. If $H(I, J)-\emptyset(I? J)<C$ the vertical element above the node is isolated from the system. C is a constant which is arrived at by trial and error. Its value must be such that only a small fraction of the system, ie. a row is isolated at each cycle of the computation (see Fig. 3.15). This is because if a large area of the model is isolated suddenly the phreatic surface becomes unstable.

Computational details are given in the appendix. Since the determination of the phreatic surface is largely one by trial and error a confirmation of the method is essential and the best possible way to do this is to use the results of the hydraulic model described in section 3.2.3.

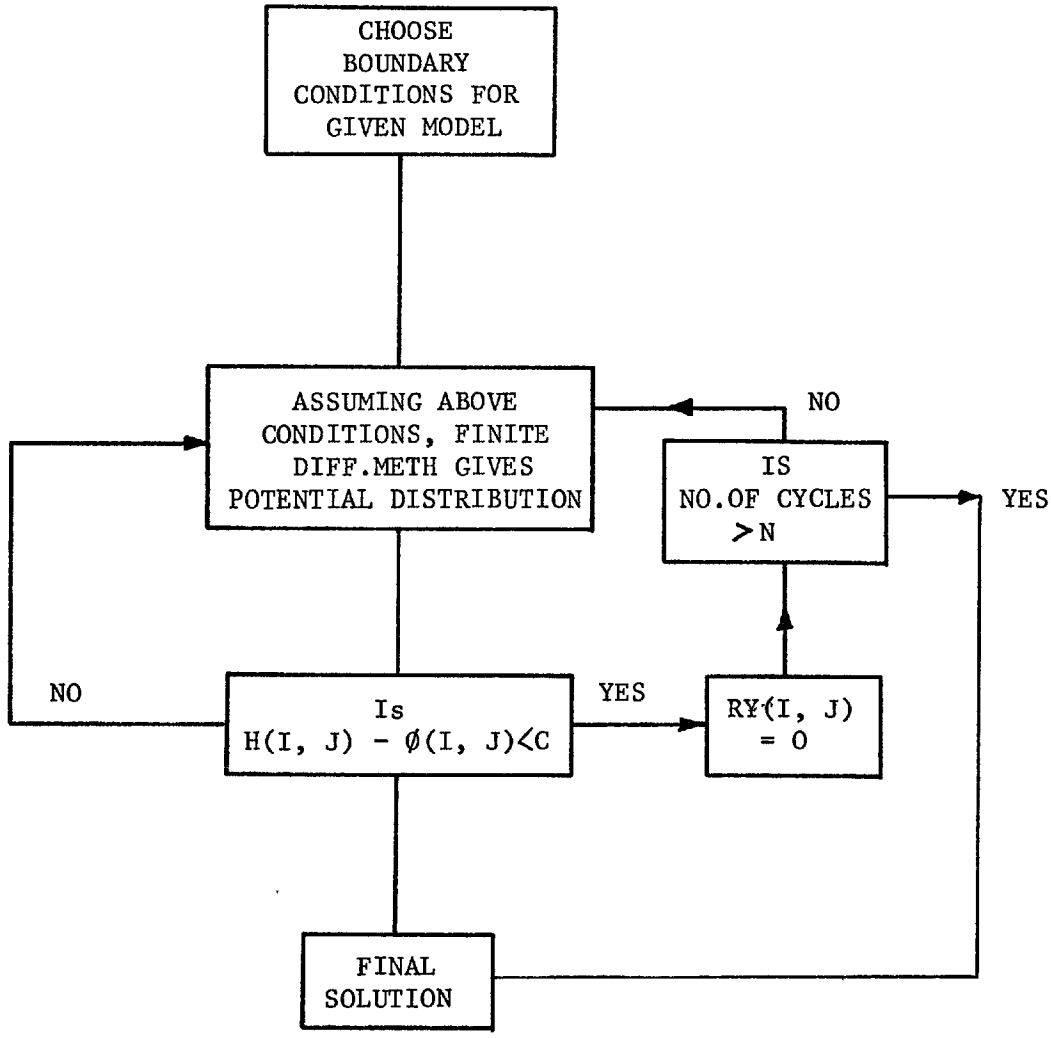


FIG. 3.15

Fig. 3.16 is a typical result of such a numerical analysis. Also on the same diagram are traces of the phreatic surface. As was explained in the previous section it is possible to define the phreatic surface in two ways, ie. a line joining the tope of the water level in the sectional fissure which indicates the pressure in the top elements or a stepped line which defines the area of flow. From these results it can be seen that the results of the physical or hydraulic model agree very closely to the computer solution. The solutions for the other different boundary conditions agree very well with the hydraulic model indicating that the method of analysis and of obtaining the free surface is correct.

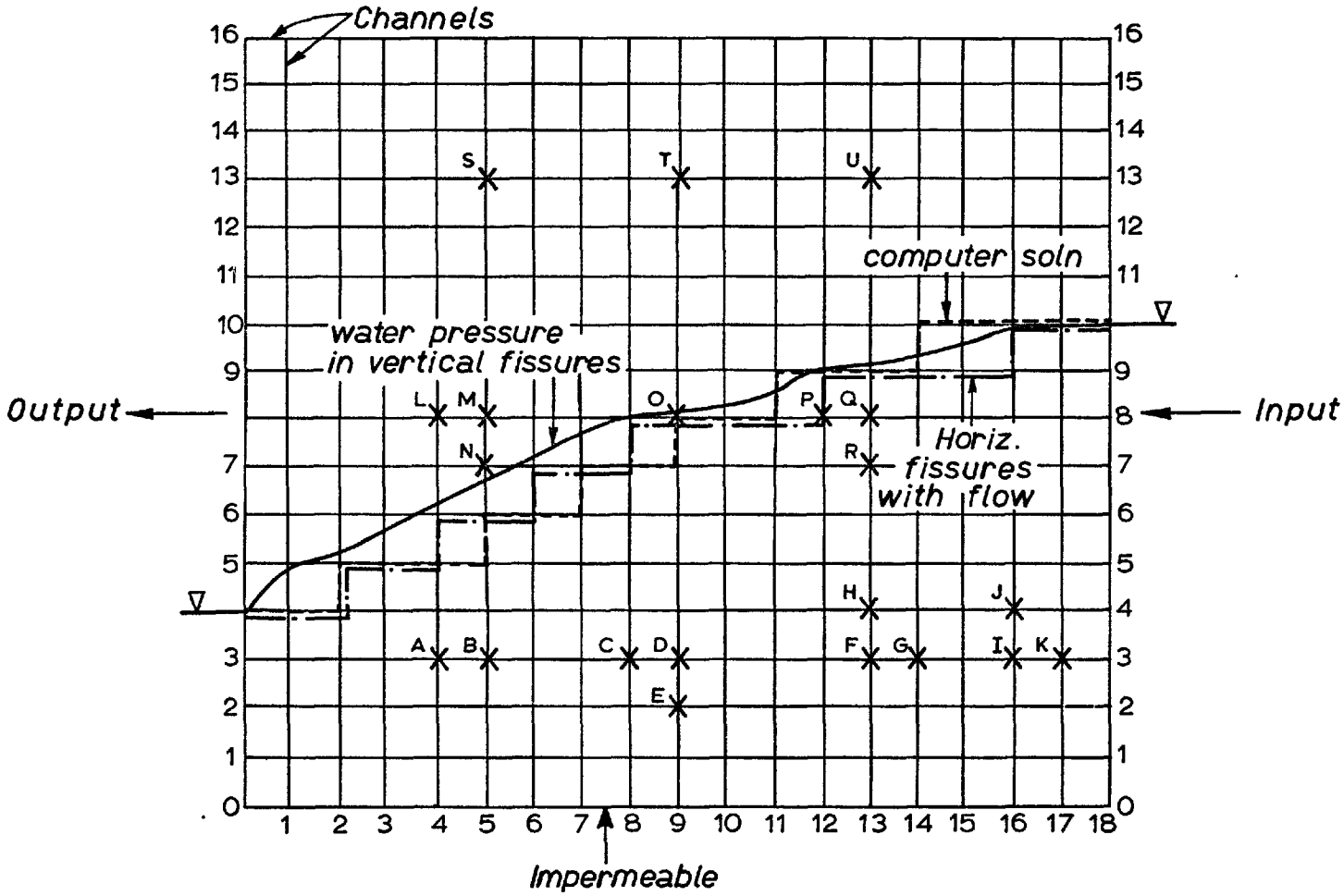

Channels
computer soln
water pressure
in vertical fissures
Output
Input
Horiz.
fissures
with flow
Impermeable
S
T
U
L
M
O
P
Q
N
R
H
J
A
B
C
D
F
G
I
K
E

FIG. 3.16.

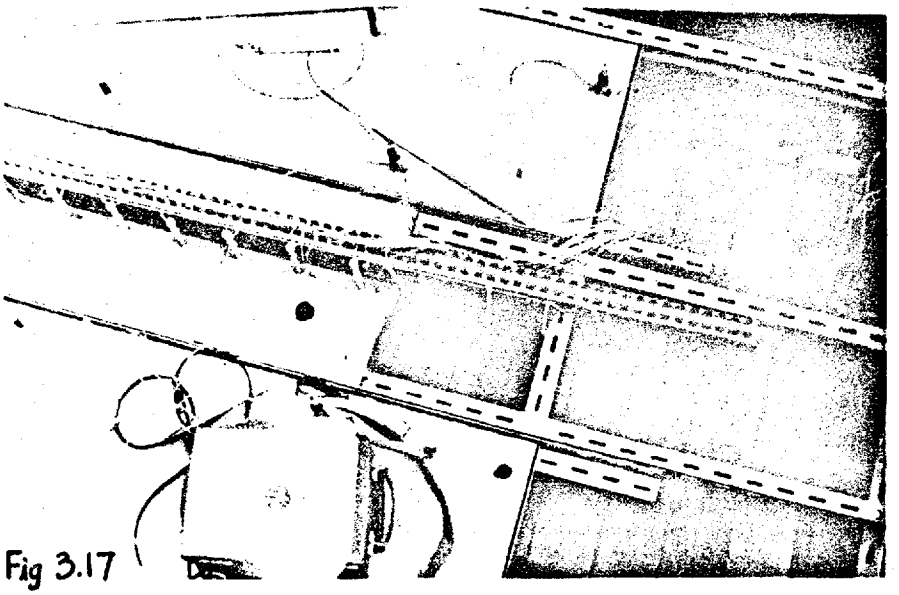


Fig 3.17

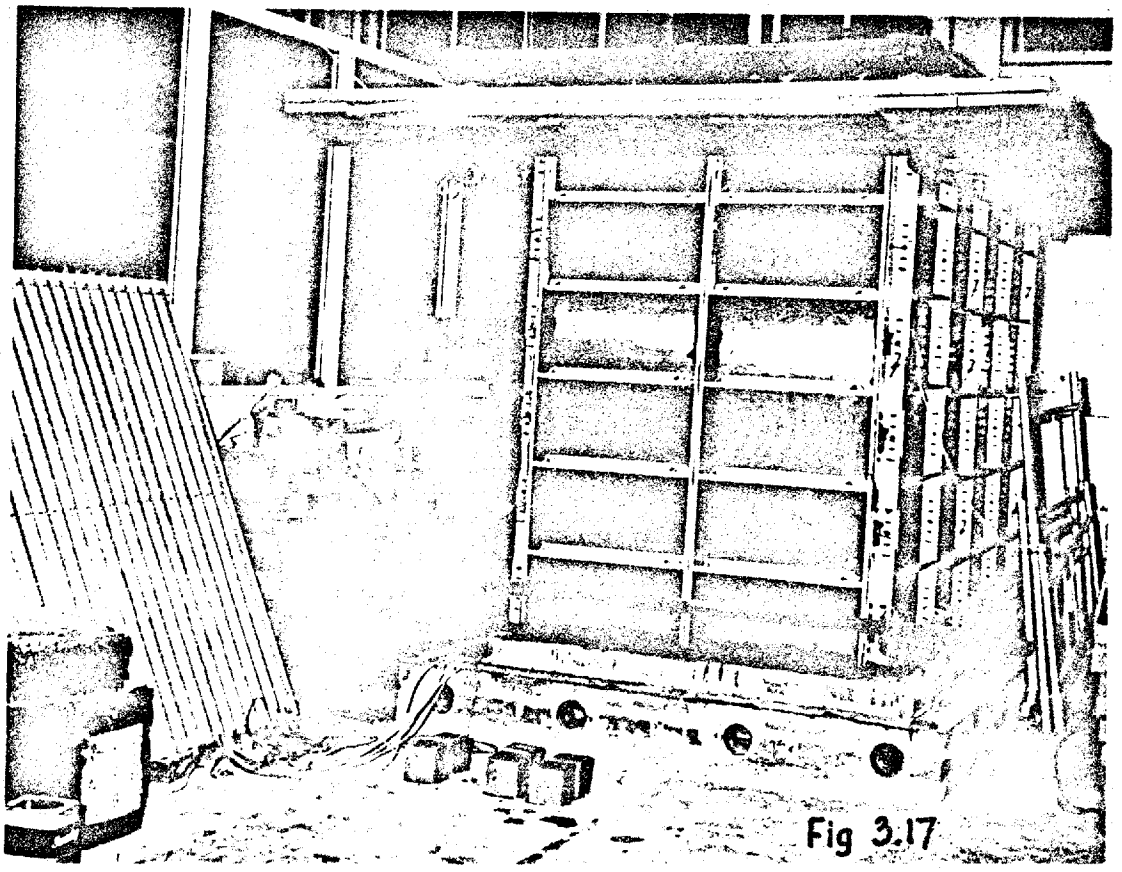


Fig 3.17

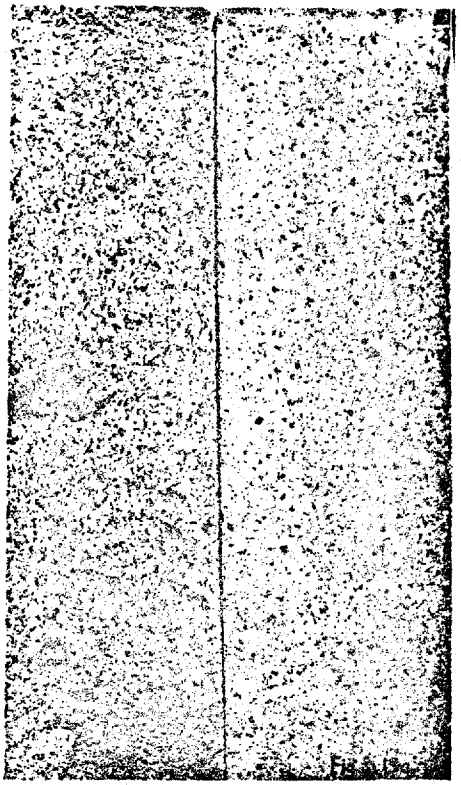
3.3.0 INTRODUCTION TO FLOW IN AN ANISOTROPIC MULTIPLE FISSURE SYSTEM

A large hydraulic model has been made at the Rock Mechanics Centre to simulate fluid flow through a fissured rock mass. Having successfully used the perspex model to test the theory under idealised conditions (section 3.2.0) it was decided (a) to consider a fissure system in which the spacing between fissures in the two orthogonal directions is different (b) the fissures are not smooth parallel plates, but have surface roughness, (c) there is a drainage gallery or tunnel in the fissure system.

With the above conditions in mind, impervious engineering bricks were chosen as the model material for the blocks which constitute a fissure system. For a variety of input pressures, measurements were carried out of the potential distribution within the model by observing piezometric levels and also the flowrates were monitored once stable conditions were achieved. Computer simulation of the above model was subsequently carried out to compare the theory with experiment.

3.3.1 DETAILS OF THE HYDRAULIC MODEL

Fig. 3.18 illustrates a section through the model which consists of 13 horizontal and 21 vertical fissures with a quadrant of a drainage gallery in one corner of the pile of bricks. By symmetry it can be assumed that the model is in fact four times the size shown in the diagram and therefore represents a fairly realistic size of problem. Pressures within the model are monitored at different locations and elevations by piezometers. A piezometer consists of a hollow nylon tube which is fixed (open ends) at the point where the measurement of pressure is required, ie. within the fissure plane. A large number of piezometers daylight above the top of the model while the installations within close proximity of the drainage gallery are connected to a manometer. Transit time or seepage velocity between any two piezometers can be made using the Schmidt trigger device (described in detail in Part IV). It consists of two bare terminals at every piezometer and the wires connected to the terminal pass through the piezometer tubes are connected to the Schmidt Trigger and a chart recorder. The depth of the water level in the piezometer is measured with two base wires connected to an Avometer which are lowered into the nylon tubing. When the wires touch the water surface, the circuit is closed, thus locating the phreatic surface.



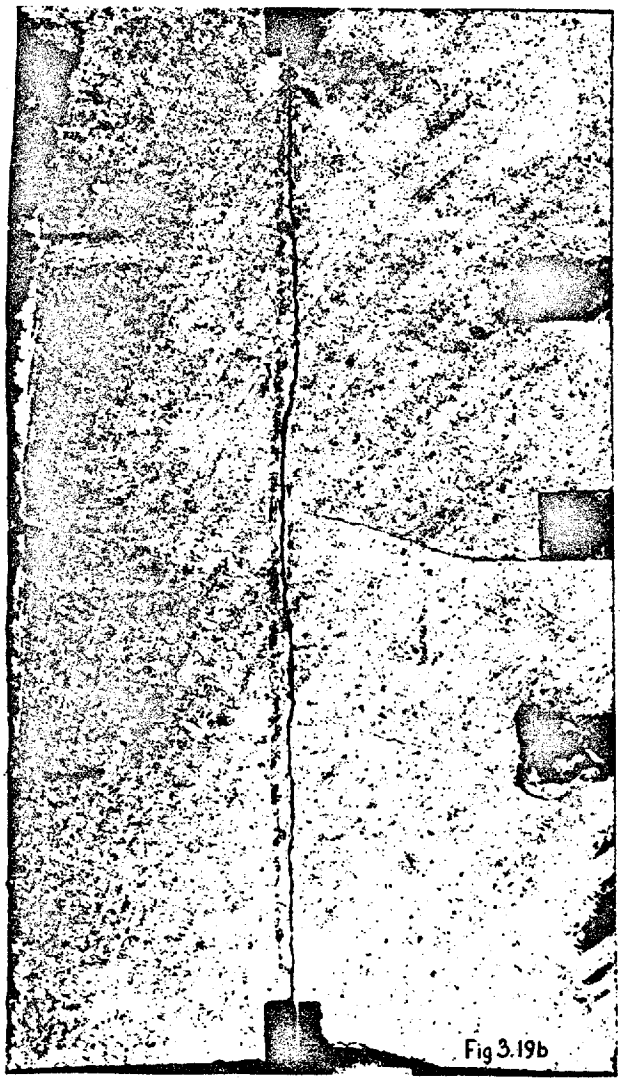


Fig 3.19b

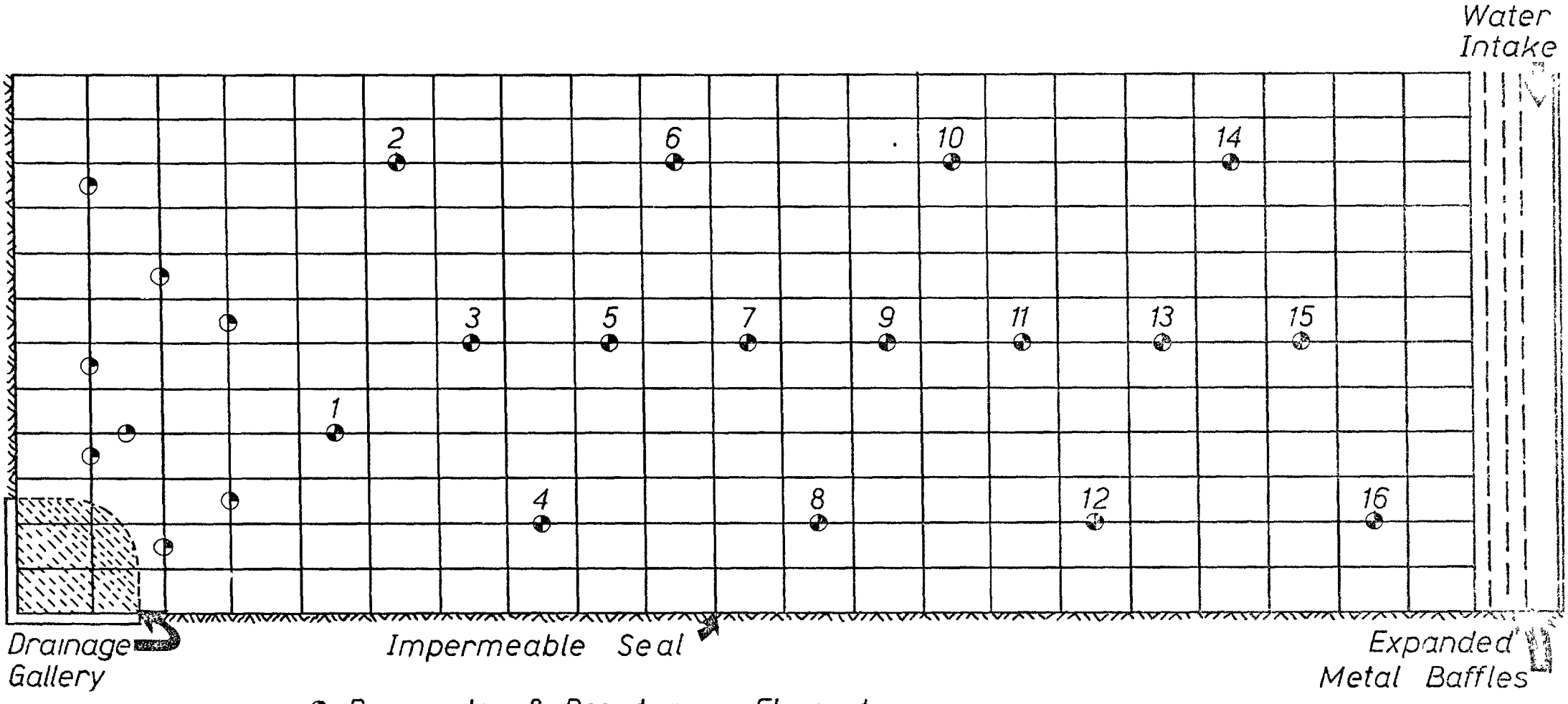

Water Intake
2
6
10
14
3
5
7
9
11
13
15
1
4
8
12
16
Drainage Gallery
Impermeable Seal
Expanded Metal Baffles
Piezometer & Resistance Element
Piezometer

FIG 3.18

3.3.2 SCALE OF THE MODEL

Distance between vertical fissures = 4 inches
Distance between horizontal fissures = $2\frac{1}{2}$ inches
Radius of gallery = 7 inches

If, for example, the gallery in the model represents one 6 ft in diameter in the field, the distance between fissures becomes 3 ft 5 in and 2 ft 2 in.

3.3.3 MODEL SINGLE FISSURE CHARACTERISTICS

Fig. 3.19(a) is a cross section along the direction of flow in the brick fissure model. The photograph does not clearly illustrate the uneven nature of the conductor as compared to Fig. 3.19(b), which is a real fissure in purphyry (9). A close examination of the fissure Fig. 3.20aillustrates how the aperture of the fissure varies.

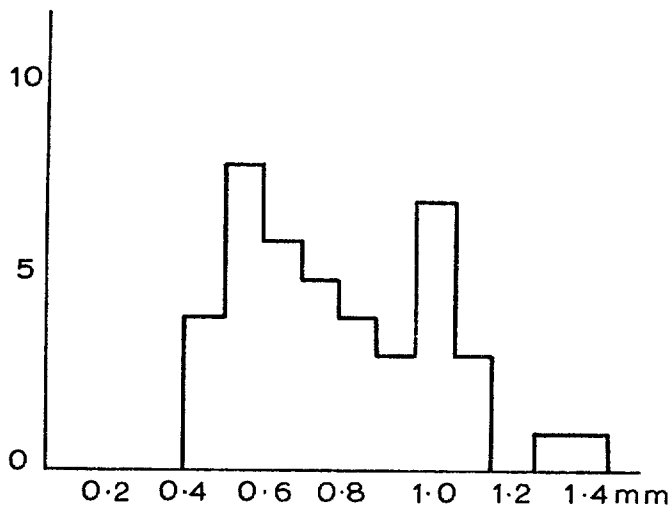


FIG. 3.20a.

These measurements were made with a reflecting microscope. It is believed that irregularities such as these cause nonlinearity in the pressure flowrate curve. The histogram also indicates that the size of the irregularity is roughly of the same order of magnitude as the aperture, as opposed to pipe roughness which is much smaller than the diameter of the pupe. The wide wave-band of aperture values indicates a convergent-divergent flow pattern and the skewness that the asperities and cavities are intermittent (9). From this roughness profile it is very likely that nonlinearity will begin at a relatively low Reynolds number.

Simple flow tests were carried out along the length and width of the fissure to (a) calculate permeability of a single fissure (b) to observe whether the pressure-flowrate curve is nonlinear, (c) to determine if there is any anisotropy to flow in the plane of the fissure. A final test was carried out on a pile of eight bricks to compare the value of permeability per fracture from this test to the previous two, see Fig. 3.20(b).

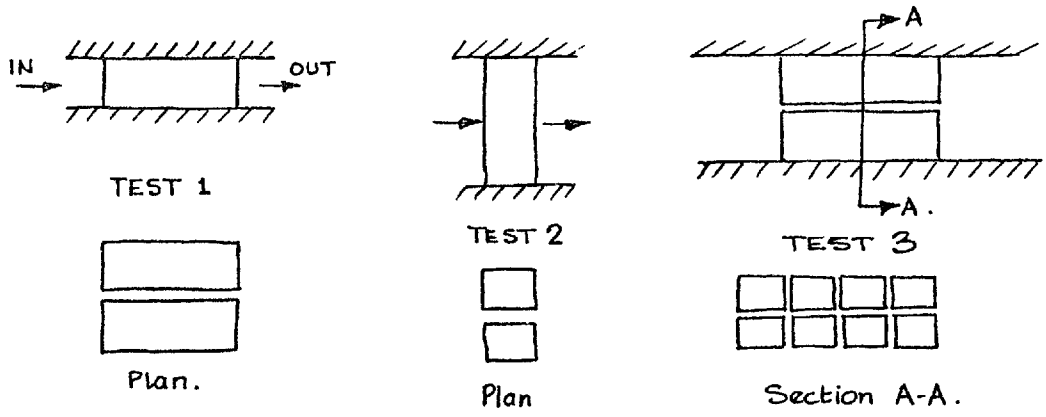


FIG 3.20(b)

Fig. 3.21 illustrates the result of the tests 1, 2, where flow-rate is plotted as hydraulic gradient. Only the very early part of the curve can be classified as a straight line. The relationship is a nonlinear one and from the experimental points there seems to be no difference between flow in two directions within one plane. There is no distinct change from laminar to turbulent flow and therefore it is no possible to define the Reynolds number at which laminar flow breaks down. In order to obtain values of permeability for purposes of comparison the initial linear part of the curve is used.

If we assume $Q = AKJ$

Q is flowrate

A cross section area of flow per unit width

K fissure permeability

J hydraulic gradient

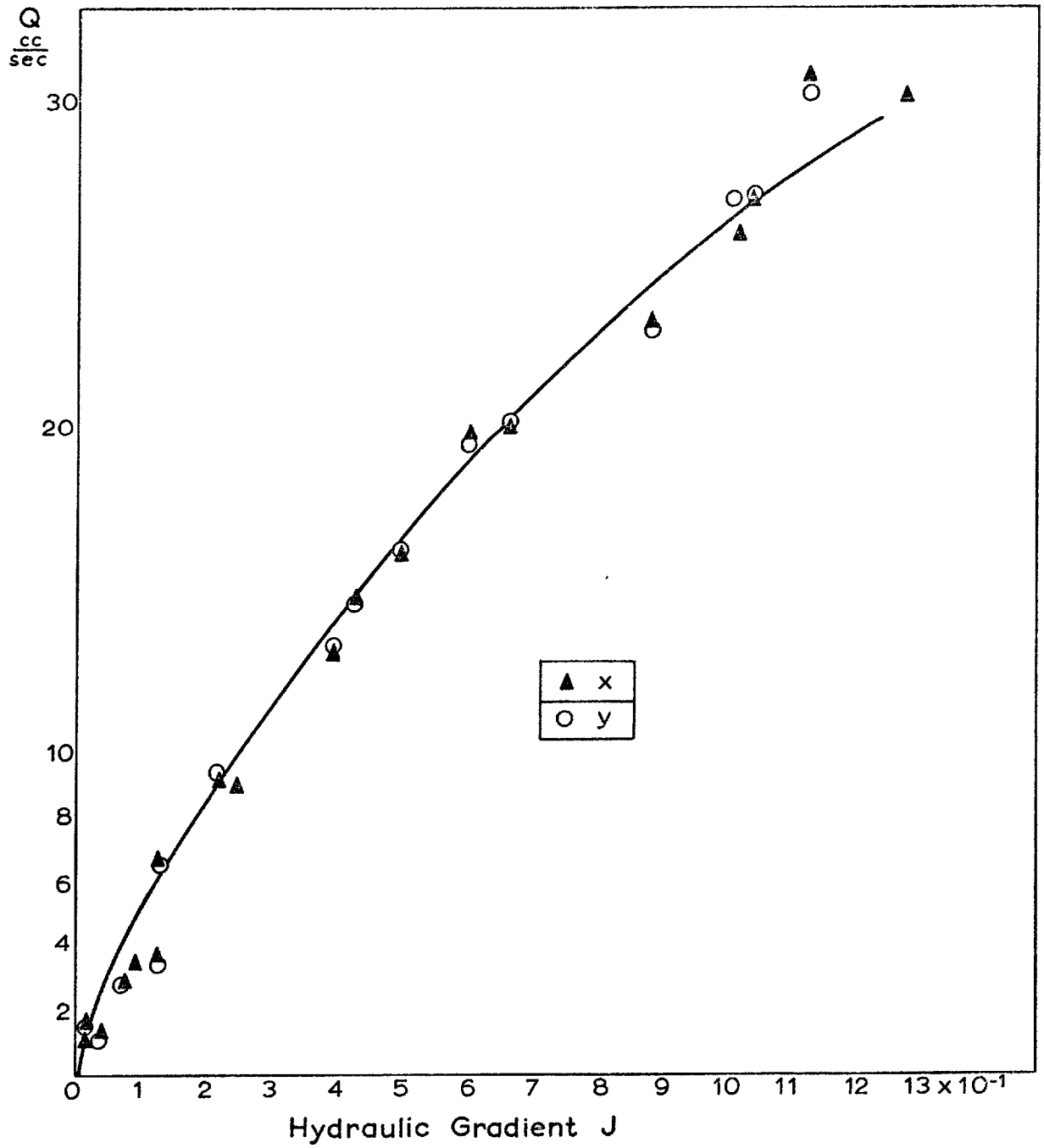

Q
cc
sec
30
20
10
8
6
4
2
0
1
2
3
4
5
6
7
8
9
10
11
12
13 x 10⁻¹
Hydraulic Gradient J
▲ x
O y

FIG. 3.21.

TABLE 1

Test 1	AK = 1.98 cm^2/sec
Test 2	AK = 3.5 cm^2/sec
Test 3	AK = 4.1 cm^2/sec

The above results can be expressed in terms of permeability if a value for mean opening can be assumed. From the histogram the value of mean opening is 0.8 mm.

TABLE 2

Test 1	K = 24.7 cm/sec
Test 2	K = 33.2 cm/sec
Test 3	K = 40.7 cm/sec

Assuming a parallel plate model with an opening 0.8 min

$$K = \frac{e^2 g}{12V} = \frac{980 \times (0.8)^2 \times 10^{-2}}{12 \times 1.14 \times 10^{-2}} = 46.1 \text{ cm/sec}$$

In table two it can be seen that the permeability between Test 3 and 1 is different. The reasons for this is that the edges of the bricks are not all sharp and therefore some liquid escapes through the gap between the brick walls which is created when an arrangement such as Test 3, Fig. 3.20(B) is used. The value of permeability of an equivalent parallel plate, ie. one with an aperture of 0.8 mm is much higher. This is reasonable because the roughness on the brick surface reduces the permeability by increasing the viscuous drag on flow.

3.3.4 MULTIPLE FISSURE CHARACTERISTICS

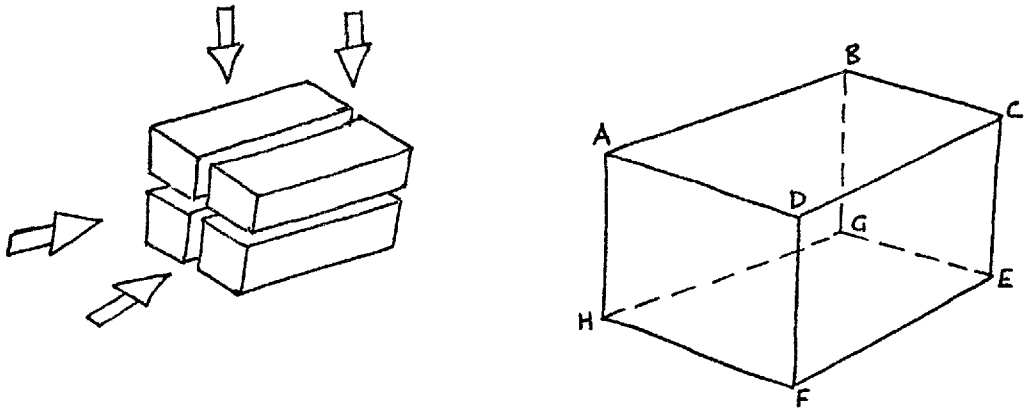


Fig. 3.22

If Fig. 3.22 is a typical block element out of the fissure system, flow will take place along three different planes, ie. ABCD, DCEF and BCEG. The flow along channel ABCD and BCEG can be thought of as flow through a two dimensional system, the flow in each plane by symmetry being reduced to a line flow as in Fig. 3.23 where xy corresponds to ABCD
zy corresponds to BCEG

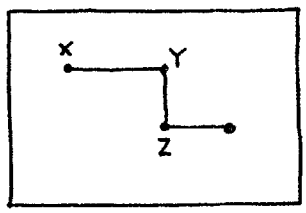


Fig. 3.23

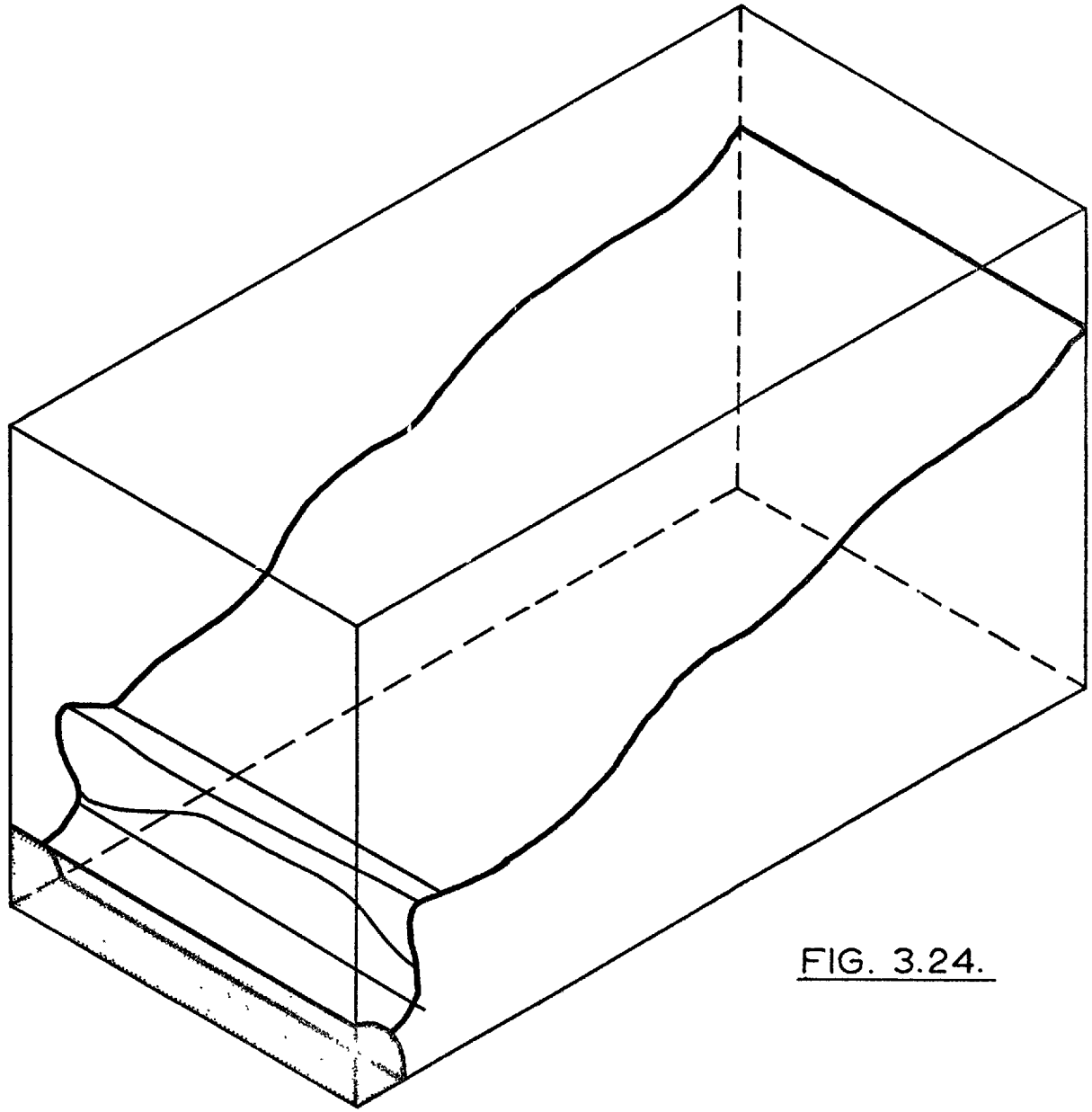


FIG. 3.24.

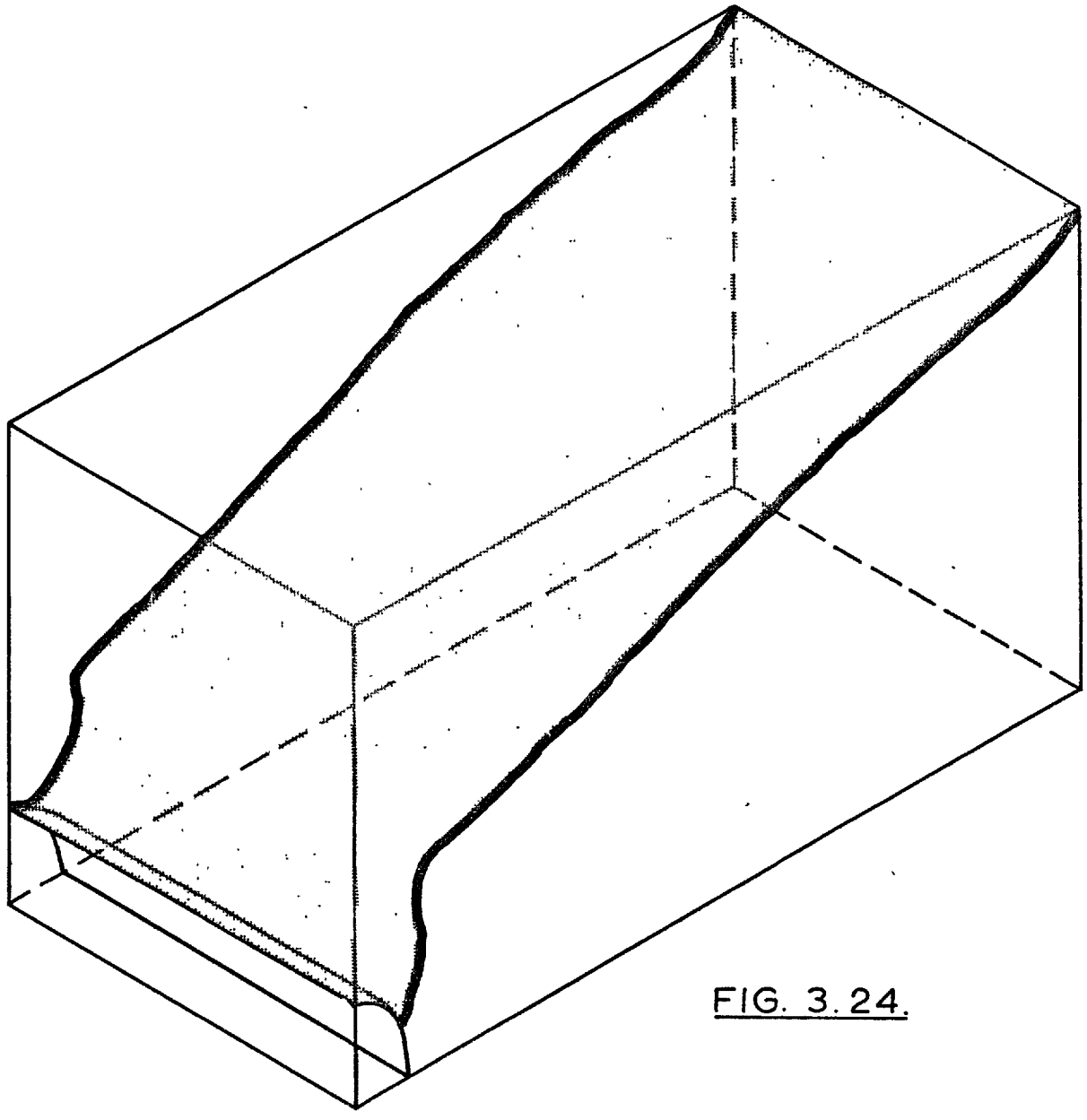


FIG. 3.24.

Flow in element DCEF and others in the same plane can be thought of as flow in one large single plane. Therefore the total flow being the superposition of the two dimensional flow in the XY, YZ direction plus flow in the plane parallel to DCEF. This superposition is clearly only possible for the case of linear flow.

For a large number of different upstream pressures the pressures within the model were measured so that a picture of the phreatic surface and hence, the potential distribution could be made up. Fig. 3.24 is a typical example of two such tests. In the first test, a head is applied which is equal to the height of the model. The second one is a case with 75% applied head. The pressure drop from the upstream end is linear most of the way towards the end where there is a sudden decrease towards the gallery. This behaviour is believed to be due to the acceleration of the fluid as it approaches the gallery.

DETERMINATION OF SEEPAGE VELOCITY USING THE SCHMIDT TRIGGER

Seepage velocity is measured within the model using aSchmidt trigger device. This method relies on injecting either hydrochloric acid or salt solution into the input end of the tank. As the tracer front (assuming little dispersion at such high velocities) moves within the model and goes past the probe an electrical signal is triggered off to indicate that the front has moved past the given point. Fig. 3.25 is such a record where the sharp peaks indicate the time at which the front passes by. Numbers 1-4 indicate the piezometer numbers. Piezometer number 2 and 4 are on the same level.

DIRECT ESTIMATE

Distance from piezometer 2 to 4 = 2 x 4 x 2.54 = 20.5 cms

Time interval from 2 to 4 (Fig. 3.25) = 1.25 x 6 = 7.5 seconds

Seepage velocity from point 2 to 4 $= \frac{20.5}{7.5}$ = 2.75 cm/sec

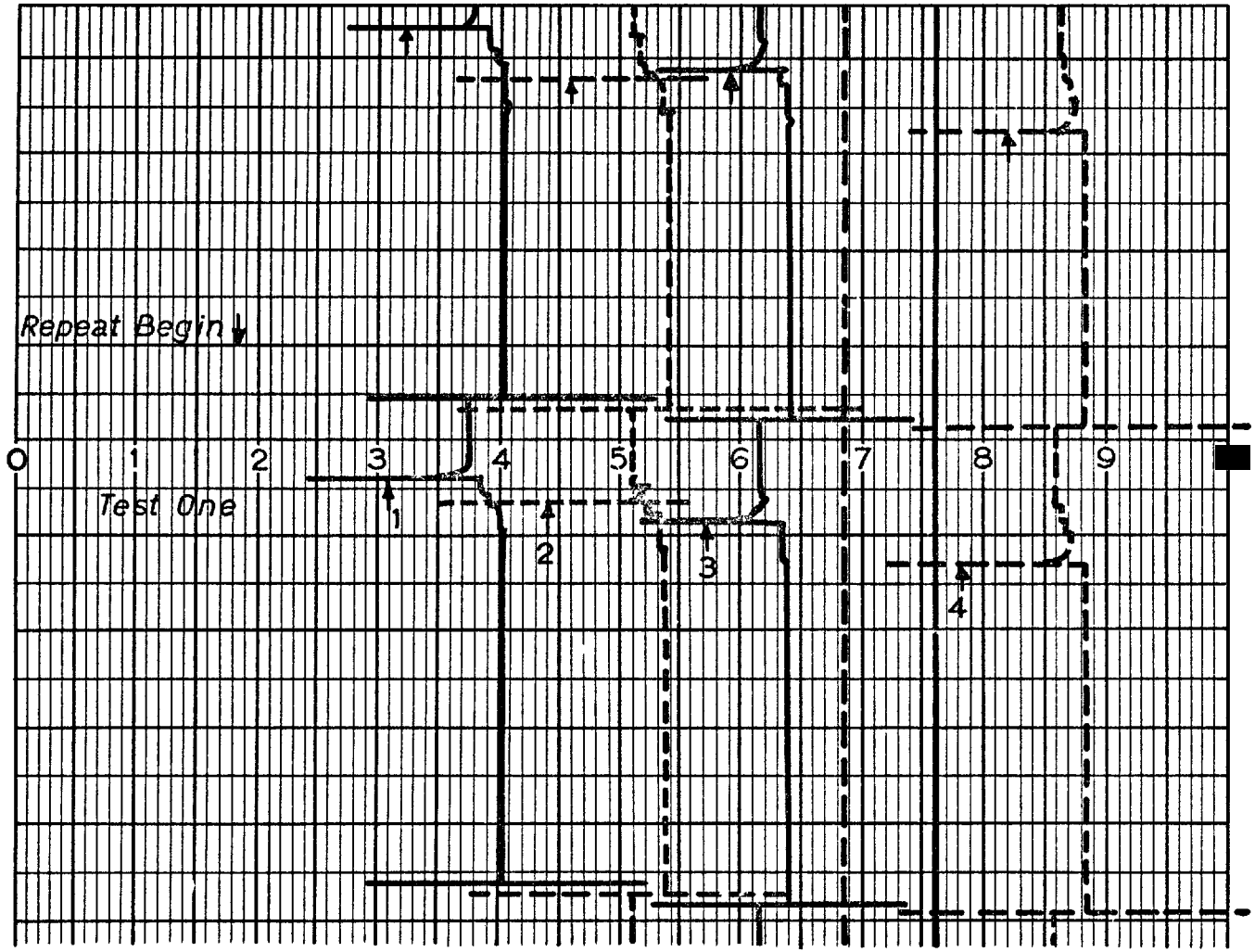
INDIRECT ESTIMATE

Pressure difference point 2 to 4 = 50.5 - 42.0 = 3.5 cms

$\therefore$ Hydraulic gradient = $\frac{3.5}{20.5}$ = 0.170

From section 3.3.3 mean permeability K_J = 32.6 cm/sec

$\therefore$ seepage velocity point 2 to 4 = 32.6 x 0.170 = 5.5 cm/sec


Repeat Begin
0
1
2
3
4
5
6
7
8
9
Test One
1
2
3
4

The degree of agreement between the two answers is not bad at all because the mean aperture estimate is subject to error, ie. a small error in aperture causes a very much larger error in the estimate of permeability.

Reynolds number upstream between point 2 and 4 $= \frac{ud}{v} = \frac{2.75 \times 8 \times 10^{-2}}{1.2 \times 10^{-2}}$

u = velocity
d = hydraulic radius
v = kinematic viscosity

$= 18.3$

Close to the gallery the velocity can be calculated from the pressure readings at point 9, 4.

Pressure drop between point 9 and 4 = 8.8 cms

$\therefore$ Gradient point 9 and 4 $= \frac{8.8}{4 \times 1.54} = 0.87$

$\therefore$ Velocity from point 9 to 4 = 37.6×0.87 = 28 cm/sec

Reynolds number $= \frac{ud}{v} = \frac{28 \times 8 \times 10^{-2}}{1.2 \times 10^{-2}}$

RN = 186

The above calculation demonstrates that the seepage velocity increases by a factor 10 times from the upstream end of the model to the downstream end near the gallery. The pressure loss due to the change in kinetic energy near the gallery is approximately 8% of the frictional loss. In this particular model the Reynolds number close to the gallery justifies the incorporation of the intersection losses, but otherwise they are sufficiently low and the value is within the inaccuracies caused by the irregularity of the block sizes, alignment of the fissures etc. Numerical analysis will be carried out to see the degree of correspondence between theory and model.

3.3.5 NUMERICAL ANALYSIS OF FLUID FLOW THROUGH ANISOTROPIC MULTIPLE FISSURE SYSTEM

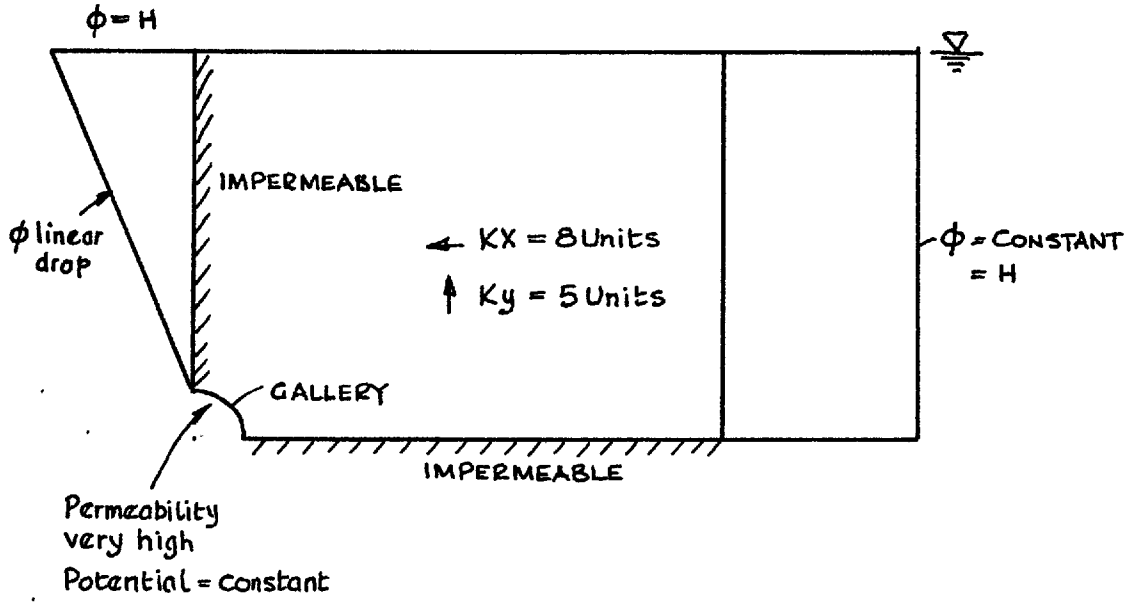


FIG 3.26

Two cases are considered:

1. Ratio of principal permeabilities = $\frac{Kx}{Ky} = \frac{8}{5}$ Fissure Horizontal and Vertical Direction

2. " " " " " = 1 Fissure in Vertical Plane

The same numerical technique as described in the previous section is used except that at the bottom left hand corner a gallery is introduced. The gallery potential is always constant and equal to the elevation potential. The permeability within the gallery is very large compared to the permeability of the fissures.

A large number of computations were carried out to establish the free surface so as to compare the numerical results with tests carried out in the hydraulic model. Figs. 3.27 and 3.28 illustrate the free surface using various techniques. As was mentioned in the previous section, the phreatic surface can be represented (9) by the stepped line which is the uppermost flow

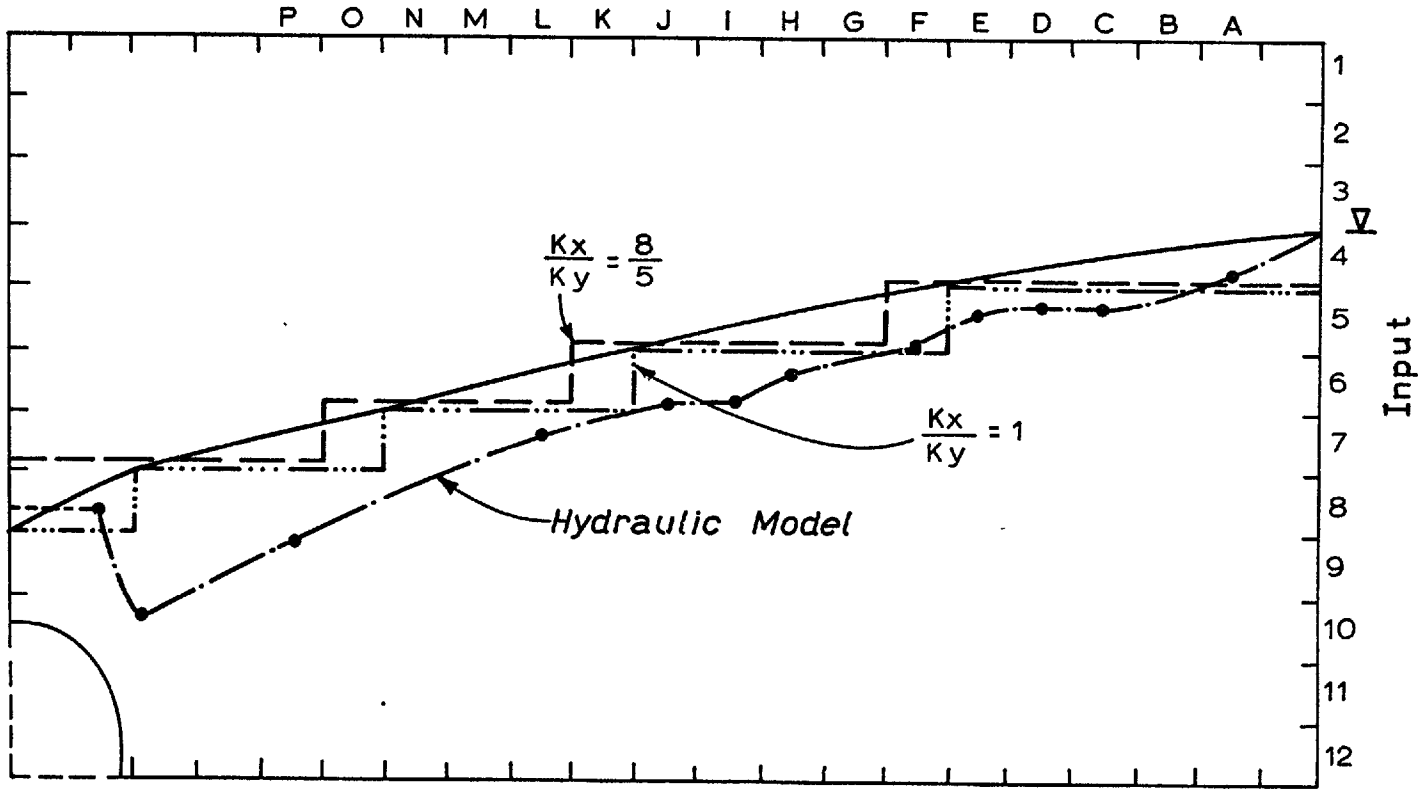

P O N M L K J I H G F E D C B A
1
2
3
4
5
6
7
8
9
10
11
12
Input
Kx/Ky = 8/5
Kx/Ky = 1
Hydraulic Model

FIG. 3.27

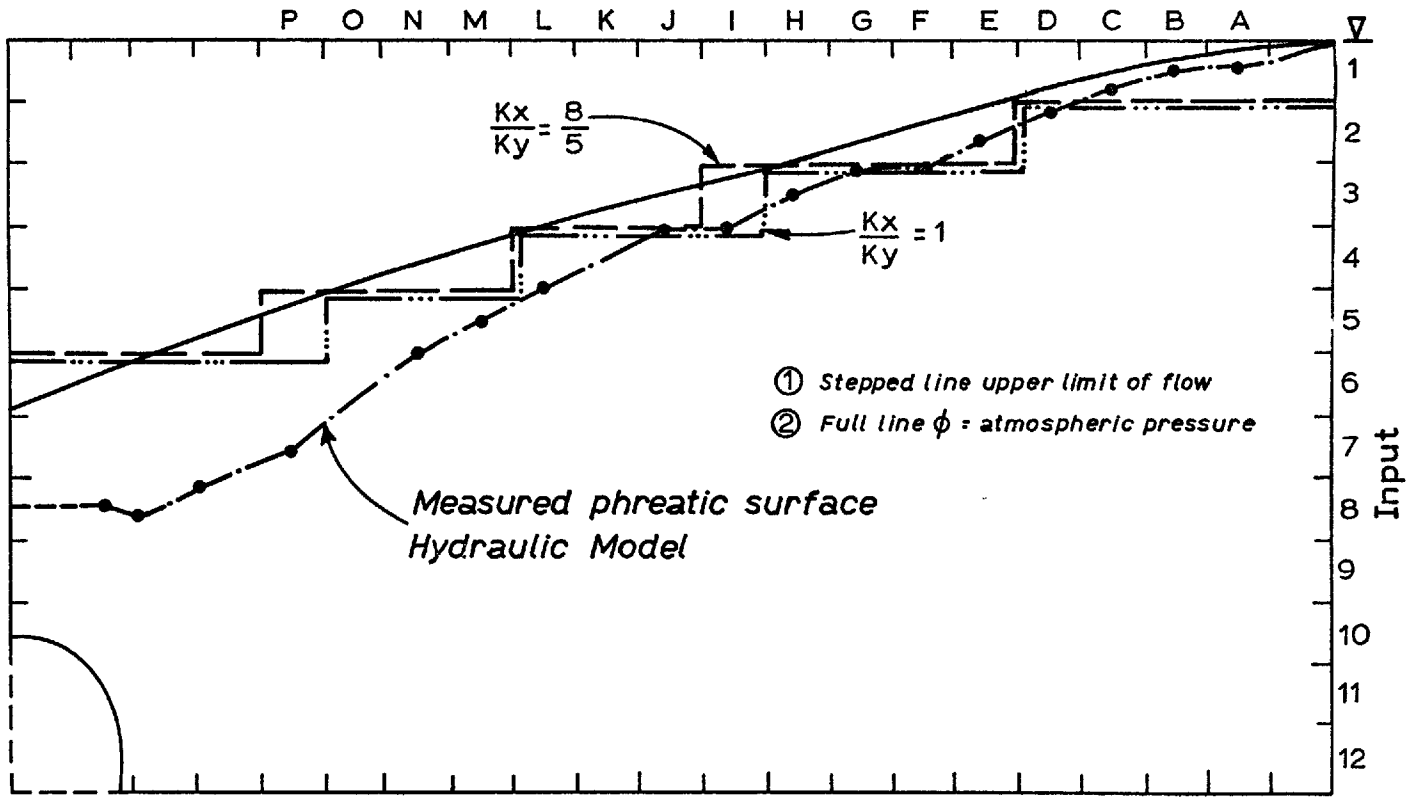

P O N M L K J I H G F E D C B A
1
2
3
4
5
6
7
8
9
10
11
12
Input
Kx/Ky = 8/5
Kx/Ky = 1
① Stepped line upper limit of flow
② Full line ϕ = atmospheric pressure
Measured phreatic surface
Hydraulic Model

FIG. 3.28.

boundary. It is strictly not the phreatic surface but if the dimensions of the problems are large ie. high hydrostatic pressure and close jointing, the error in using the stepped version is small. If, on the other hand, the slope is not too high and with widely spaced fractures, the uppermost flow boundary will not correspond to the phreatic surface. In this case it is suggested that pressures at each node are recorded (in terms of head of water) and a line is drawn joining the top of these pressure lines as in Figs. 3.27 and 3.28. The slight irregularity in the free surface of the hydraulic model is due to the surfaces of the bricks being uneven. As far as the computer solutions are concerned the phreatic surface is represented by either the smooth line or the stepped version which is the uppermost boundary of flow. The free surface is represented in Fig. 3.27 and 3.28 for the isotropic and anisotropic case, the two conditions corresponding with flow either in the plane parallel to the gradient or in the vertical and horizontal directions. The total flowrate in the gallery is given by the sum of the two flows (by superposition). As far as the free surface, there is no rigorous solution to such a problem and therefore the mean of the two free surfaces should represent the phreatic surface.

The numerical solution agrees reasonably well with the hydraulic model, allowing for the fact that the geometry of the hydraulic model is not exact, the flowrate-pressure law is nonlinear and finally the pressure drop due to the kinetic energy has been neglected in the numerical solution. It was shown in the previous section that this difference at a distance equal to twice the radius of the gallery from the bottom left hand corner of the model (Fig. 3.27 and 3.28) the effect of neglecting the losses due to acceleration were as much as 10%. Closer to the gallery in the hydraulic model no measurements were possible, but an example can be considered from the numerical solution.

Prior to examining conditions downstream, let us compare the gradient in numerical model to the actual measured value at the same position.

In section 3.3.4 the measured hydraulic gradient between point 2 and 4 is given by $\underline{J = 0.17}$

From the computer solution the gradient at the same location, point 2 to 4 is given by

$$J = \frac{0.4 \times 2.5 \times 2.54}{4 \times 2.54}$$

$$= \underline{0.25}$$

This agreement is considered to be reasonable since the numerical model is an approximation to the brick model in that the problem is solved by the superposition of two dimensional flow in two orthogonal planes and further in the hydraulic model, the different elements are not strictly homogenious.

Assuming full head at the upstream end the gradient close to the gallery is:

$$J = \frac{5.0 \times 2.5}{4} = 3.1 \text{ (As opposed to gradient of 0.2 upstream)}$$

From Table 2, section 3.3.3

K mean = 32.6 cm/sec

Assuming linear conditions:

$$V = 32.6 \times 3.1 = 100 \text{ cm/sec}$$

$$\therefore \text{ Kinetic Energy losses} = \frac{V^2}{2g} = \frac{100 \times 100}{2 \times 980} = \underline{5.1 \text{ cms}} \text{ Head of Water}$$

Difference between measured phreatic surface and theoretical surface = $\underline{9.7 \text{ cms}}$ Head of Water

The discrepancy between the measured and calculated phreatic surface can be explained in terms of the kinetic energy losses that occur as the fluid accelerates on approaching the gallery.

CONCLUSIONS

The perspex and brick model have proved that the use of simple numerical methods in a discontinua can give reliable answers, provided the inertia effects are small. Having established that it is possible to use numerical methods in such problems it becomes possible to attempt to solve difficult geometries and varying permeabilities with greater confidence. Variation of parameters is very much easier in a numerical study as opposed to a hydraulic model. It will obviously not be possible to model field problems in detail due to the difficulty in obtaining enough input data and therefore, the numerical tool provides a further advantage in being able to vary the input data and then study the influence on either the stability of the structure or the variation in the total amount of flow in a given system.

INTERACTION BETWEEN STRESS AND PERMEABILITY IN JOINTED ROCK.

Synopsis

In jointed rock the relationship between permeability and stress is a non-linear one such that a small change in stress produces a correspondingly very large change in permeability. The deformation of a rock mass is consequently a complex interaction between the solid body stresses and seepage pressures. To date the seepage of water through a network of fissures has been considered as that through non deformable conductors. Analytical expressions describing such a phenomenon are cumbersome and applicable to only simplified cases. It is proposed to use two separate numerical models, one performing the structural analysis and the other calculating seepage pressures, suitably coupled to study the interaction problem.

Seepage pressures as obtained from a non-deformable analysis are compared with those from a coupled analysis for the case of a rock slope. Such a coupled analysis requires certain assumptions about the behaviour of the conductors under normal and shear stresses. Information from published literature is used for the determination of the conductors under normal stresses. An experiment was carried out to get an idea of the change in permeability with shear displacement at low normal stress.

4.1.0 INTRODUCTION

Let us consider flow through a "parallel plate" idealisation of a fissure. For laminar flow from Chapter 2,3.

$$Q = AK_J J$$

K_J conductivity of the fissure
J Hydraulic gradient
A Effective area of flow
Q flow rate

where $K_J = \frac{e^2 g}{12V}$

for unit width of fissure

$$\therefore \quad Q = \frac{e^3 g}{12V} J$$

$$\therefore \quad Q \propto J$$

and $Q \propto e^3$

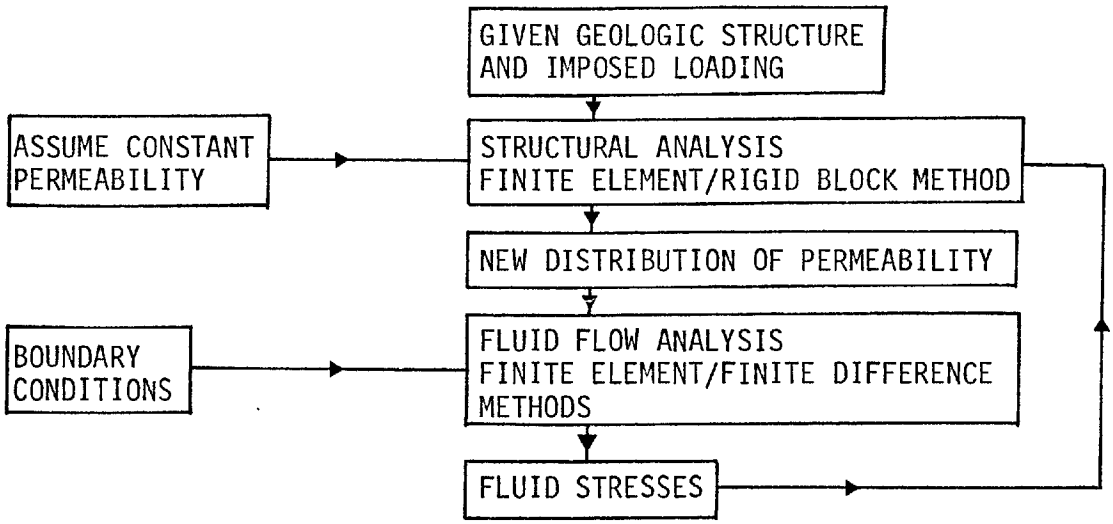
A small change in "e" produces a large change in Q or in J which is related to the uplift forces in a rock mass. On the laboratory scale Bernaix has shown (Chapter 2 part II) how the application of confining pressure in a triaxial cell changes the permeability of fissured rock by three or four orders of magnitude while for an intact specimen there is no appreciable change. In practical terms this suggests that if there is a constant volume of recharge in a fissured rock mass, such as the upstream end of a dam, stress concentrations at the toe of the dam lead to daming up of the water, thereby building up excessive seepage pressure in the area. A further very important implication of consideration of stress and its influence on permeability is that it causes anisotropy in the system. Consequently the analysis of boundary value problems becomes very difficult and often soluble only by numerical methods.

The simple case of the interaction between permeability and stress for a case of parallel fractures with self weight loading has been analytically solved by Snow (33) using continuum mechanics equations. This work was initiated in order to understand the mechanism associated with seismic events which may be caused by fluid injection into deep disposal wells. Owing to the very complex nature of the problem the analytical approach does not constitute a realistic model. Features such as the deformation of blocky nonlinear systems (caused by fissuration) cannot be simulated with such an approach.

4.2.0 INTERACTION MODEL

In order to calculate the deformation of a rock mass under the combined structural and hydraulic loading two separate numerical schemes are suitably linked to calculate stresses and water pressures.

The essential concept behind the interaction model is best described graphically as in Fig.4.1.



COUPLED STRESS FLOW PHENOMENON

Fig. 4.1.

To begin with it is assumed that in a given problem the geological structure is given and so is the imposed loading. Initially a constant permeability is assumed, i.e. no strain in the system. A structural analysis is carried out assuming no water pressures. This analysis can be a continuum or jointed finite element analysis (76) or a rigid block type analysis (34). From such an analysis it is possible to obtain stresses and strains in the system. The strains give new values of permeability which together with the boundary conditions are used in the fluid flow analysis to give a distribution of seepage forces. Once again for this part of the analysis it is possible to use Finite Element or Finite Difference techniques.

Seepage forces are now fed back into the structural analysis of the problem in order to obtain a new loading due to water in the system and consequently new joint closures. With the recalculated values of permeability a seepage force distribution is obtained and fed back into the structural analysis.

This process is repeated until the deformation or seepage pressures converge to a steady value for a further one or two cycles. It is believed that this is the final deformation of the rock mass under combined structural and hydraulic loading.

4.2.1 STRUCTURAL ANALYSIS OF THE ROCK MASS

A vast number of methods are available for this part of the analysis in which the rock mass is treated as a continuum with elastic or non elastic properties and others which take into account the properties of the fractures under imposed loading (76). For the first attempt at the interaction model a continuum model is chosen and is described in detail elsewhere (76). A finite element method is used to analyse the stresses and strains in the model and for ease of computation it is assumed that the rock mass behaves elastically (this however, is not an essential assumption).

Input information for this part of the programme includes the boundary conditions, loading and elastic properties of the rock mass, such as modulus of deformation, poisson's ratio, etc.

4.2.2 FLUID FLOW ANALYSIS

The analysis of seepage pressures is as described in Chapter 3, Part I. A finite difference method is used to solve the distribution of seepage pressures assuming certain boundary conditions and a permeability distribution.For the case of a phreatic surface an iterative technique is used to simulate gravity. For complex fissure systems it is perhaps easier to use the finite element method (61). The interaction or coupling of the two numerical methods becomes easier if both the methods are similar.

4.2.3 LINKAGE OF THE TWO NUMERICAL SCHEMES

In order that the two numerical schemes can be linked it is important that the two grid systems are compatible.

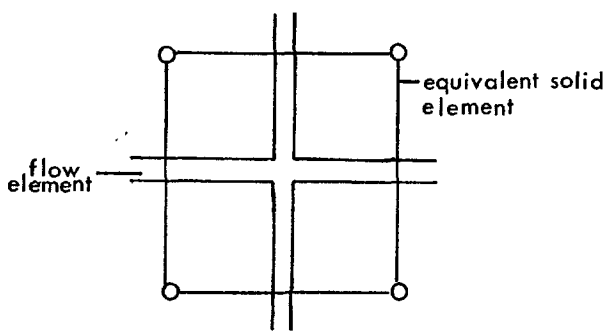


FIG 4.1

In the subsequent analysis that is going to be carried out the finite element method in the structural analysis was successfully linked to the finite difference fluid flow analysis by St. John (76). Fig.4.1 shows the equivalent solid element and the fissure system each with its own numbering and grid system. In the fissure system the forces are transmitted from within the fissure to the continuum structural element through the nodal points as shown in Fig.4.2.

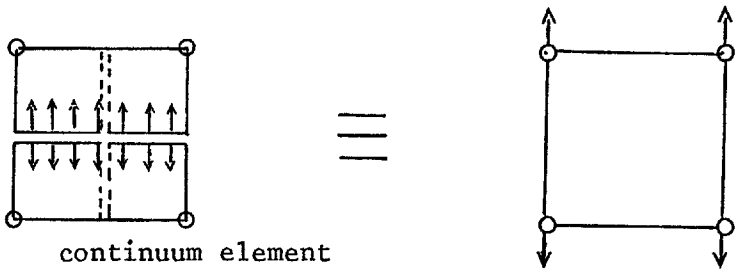


FIG 4.2

4.2.4 DETAILS OF THE ROCK SLOPE MODEL

Fig.4.3 shows the boundary conditions, size, elastic constants etc that were used in the model.

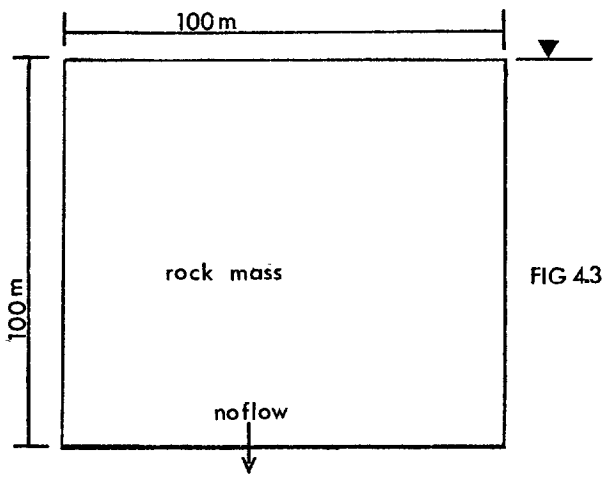
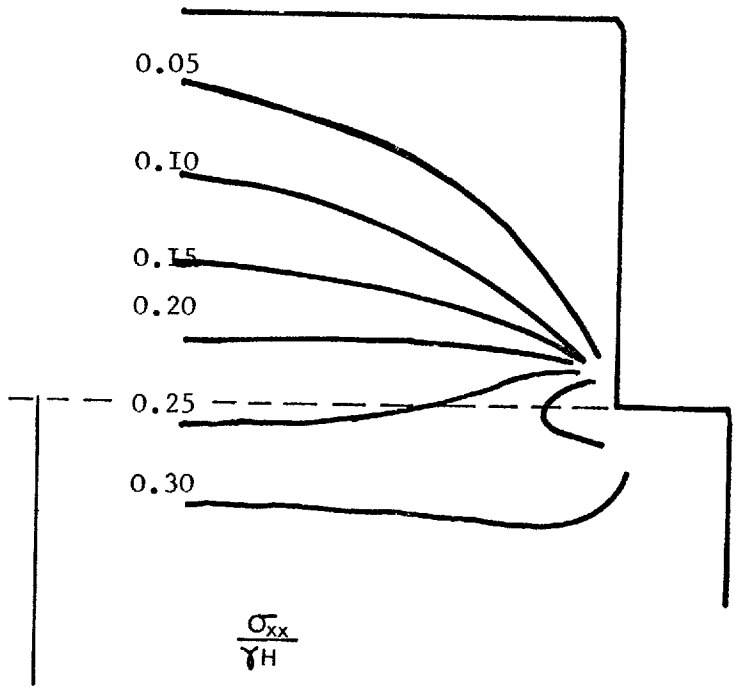


FIG 4.3

Compression modulus	=	1000 kg/cm^2
Poisson's Ratio	=	0.2
Compression mod of fissure	=	500 kg/cm^2
Initial fissure opening	=	0.1 mm.
Height of model	=	100 metres
Width of model	=	100 metres
Joint spacing	=	5 metres.



Impermeable base of flow model

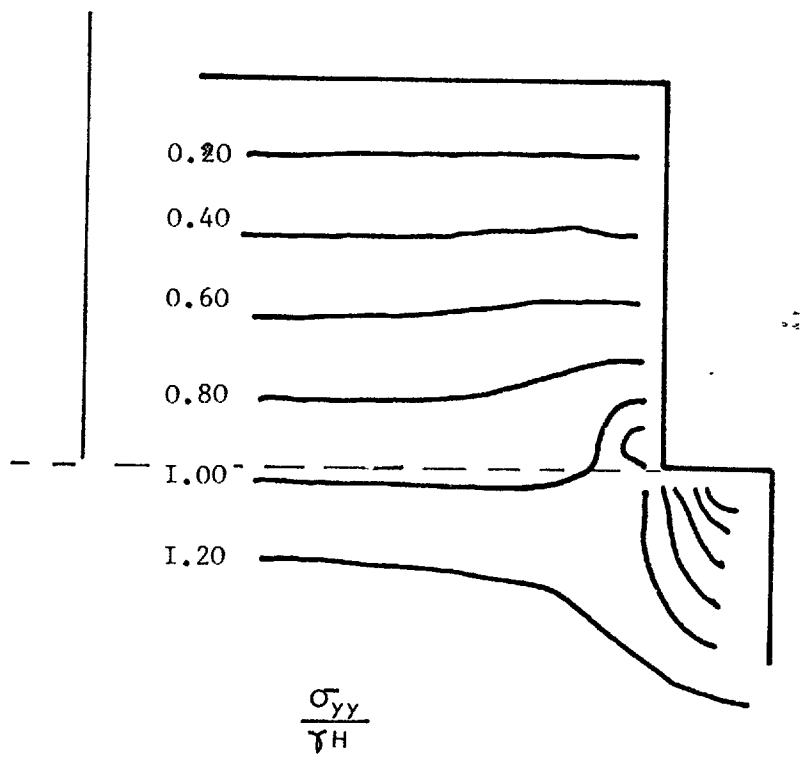
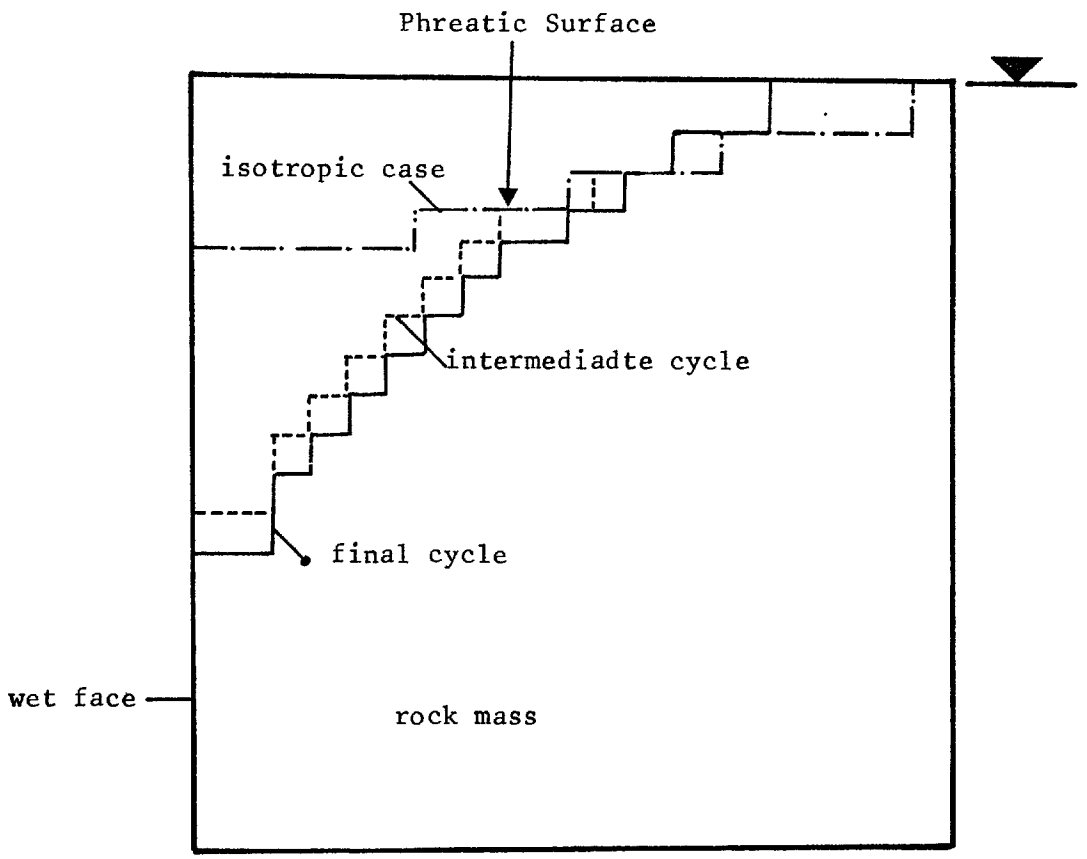


FIG 4.4



Interaction model

FIG 4.5

4.2.5 RESULTS OF ANALYSIS

In section 4.2.0 the flow chart for the interaction model shows how the first step of the calculation is to determine the stress distribution without water. Fig.4.4 shows the result of a typical stress distribution in such a case where the contours are non-dimensionalised. It is interesting to note that the influence of the toe in as far as stress concentrations are concerned is very localised and unlikely to cause any damming up of water, on a large scale.† In effect as a result of excavation the slope heaves outwards.

During the first cycle of the calculations for seepage pressures it is assumed that the permeability in the model, as in Fig.4.3 is constant everywhere and given by:

$$K_J = \frac{e^2 g}{12V}$$

e = aperture of the fissure = 0.1mm.
g = gravitation constant
V = kinematic viscosity

Initially it is assumed that the entire model is submerged under water. The effect of this is one of buoancy, fluid pressures being a function of depth. These seepage pressures are fed into the structural analysis so that new deformations based on effective stress are computed. These stresses produce new strains and consequently a new distribution of permeability. The fluid flow analysis is now carried out with these values of permeability and the original boundary conditions.

This time, however, the phreatic surface is calculated iteratively. The result of such a calculation is new seepage pressures. This process is repeated until convergence is obtained. In Fig.4.5 the phreatic surface can be seen during an intermediate cycle until it finally settles down to a position from which it does not change with further cycling. In this particular problem it was found that the solution converges after three intermediate cycles.

Also in Fig.4.5 is plotted the phreatic surface for the case of flow through the model assuming that the conductors are non deformable (marked isotropic flow). It can be seen from the model that the phreatic surface for the deformable model is much lower than the isotropic case. This indicates lower seepage pressures in the system or better drainage. The effect of water is to heave the model up and to the left as a result of which the fissures open up increasing the drainage of the rock mass.

† This ofcourse assumes that there is no impervious boundary near the base of the excavation.

In this particular model the change of permeability with shear displacement is ignored because it is not certain what the relationship is, short of knowing that a joint dilates during shear.

4.3.0 EXPERIMENT TO OBSERVE CHANGE IN PERMEABILITY WITH SHEAR DISPLACEMENT

It is not possible to carry out measurements of permeability in the 50 ton shear machine at Imperial College. It was therefore decided to carry out an initial test on a very simple experimental set up. The test was performed at a low normal stress and this eliminated the need for a complicated loading system. The choice of low normal stress was made to be consistent with the evidence put forward of the existance of low stresses that are found in rock slopes (34, 76).

4.3.1 TEST SET UP

The shear box is made out of 1" thick perspex and the sample is housed in the middle as shown in a schematic sketch, Fig.4.6.

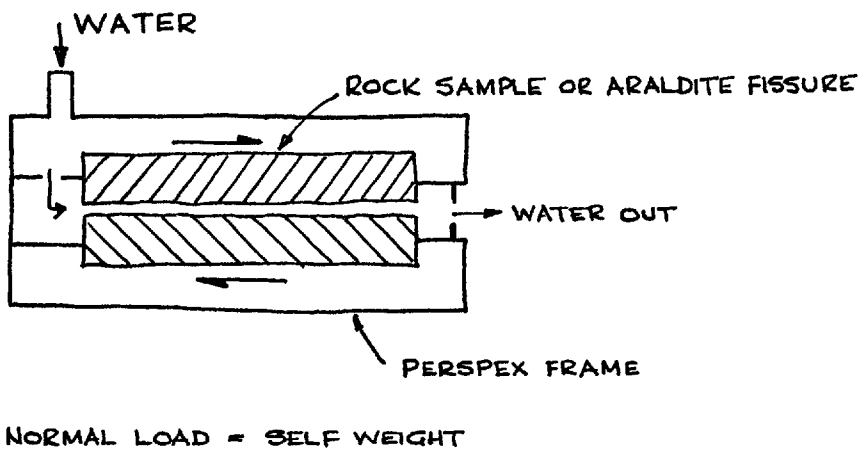


FIG 4.6

The sample used for the test was a 25 sq.in. slab of slate which was split along a cleavage plane. The two halves were mounted carefully as in Fig.4.6. The first permeability measurement was made at zero shear displacement, i.e. when the two halves of the sample fitted each other and although there was a small gap to allow fluid flow through it, the vertical displacement was assumed to be zero. The sample was sheared along the direction of lineations.

4.3.2 Results

Permeability measurements were made at shear displacement intervals of approximately 0.2cm. Fig. 4.7 shows the result of the experiment where for a shear displacement of 1cm. the permeability has changed from approximately 10^{-2} cm/sec. to 1 cm/sec., the dilatation due to the shearing being just under 0.2cms. This experiment illustrates how the permeability changes substantially with shear displacement. This phenomenon must play a part in the progressive failure of a slope, for example, where excessive pore pressures cause sliding of the rock mass along discontinuities and a result of the movement the rock drainage increases, possibly thereby stabilizing the system for such a time when the pore pressure builds up again, to cause further movement. The experiment illustrates the importance of the change of permeability with shear displacement and it is suggested that more controlled tests in terms of stress application should be carried out to study this phenomenon.However, in reality it is expected that the change in Permeabity may not be as large as shown in Fig 4.7 since (a) even at low normal stresses the dilation is less than at zero normal stress and (b) fines develop which may block the fissures thus reducing the effective aperture.The increase in permeability is likely to be higher in hard rocks than in soft rocks like schists.

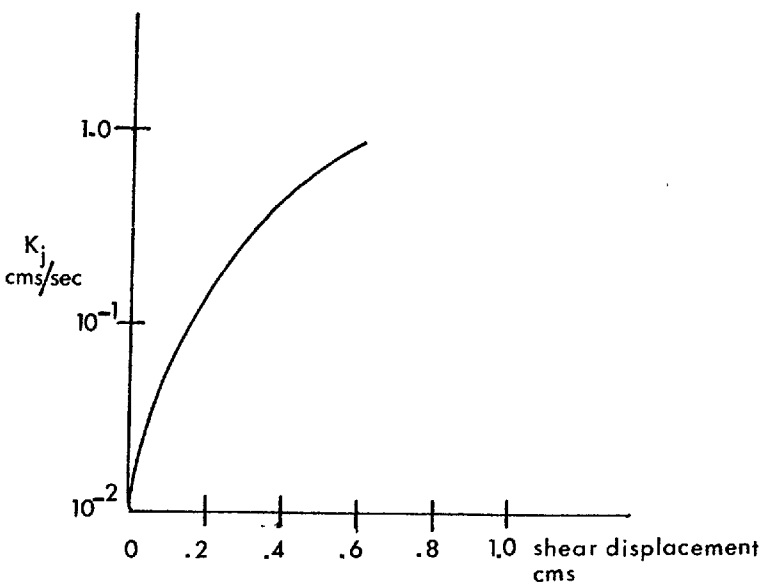


FIG 4.7

CONCLUSIONS 4

The strong interaction between stress and permeability in fissured rock is an extremely important phenomenon which has been ignored so far and is just beginning to attract attention. This is largely due to the fact that the equations of state of this combined phenomenon have not been formulated or solved and the problem is soluble only by coupling two numerical schemes iteratively until convergence is achieved. The linkage of the flow programme to the jointed rock mass analysis of St. John (76) and Cundall (34) will provide further very interesting insight into the deformation of fissured rock under the combined structural and hydraulic loading. A preliminary analysis of a rock slope shows the vast difference in the seepage pressure distributions. As a result of the interaction programme it can be seen that a slope has a much higher drainage than postulated by the rigid element analysis of Louis (8) and Sharp (9).

It is felt that in the case of a dam foundation where both the stresses and hydraulic gradients are high (unlike slopes) this effect will be even more pronounced. The interaction problem needs much more detailed evaluation especially the practical aspects where little is known about the change in permeability of fissures with normal and shear stresses. An attempt has been made to stimulate further interest in this area and it is hoped that more results will become available in the near future.

PART 2

INTRODUCTION TO PRESSURE TESTING IN ROCK

SYNOPSIS

A brief historical introduction of flow from or into a cylindrical cavity is provided so that some sort of perspective can be gained into the present state of knowledge - and consequently, current practice. Quite often the assumptions behind a theory are forgotten in practice and the unreliability of the test results is blamed on the inaccuracy of the method. Recent research obviously follows the historical development of the subject and before considering any further research it is important to know which areas have been studied or are at present being looked at by Engineers interested in the flow of fluids through fissured media.

1.1.0 FIELD OF APPLICATION

The study of flow of water through soils and rocks illustrates the principle of the university of modern sciences. It is here the hydrologists, geologists, meteorologists, engineer and agronomists overlap in their activities. As a result of this diversity, the approach to the problem has been extremely varied, from the very practical approach of the farmer, through the descriptive mode of the geologist and the semi-empirical approach of the engineer to finally, the rigorous solutions sought after by the applied mathematicians. However, the complexity of the problem has even lead a genious like Leonardo da Vinci to comment "that water flows from the vast depths to the mighty ocean in the deep caverns that lie hid within the bowels of the earth, whence, through the spreading veins upwards against its natural course, incontinual assent to the high summits of the mountains, it returns through the burst veins to the deep".

1.2.0 HISTORICAL DEVELOPMENT

It was as early as 1848 when the French eingineer Dupuit (1) developed the theory of filtration to be soon followed by Darcy (2) in 1856. It was, however, Dupuit who calculated the flow of water into wells in unconfined and confined acquifers. Shortly afterwards in 1886 Boussinesq (3) and Zhukorskii (4) developed equations and solutions to three dimensional, nonhomogenious and time dependent problems with simple boundary conditions.

It was not until 1955 that any serious interest was shown in fluid flow through fissured media (4). At the same time a paper of considerable interest was published by Baker (5).

Baker considered the case of axisymmetrical flow of water in a fine fracture towards a cylindrical cavity. Model tests on a fissure proved that analytical solutions based on a parallel plate model could be used to describe flow within the laminar regime. Further, he was the first person to demonstrate the large volume of fluid that could flow within a fissure compared to an unfissured formation. For example, a single fissure with an aperture of 0.01 inch is equivalent to 454 feet of infissured formation having a uniform permeability of 10 millidarcys or 10^{-3} cm/sec. Another important conclusion in Baker's paper is that the pressure drop within close proximity of the hole, as a result of flow into or from a hole, is extremely severe compared to the case of a porous media. In the case of a 1 mm aperture fissure, Baker shows that 80% of the pressure drop takes place within a foot of the hole. In the case of a pumping test in fissured media this obviously proves that it is the aperture of the fissure within the 'confines' of the hole that determines the flow capacity under a given applied gradient.

Polubarinova-Kochina (6) summarizes a vast amount of work which has been done by Russian Engineers and gives detailed solutions to a large class of problems of fluid flow through porous media. The approach used is that fractures occur randomly and if the correct scale is sued to analyse problems, continuum mechancis equations can be applied as in a porous medium. However, an essential difference is made in the case of fractured media. The medium is given two distinct permeabilities; primary permeability to the intact material and secondary permeability to the fissures; the secondary permeability, obviously, being much greater than the primary permeability. Navier-Stokes equations are now applied to a medium where there are two pressures; i.e. pressure in the pores and in the fissures, taking into account the transfer of liquid from the pores into the fissures. Solutions are thus given for certain specific problems of non-steady state seepage in a fissured rock. Although the derivations are extremely rigorous within themselves and a feat in Applied Mathematics they cannot be easily applied in Civil Engineering or Mining problems for two reasons. The first one is that very often the fracture systems have some form of symmetry, e.g. sedimentary environments, and also the degree or intensity* of fissures is comparable to the size of structure under consideration. Therefore mean characteristics, whereby the averaging is carried out on a scale which is large compared to the dimensions of the individual blocks, is inadequate. Secondly the transfer of fluid from the porous media into the fractures takes place so slowly, if at all, because the input boundaries of near surface strctures are probably directly connected to the fissure systems, e.g. during a pumping out test in a saturated fissured rock mass water would be transmitted from the fissures directly to the cavity at relatively low pressures, making it impossible for water within the intact material to move towards the fissures sufficiently quickly to maintain a high constant flowrate.

In 1965 Snow (7) presented a theory of flow from a cylindrical cavity into a jointed media. Snow begins his hypothesis on the basic assumption that a fissure in a rock mass can be represented by an equivalent parallel plate model. He further assumes that the flow within such a parallel plate will stay laminar under all conditions.

Individual fissures or fissure sets can have any orientation in space and they have different apertures and spacing. If a hydraulic gradient is applied to such a medium, the direction of flow does not necessarily follow the same direction. Such a flow is termed anisotropic flow. The anisotropy in the medium is a result of the strctural skeleton of the conducting elements and their individual apertures. However, such a medium

Degree or intensity applies to the spacing between fissures in this thesis

has principal values of permeability and also principal directions of flow. Snow presents the equations of fluid flow from a cavity in such a medium in a tensoral form. This approach makes the three dimensional nature of the problem easier to appreciate and manipulate mathematically. Snow's main conclusions were that in a parallel plate model the discharge is proportional to the cube of aperture and consequently in a fissure system with coarse and fine fissures the coarse ones will dominate the discharge. Anisotropy could be a result of orientation, spacing between fissures, varying apertures and due to surface texture such a foliation of rock fabric, and lastly, Snow proposes that statistical techniques can be used to predict the fissure frequency and apertures from standardised pressure tests in a borehole. Snow's method can solve a large number of problems adequately provided that that the fracture frequency is high enough with respect to the scale of the test and the fracturing is apparently random.

A vast amount of very interesting analytical and field experience is available in the Oil Industry on fluid flow through heterogenious reservoirs. These studies have ranged from investigations of behaviour of wells near faults to performance of wells in naturally fractured reservoirs. For example, methods exist whereby the distance to a fault can be very accurately determined by a pressure build up test (39). Pollard (40), Warrent and Root (41) Odeh (42) have all considered the flow of fluid, in a naturally fractured reservoir, towards a well. Essentially, the above analyses are numerical solutions to Navier Stokes equations assuming a slightly compressible fluid. Idealisations are made of the fracture systems prior to the application of numerical methods. A typical plot from a pressure build up test is one of log pressure v time. The result is in the form of three straight lines, each with a different slope indicating the pressure build up within close proximity of the well, the coarse fissures and the fine fissures. In view of the vast importance of the Oil Industry in Economic terms a large number of controlled experiments have been carried out and proved to be useful. However, the use of existing methods in Civil Engineering and Mining is not really possible because of a fundamental difference in one of the assumptions. Owing to the great depth at which petroleum work is carried out, all the methods assume that the fluid is slightly compressible under large stresses. It is this factor which gives the time dependents to the equations of flow. In the majority of civil engineering problems the water is assumed to be strictly incompressible and if there is a time dependence in the test it is due to changing boundary conditions.

1.3.0 CURRENT PRACTICE

Prior to the introduction of the Lugeon test, all field tests were carried out in wells and open holes. To obtain representative parameters for filtration of water through a soil or rock mass, either the well was pumped out in which case the flow rate and pressure in the well together with the drawdown in surrounding holes was observed, or water at a known rate was pumped down a hole and the subsequent changes of the water level observed. With the advent of large civil engineering structures on soils and rocks the need for a better test was felt and the Lugeon test emerged. A Lugeon test consists of pumping water into the rock mass between two inflated packers in a borehole, Fig 1.1. Water is subsequently pumped into the hole at a standard pressure of 10 Kg/cm^2 and the corresponding flow rate measured. A Lugeon is defined as a flow of 1 litre/metre/minute at an excess pressure of 10 Kg/cm^2.

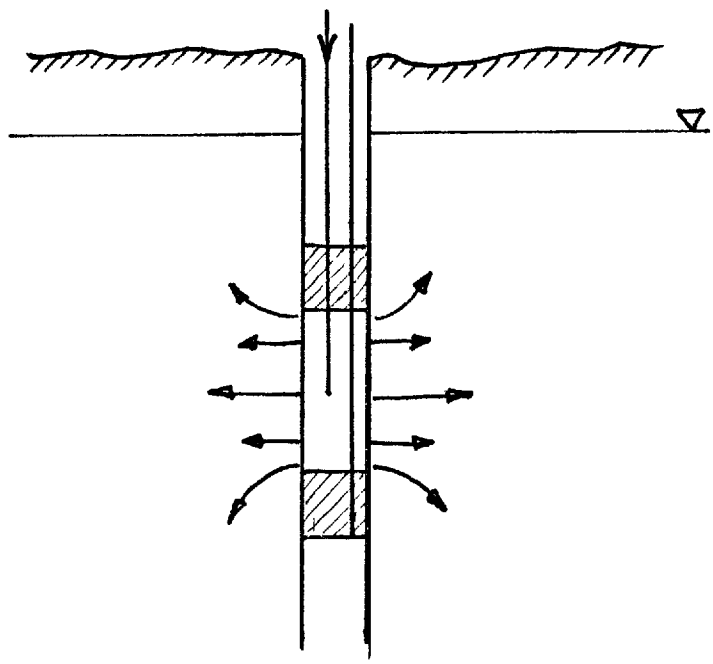


FIG 1.1

A rock mass is grouted if it's absorbtion of water is greater than one Lugeon (32). This criterion is based on experience in the civil engineering industry. The test is well over 50 years old and is still used in its original form in a large number of projects. In order to examine its validity, the assumptions of a Lugeon test must be very clearly stated.

(a) An acquifer of infinite extent
(b) Homogeneous and isotropic conditions
(c) Steady state conditions
(d) Relationship between pressure and flowrate is linear (Darcy's law)
(e) Inertia terms negligible
(f) No communication between the packed off section and the remainder of the hole

These assumptions lead to a relationship between pressure and flow rate as follows

$$Q = \frac{2\pi L K (P_1 - P_2)}{\log_e (r_2/r_1)} \qquad (1.1)$$

Q = Flow rate cm^3/sec

L = Length between packers in cms

K = Permeability cm/sec

P_1 = Pressure at the hole in cm of H_2O

P_2 = Pressure at radius r_2 in cm of H_2O

r_1 = Radius of hole, cms.

Unfortunately, equation 1.1 has been used rather indiscriminately - i.e. without fulfilling the assumptions. In most soils this equation gives reasonable results, if the distance between the packers is kept large. This, in fact, implies that any small internal variations in permeability are statistically swamped. However, even the most optimistic soils engineer finds it difficult to establish conditions (a) and (b) in the field. There is remarkably little information on the comparison of permeability values of the same medium as obtained by different methods. Moser (11) has carried out very extensive laboratory tests. In the laboratory using a homogeneous material such as sand he has been able to correlate successfully different methods of determining permeability. However, in the field this has proved virtually impossible. The difference in permeability of a saturated soil as determined by a pumping out test and two different tracer tests is greater than 50%. The two different tracer tests were (a) transit time method and (b) Point dilution method (11, 10).

Both the tracer tests gave consistent results while the pumping test lead to a smaller value. This difference is attributed possibly to the factors (a) to (f) not being fulfilled. Childs (12) after a very exhaustive account of permeability measurements in the field concludes that the methods are difficult and subject to considerable errors: "Some of the objections reported are associated with genuine difficulties of soil properties, such as

instability which makes it impossible to maintain a borehole or cavity of known dimensions. Some, however, are the result of an inadequate appreciation of the nature of hydraulic conductivity as a statistically averaged soil property". It is this last factor which has contributed most to serious errors in the measurement of fissured rock mass permeability.

If a pumping test is carried out in a fissured medium it is important that the above assumptions are kept in mind. Since deviations from these assumptions are more likely (8, 10) in a fissured rock mass than in a soil they will be discussed in subsequent chapters in this part. Because of the diverse nature of a rock mass it is difficult to generalise on remedial measures and therefore where possible, special cases will be put forward and discussed.

1.4.0 RECENT RESEARCH

The assumptions outlined in Section 1.3 have been examined more recently by Snow (15) for the case of a fissured rock mass. A method of analysis is proposed and examples worked out for the case where the three principal permeabilities and their directions can be worked out from a three-borehole test (mutually perpendicular) arbitrarily oriented in space. This method is extremely powerful if the rock mass is heavily fractured and the spacing between fractures is small. In a further paper Snow (43) has used data from pumping tests to obtain an estimate of average spacing and average apertures of water conducting fractures in undisturbed rock masses. This work is supported by complex statistical techniques in the hope of generalising the method.

Sharp (9) has considered the flow of water from a cavity into a homogeneous fissure system, one in which the fissures are equally spaced. The influence of increasing the test section length on the pressure-flowrate relationship are considered. If the test cavity is small compared to the depth of the impermeable boundary the flow from it is spherical. In a two dimensional system, for example, this means that the permeability value is a mean between the permeability in a direction parallel and the one at right angles to the cavity. Sharp demonstrates that by increasing the length of the test section, flow becomes cylindrical and therefore the predominant flow is in a direction at right angles to the cavity. In this way a test becomes directional and in the context of a fissured rock mass, more meaningful. These studies have been carried out by him on an analogue and also on a digital computer. Another important aspect of this research is that the pressure drop within the vicinity of the borehole is significant (80%) due to the limited cross section area which is available for water to flow out of a

hole. Sharp reports that a variation of conditions at some distance from the hole makes little change in the pressure-flowrate relationship. Conversely it is the area close to the hole that controls the response of the rock mass to the test.

Another important assumption which has been considered recently is validity of the linearity between flowrate and pressure. In a recent paper by Trollope et al (13) this aspect of flow behaviour has been tested rigorously. Although this work was carried out on crushed granite aggregate (3/16" size) the Reynolds number is very similar to that in fissures. However, for such high velocities as they have measured they propose the use of the Forchheimer relationship between flow and pressure. In the case of a confined axisymmetric flow into a well the Forchheimer relationship gives a flowrate which is well within 1% of the measured flowrate. The Darcy approach however, leads to an error of well up to 20%. Baker (5) evaluates the importance of non-linearity and the subject is considered by others (9, 10).

EQUATIONS OF MOTION OF FLUIDS

SYNOPSIS

In this chapter equations are derived for the axisymmetric flow from a cavity into a fissure system. These equations are for laminar and turbulent flow and it is assumed that the tests are performed in an infinite aquifer. Methods are provided to deal with the case of anisotropic flow. The influence of a three dimensional fissure system on such a test is discussed. Reasons are put forward for the substantial amount of space given to axisymmetric problems in view of the possibility of three dimensional flow.

2.1.0 AXISYMMETRIC SEEPAGE

It is proposed that equations of motion of a fluid are developed for the case where pumping-in of a fluid takes place. The following assumptions are made:

(a) Fissure of infinite radial extent (SINGLE FISSURE).

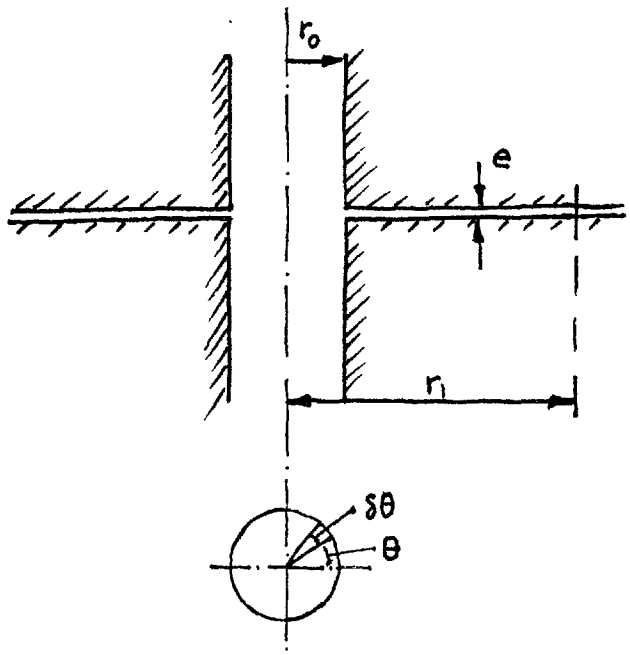
(b) Linear Flow Law.

(c) Radial Flow, ie. equipotential lines are circular - isotropic in fissure plane.

(d) No inertia effect as a result of acceleration of fluid.

(e) No influence of secondary fissures, parallel to the hole, eg. no influence of gravity.

Note: This special case of a fissure at right angles to the borehole is considered to make the mathematics simple and clear. Influence of gravity, as would be the case in an inclined joint, is simply allowed for by linearly superimposing the gravitational component g.sind to the gradient (see Ref.10).



Consider Fig.2.1 using polar coordinate system:
Darcy's Law applied to a parallel plate model

$$V = K_J \frac{\partial P}{\partial r} \qquad (2.1)$$

where K_J = joint permeability
V = mean velocity
e = mean opening

The flow from a cavity into a fissure is

$$Q = 2\pi re.\bar{V} \qquad (2.2)$$

Substituting 2.1 into 2.2 and integrating gives

$$\frac{Q}{2\pi re} = K_J \frac{\partial P}{\partial r}$$

$$\int_{r_o}^{r_1} \frac{dr}{r} = \int_{P_o}^{P_1} \frac{2\pi e}{Q} K_J \, dP$$

$$\log_e \left(\frac{r_1}{r_o}\right) = \left(\frac{2\pi e}{Q}\right) K_J (P_o - P_1)$$

$$\therefore \quad Q = \left\{ \frac{2\pi e K_J}{\log_e \left(\frac{r_1}{r_o}\right)} \right\} (P_o - P_1) \qquad (2.3)$$

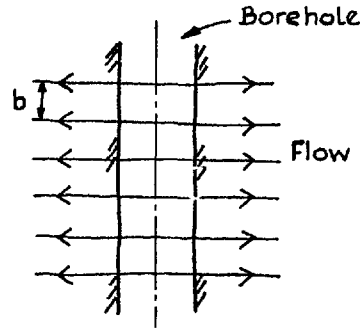
2.1.1 INFLUENCE OF FISSURE FREQUENCY IN DIRECTION ORTHOGONAL TO BOREHOLE.

If within a given test section the fracture frequency orthogonal to the hole is considered as regular, ie. the spacing between joints is constant, equation 2.3 is very simply modified to the following, by the principle of superposition:

$$Q = \left\{ \frac{2\pi e n K_J}{\log_e \left(\frac{r_2}{r_1}\right)} \right\} (P_o - P_i) \qquad (2.4)$$

where n is the number of fissures.

In such a case, it now becomes possible to use the term equivalent permeability if the fissures are identical in aperture.



If we consider flow from a borehole into a set of fissures, the discrete element approach gives us the flowrate as:

$$Q = \left\{ \frac{2\pi e n K_J}{\log_e \left(\frac{r_i}{r_o}\right)} \right\} (P_o - P_i) \qquad (2.5)$$

where K_J is the fissure permeability.

Using the continuum concept, for the same problem

$$Q = \left\{ \frac{2\pi b n K_s}{\log_e \left(\frac{r_i}{r_o}\right)} \right\} (P_o - P_i) \qquad (2.6)$$

where K_S is the system permeability.

Since flow is the same in both cases : $e K_J = b K_S$

$$\therefore \quad \frac{e}{b} K_J = K_S \qquad (2.7)$$

An alternative way is to use L, the test section length instead of bn

$$\therefore \qquad e K_J = \frac{L}{n} K_S$$

However, an important class of problems exist, ie. most practical cases, where the distribution of fissures is random with respect to the hole or alternatively they occur in clusters. In this case, it is essential to find out the scale on which the pumping test results are going to be used in a subsequent analysis (10).

If the information from a pumping-in test is going to be used to determine the fracture frequency as proposed by Snow (7) then some form of statistical evaluation might prove to be fruitful. However, if the results are going to be used for computing leakage from under a dam or pressure distributions in a rock slope some other form of method will have to be adopted.

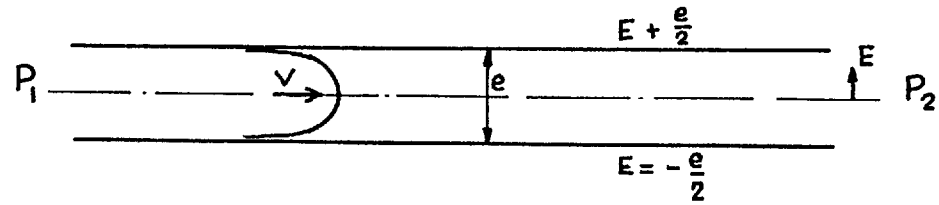
In the ideal case, the problem can be solved by splitting up the area of interest in discrete zones of different fracture frequencies, information of the frequency being obtained from geotechnical logging. These different zones would then be tested individually using the correctly scaled packer spacing (discussed elsewhere) and values of permeability assigned to these zones. In this way, a model could be made up of the area, and leakage, and pressure distributions could be calculated using numerical methods.

Unfortunately, the ideal case where such zones can be delineated by the geologist is far from being practical and also the variable packer spacing type of test demands a technology which has not arrived yet in commercial projects. If a case occurs where the packer spacing is fixed and clustering occurs in the test section, either the spacing b is recalculated as a geometric means from all the values of b to obtain equivalent permeability or alternatively, the concept of equivalent permeability is dropped completely in favour of equation (4) in which case eK_J can be calculated per joint and this information fed into the numerical model. This topic will be dealt with in detail in the chapter on Field Testing.

EFFECT OF INERTIA IN A LINEAR SYSTEM

Consider the case when a large amount of water flows through the pipe and down the hole where it enters the packed off section. Passage of water now changes from a circular smooth tube to either one or many very fine fissures. This process results in a sudden acceleration of the fluid and consequently, a change in kinetic energy. In order to estimate the influence of this phenomenon it is proposed to treat a fissure as a parallel plate model.

This is done because calculating kinetic energy assumes a knowledge of the velocity profile. In the laminar case it is assumed that the velocity distribution is parabolic.



At any point F from the axis the velocity is given by

$$V = \frac{(P_1 - P_2)g}{\mu L}\left\{\frac{e^2}{8} - \frac{E^2}{2}\right\}$$

where μ is Kinematic Viscosity & P_1 and P_2 are pressures
the mean square of the velocities

$$(V^2 m) = \int_{-e/2}^{+e/2} \left(\frac{\frac{e^2}{8} - \frac{E^2}{2}}{e}\right)^2 dt \cdot (P_1 - P_2)^2 g^2 \frac{1}{\mu^2 L^2}$$

$$\therefore (V^2)m = \frac{(P_1 - P_2)^2 e^4 g^2}{120 \mu^2 L^2} \qquad (2.10)$$

the drop in pressure due to change in KE

$$P_K = \frac{1}{2g}(V^2)m$$

units of P_K = Cms/head of water

substituting Eq.2.10 in the above

$$P_K = \frac{(P_1 - P_2)^2 e^4 g^2}{240 \mu^2 L^2 g} \qquad (2.11)$$

Poiseiulles law for parallel plate model is

$$V_m = \frac{e^2 g}{12\mu}\left\{\frac{\Delta P}{L}\right\} \qquad (2.12)$$

Substituting (4) in (3)

$$P_K = \frac{3}{5g} V_m^2 \qquad (2.13)$$

For radial flow the friction or inertia loss is given by (5)

$$P_k = \frac{3Q^2}{20\pi^2 e^2 g}\left\{\frac{1}{r_1^2} - \frac{1}{r_o^2}\right\} \qquad (2.14)$$

where r_o = radius of hole
r_1 = radius at which pressure has dropped to minimum value

Thus equation 2.14 represents this loss of energy, due to sudden acceleration. For the case of n fractures

$$P_{Kn} = \frac{3Q^2}{20\pi^2 e^2 n^2 g}\left\{\frac{1}{r_1^2} - \frac{1}{r_o^2}\right\} \qquad (2.15)$$

Eq.2.15 can be simplified to the following expression:

$$P = \frac{CQ^2}{e^2 n^2}$$

where C is a constant

For a given Q if the size of fissure is reduced the denominator becomes small and therefore the KE loss terms becomes very large. This expression should be incorporated into the original equation for estimating the permeability.

A hypothetical example illustrates the point and also the importance of the aperture in such a test. Assume a pressure test with 20 fissures - discharge 20 litre/min. r_o = 1.5inches, r_1 = 120inches.

For a fissure system with apertures of 1mm P_{Kn} = 0.025 cm.head of water.
1/10mm P_{Kn} = 2.5 cm. head of water.
1/100mm P_{Kn} = 250 cm. head of water.

The relationship between flow and pressure now becomes for the linear laminar case:

$$P = \frac{Q \log_e (r_1/r_o)}{2\pi K_J n} + \frac{3Q^2}{20\pi^2 e^2 n^2 g}\left\{\frac{1}{r_1^2} - \frac{1}{r_o^2}\right\}$$

or very simply

$$\therefore P = AQ + BQ^2 \qquad (2.16)$$

However, it was found in the field trials that the term BQ^2 is very small and can be ignored in general. If in a field evaluation the pressure-flow curve is non linear, it is advisable to calculate BQ2 before proceeding on to apply a non-linear flow law.

THE USE OF NON LINEAR PRESSURE-FLOW LAW

Numerous pressure-flow laws exist for the case of turbulent flow. The most general of them being the Forchheimer law and the Miessbach law (13). For these calculations the latter of these two is adopted. The reason for this choice is that it is easier to manipulate mathematically the Miessbach law to fit equations of motion of a fluid either from or to a cavity in a discontinuum model. It is interesting to note that the field data of Pressure v Flowrate fits the Forchheimer Law extremely well. However, the extraction of the generalised permeability factor from a radial test is a bit cumbersome if the Forchheimer law is used. Miesbach law for flow in a parallel plate model is given as:

$$(V_m)^n = C \frac{\partial p}{\partial r} \qquad (2.17)$$

where n is the degree of non-linearity and its value lies between 1 and 2. When n = 2 flow is generally assumed to be fully turbulent. C is a constant which depends on the medium and the viscosity of the fluid that is used. Various people have worked on what this value C is in terms of pipe flow. Louis (8) has done considerable model work on planar conductors, both rough and smooth to further define C in terms of roughness, degree of separation, angularity of the asperities in a fissure etc. And in each case this definition is bound up with Reynolds number. While this work is important in so far as research is concerned into the relationship between the aperture obtained from a non linear test to a linear one, it is felt that in practice, no further definition of C is essential as it is a parameter that will be determined experimentally in the field anyway.
Let us assume that

$$\text{Mean velocity} = V_m$$

the flow from or into a cavity in a single fissure system is

$$Q = 2\pi r e V_m \qquad (2.18)$$

r is radius at any point
e is effective opening of the fissure

substitute Eq.2.17 into Eq.2.18.

$$\left\{\frac{Q}{2\pi r e}\right\}^n = C \frac{\partial P}{\partial r}$$

$$\int_{r_o}^{r_1} \frac{\partial r}{r^n} = \frac{C(2\pi e)^n}{Q^n} \int_{P_o}^{P_1} \partial P$$

$$\left\{ \frac{1}{r^{n-1}} \right\}_{r_o}^{r_1} = \frac{C(2\pi e)^n}{Q^n} (P_o - P_1)$$

$$\frac{1}{r_o^{n-1}} - \frac{1}{r_1^{n-1}} = \frac{C(2\pi e)^n}{Q^n} (P_o - P_1)(1-n)$$

$$\text{or} \quad Q^n = C(2\pi e)^n \left\{ \frac{r_o^{n-1} \cdot r_1^{n-1}}{r_1^{n-1} - r_o^{n-1}} \right\} (P_o - P_1)(1-n) \qquad (2.19)$$

P_1 = pressure at point r

r_1 = pressure to a point r

r_o = radius of the hole

Alternatively, $EQ^n = (P_o - P_1)$

$$\text{and} \quad n \log Q + \log E = \log (P_o - P_1) \qquad (2.20)$$

In the case of non linear flow, a curve of log (Po-P1) vs log Q should be a straight line. The slope of the curve indicating the degree of non-linearity and from the intercept on the pressure axis a value of Ce can be obtained. This value will be termed the "non linear permeability function" (N.P.F.) to distinguish if from the permeability in the laminar case.

Examples of this type of behaviour will be discussed in the chapter on Field Evaluation.

2.1.4 USE OF INERTIA TERM IN THE NON-LINEAR PRESSURE-FLOW RELATIONSHIP

As in section 2.1.2. equations will be developed for the isotropic case of radial flow in the horizontal plane where K.E. changes due to acceleration changing the pressure.

$$P_{KT} = \frac{1}{2g} \frac{Q^2}{4\pi^2 e^2} \left\{ \frac{1}{r_0^2} - \frac{1}{r_1^2} \right\} \qquad (2.21)$$

As in the case of linear flow this quantity is negligible and therefore will not be further considered.

2.1.5 AQUIFER OF INFINITE RADIUS - IMPLICATIONS

It can be seen from equation 1.1 that the most elementary formula relating pressure and flowrate requires two observations of pressure-one at the borehole and another one at some radius rl from the hole. In a Lugeon type of test, this second observation is not made but a large enough value substituted into radius rl to give what is supposed to be an accurate answer. The argument put forward generally is that since this relationship is a logarithmic one, any changes in rl do not make significant changes in the final answer (9)(10).

A term which is used quite often for rl is the radius of influence and has been empirically derived by Sichardt to be (9)

$$r_e = 3000 \left(\phi_b - \phi_e \right) \sqrt{K} \qquad (2.22)$$

r_e is radius of influence potential at the hole

b_e potential at distance r_e

K permeability; cm/sec.

Equation 2 leads to a reasonable answer for the case of porous media flow according to the author, but there is no evidence of either its validity or practical use in fissure flow. The concept of infinite aquifer yields reasonable answers in most cases in porous media, and therefore it is interesting to see its implications theoretically.

Eq.2.4.

$$Q = \left\{ \frac{2\pi e n K_J}{\log_e \left(\frac{r_1}{r_0} \right)} \right\} (P_0 - P_1)$$

rewriting for permeability

$$K_J = \left\{ \frac{Q}{2\pi e n (P_0 - P_1)} \right\} \log_e \left(\frac{r_1}{r_0} \right)$$

suppose the term in the big bracket = 1, the above equation reduces

to: $K_J = \log_e (r_1/r_o)$

for a 3" diameter hole, $r_o = \frac{3}{2 \times 12} = \frac{1}{8}$ ft.

r_1(ft)	1	10	100	1000	10000	100000	10^6
r_1/r_o	8	80	800	8000	80000	800000	8×10^6
K_J	2.079	4.4	6.7	9.0	11.3	13.6	15.9

TABLE 1

Table 1 shows that the maximum possible error could be not more than an order of magnitude, if the above concept of infinite aquifer was used.

Unfortunately, the above reasoning which has been reiterated before is not strictly true. Two possibilities could exist. The first one is that at a certain radius from the hole there is a boundary which is impermeable, ie. change of topography or geological change in strata and lastly, a major discontinuity such as a fault or a dyke. The second possibility is a constant pressure boundary eg. a recharge area. The result of these two boundaries is to completely change the form of the solution. Qualitatively, the first case can be thought of in this way: continuous pumping-in of water from the borehole into the surrounding rock will build up the water pressure in the system. This build-up will be non uniform in the radial direction because of the continuously changing back pressure. In effect this build-up amounts to a non-steady state solution in which the pressure distribution not only varies with radius but also with time. It is absolutely essential that in a field test if pumping is being carried out in one hole, observations of pressure changes should be made in a nearby hole, for the above reason and also because the pressure drop in the radial direction is non-linear. (See Chapter 3).

2.1.6 ANISOTROPIC FLOW IN THE HORIZONTAL PLANE

So far all the different conditions that have been considered assume that a fissure is isotropic in the horizontal plane. This assumption amounts to conditions of radial flow (see Fig.2.4.).

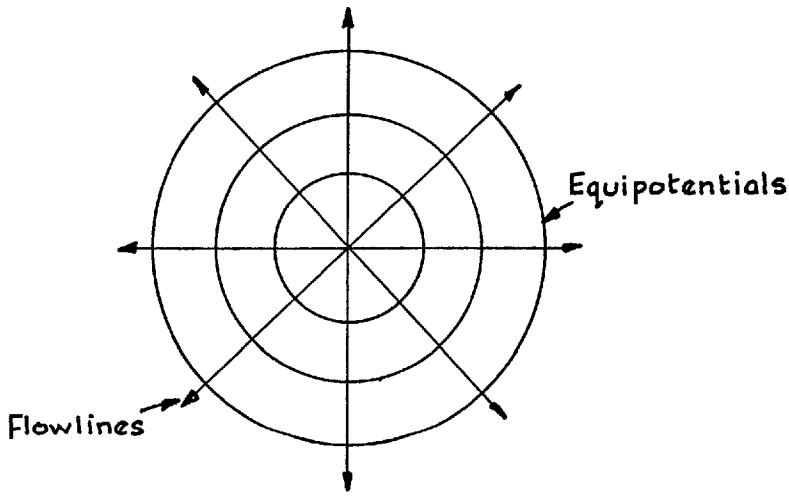


Fig 2.4 Isotropic flow

Very often the nature of the fissure topography is such that it is easier for flow to travel in one direction rather than another. This could be due to lineations on the fissure surface either as a result of erosion (eg. Karst) or due to tectonic movement. This alteration and its subsequent hydraulic effect causes anisotropy. For a two dimensional case, the complete permeability of the fissure is described by the following case tensor. The tensoral representation of permeability has been derived from first principles by Irmay, Childs and Scheidegger and therefore, will not be repeated.

$$|K| = \begin{vmatrix} K_{11} & K_{12} \\ K_{21} & K_{22} \end{vmatrix} \qquad (2.22)$$

Where K11 for example is the resistance to flow in the one direction given a gradient in the same direction and K12 is the resistance to flow in the one direction if there is a gradient in the 2 direction. K12 = K21 is normally accepted for reasons of continuity.

A graphical representation of anisotropic permeability can be made to make it clear what the principal directions are in such a case. A method analogous to Mohr's circle is proposed by Irmay (4). Fig 2.5is self-explanatory. Kx, Ky are the two principal permeabilities, mathematically this amounts to equation 2.22 changing its form to

$$|K'| = \begin{vmatrix} K_x & 0 \\ 0 & K_y \end{vmatrix}$$

If 1, 2 are two orthogonal but arbitrary directions, by applying a known gradient in either of the two directions, the flow component can be measured in both the direction of the gradient and orthogonal to it. Then by applying a known gradient in the other direction it is possible to measure flow components as in the previous case. In this way three of the constants K11, K12, K22 can be calculated and then using the Mohr circle method (Fig.2.5) it is possible to obtain the direction and value of the principal permeabilities.

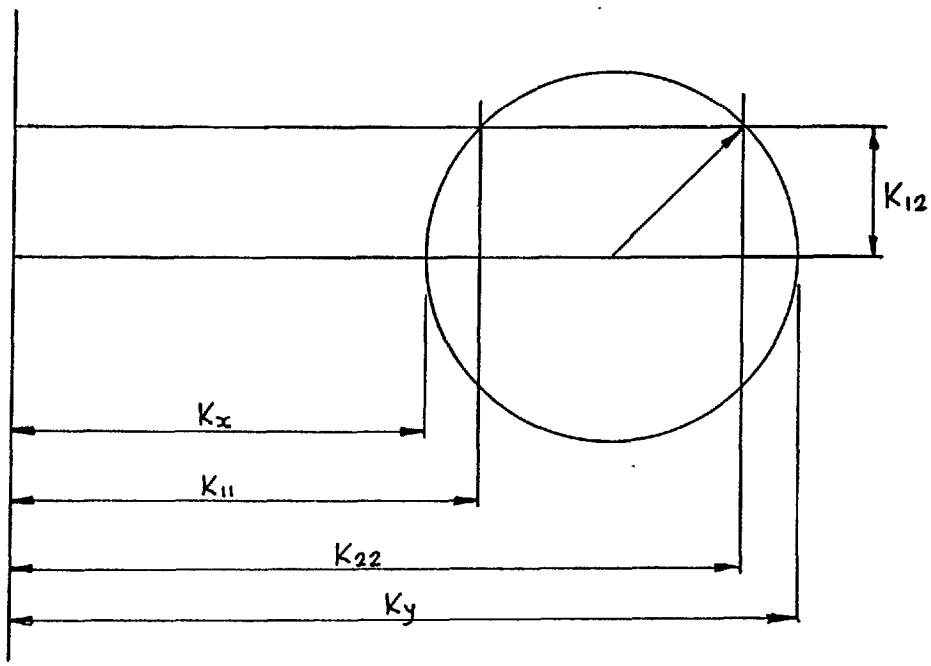


Fig. 2.5.

Anisotropy in the horizontal plane means the flow travels more easily in one direction than another. Fig.2.6 illustrates an equipotential due to anisotropy in a system where flow is either from or to the origin.

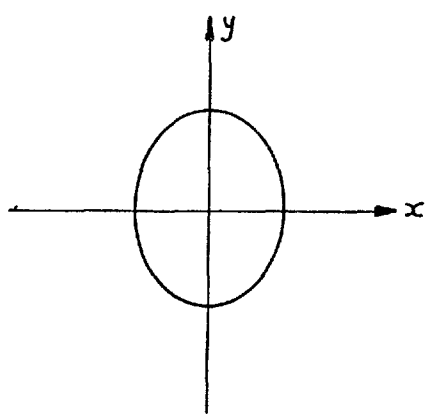


Fig. 2.6.

It is rather cumbersome to deal with problems of flow from a cavity into an anisotropic medium by analytical means. It is very often much easier to use numerical models and these will be discussed in the chapter on Numerical Analysis. Also the case of the non-homogeneous, and anisotropic flow will be considered in the chapter on model work, since this aspect is intractable even with a computer model.

Anisotropy in the plane of the joint can be extremely difficult to detect. Lack of detection of such an existing anisotropy can give completely midleading computations of flow rates. And, further, the flow test as it exists can completely miss the anisotropy, because the relationship between pressure and flow is derived on the basis of radial flow, in which case the radial permeability is equal to permeability in any direction. It seems virtually impossible to obtain the anisotropy from one test and therefore, it is proposed that during a pumping-in test the pressures are monitored in two observation holes as in Fig.2.7, where r is an arbitrary length. The Numerical and Field sections will deal with this aspect of the problem in detail.

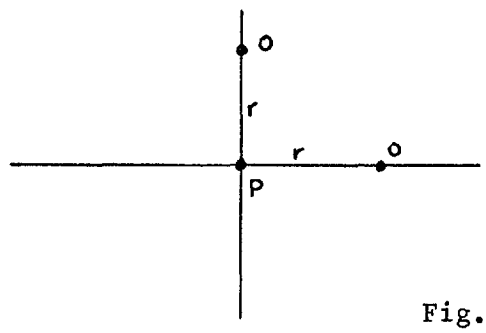


Fig. 2.7.

2.1.7 INFLUENCE OF SECONDARY FISSURES

So far, a great deal of emphasis has been placed on the particular case of flow from a borehole into a single set of fissures which intersect it. There are two reasons for this. The first one is that there are a great deal of problems in the range of sedimentary rocks where the bedding can play an important part in fluid transport, especially if this bedding is associated with some form of stress relief. There are numerous other cases of schistosity, zones of shear joints and faults which come into this category of flow-structure relationship. Faults as the dominant fluid carriers, in fractured rock, have been generally disregarded. The second reason is a hydraulic one.

It was Muskat and later Baker (5) who demonstrated that the pressure drop within the vicinity of the borehole is so large that the performance of a well in the oil field or a borehole is consequently governed largely by what happens near the hole. Fig.2.8 demonstrates this very clearly.

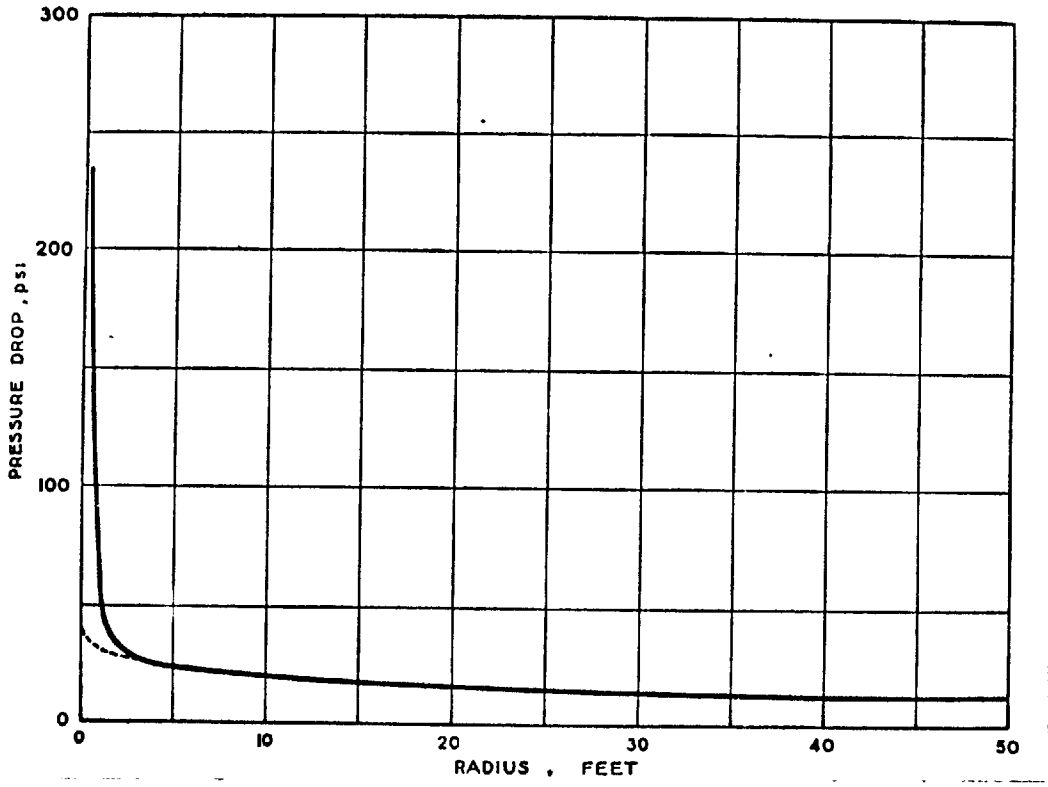


FIG 2.8

Pressure drop occurs as fluid flows from horizontal fractures into a cavity. In the case of a fissured media the drop is a very much more severe one. Baker attributes this behaviour to the limited area available for flow of a fluid in a fissure system and the acceleration of the fluid as it approaches the cavity. It is worth considering a hypothetical numerical model to illustrate this point in view of its great importance. Equation 2.4 gives. $Q = \left\{\frac{2\pi e n K_J}{\log_e (r_2/r_1)}\right\}(P_o - P_i)$

Let us assume the following conditions:

$n = 1$

$e = \frac{1}{10}$ mm

$K_J = \frac{e^2 g}{120}$

$Q = 1$ Litre/min

$P_o = 800$ cms. head of water (Approx. 26ft.)

$r_o = 3$ cms.

$r_1 = 6$ cms.

P_i at $r_1 = ?$

substituting these values in the above equation:

$$\frac{1000}{60} = \frac{2 \times 10^{-2} \times 1 \times 10^{-4} \times 980}{12 \times 1.45 \times 10(-2) \times 0.7} \quad (800-P_1)$$

$$\frac{1000}{60} = 0.05\ (800-P_1)$$

$$\underline{800}-P_1 = \frac{1000}{60 \times 0.05} = 333$$

$$P_1 = 467 \text{ cms head of water}$$

Pressure drop = 58.5% in a distance twice the radius from the hole.

Now consider a continuum approach: Eq.1.1

$Q = \frac{2LKs}{\log (r_1/r_o)} (P_o-P_1)$, L = distance between packers = 1 metre

the permeability of one fissure $K_J = \frac{e^2 g}{12\nu} = \frac{10^{-4} \times 980}{12 \times 1.45 \times 10^{-2}} =$

0.56 cm/sec. $= 5.6 \times 10^{-1}$ cm/sec.

Now let us assume that the continuum permeability K_s is the same = 5.6×10^{-1} cm/sec.

$$\frac{1000}{60} = \frac{2 \times 100 \times 5.6 \times 10^{-1}}{0.7} \quad (800-P_1)$$

$$\frac{1000}{60} = 160\ (800-P_1)$$

$$800-P_1 = \frac{1000}{9600}$$

$$P_1 = 800 - 0.11 = 799.89 \text{ cms head of water.}$$

In a continuum at a distance twice the value of the radius hardly any pressure drop has occurred.

This exercise illustrates how the pressure drop is substantial in a fissure system. Therefore it is the permeability characteristics of fissure near the borehole that will decide how pressure-flowrate is related. Since a large number of fissure systems exist where the spacing between fractures is greater than 6 cms. it is clear that the influence of the secondary fissures which do not intersect the borehole cavity is not substantial. The pressure drop near a borehole was also observed by Sharp (9) who has indicated how pressure drop from a hole changes under varying ratios of borehole diameter/length. As was mentioned previously it is important in a Field situation to perform tests in one hole, and observe the effect, in terms of pressure changes in another hole which is at a known distance. In such a way it is possible to decide; how severe the pressure drop is away from the hole. If the drop is not substantial the influence of secondary fissures must be taken into account (see section on Numerical Analysis) otherwise the analysis described in the chapter can be used.

2.1.8 INFLUENCE OF FLUID STRESSES DURING A PUMPING TEST

It is often very difficult to predict from the results of a pumping test if the fissures have opened up. A conventional plot of pressure vs flowrate may be non-linear; but it is difficult to see from this plot whether the nonlinearity is due to fissure-widening or a host of other factors. Therefore it is suggested that a curve of P/Q vs Q is plotted. If the relationship between the pressures and flows is given by the polynomial,

$$P = AQ + BQ^2$$

the second term indicates changes in kinetic energy. A curve as in Fig.2.9 will indicate a decrease in kinetic energy loss with increasing flowrate. This is only possible in a system where the water carrier ie. a fissure in this case, increases in its aperture.

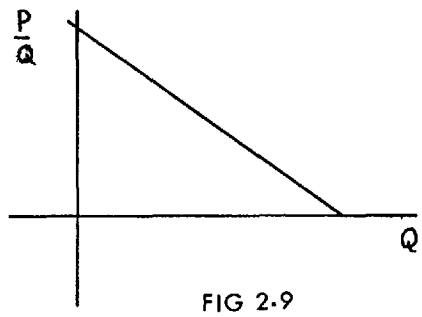


FIG 2.9

Bernaix (14) considers the problem of radial percolation in an isotropic medium and its influence on the total stress field. For example, given a constant percolation pressure, or alternatively, the hydraulic gradient the permeability is much higher with divergent percolation (10 (-8) cm/sec.) than with convergent percolation (2 x 10 (-9) cm/sec.). In the two cases the effective stress field has changed, (see Fig.2.10) as a result of the fluid pressure.

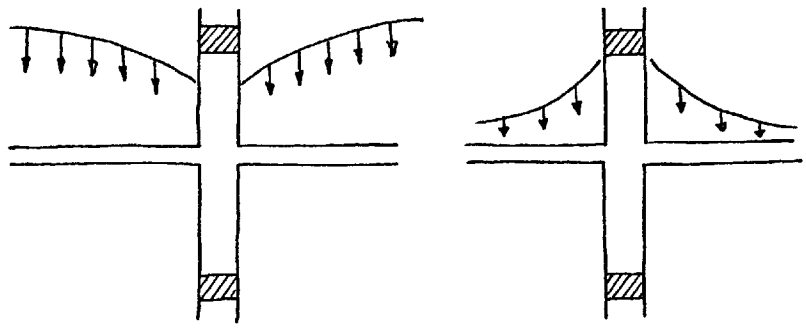


FIG.2.10

Since the relationship between permeability and aperture is a cubic one, it is obvious that small changes in stress will cause much greater changes in permeability. Fig.2.11 describes the results of laboratory tests carried out by Bernaix to show the importance of fluid stresses on permeability. Since the analytical solution has been described by Bermaix for the isotropic case, the author has considered various cases of anisotropy and stress application to a pumping test. These results are discussed in the section on Numerical Methods.

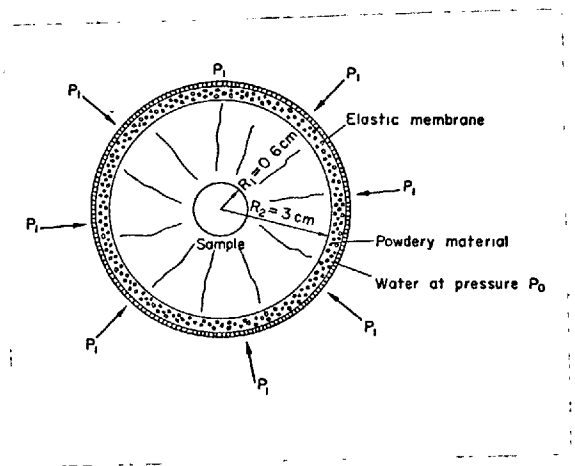
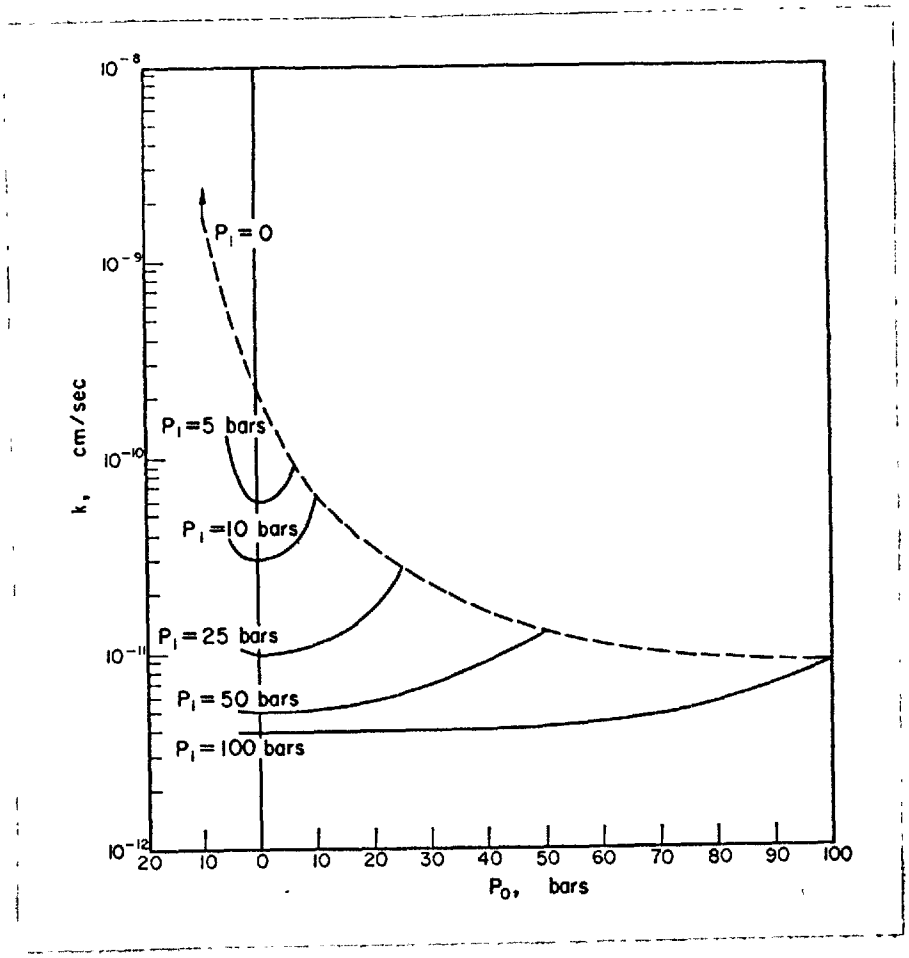
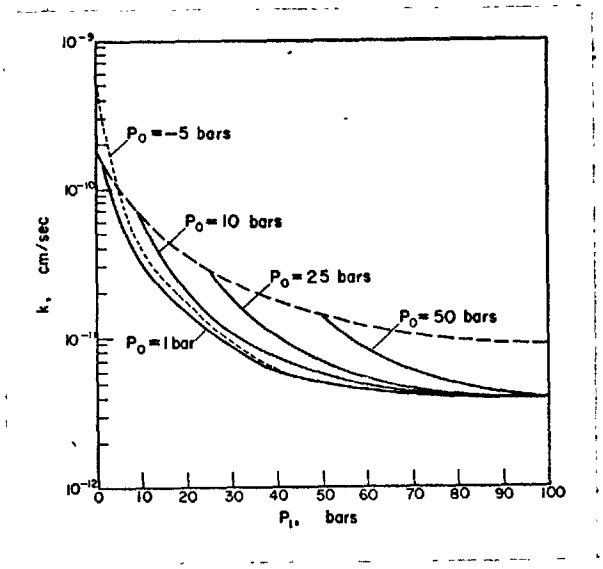


FIG 2.11


10^{-8}
10^{-9}
10^{-10}
10^{-11}
10^{-12}
k, cm/sec
$P_i = 0$
$P_i = 5$ bars
$P_i = 10$ bars
$P_i = 25$ bars
$P_i = 50$ bars
$P_i = 100$ bars
20 10 0 10 20 30 40 50 60 70 80 90 100
P_0, bars


10^{-9}
10^{-10}
10^{-11}
10^{-12}
k, cm/sec
$P_0 = -5$ bars
$P_0 = 10$ bars
$P_0 = 25$ bars
$P_0 = 50$ bars
$P_0 = 1$ bar
0 10 20 30 40 50 60 70 80 90 100
P_i, bars

FIGS 2.11

2.2.0 TWO AND THREE DIMENSIONAL SEEPAGE FROM A CAVITY (GRAVITY FLOW)

As it was stated in section 2.1.7 the influence of secondary jointing is to introduce flow in different directions. However, it must be once more stated that the jointing has to be comparable in spacing to the diameter of the hole in order to cause dominant non axisymmetric flow. Fig.2.12 demonstrates a general case of a two dimensional fissure system where the fissures intersect at an angle to each other. Now the two fracture systems may have completely different in permeabilities and therefore, cause anisotropy. In theory, it is possible to measure the ratio of anisotropy if two pumping tests are carried out in holes orthogonal to each other and arbitrarily oriented in space (section 2.1.6 or Ref. 15). If the degree of jointing is high and random, the system can be regarded as a continuum, and then it is possible to calculate the ratio of permeability using the method proposed by Snow (15).

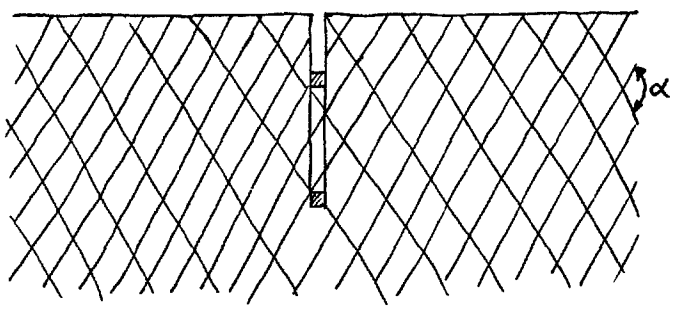


FIG 2.12

If the frequency of the two sets varies, the problem becomes rather more intractable and cannot be solved analytically. The only possible way then is to build a numerical model of the system. Since the permutations can be enormous, it was felt that little could be gained by setting up a totally general model. A more specific model was considered which could be treated numerically, and subsequently a check made on the method with either a perspex model in the laboratory or in the field.

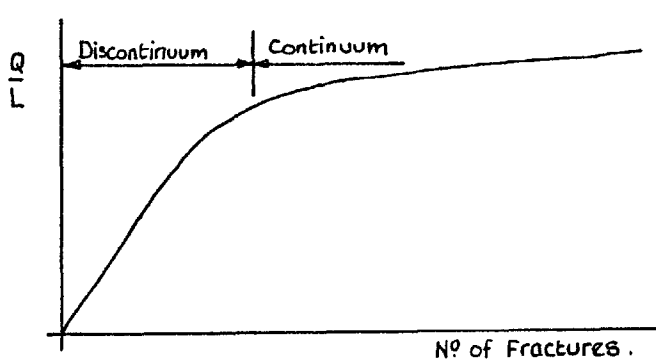


FIG 2.13

Fig.2.14 shows the model which has been treated numerically. The frequencies of jointing can be varied with great ease and so can the length of the test section. Using this model it has been possible to solve for the anisotropic case of permeability. Also the influence of the test section has been examined in order to arrive at a reasonable idea of scale for the test, given a certain fissure frequency. (See section on Numerical Modelling).

By scale is meant this - if a pumping test was carried out with a given packer section, for a given pressure, the flow will be an amount proportional to the fissure permeability. Now, if the length is doubled the flow should double too - should the system be homogenious and isotropic. However, this does not happen in a realistic fissure system until a large enough number of fissures are taken. Fig.2.13 shows this concept described graphically. Details of this will be discussed in the sections on Numerical Models and Field Work.

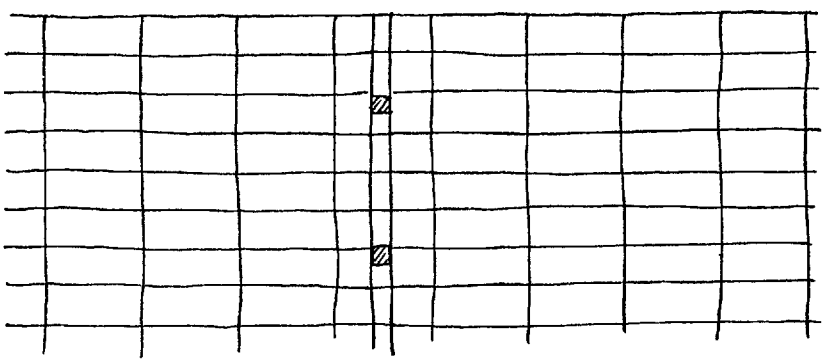


FIG 2.14

2.2.1 END EFFECTS IN A GRAVITY SYSTEM

In a two or three dimensional system the end effects at the cavity cause a problem in computation of permeability. Many authors have discussed this problem but no analytical proof exists where this effect has been calculated. However, with a numerical solution it is possible to correct for this effect. Numerous shape coefficients exist which have been obtained for the case of isotropic flow. In the section on Numerical Work this problem will be discussed in detail for the case of anisotropic flow. Two practical solutions exist to treat this problem. The first one is to increase the test section length to such a degree that the spherical component at either end becomes negligible. The alternative to this is the method developed at Imperial College (45) where a system of four packers is used. The end packers act as flow linerarisers and the middle section is where the measurements are taken. In this way it is possible to measure the contribution to resistance in a direction normal to the hole without bringing in any other factor. Field tests with this type of packer have been performed by the author and they are dealt with in a later section.

CONCLUSIONS

In view of the geologic nature of problems and the effect of fine fractures on flow from a cavity, axisymmetric flow equations have been developed for the case laminar and non-linear flow. Although the equations for the laminar case are not original, they have been rederived with a discontinuum model of a fractured rock mass in mind. The non-linear equations are new and must be further tested both in the field and in the laboratory. Although in nature the problem of fluid flow in fissured media is complex and needs numerical models to solve boundary value problems the equations in Chapter 2 can be the first step in describing the response of the rock mass to flow of water within it. Field trials were carried out and the methods developed in Chapter 2 were used and proved to be relatively consistent. Where possible these equations have been tested for their validity in the laboratory under controlled conditions. The results were satisfactory for both the idealised case and the "real cases", where tests were performed on araldite replicas of real fissures.

MOTION OF A FLUID FROM OR TOWARDS A CAVITY - NUMERICAL SOLUTIONS

SYNOPSIS

Numerical methods are discussed which make it possible to solve otherwise intractable problems of fluid flow through an anisotropic media. Different cases are considered where the flow occurs from a borehole into a single set of fissures and also into a two dimensional intersecting set of fissures. In both these cases the influence of anisotropy is considered on the pressure distribution and also on the flowrates. Methods are discussed whereby the ratio of principal permeability can be measured in the field. The influence of the cavity size relative to the fissure frequency and also the influence of boundary is analyzed for the case of isotropic and anisotropic flow.

3.1.0 INTRODUCTION

The advent of digital computers has made the solution of complex boundary problems relatively easy. Whereas in the past, solutions to differential equations with simple boundary conditions and relatively straight-forward material properties were possible, realistic and consequently generally complex problems were not attempted. Techniques such as the Finite Difference and Finite Element computer-based methods exist which can solve, anisotropic non-linear systems. For example, Freeze and Witherspoon (16) have used the Finite Difference method to study geohydrological problems under steady state conditions. This method of computation is essentially based on the relaxation technique of Southwell (17). Use of Finite Element method has been made by Zienkiewicz (18) to treat two-dimensional anisotropic flow. However, both these methods are solutions of groundwater flow in a continuum under steady state conditions.

Treatment of fluid flow through a discontinuum has been described by Louis (8) who studied numerous cases of groundwater flow in slopes, under dams and into tunnels. The method used is basically analogous to electrical networks. The different joint systems constitute a network. Two criteria are used to solve the equations and they are identical to Kirchhoff's Laws. Equations are written in such a way that the mathematical formulation is in a matrix form between potential, flow and permeability. Sharp (9) has used the relaxation technique described Southwell to solve two and three dimensional problems; with modifications for free surfaces, drainage and impermeable layers. A completely different approach is used by Stark and Volker (19) who solved numerically the Navier-Stokes equations of flow through a clastic material. This approach is extremely rigorous in that it takes account of the inertia terms and the solution yields the detailed flow path through the clastic system. In addition a completely general flow law is used. In this section the solutions to various problems are based on the relaxation technique (9).

3.1.1 FLOW FROM A VERTICAL CAVITY INTO A TWO DIMENSIONAL ANISOTROPIC FISSURE IN THE HORIZONTAL PLANE

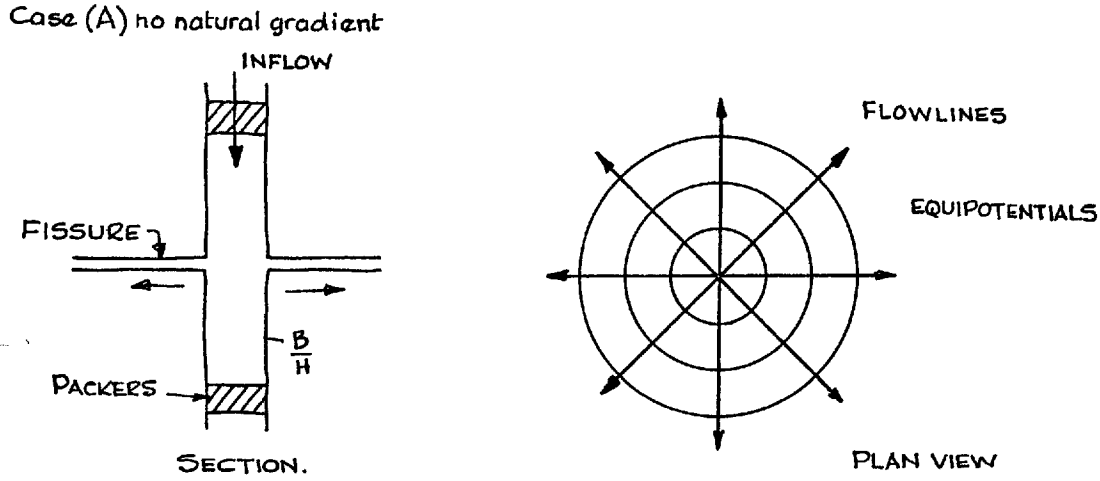


FIG 3.1

Consider the case of flow of water from the cavity as in Fig.3.1. Water either flows into a single or multiple fissure system. In an isotropic system, the equipotentials will be a series of concentric circles and flow will be radial. If the surface profile of the fissure is such that it allows water to flow preferentially in one direction rather than another the permeability of fissure will be termed ANISOTROPIC. Such profiles are for example generated as a result of tectonic movement, ie. faults or shear joints. On a large scale, the presence of lineations has been described by Ramsay (50) as a result of complex folding. In a Karstic environment solution cavities can be formed within the plane of the fissures, thereby allowing preferential flow. Therefore the potential distribution in such an environment will depend on the degree and extent of anisotropy. Very often permeability tests are carried out in such systems on the basis of isotropy. It is proposed to simulate a water pressure test in an anisotropic fissure plane to study (a) the pressure distributions in the principal permeability directions; (b) the influence on the flowrate from a cavity; (c) detection of anisotropy. In each case comparisons will be made with an isotropic condition which is generally assumed.

3.1.2 NUMERICAL MODEL

In Chapter 2 is has been shown that the optimum direction for a borehole is orthogonal to the fissure set under examination. Fig. 3.1 shows such an intersection and since the problem is two dimensional flow only in the plane of fissure is considered. Although it has been assumed that the aquifer is infinite, for practical reasons a finite model has to be used in which the borehole is very much smaller than the size of the boundaries. This assumption will, however, be tested at a later stage.

The entire area of the fissure is considered as a continuum and divided into elements with a central hole as shown in Fig.3.2. The borehole is defined by 5 nodes. This configuration was chosen after preliminary trials on a single node and four node configurations (Fig.3.2). The four and five node systems gave approximately the same answer and were well within 10% of the total flowrate. This total flowrate is obtained by having a large number of nodes to simulate a hole, obviously suggesting that the greater the number of nodes that define the hole, the better is the convergence of the flowrate to the true value. These conclusions agree with those of Sharp (9) that unless a hole is well connected, as shown above, considerable errors creep into the system due to the non-simulation of radial flow conditions.

In all the computations that follow flowlines and equipotential lines are identical whether the flow occurs from the cavity into the fissure system or conversely from the fissures to the cavity. Therefore it is quite arbitrary whether the borehole is at a higher or lower potential than the surroundings. In the examples that follow it is assumed that the borehole potential is zero while the boundary is at 10 arbitrary units. The resistance in the x and y direction is fixed by the ratio of the principal permeabilities.

3.1.3 METHOD OF SOLUTION

Solutions to Laplace's Equation provide the potential distribution in most flow problems. The derivation and assumptions of the equation are outlined in numerous papers (6,8,9,12). The Laplace Equation can be rewritten in terms of a Finite Difference Equation and then solved using Relaxation Techniques. Having fixed the boundary potentials at 10 and 0 units (Fig.3.2) all the remaining nodes in the mesh are given an arbitrary but temporary value of 10 units. By a suitable relaxation technique which is outlined in the Appendix, a solution for the potential distribution is obtained. Contours of equipotentials are then drawn by joining points of equal potential at suitable intervals.

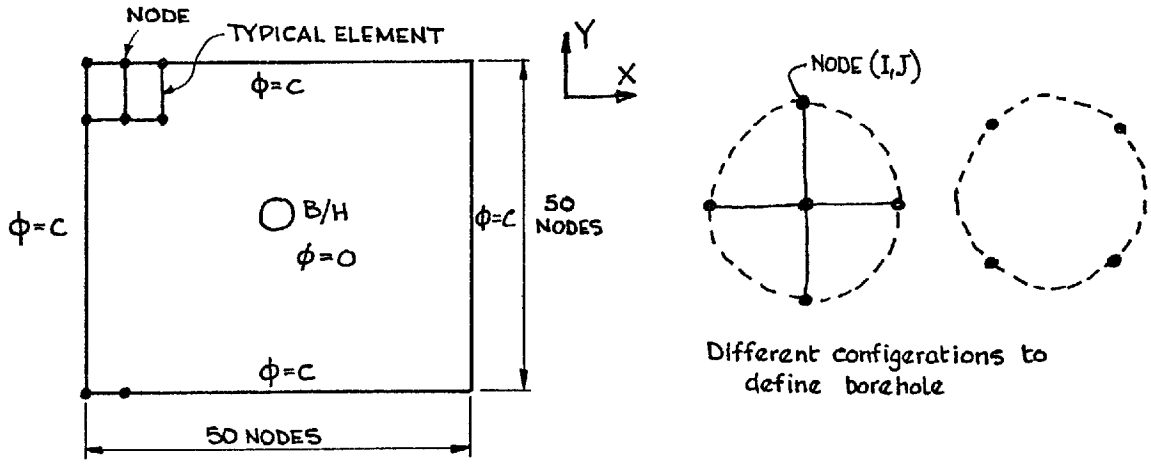


FIG 3.2

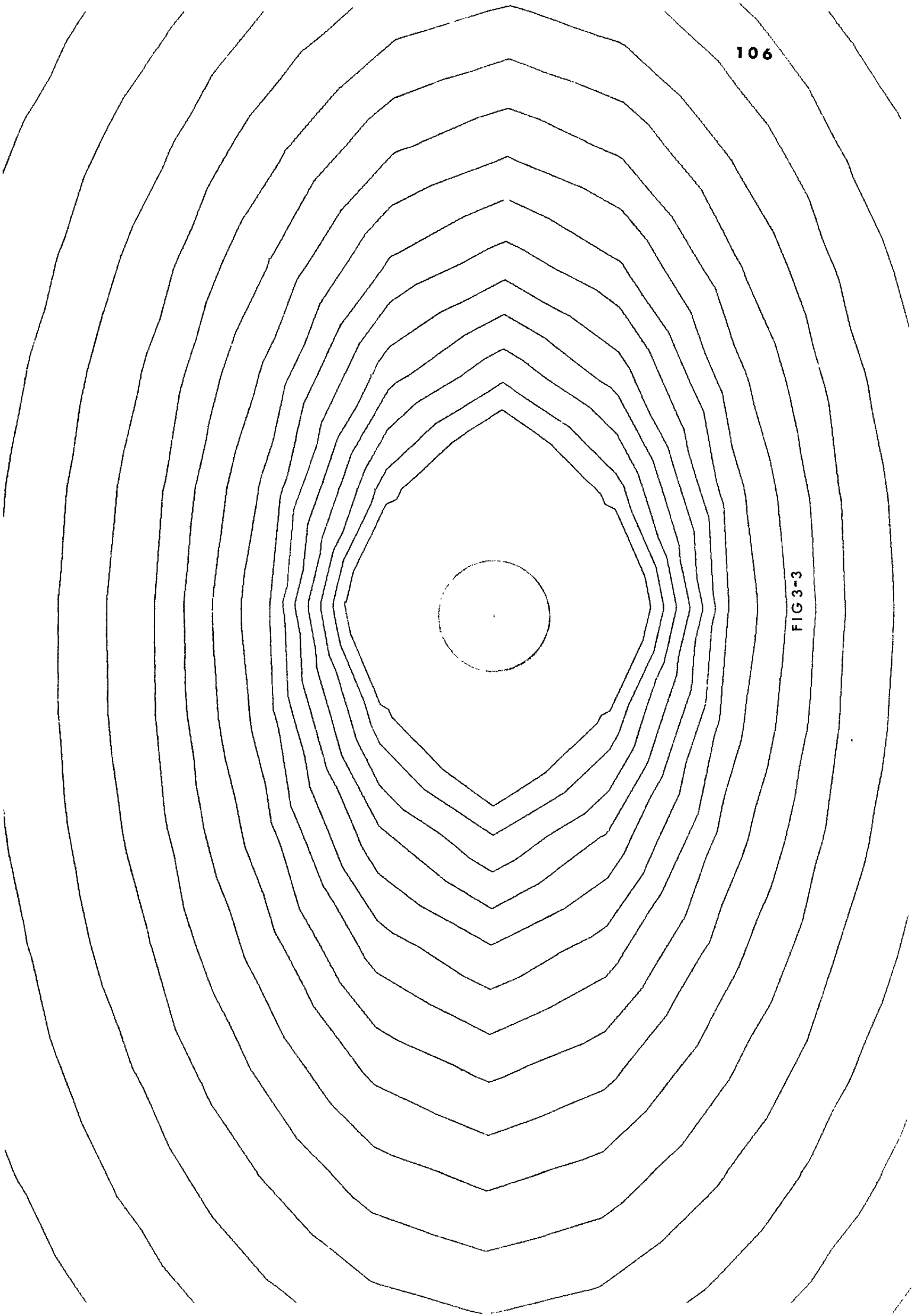


FIG 3-3

3.1.4 NUMERICAL ANALYSIS

The following cases were considered where the ratios of principal permeability are given as:

$\frac{Ky}{Kx}$ or $\frac{Kx}{Ky}$

Kx = permeability in x-direction

Ky = permeability in y-direction.

The following cases have been examined using the numerical model.

(a) $\frac{Kx}{Ky} = 1,2,5$

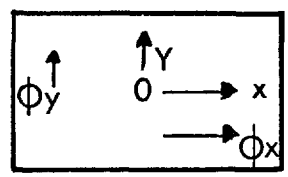
(b) $\frac{Ky}{Kx} = 1,2,5$

When the ratio of principal permeabilities in one flow is isotropic and the equipotentials are circular as in Fig.3.2. In anisotropic flow, however, the potentials are in the form of ellipses and the principal axis of such coincide with the principal permeability directions. This can be seen in Fig.3.3 where the ratios of principal permeabilities are marked.

Since the equipotential lines are elliptical in shape it is obvious that the pressure distribution along any axis taken from the hole, is dissimilar to the isotropic case. Fig.3.4 is a dimensionless plot of Potential in the x-direction vs distance from the hole. For the case where the ratio Kx/Ky is greater than 1 the pressure distribution in the x-direction is less than in the isotropic case. This is because it is much easier for the fluid to flow in the x-direction than in the y-direction and therefore the frictional loss is smaller in the x-direction . The converse is true for the case where Kx/Ky is less than one. If a pressure test was carried out as described in Chapter 2 and the fissure-set was anisotropic in its plane the error in determining permeability (eq.2.3) could be calculated from Fig.3.4. For example if the observation hole is at a distance five times the diameter of the hole and the ratio of principal permeabilities Kx/Ky = 1/10, the difference in the pressure from the isotropic case is given by:

$$\left[\frac{\phi_x}{\phi_o}\right] \frac{Kx}{Ky} = \frac{1}{10} = 0.95$$

$$\left[\frac{\phi_x}{\phi_o}\right] \frac{Kx}{Ky} = 1 = 0.76$$



Kx PRINCIPAL PERMEABILITY

Ky PRINCIPAL PERMEABILITY

ϕ POTENTIAL (PRESSURE)

ϕo POTENTIAL (PRESSURE) at B/H

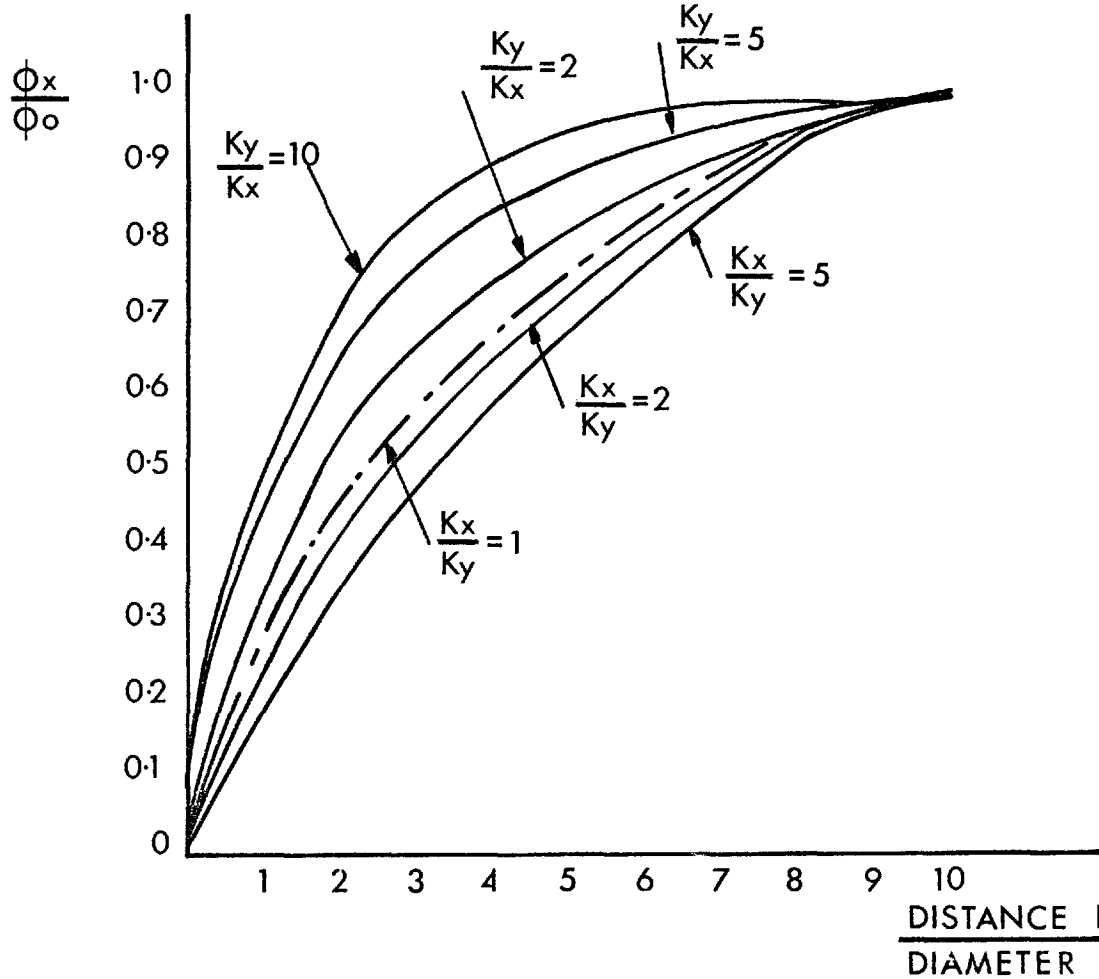


FIG 3·4

DIMENSIONLESS PRESSURE DROP VS DISTANCE FROM HOLE

In an anisotropic system the flowrate in the two principal directions is governed by the ratio of principal permeabilities. Fig.3.5 shows how the dimensionless flow varies with the permeability ratio. When Kx/Ky = 1 the ratio of the flow is also equal to 1; thus indicating isotropy. It is interesting to note that initially the curve is extremely non-linear and when Kx/Ky = 3 it begins to straighten out; suggesting that for higher values of Kx/Ky the dimensionless flow in the x-direction increases linearly with Kx/Ky. An implication of this result is that if a pressure test is being carried out with respect to the plane of the fissure with Kx/Ky > 3 the permeability will approximate the maximum of the two principal permeability directions. Very careful use should then be made of such a result in solving a boundary value problem.

3.1.5 DETERMINATION OF PRINCIPAL PERMEABILITY RATIO: APPROXIMATE METHOD

In problems where the ratio of principal permeabilities of a single set of joints or faults is important in terms of flowrates or pressure distributions it is proposed that a test is carried out as part of a routine to assess the magnitude of such an anisotropy. The test very simply consists of pumping water into/out of a borehole which intersects the fissures orthagonally. During pumping it is essential to monitor pressures in the observation holes. This particular section refers only to an approximate determination because the principal directions have to be guessed, unless of course, a lot of trial holes can be drilled for an accurate determination of the principal directions of permeability.

Indirect methods could be used to determine the principal permeability directions. For example, the direction of the tectonic movement in a fault system can be used as one of the principal directions. This assumption has been tested on a model and the details are reported in Chapter 4. Sharp (9) has demonstrated how a histogram of surface topography can represent different fissure models. Clearly some histogram shapes such as in Fig.3.6 indicate anisotropy.

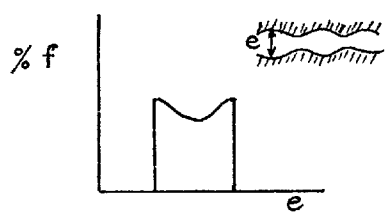
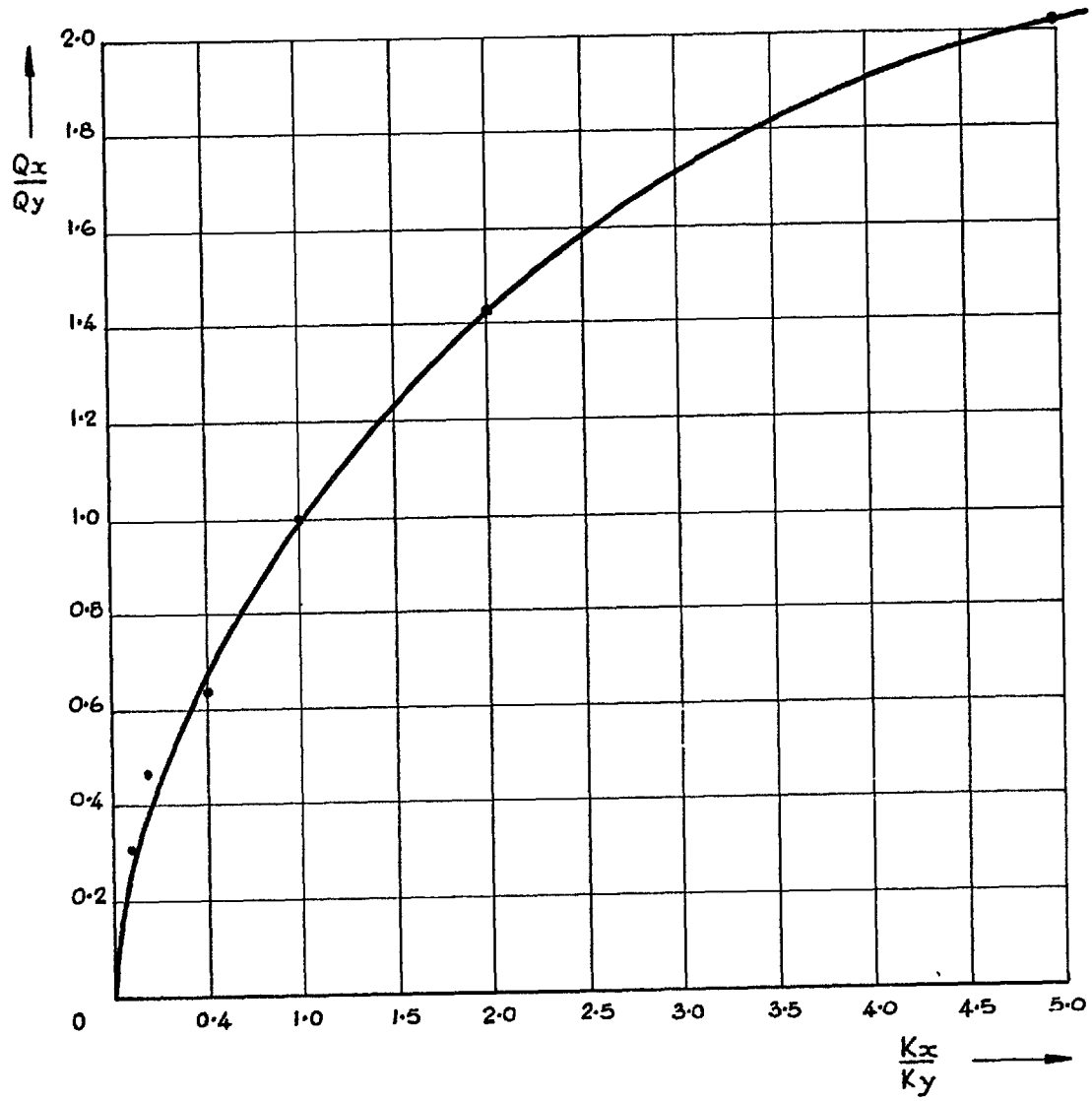


Fig 3.6

Stress distributions can result in the fissure becoming anisotropic. Since the permeability of a fissure is proportional to the cube of the aperture (for a simple model) any small changes in aperture as a result of stress would plainly effect the ratio of principal permeabilities. Therefore, prior to a test on a single set of fissures it is important to examine the stress distribution along the plane of the fissures to see if there are any serious stress concentrations which would result in anisotropy.



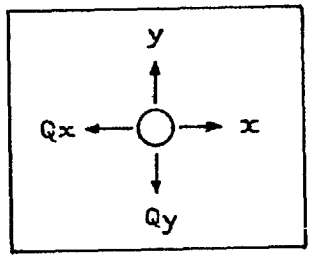


FIG 3.5 K_x / K_Y = RATIO OF PRINCIPAL PERMEABILITY

If x, y were the principal directions, three holes, as in Fig.3.7 should be used. The hole marked P is where water is either pumped in or out. Points O at distance x from P are the observation holes. By pumping water at a constant rate into P (assuming steady state), the pressures are monitored in O. If the fissure or set was isotropic the pressures in the two holes O would be identical. Any deviation indicates an anisotropy.

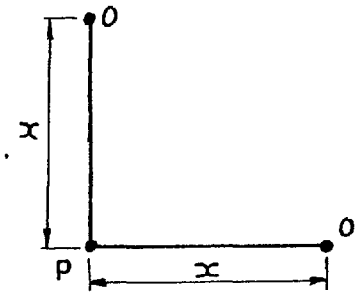
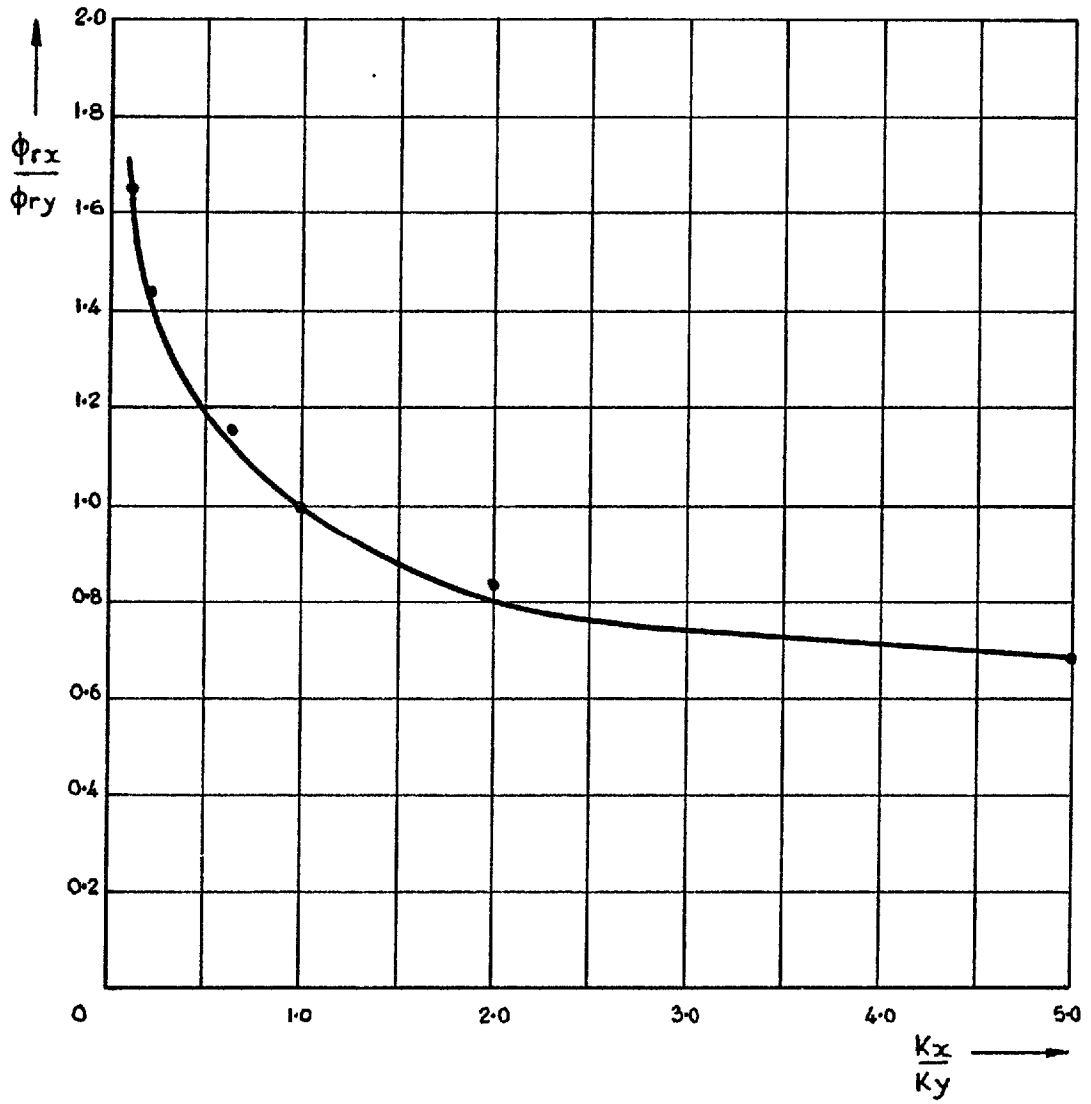


FIG 3.7

If the observation holes O lie on concentric circles generated from the pumping well, the ratio of the potentials during pumping should give an indication of the ratio of the principle permeabilities. The greater pressure drop obviously occurring in the direction of minimum permeability. Fig.3.8 illustrates the ratio of potentials in orthogonal directions at one given radius plotted vs increasing permeability ratio in the same directions. For a permeability ratio of 1 the ratio of the potentials is unity indicating equal flow in the two directions. As $\phi rx/\phi ry$ decreases the ratio of principle permeabilities increases. It can be seen from Fig.3.8 that very small differences are required in potential in the two orthogonal directions to provide large changes in Kx/Ky. The results as shown in Fig.3.8, when replotted on a log-log scale lie extremely well on a straight line. Several cases have been considered of potential ratios in orthogonal directions at varying radii, Fig.3.9. The straight lines pivot about 1, the steepest gradient being the ratio of potentials very close to the hole. As one gets further away from the hole, the line rotates anticlockwise about point 1 tending towards the horizontal at infinity where the ratio of potentials approaches one.

By giving a suitable distance for the two observation holes, say 10r/o readings should be taken of the pressures while water is either pumped into or out of hole P. The ratio of the pressures or potentials can then be located on Fig.3.9 to obtain an idea of the ratio of principal permeabilities.



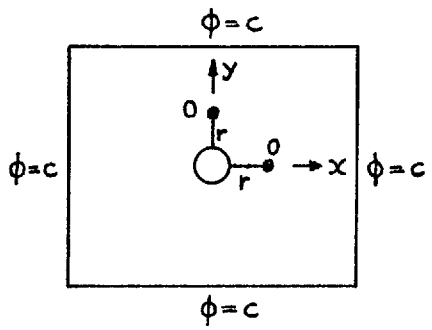


FIG 3.8 r = 4× DIA. OF BOREHOLE

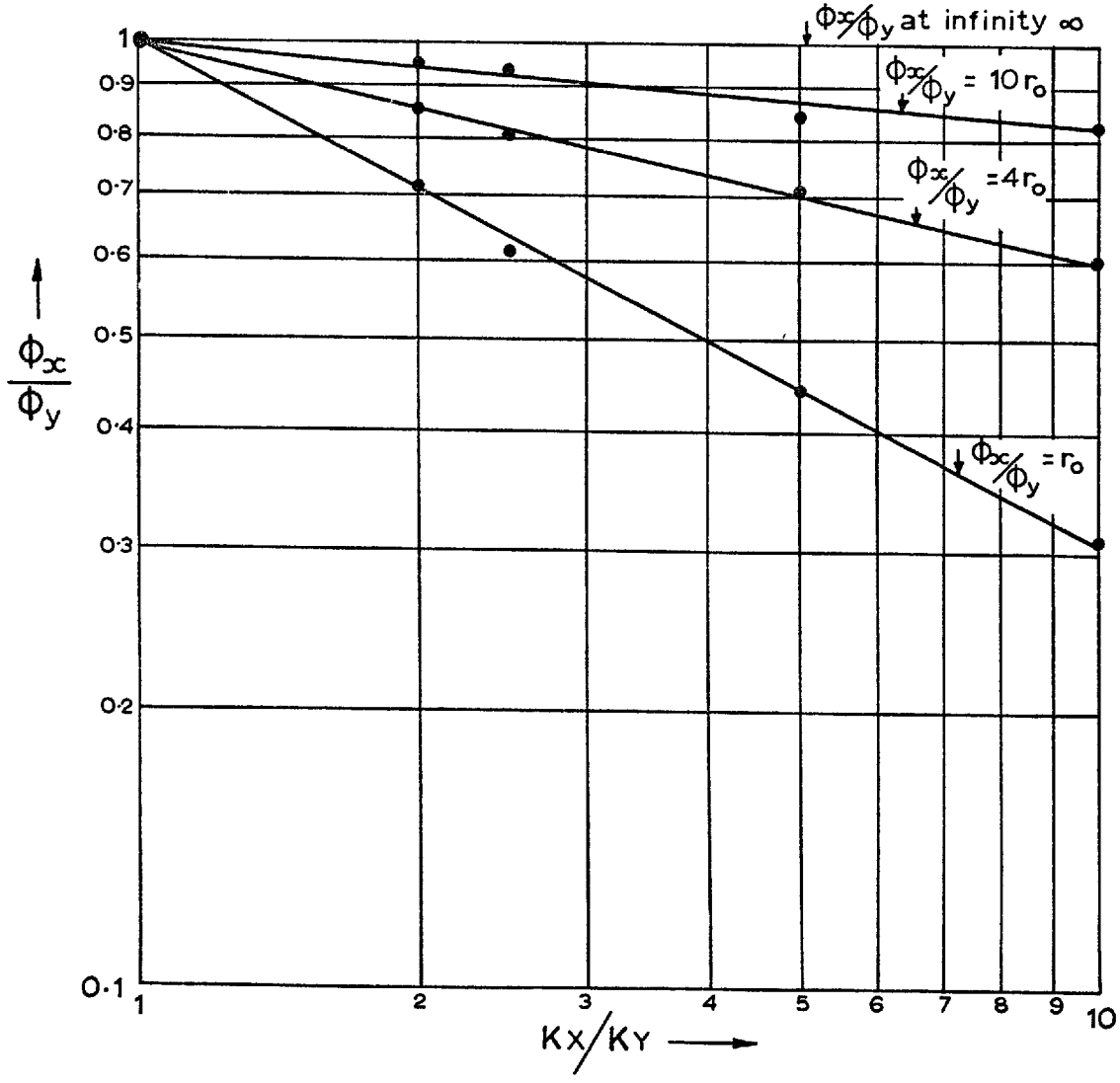

Φx/Φy at infinity ∞
Φx/Φy = 10 r0
Φx/Φy = 4 r0
Φx/Φy = r0
Φx/Φy
1
0·9
0·8
0·7
0·6
0·5
0·4
0·3
0·2
0·1
1
2
3
4
5
6
7
8
9
10
KX/KY

Fig. 3.9.

3.1.1 CASE (B) PRESENCE OF A FIELD GRADIENT "J"

The presence of a field gradient on pumping tests can be treated by superposition of the two potential fields. In the previous numerical model for example instead of keeping the boundaries at constant potential, a gradient is applied, thus in a linear system the summation is quite straight forward.

3.2.1 TWO AND THREE DIMENSIONAL FLOW SYSTEMS

As was mentioned in section 2.1.7 two and three dimensional flow systems become important as far as the water test is concerned when the degree of fissuration is high. Since the whole phenomenon of flow from a cavity into an arbitrary system is so complex, models that are considered are at best speculative. Therefore, it is hoped that by studying a few idealised examples, it may be possible to get some form of a picture. In this section it is assumed that the relationship between cavity size and fissure spacing is such that a two or three dimensional flow system is possible.

3.2.2 DETAILS OF THE NUMERICAL MODEL

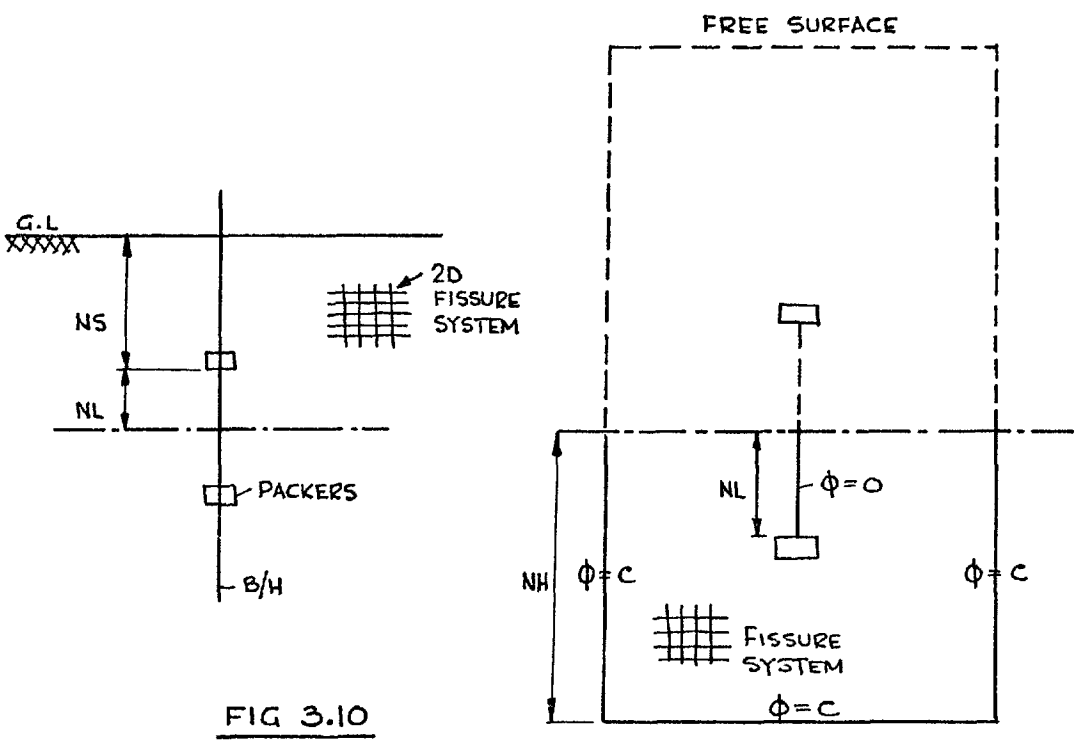


FIG 3.10

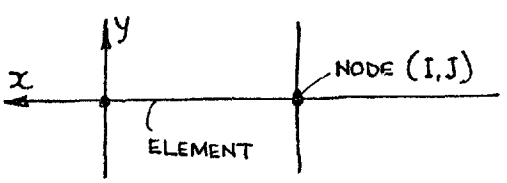


FIG 3.11

The case is now considered of a borehole intersecting a two dimensional fissure system in an infinite medium. One set of fissures intersects the borehole orthogonally while the other one is parallel to the axis of the borehole. It is proposed to study the influence of a pressure test on the potential field in such a medium. By increasing the spacing between the packers (Fig.3.10) it is possible in theory to obtain flow which is dominantly orthogonal to the borehole. It is also possible to obtain the ratio of principal permeability by carrying out a series of tests with different packer spacing. Obviously, altering the packer spacing introduces the variability of the sample size (of fissures) and consequently the value of permeability. The results of this enumerative study will be compared with those of Snow (7) which are based on statistical studies. The following assumptions have been made in the numerical study:

(i) Linear system

(ii) $NS \gg NL$

(iii) Two Dimensional Fissure System

(iv) Const. Potential at a large radial distance from the hole.

(v) Const. Potential in the hole between packers.

(vi) STEADY STATE conditions

(vii) Borehole is a line source or sink.

(viii) The distance between fissures and the total number of fissures in the entire model is constant.

The infinite medium is represented by 10,000 elements or fissures. Each element has two nodes either side of it as in Fig.3.11. The elements in the y-directions represent the fissures in that direction and similarly in the x-direction. Each element had its prescribed permeability value. A borehole in the y-direction for example is described by a chain of nodes linked by elements in the y-direction. All the nodes within the borehole are at constant potential and the permeability in the y-direction in the borehole is infinite. A line source or sink is justified on the basis that overall changes in flows and potentials are considered with changing permeability ratio and therefore the detail pressure distribution near the hole is not essential and further, in the real situation, a 3" diameter hole is very small compared to the areal dimensions of fissures and therefore appears as a line source anyway. The boundary potentials are clearly labelled in Fig.3.10. Since the problem is symmetrical about the midpoint between the packers, only one half of the problem is considered.

3.2.3 NUMERICAL ANALYSIS

A constant potential of 50 arbitrary units is applied to the boundaries as shown in Fig.3.10. The borehole has a potential of 0 units. The following cases have been considered in the numerical model.

(a) $\frac{Kx}{Ky}$ = 1,2,5

(b) $\frac{Ky}{Kx}$ = 1,2,5

The method of solution is as in Section 3.1.3 where having fixed the boundry potentials, temporary values of potential are given to the rest of the system and by a process of relaxation a solution is obtained to the problem. The details are listed in the appendix.

3.3.1 END EFFECTS IN A PRESSURE TEST

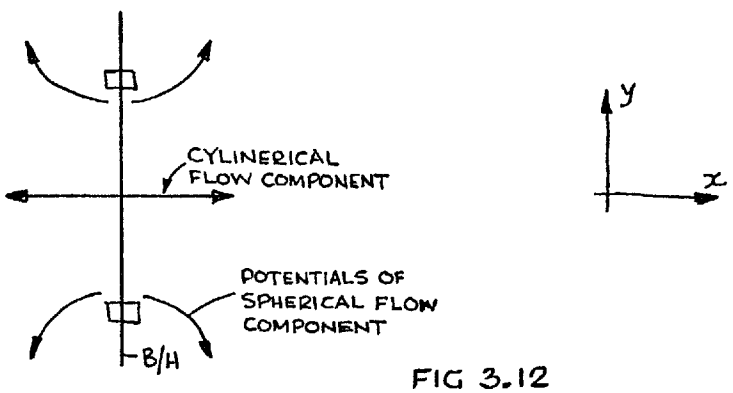


FIG 3.12

Fig.3.12 illustrates the cylindrical and spherical components of flow during a pressure test in a fissured media as described in section 3.2.2. Since the flow direction is not unique, ie. either the x or y direction; the value of permeability thus obtained has no directional significance.

Using the methods outlined in section 3.2.2 and 3.2.3 the influence of increased packer spacing in an isotropic and anisotropic medium was studied. This amounted to beginning with a small value of NL (Fig.3.10) which was subsequently increased to include more fissures.

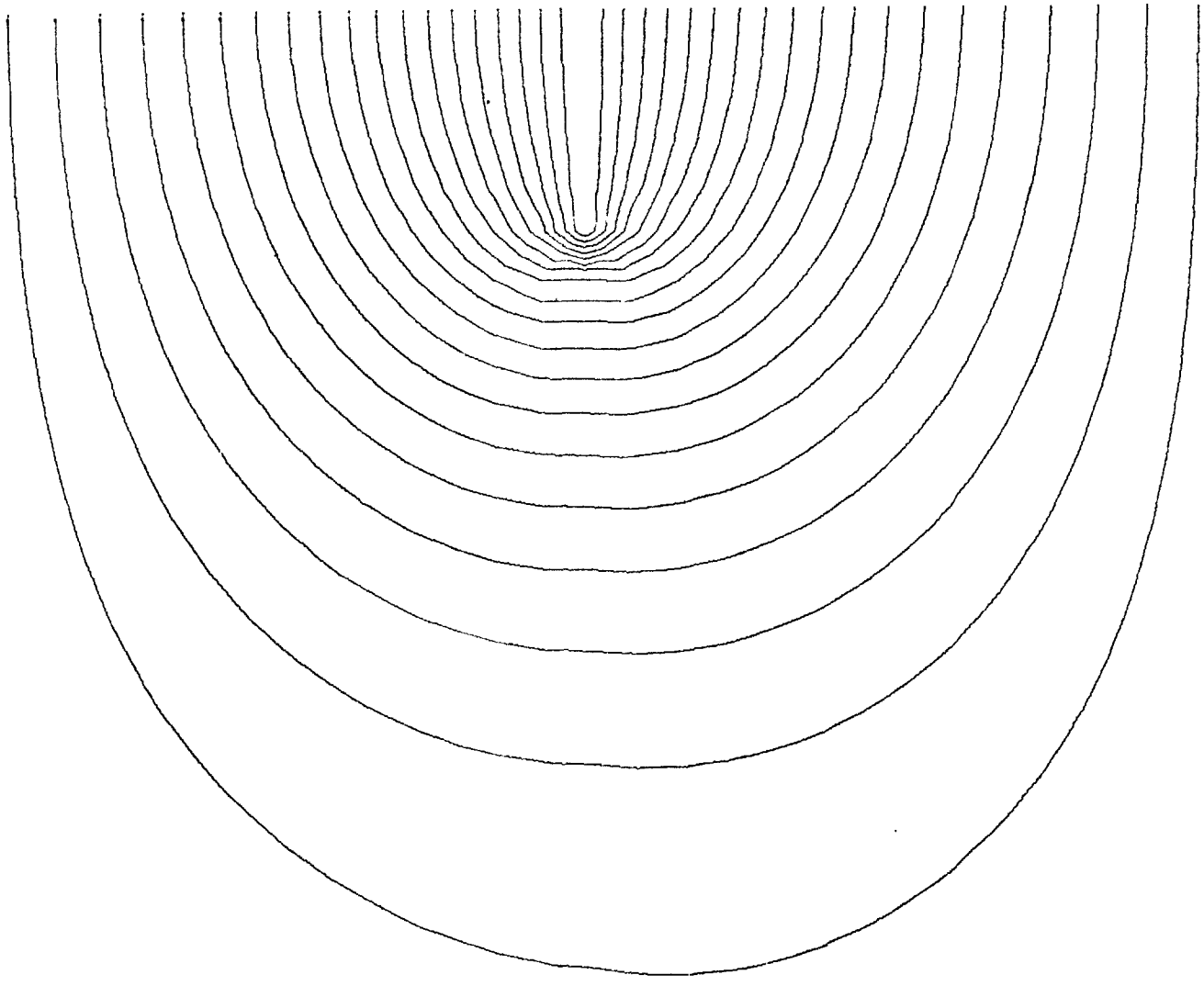
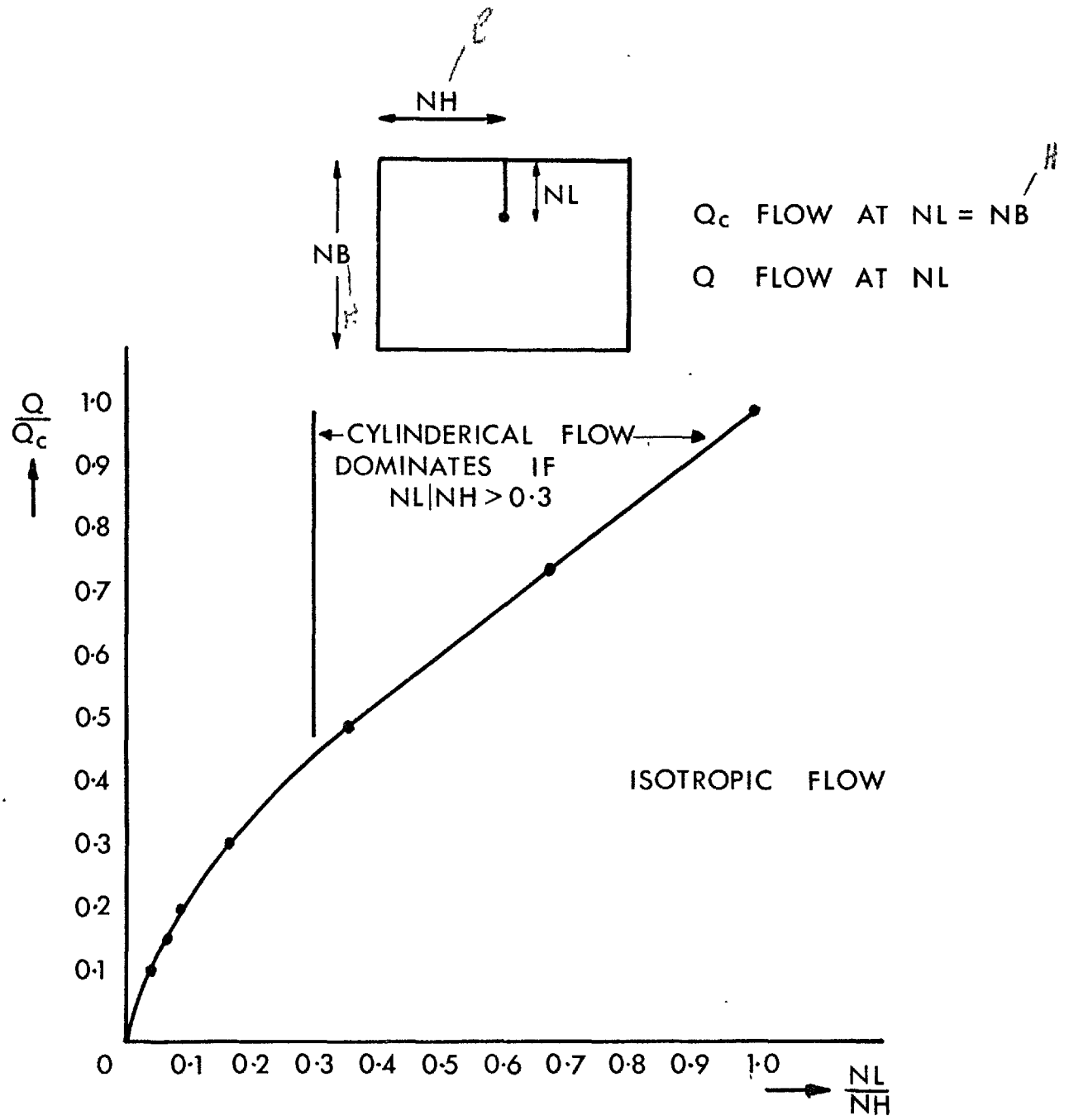
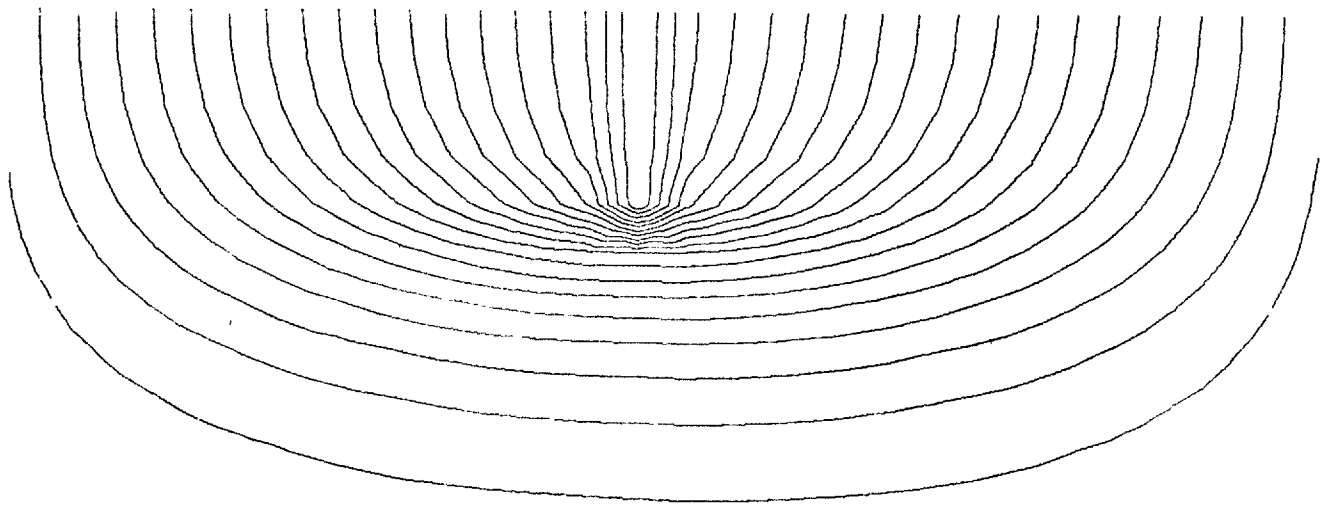


FIG. 3.13. Potential Distribution During a Pumping Test



DIMENSIONLESS PLOT TO SHOW INFLUENCE OF INCREASED PACKER SPACING

FIG 3·14



$K_X = 1$
$K_Y = 1/10$

FIG. 3.15.

Fig.3.13 is a typical result that was obtained from the computer analysis and shows lines of equipotential surrounding the borehole during a test. A visual examination of the contours shows the area which has predominantly cylindrical flow and that with spherical flow. An obvious way to produce predominantly cylindrical flow is to increase the packer spacing. Fig.3.14 shows such a phenomenon occurring when dimensionless flow from or to the borehole is plotted vs the distance between the packers. Initially the curve is non linear showing the complex interaction that must occur between the cylindrical and spherical components of flow. Once the ratio of NL/NH $\geq$ 0.3 the relationship becomes linear and flow is directly proportional to the surface area of the cavity; thereby indicating that the majority of the flow is cylindrical.

The same problem was repeated for the case of anisotropic flow. Fig.3.15 demonstrates a typical pressure or potential distribution when Kx/Ky = 10. The ratio NH/NL was varied as in the isotropic case. Fig.3.16 illustrates the relationship between dimensionless flow and packer spacing when Ky/Kx = 5. Unlike the isotropic case the curve is non-linear for almost the entire range, thus indicating the difficulty in obtaining a predominance of cylindrical flow. The obvious solution of increasing the packer spacing will not help in such a situation. Instead practical tools such as four packer systems can be tried to improve the situation (see Chapter 4).

3.3.2 DETERMINATION OF ANISOTROPY RATIO IN A TWO DIMENSIONLESS FISSURE SYSTEM.

The importance of anisotropy in nature cannot be over-emphasised. It's occurrence in the form of different fracture frequencies in different directions and or variations in apertures of fissures is more likely than not (7,15). Isotropic systems where fissure frequencies and apertures are identical are difficult to envisage. If anisotropy is so common, must there be an easy way of detecting it?

The simplest and most obvious way to determine the anisotropy in a model such as the one outlined in section 3.2.2 is to measure permeability of individual sets of fissures. The problem with this is that for an n fissure system, n holes are required - or very simply in a two fissure system, ie. bedding and orthogonal fissures, one requires two holes. The alternative for a highly complex fracture system where there is no pattern in the fissure directions, it is proposed that the method suggested by Snow is used (15). Numerical studies carried out on simple but anisotropic systems have yielded a method whereby anisotropy ratio can be arrived at by only one test. This model is theoretical and therefore any field application of it must be made with extreme caution. The model is justified on the basis that it provides insight into the mechanics of the problem.

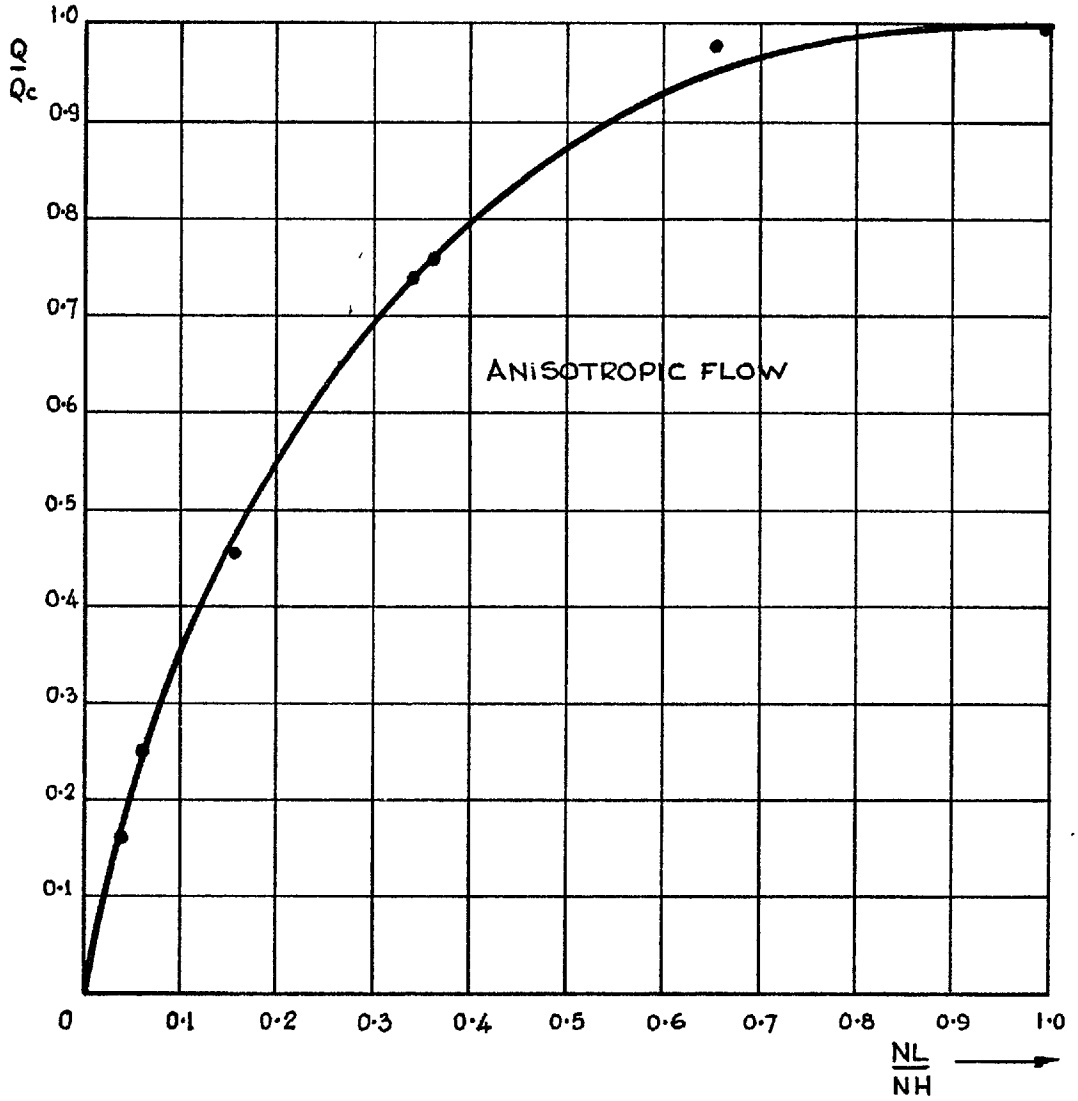


FIG 3.16 MODEL AS IN FIG 3.14

$K_Y / K_X = 5$

DIMENSIONLESS FLOW verses PERMEABILITY RATIO

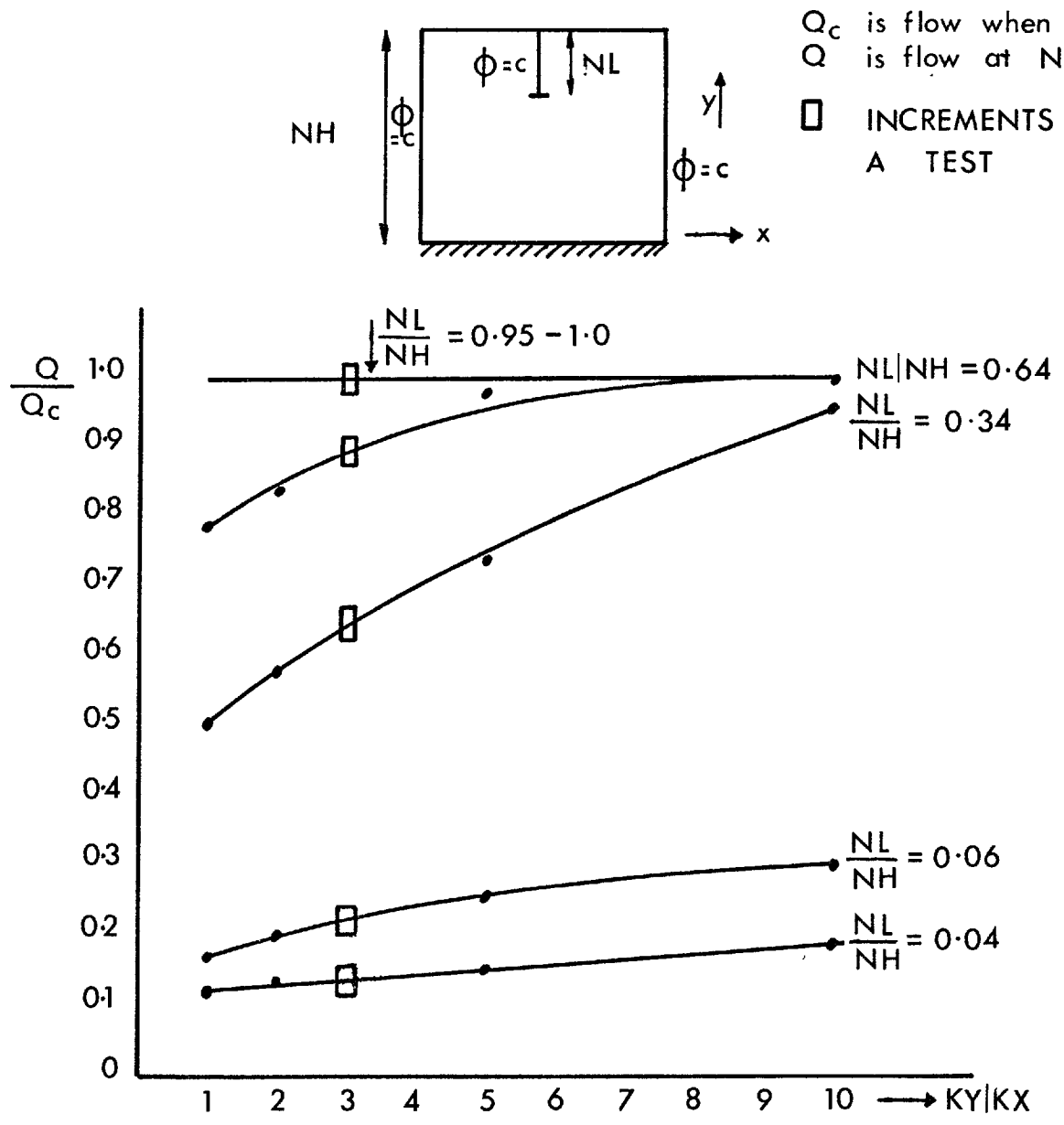


FIG 3·17

3.3.3 A SIMPLE ONE HOLE METHOD TO ESTIMATE THE DEGREE OF ANISOTROPY IN A TWO DIMENSIONAL SYSTEM.

It is proposed that a pumping out test is carried out in a hole which is perpendicular to at least one of the fissure sets. Depending on the mean spacing of the fissures, the first test is carried out with the minimum packer spacing, section 3.3.1. This spacing is then gradually increased in stages. Fig.3.17 illustrates the dimensionless flow into the cavity vs the ratio of principal permeabilities. A number of such curves are drawn for increased packer spacing or the ratio NL/NH. By allowing for different increments in packer spacing as indicated in Fig.3.17 and measuring the flow rate under a given head a series of points are obtained. The line joining these points should give an intercept on the x axis which is the ratio of permeability.

This method, although not totally rigorous gives an idea of whether the ratio of principal permeabilities is large or small. If it is large, it is proposed that tests are also carried out in boreholes orthogonal to each set, taking into account the number of fissures each time. In this way, the anisotropy can be obtained first on a global and secondly on a localised level. The global parameters being used in analysis where the rock mass is equated to some form of a continuum.

A large number of cases were considered, but not all of them are plotted for two reasons, in Fig.3.17. The first one being that it overcrowds the diagram and therefore makes the determination of the ratio of principal permeabilities confusing. Further in the field economic limitations make it impossible to carry out a vast amount of testing. It is interesting to note that all the curves lie on straight lines when plotted as log Q/Qc vs log Ky/Kx. For a value of $NL/NA < 0.06$ the curves can be reduced to a single line as shown in Fig.3.18. This obviously has the advantage that only one test is required to determine the ratio of principle permeability. Practical use of the above method is obviously limited; but it demonstrates the principle that lies behind the mechanics of the problem.

3.3.4 INFLUENCE OF TEST CAVITY SIZE ON PERMEABILITY VALUE

In Chapter 1 and 2 it has been suggested that the size of cavity used during a test could have an important bearing on the value of permeability. In soils for example, the size of cavity should make no difference, since the pores through which flow takes place are so very small compared to the size of the borehole. In a fissures media no simple law exists which describes the scale effect during a test.

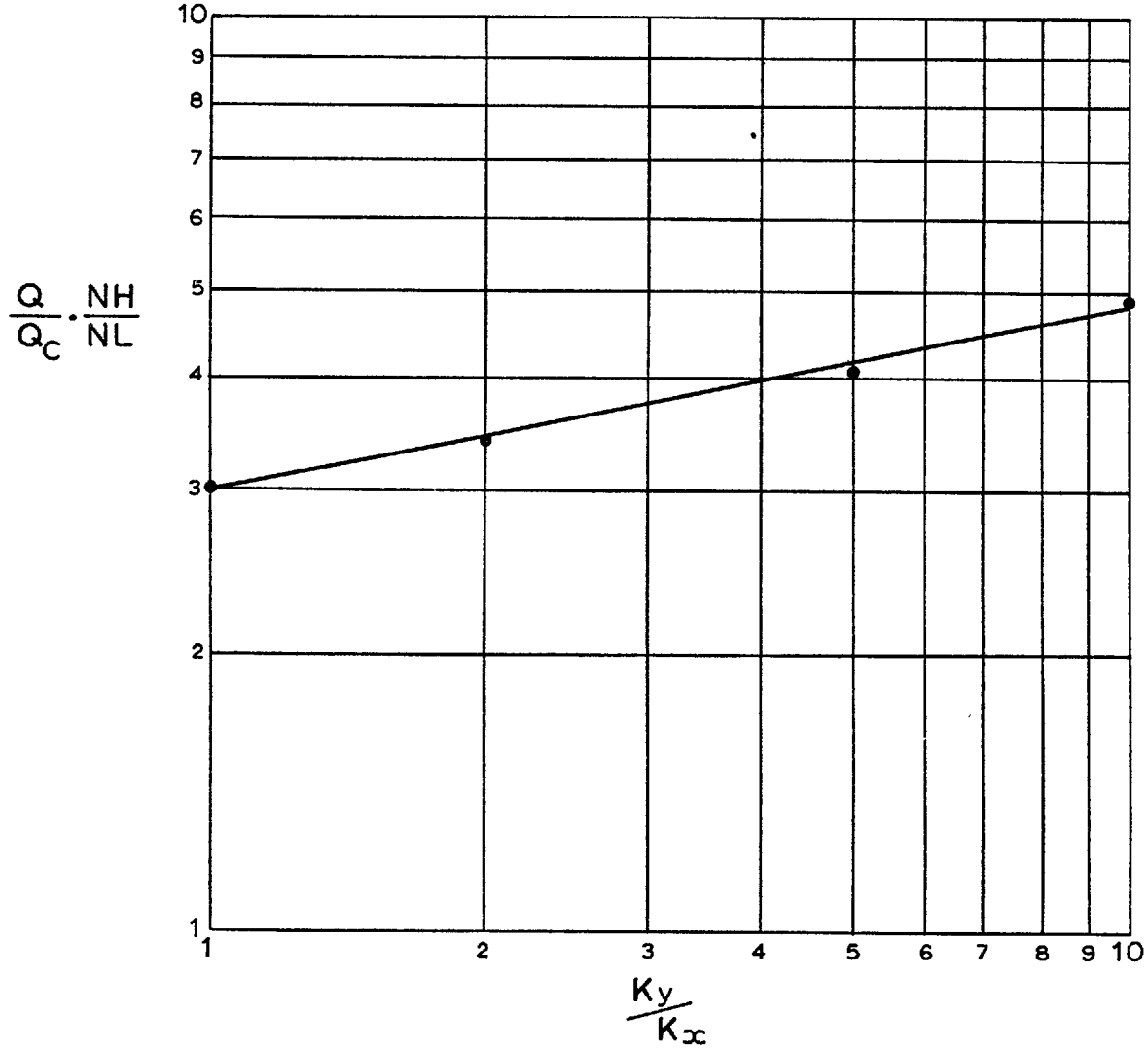


FIG. 3.18. General Method for Obtaining Ratio of Principle Permeabilities when $\frac{NL}{NH} < 0{\cdot}06$

In the oil industry attempts have been made to correlate the values of permeability obtained in the laboratory to those in the field. Warren and Price after an exhaustive approach and computer simulation arrive at the conclusion that permeability is well estimated by the geometric mean of individual measures. Snow (7) has considered this problem from the statistical angle suggesting that the permeability increases with the number of conductors as in Fig.3.19.

Before examining this phenomenon it is important to decide which concept of permeability is going to be used in the fissured media. From Eg.1.1.

$$K_s = \frac{Q\log e\ (^{r}2/r_1)}{2\pi L(P_1-P_2)}$$

where K_s system permeability other symbols defined before

Using the Discontinuum approach this equation is reqritten as

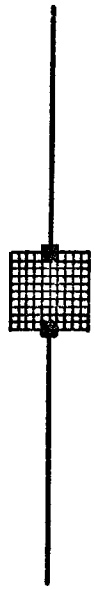
$$K_J = \frac{Q\log e\ (^{r}2/r_1)}{2\pi en(P_1-P_2)}$$

Assuming a fixed spacing between the packers an increase in n will obviously result in a decreased value of K/J. Alternatively, an increase in the number of fractures will give a higher value of K/S because:

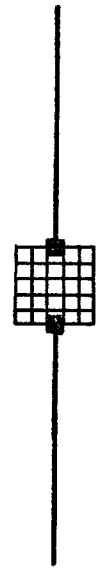
$enK_J = LK_s$ if e, K_J, L constant then increase in n will result in higher K_S

The permeability referred to by Snow is the system permeability and therefore the hypothesis that system permeability increases with the number of conductors could be correct.

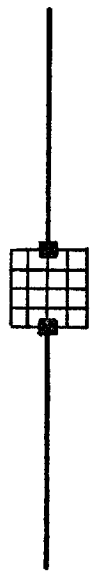
If the concept of system permeability is to be used, the test section should take account of the mean spacing between fissures. Consider Fig.3.19A which indicates that the joint frequency within the test cavity is 6 inches. Let us assume that the boundry of the test will be given by an area 36' x 36'. Diagram B to E illustrates how the fissure frequency is reduced in stages while the test section length is kept constant at 5ft. If the value of system permeability is evaluated in each case A to E it is observed that the value reduces as predicted by Snow. Computer simulations were made to test this concept while increasing the fissure frequency and the overall boundries of the problem. Fig.3.20 illustrates the result of such an analysis. The initial part of the curve is non-linear; but it soon becomes assymptotic to the final system permeability.



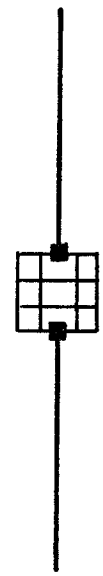
A



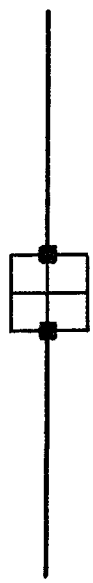
B



C



D



E

FIG 3.19A

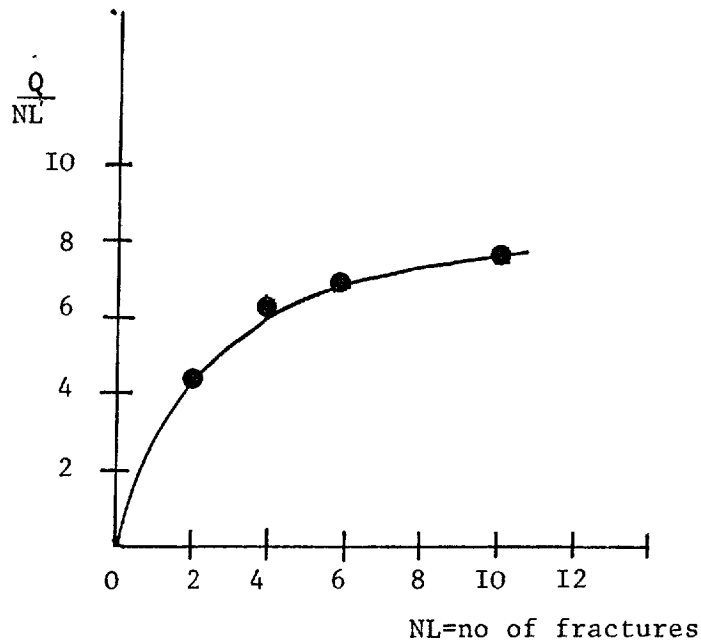
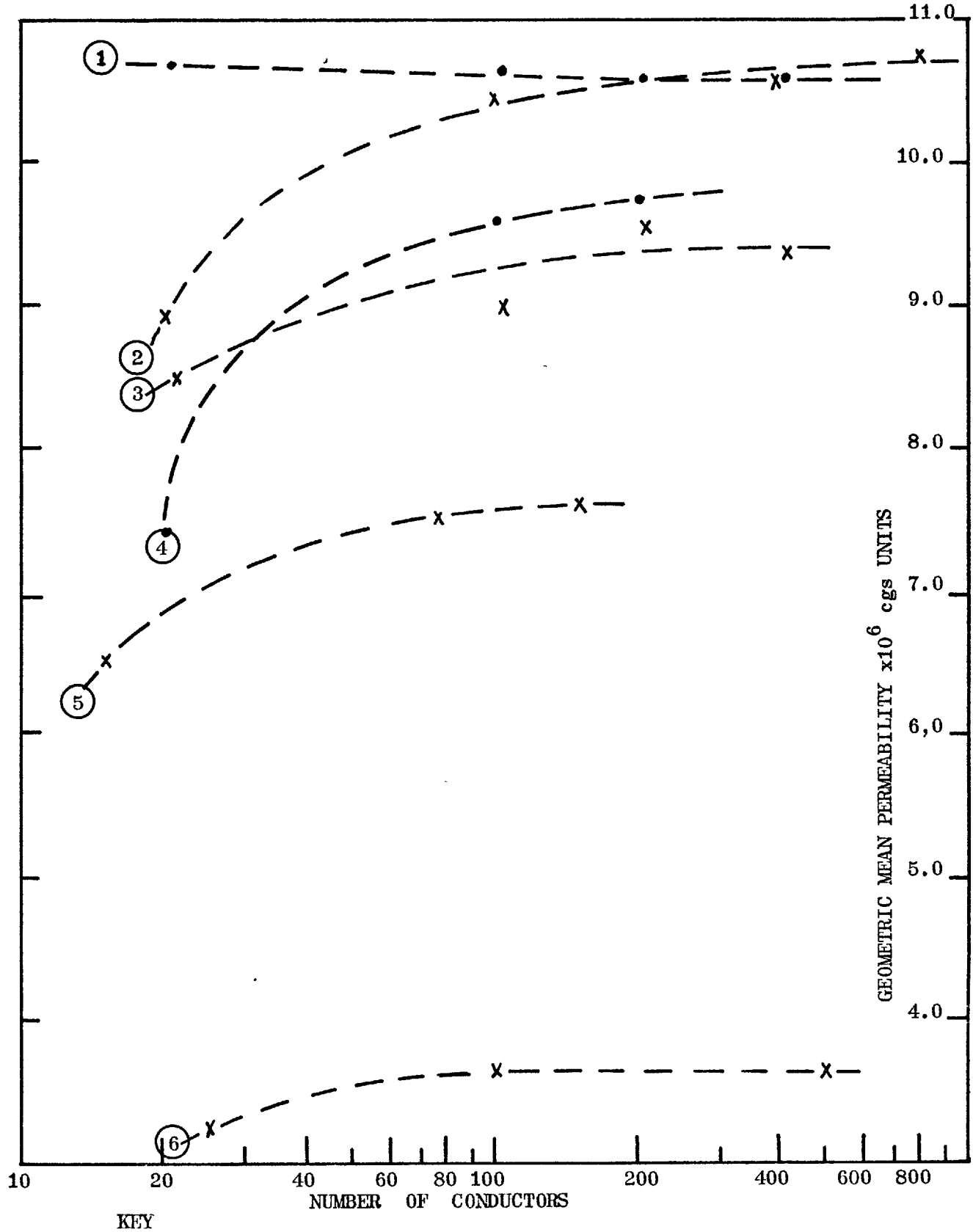


FIG 3.20



KEY

1 2 NORMAL SETS, DIFFERENT DISPERSIONS

2 2 EQUAL, NORMAL SETS

3 2 NON-NORMAL SETS, DIFFERENT DISPERSIONS

4 2 EQUAL NON-NORMAL SETS

5 2 NORMAL SETS, DIFFERENT SPACINGS

6 1 SET

FIG 3·19 SNOW

If system permeability is going to be used in the field obviously tests should be carried out with a changing packer spacing until an assympotòtic value of system permeability is obtained. This phenomenon which is predicted by the statistical and enumerative approach was observed in the field and is reported in Chapter 4.

Use of such a method in the field is, however, very difficult because the method relies on the fact that the fissures belong to the same family and therefore have roughly the same effective aperture and constant spacing. Very often cases occur in a sedimentary environment for example where the fissures occur in clusters each with different value of aperture and spacing. In such a case system permeability should be discarded and a numerical model built on the joint permeability values for each cluster, where the overall permeability of the cluster is given by the number of fissures x K_J.

Heterogenities can be built into the computer simulation of the test very easily. These can be in the form of anisotropy, impermeable boundaries etc.

3.3.5 INFLUENCE OF BOUNDARY CONDITIONS ON THE TEST

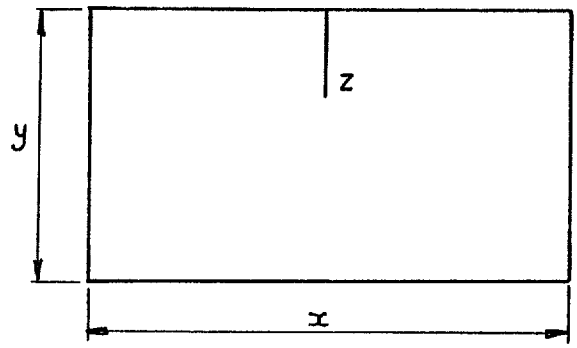


FIG 3.21

Fig.3.21 shows the numerical model in which the number of fissures that intersect Z the borehole remain constant while x and y are changed simultaneously.

Fig.3.22 shows how for different permeability ratios the boundary affects flow into or from a cavity. In most cases, after a ratio of $2R/L > 8$ very little change takes place in the total flowrate that leaves or enters the borehole.

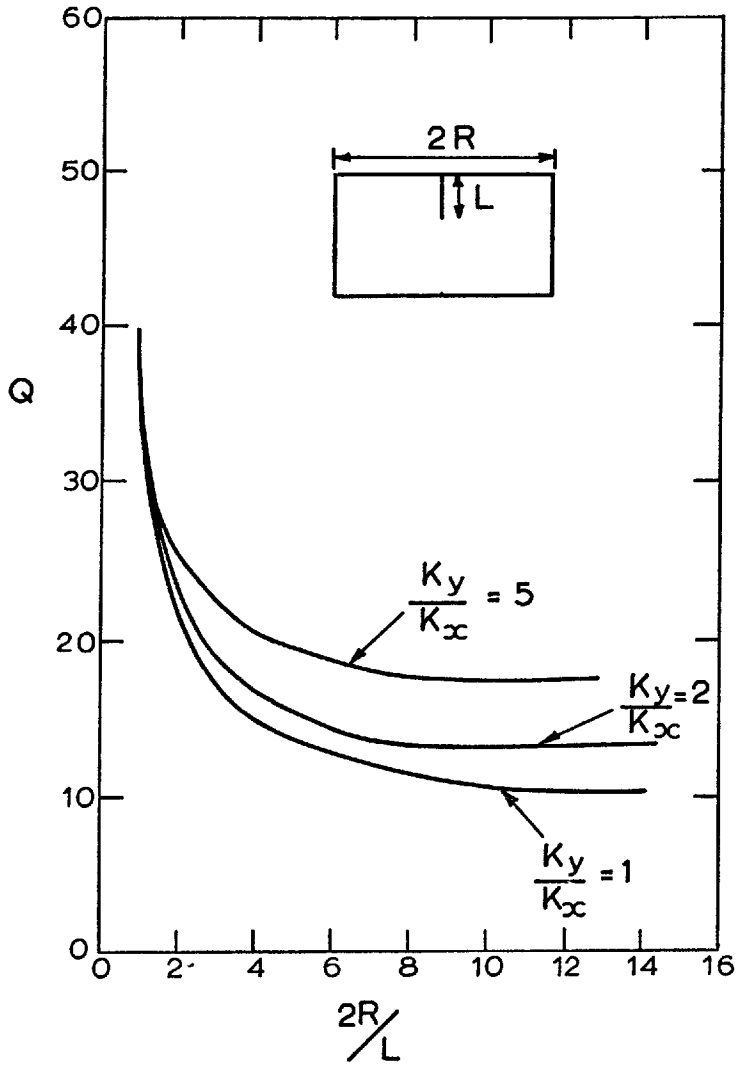


FIG. 3.22. Influence of Boundary on Flow into Bore Hole

This is important in deciding how long the test section should be in case the boundaries are nearby. Alternatively, it gives an indication of the importance of boundaries, such as dykes or faults in the vicinity of the test zone. If a situation exists whereby the fracture frequency is such that a long section is required and further if the boundaries are a bit too close, the various equations previously derived to determine permeability cannot be applied, since they are all based on the concept of an infinite aquifer. For such special cases the various criteria outlined in Chapter 3 should be recomputed using the programs which are listed in the appendix with changes to allow for the particular boundaries.

The case of a hole intersecting an arbitrary three dimensional fissure system has not been considered since it is felt that in the case of a close but random system it is best to use the methods proposed by Snow (15). However, for a fissure system where the spacing is larger, numerical modelling has not been attempted because most situations lend themselves readily to two dimensional study and further, the computer storage for a three dimensional problem is so enormous that it is rarely justified. A physical model was constructed for such a case and it will be dealt with in another section.

CONCLUSIONS

This chapter has exploited the use of numerical analysis to study fluid flow from a cavity into an anisotropic media. Analysis along these lines is virtually impossible with analytical methods, but the methods discussed so far have showed the ease with wich numerical models can deal with complicated situations.

The analysis shows that during a pressure test where water is being pumped into or out of a rock mass at least one observation hole is required in the isotropic case and two in the anisotropic case. Various dimensionless plots of pressure, flow and ratio of principal permeability in a given system are given so that (a) it is possible to understand the mechanics of the problem (b) comparisons can be made with field situations not to pin point answers but to study the sensitivity of different parameters. Methods are discussed for measuring the ratio of principal permeabilities in the plane of the fissures and also in systems where the anisotropy is caused by different sets of intersecting fissures.

Flow from a borehole into a two or three dimensional fissured media is a combination of cylindrical and spherical flow. This obviously leads to a value which is non-directional, unless the test takes this effect into consideration. In the isotropic case for example cylindrical flow begins to completely dominate if $NL/NH > 0.3$ where NL is half the test cavity size and NH is the distance from the test cavity to the impermeable barrier. Obviously this is not easy to obtain in practice and it is suggested that either $NL/NH > 0.15$ is used where a large amount of flow is cylindrical or the four packer system is used in such a case (see Chapter 4). In an anisotropic case it is virtually impossible to achieve cylindrical flow when the permeability in the direction parallel to the cavity is higher than in the orthogonal direction. In a field situation obviously a compromise has to be made in view of a large number of other factors which influence a test. The number of fissures that must be used to give a representative sample in a test are discussed. If the system concept of permeability is to be used it is suggested that pressure tests are carried out on the same family of fractures but with varying packer spacing until an assymptotic value for the system permeability is obtained for that one particular case. If on the other hand the concept joint permeability is to be used in a numerical model there is no further need to consider the scale effect because the value of joint permeability in such a model is always used in conjunction with a given number of fissures at a particular location.

LABORATORY EVALUATION OF PUMPING TESTS

SYNOPSIS

In Chapter 1, 2, 3 methods have been outlined to predict the permeability of a fissure system on the basis of results obtained from a pumping test in a borehole. It is proposed in this chapter to verify some of the equations which describe flow from a cavity into an idealised and a real fissure system. For the ideal case the model consists of smooth parallel perspex plates and the real situation is modelled by producing an exact geometrical replica of a porphyry fissure by using liquid araldite which sets hard at room temperature. Water is pumped either in or out of boreholes in the above models and the relationship between "pressure-flowrate" is studied at the borehole and within the flow field.

4.1.0 INTRODUCTION

The earliest and about the only physical modelling of flow from a cavity into a fissured medium has been carried out by Baker (5). Several attempts have been made by research workers to model flow from a borehole in a soil. Childs (12) has achieved a remarkable degree of success, while examination of the ASTM (20) shows the large degree of variation in the answers using different methods of obtaining permeability. The difficulty has been attributed largely to the difficulty in obtaining a reproducable packing or porosity in the model and the inaccuracies which are inherent in the methods themselves. Baker's model work consisted of proving the validity of the radial flow equations (Chapter 2) and also finding the region of turbulance, surrounding the borehole. Fig. 4.1 demonstrates the test outlay.

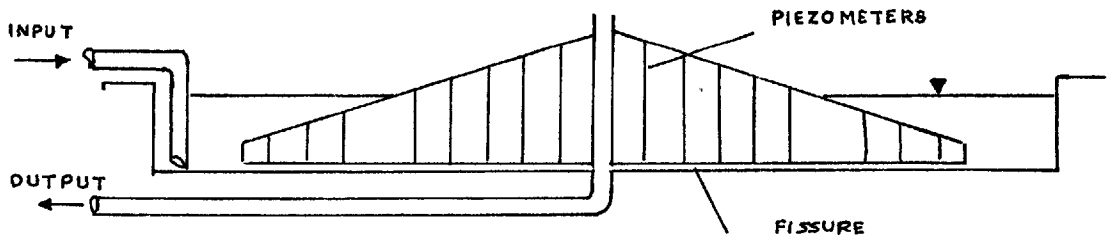


FIG 4.1

The model consisted of two concrete blocks 10ft. in diameter. The aperture of the fissure was varied from 0.05 inches to 0.4 inches. For different flowrates the pressure distribution was obtained. Fig.4.2 shows how rapid the drop is for a fissure system as opposed to a continuum in the radial direction. This has important implications in that it makes the test very much more difficult to analyse and also the radius of influence, or the area of representation of the test is reduced tremendously. For example, changes in aperture of the fissures at a radial distance 2 x diameter, makes little impression on the majority of the pressure drop in the test. Another factor that was highlighted by Baker's work was that large volumes of fluid were involved in the transport phenomenon. His theoretical and practical work shows that a fissure with an aperture of 0.01 inches is equivalent to 454ft. of unfissures formation having a uniform permeability of 100 millidarcys*. Baker's work shows the ease with which a fluid communicates in a fissure system in spite of the low fissure frequency provided there is an adequate interconnection in the system.

* *I Darcy* = 10^{-3} *cm/sec.*

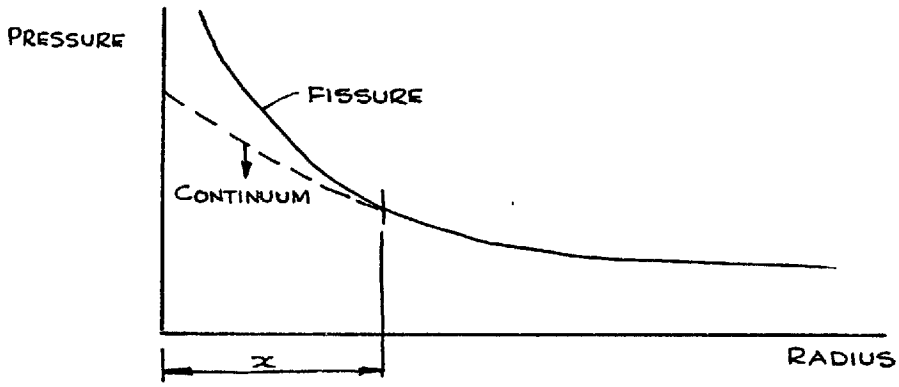


FIG 4.2

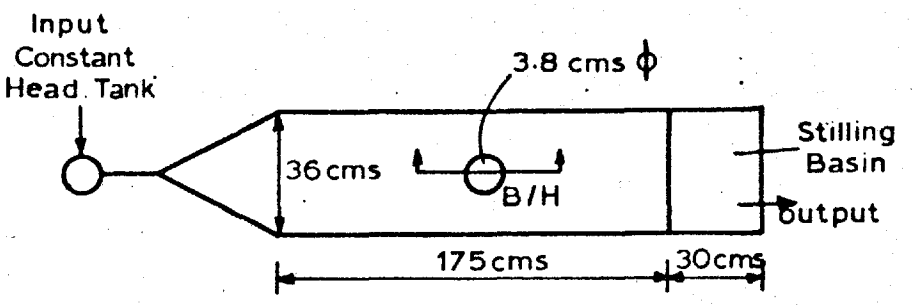
Since the flow from a cavity into a fissure can at best, be only approximated, and that badly in detail near the hole, it is best to physically model the situation. For this, two simple models were conceived. The first is a parallel plate model, but instead of using a "radial flow" situation, a fissure with a flow occurring due to a natural gradient is modelled, with a hole in the middle of the flow field. The second case is one in which an araldite model of a natural fissure is cast, giving the exact replica of the fissure topography, and then a hole is made into the fissure and tests carried out to simulate a real field situation. The second test is an extension of Baker's work by using real fissure surfaces. The object of this exercise is not to produce generalised laws; but to study the mechanics of the problem in one real but arbitrary situation.

4.1.1 PRESSURE TEST IN A FISSURE UNDER A NATURAL FLOW FIELD

Fig.4.3 illustrates the general outlay of the model; dimensions of which are given in Fig.4.4. The model material is perspex and the fissure is formed by two smooth parallel plates with a mean opening of 1.25 mm. The diameter of the hole is 3.8 cm. and the fissure is 36 cms. wide. The "fishtail" entry to the model together with the available length of the fissure prior to the borehole ensures that the turbulence is a minimum as flow enters the model via a circular pipe and then flows into a thin rectangular box section. An obvious problem with such a model is to maintain a constant fissure aperture of 1.25 mm. Care was taken during construction to maintain this opening but on examination after the tests were over showed that the aperture varied from about 1-1.25 mm. The sides of the model are considered as "no-flow" boundaries. Since the gradient is applied in only one direction, ie. parallel to the "no-flow" boundaries, the distance of the boundary from the hole is considered as adequate as regards interfering with the flow field.



FIG. 4.3. Influence of Bore Hole on Flow Field.



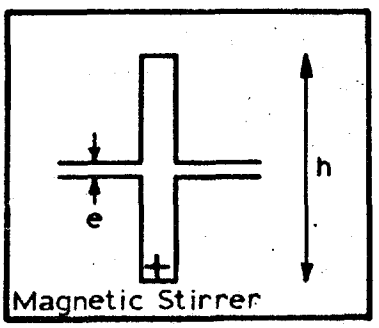


FIG. 4.4.

Different hydraulic gradients are applied and these resulted in different flowrates. Pumping tests are carried out under these different flow conditions once steady state is achieved in the model. (By steady state is meant that there is no change in flow-rate with time). Throughout the test the fluid temperature was measured.

4.1.2 TEST RESULTS

In Chapter 2, section 2.1.2 the pressure change as a result of flow into or out of a cavity in a fissure system is given by the following equation.

$$P = \frac{Q \log_e (r_1/r_o)}{2\pi K_J e n} + \frac{3Q}{20\pi^2 e^2 n^2 g} \left[\frac{1}{r_o^2} - \frac{1}{r_1^2} \right] \qquad (4.1)$$

or very simply: $P = AQ + BQ^2$ where A and B are friction and kinetic energy term constants respectively. In the presence of a flow field this is altered by (superposition in a linear system) to:

$$P = AQ + BQ^2 \pm \frac{QnL}{AK_J}$$

$\pm$ depending on whether the test is pumping in or out of the cavity.

Q' is flow in the fissure under natural gradient.

n = 1 no. of fissures

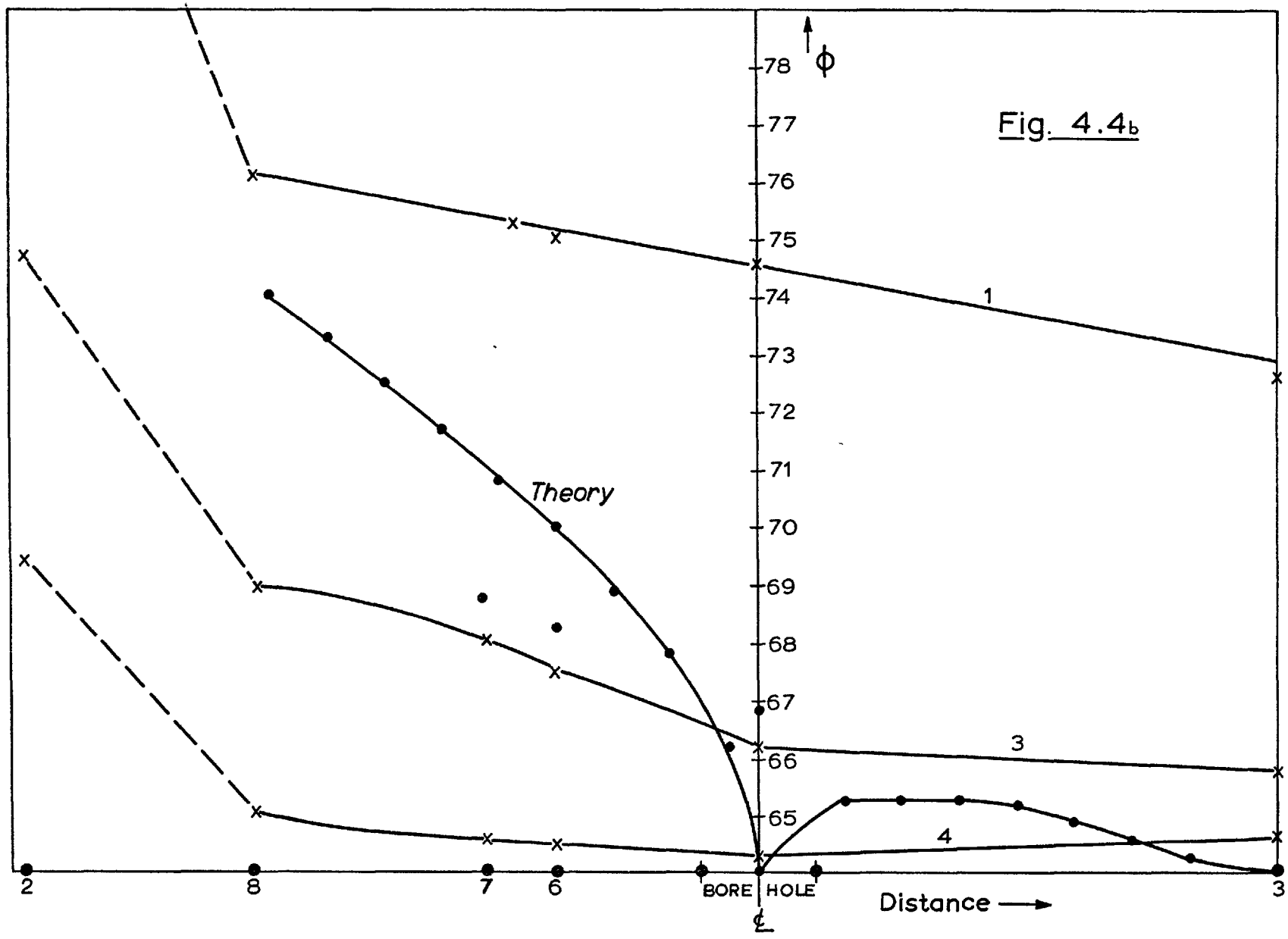
A = cross section area of fissure

K_J = permeability of fissure

where $\frac{Q'nL}{AK_J}$ is pressure drop due to flow in the fissure (Darcy's Law).

Numerous pumping out tests were carried out because it was found that it was easier to maintain a steady suction from the cavity rather than a steady supply. Fig.4.4bshows some of the results of the actual pressure distributions along the length of the model, ie. in the direction of the gradient. For a given constant flow-rate in the model pumping out is performed at three different steady rates.

Fig.4.5 shows the pressure distribution along the centre line in the direction of flow close to the hole. The problem was simulated with a computer model and it is clear from the diagram that the pressure drop is severe in the practical case within the vicinity of the hole. This difference is due to the fact that the kinetic energy terms as well as turbulence and non uniformity of flow are ignored in the computer simulation.


Fig. 4.4b
ϕ
78
77
76
75
74
73
72
71
70
69
68
67
66
65
1
3
4
Theory
2
8
7
6
BORE HOLE
℄
Distance
3

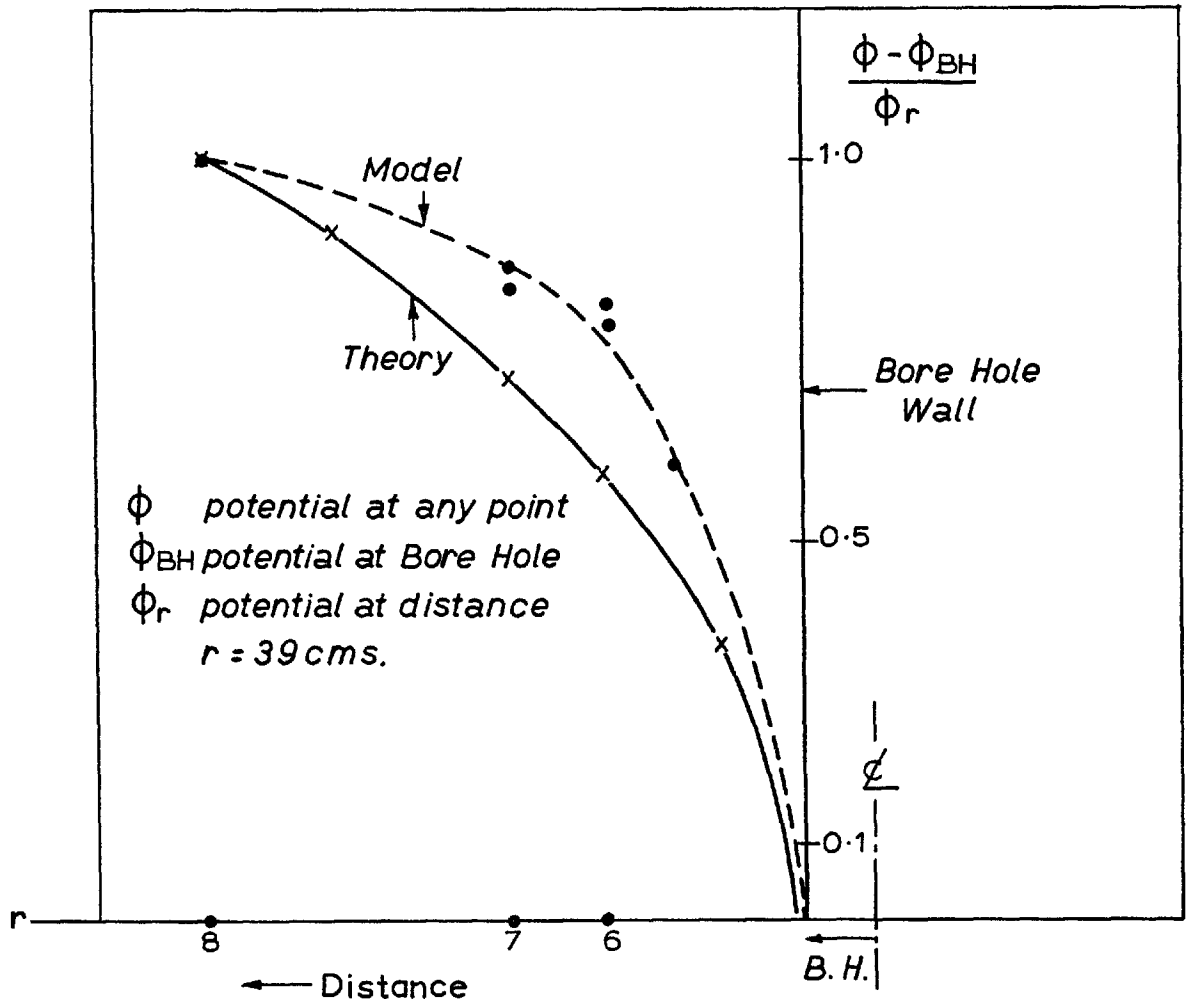


FIG. 4.5. Pumping Out Test Single Fissure

Further this experiment confirms the findings of Baker that the pressure drop is steep in a fissure system near the hole. In a continuum the decline of pressure would be much more gentle owing to a larger available surface area and lower velocities.

One of the tests has been considered in detail. Numerical calculations have been carried out to test (i) the validity of the assumptions in Chapter 2 and equation 4.2. (ii) the magnitude of the different components. (iii) to calculate permeability from a pumping test and compare it with the theoretical value and also one obtained by applying Darcy's Law directly, since the flowrate, cross-sectional area and gradient are known.

Q' = flowrate under natural gradient = 45 cc/sec.

Q = flowrate during pumping test from B/H = 22 cc/sec.
Pressure at hole with no pumping out = 74.6 cms. Head of H_2O

Pressure at hole during pumping out = 64.3 cms. Head of H_2O

Net pressure drop = 10.3 cms. Head of H_2O

Frictional component due to radial flow =

$$\frac{Q\log_e(r_1/r_0)}{2\pi e K_J} = 0.89 \text{ cms.}$$

where $(K_J = \frac{e^2 g}{12U})$

and U = kinematic viscosity

K_J = 111.0 cm/sec. @ 15 deg.C.

$\log_e(r_1/r_0) = 3.5.$

Kinetic energy component $= \frac{3Q^2}{20\pi^2 e^2 g} \quad (1/r_1 2 - 1/r_0 2)$

Cross section area of fissure = 4.5 cm^2, L = 127 cm.

Pressure drop prior to pumping out in the fissure = $\frac{Q'nL}{AK_J}$

= 11.5 cms.

From Equation 4.2.

$$P = AQ + BQ^2 \pm \frac{Q'nL}{AK_J}$$

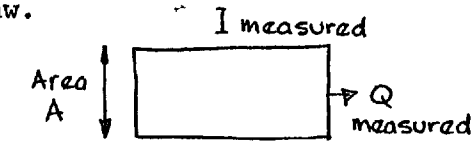
= 0.89 + 0.13 - 11.5 = 10.48 cms.

Measured pressure drop at the hole = -10.3cms.

These results indicate two things. The first is that the pressure drop due to the kinetic energy term is significant compared to the frictional term. Secondly, the use of the complete expression in Equation 4.2 gives an extremely accurate picture of what is happening.

COMPARISON OF PERMEABILITY VALUES

(A) Value based on Poiseiulle's Law.



$$Q = A K_J I$$

$$I = 1/36$$

$$K_J = \frac{Q}{AI} = \frac{23.4 \times 36}{4.5 \times 1} = 187 \text{ cm/sec}$$

(B) Value based on Theoretical model.

$$K_J = \frac{e^2 g}{12V} = \frac{1.55 \times 10^{-2} \times 980}{12 \times 1.15 \times 10^{-2}} = 111 \text{ cm/sec.}$$

(C) Value based on Pumping Test (Lugeon Type).

$$P = -\frac{Q \log_e (r_1/r_0)}{2\pi e K_J} + \frac{Q n L}{A K_J}$$

$$11.5 - 10.3 = AQ$$

$$\therefore \frac{Q \log_e (r_1/r_0)}{2\pi e K_J} = 1.2$$

$$\therefore K_J = \frac{22 \times 3.5}{2\pi \times 1.25 \times 10^{-1} \times 1.2} = 81.5 \text{ cm/sec.}$$

(D) Value K based on Modified Pumping Test.

$$P = -AQ - BQ^2 + \frac{Q' n L}{A K_J}$$

$$1.2 = -\frac{Q \log_e (r_1/r_0)}{2\pi e K_J} - \frac{3Q^2}{20\pi^2 e^2 g} \left[\frac{1}{r_0^2} - \frac{1}{r_1^2}\right]$$

$$1.2 = -\frac{22 \times 3.5}{2\pi \times 1.25 \times 10^{-1} K_J} - 0.13$$

$$\therefore K_J = \frac{22 \times 3.5}{2\pi \times 1.25 \times 10^{-1} \times 1.07} = 92.5 \text{ cm/sec}$$

Summary of Permeability Values

(A) Direct Estimate	187	cm/sec.
(B) Theoretical Value	111	
(C) Pumping Test, Lugeon	81.5	
(D) Pumping Test Modified	92.5	

From these values it can be seen how the permeability varies even for a uniform fissure. The first value is assumed to be the correct one. The Lugeon test gives a very much smaller value whereas the modified Lugeon is nearer the first value, because of the inclusion of the Kinetic Energy term. The theoretical value is so small because there may be errors due to variations in the fissure opening. Small errors in the aperture term can lead to large errors in permeability.

4.2.1 PRESSURE TEST IN A MODEL FISSURE

Analytical solutions for the case of flow from a cavity into a fissure system have been derived in Chapter 2. The case of more complex boundary conditions are outlined in Chapter 3. In section 4.1.1 experimental work has proved the validity of some of the mathematical expressions. Having established the basis of a theory for testing under ideal conditions the method should be applied to real fissures. Since large rock samples can be so cumbersome in the laboratory in terms of weight, machining, cutting and drilling without disturbing the two mating surfaces of a fissure an alternative was sought which would cut down some of these problems.

The important factor which controls the relationship between pressure and flowrate at low stress levels in the geometry of the fissure surface. (8,9,10). Therefore if we can reproduce the surface exactly it does not matter what the material is as long as it is stable. Liquid araldite which sets at room temperature takes the shape of the cast it is moulded in without much shrinkage. Further it has the advantage that the finished replica is completely transparent. This is extremely useful in experiments on fluid flow because it is possible to visualise the streamlines to see whether the flow is laminar or turbulent and also how the "dead water" areas change with applied gradient.

In this experiment the model fracture is cast from a fissure in Porphyry which has already been tested in a direct shear machine. The model fracture consisted of two castings. The first cast is made by pouring liquid araldite on to the porphyry fissure and allowing it to set. Once set it is easy to tear it away without damaging the surface. The first cast flow acted as a mould for the second casting. The above procedure is repeated after suitable lubrication of the surface. As a result of the two castings two halves of a fissure are obtained which perfectly match each other (see Fig.4.6) and Fig.4.7 . Fig. 4.7 illustrates the actual fissure used.

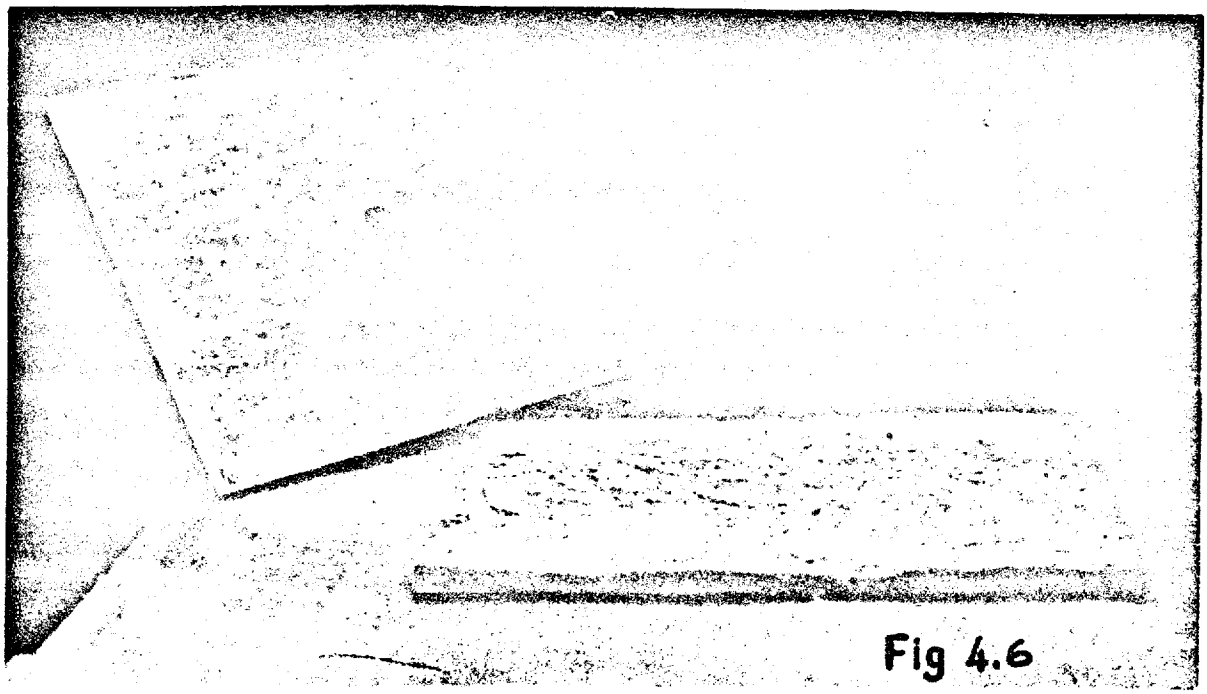


Fig 4.6

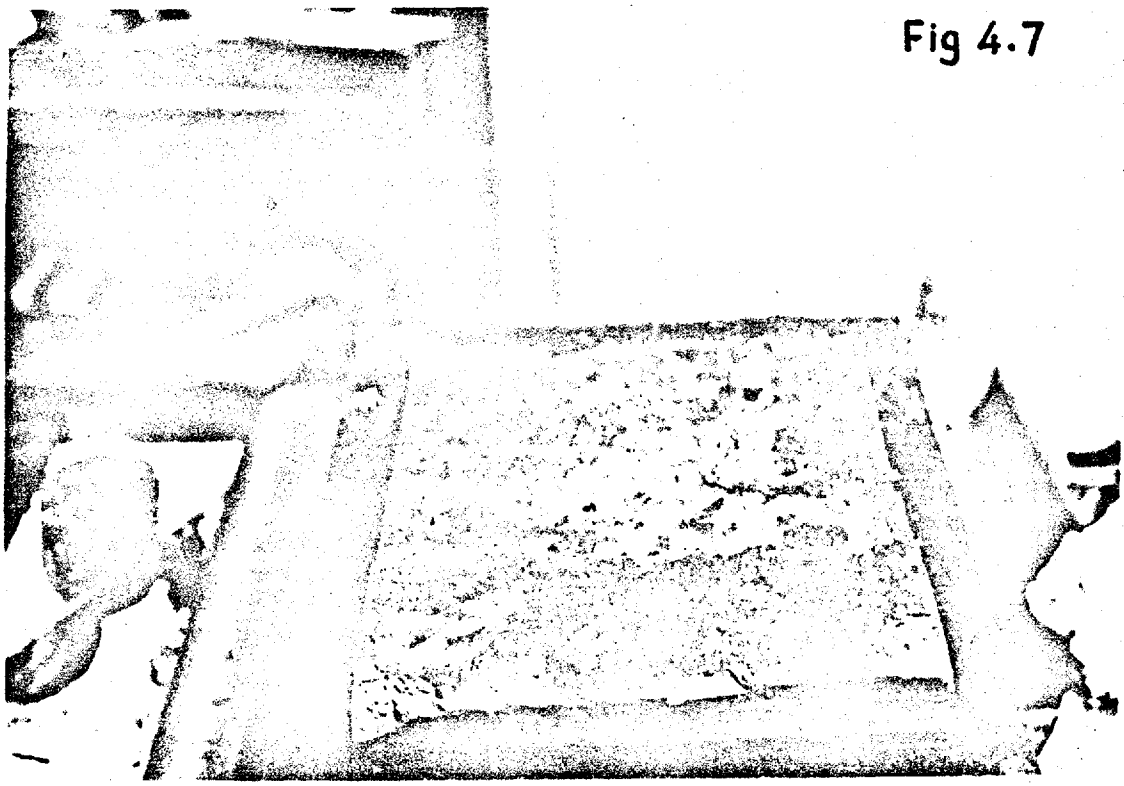


Fig 4.7

Since equations of radial flow are to be examined in the case of a real fissure the model has a circular outer boundary with a borehole in the middle. The radius of the outer boundary is 12 cms. and the radius of the borehole is 1.25 cms. The aperture of the fissure cannot be measured since it represents a rough surface with a wide spectrum of values. Only an estimate can be made indirectly from the relationship between pressure and flowrate.

During an experiment the aperture of the model can be fixed by a mechanism which consists of adjusting screws which separate the two halves of the model. Input into the borehole consists of water supply from a constant head device via a needle valve. The output from the model consists of flow through the fissure into a stilling basin, ie. the output is always submerged so that a constant back pressure is applied.

One of the test results will be dealt with in detail to illustrate the mechanics of the problem.

4.2.2 TEST RESULTS

A constant pressure of 5.7 cms. head of water was applied at the borehole and pressures were monitored at several different positions which all lay on concentric circles. As has been described in Chapter 2 and 3 the pressure drop is very sudden and most of it occurs with a few radii of the hole as in Fig.4.9. This further confirms the previous tests in section 4.1.0. There is a slight difference in pressures in the observation points along any one concentric circle. This indicates that there is a certain amount of anisotropy in the flow system as a result of the shearing of the model. Evidence of the anisotropy can also be observed in Fig.4.8 where a coloured dye was introduced into, firstly, the middle section, where it can be seen that the fluid front is far from being circular and hence isotropic, and secondly, the streamlines are not radial but have a definite bend in the direction of anisotropy. From this test, it is further proposed to calculate:

(a) the permeability of the fissure
(b) the ratio of principal permeabilities
(c) comparison of permeability value with non-steady state solutions.

(a) Permeability of the Model Fissure from a Constant Pressure Test

Since the applied pressure is so small (6 cms. head of water) we can assume linear conditions: from Equation No.3, Chapter 2, Section 2.1.0.

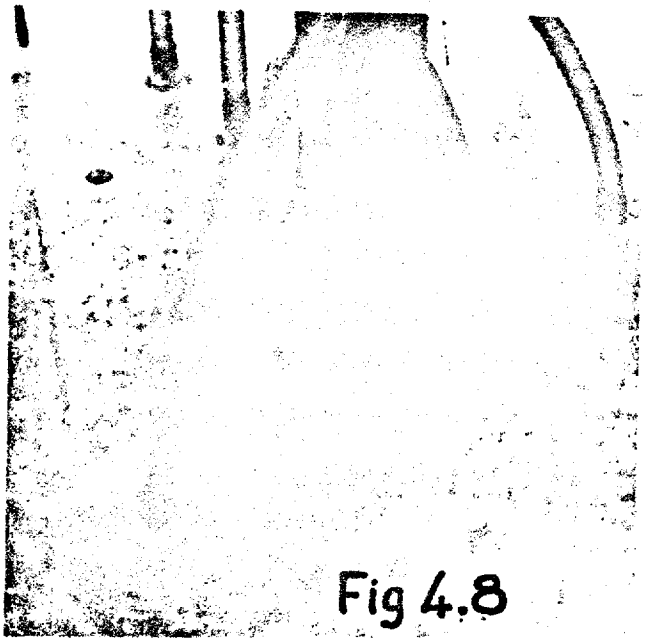


Fig 4.8



Fig 4.8

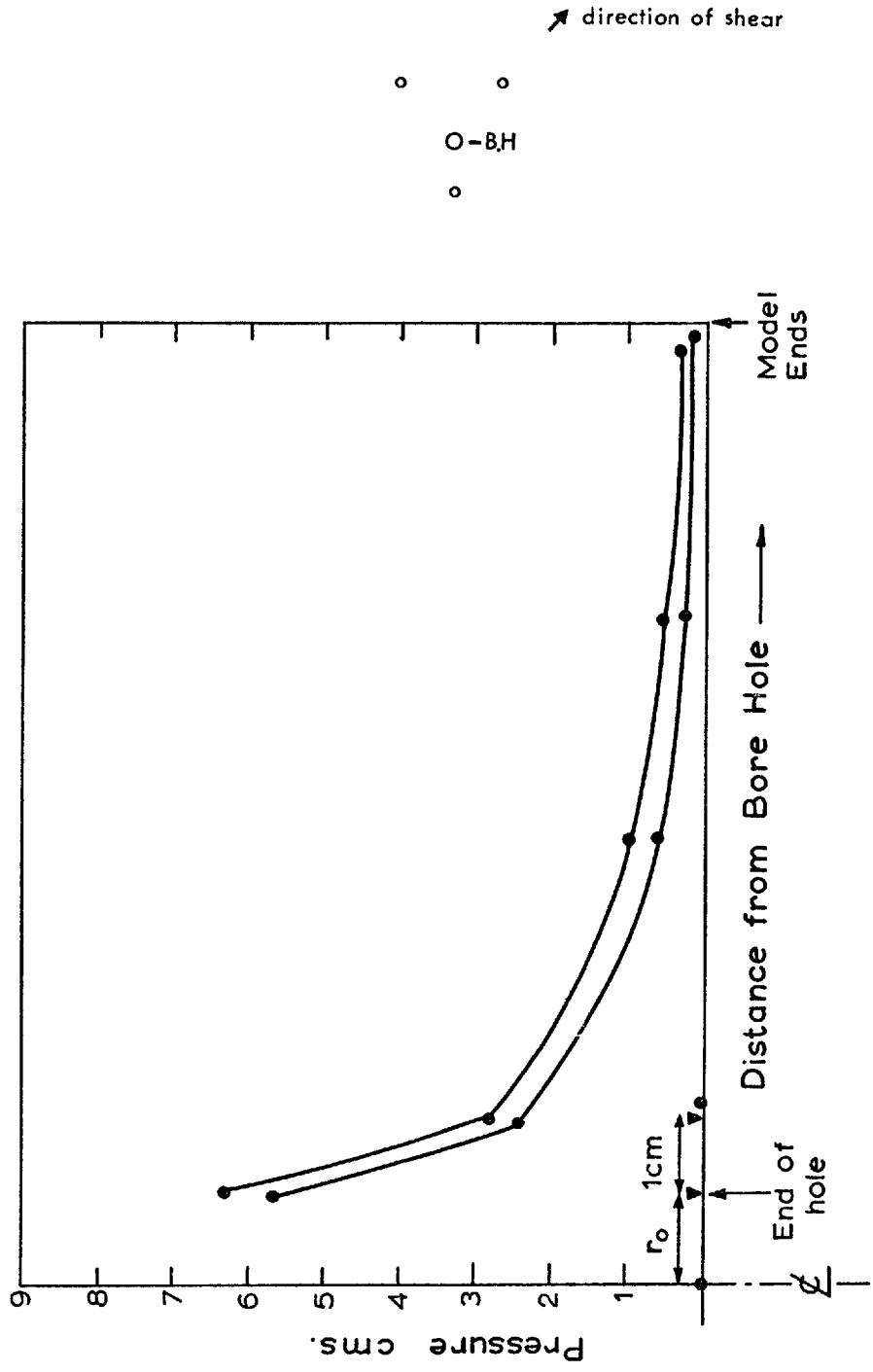

direction of shear
O-B.H
Model Ends
Distance from Bore Hole
End of hole
1cm
r_o
Pressure cms.
1
2
3
4
5
6
7
8
9

FIG. 4.9.

$$Q = \left[\frac{2\pi e K_J}{\log_e (r_1/r_o)}\right] (P_o - P_1)$$

Q Measured = 4/9 cc/sec.

$(P_o - P_1)$ measured = 5.7 cms.

$$eK_J = \frac{4 \times \log_e (\frac{12.5}{1.25})}{9 \times 2 \times \times 5.7} = 2.85 \times 10^{-2} \text{ cm}^2/\text{sec.}$$

K_J for an equivalent parallel plate is given by

$$K_J = \frac{e^2 g}{12V}$$

$$\frac{e^3 g}{12V} = 2.85 \times 10^{-2}$$

$$e^3 = \frac{2.85 \times 10^{-2} \times 12 \times 1.15 \times 10^{-2}}{980} = 4.0 \times 10^{-6}$$

$$e = 1.58 \times 10^{-2} \text{ cms.}$$

$$e = 0.158 \text{ mm.}$$

In section 2.1.5 a formular for radius of influence was quoted from Sichardt which was reported in Sharp (9). It is proposed to test this equation in the following example.

Radius of influence from equation 1, section 2.1.5.

$$r_e = 3000 (\phi_o - \phi_e) \sqrt{K}$$

$$= 3000 \times 5.7 \times \sqrt{1.2}$$

$$\triangleq 1.7 \times 10^4 \text{ cm.}$$

where ϕ is the potential in cms

K is the permeability in Cm/sec

This does not seem to be correct for the model. The pressure drop is considerably more severe in a fissure system compared to a homogeneous material and therefore the use of such a formula will give a conservative estimate of r/e. Since it is fairly empirical and not experimentally or theoretically justified in a fissure system it is proposed that this formula is not used at all, rather suppliemntary holes should be made to ascertain the pressure drop away from the hole. The presence of supplimentary holes will not only give an estimate of radius of influence, but they provide more control in the evaluation of permeability. The water levels in the observation wells during pumping provide a good indication of anisotropy and also can be used for tracer tests.

(b) The Degree of Anisotropy

As outlined in Section 3.1.5 the detection of anisotropy is very important in pumping tests. The ratios of pressures along any concentric circle (with centre at BH) should give a value of unity for the case of isotropic flow. Any deviation from this suggests anisotropy. A very simple method is outlined in section 3.1.5 where this estimate of anisotropy can be made.

In Fig.4. 9 the direction of shearing of the specimen is shown, this is the direction in which the lineations lie, and therefore, from a pure geometrical argument there should be a certain degree of anisotropy. Pressures were measured of points 1, 2, 3 (see Fig.4.10) and from the experiment:

$$\frac{\phi_2}{\phi_3} = \frac{2.2}{2.8} = 0.785.$$

substitute this value in Fig.3.9 r = r/o assuming that the direction of shearing is one of the principal directions.

$$\frac{K_1}{K_2} = 1.6$$

The ratio of max/min. principal permeability is approximately 1.6. It must be emphasised that this is an excercise to show how anisotropy can be obtained from a simple test. The result of such a simple application of theory agrees well with the observation in that the greatest amount of flow was in the direction of maximum permeability. It does not provide a universal law for application under any field condition. To obtain a more accurate estimate in the field each problem should be modelled in detail.

CONCLUSION

The equations of flow from a borehole into a parallel plate model in the presence of a natural flow field have been shown to be correct. Owing to the fairly high velocities involved in this model the kinetic energy terms had to be included for the predicted answers to agree with experimental verification. This experiment also showed the large amount of pressure drop that occurs in the vicinity of the borehole as had been predicted in Chapter 2 and 3. Radial flow equations have successfully been applied to the case of a real fissure and it has been demonstrated how it is possible to obtain the ratio of principal permeability using the results of the numerical analysis in Chapter 3. The result of such anisotropy was demonstrated by using coloured dye during a test. Once again in the case of a real fissure it is possible to show that the majority of pressure drop occurs close to the borehole.

NON STEADY STATE FLOW-AXISYMMETRIC CASE

SYNOPSIS

The falling head test is very popular for the determination of permeability due to its ease of execution. Solutions exist for the falling head test as carried out in open holes in a soil mass where the flow takes place either through the bottom of the hole if the sides of the hole are lined or it can be a combination of flow through the bottom and sides of the hole. If the hole penetrates a very short distance into the aquifer the flow is spherical and if it fully penetrates the aquifer as far as the impermeable boundary the flow is essentially cylinderical from the cavity. Further the solutions are for tests carried out below the water table and shape factors are used to correct for the size and shape of the cavity relative to the boundary conditions.

A falling head test in a fissured rock mass is a very special case owing to the geometry of the system. Equations are derived for the case where the borehole intersects the fissures orthogonally so that it is possible to calculate permeability from a falling head test data. The different boundary conditions considered are (a) unsaturated fissures of infinite radial extent (b) saturated fissures of a known finite dimension. Model tests are carried out to test the validity of the equations. Field results are reported in Chapter 4, part III.

5.1.0 FIELD OF APPLICATION

Investigation into unsteady seepage began at the time of Boussinesq (2) and it is one of the most difficult problems in the theory seepage. Unsteady or transient conditions can exist in two ways. The first, is the case of incompressible fluid where the boundaries change, eg. variations in flowrate, depletion of head or rainfall. The second case is where the compressibility of the fluid causes transient conditions. Here time enters as an independent variable. In the solution to the first type of problem it must be assumed that at each instantaneous time step pressure distribution and flowrate will correspond to the boundary conditions at that instant, as if these conditions had been maintained for an infinitely long time.

The second type of problem where the compressibility of the fluid causes transient conditions has been studied in great detail by the petroleum engineers (26, 27). Very rarely are civil engineering or mining problems at depths comparable to those in petroleum engineering and consequently at a low stress level, and therefore for purposes of analysis, water is assumed to be incompressible. The first approach when determining permeability is commonly referred to as the falling head test. In such a test the borehole is filled with water and the drop in level monitored with respect to time.

The falling head test was originally derived for the case of flow through a permeameter where the flow is one dimensional (29). This was further extended to the case of flow in a cased borehole where the flow field is entirely spherical. In practice a large number of holes exist which are not cased so that flow can occur from the sides of the cavity. It is proposed to derive analytical equations which describe the radial phenomenon in a fissure system. However, to fully appreciate the difference in the two methods and for the sake of completeness the spherical flow equation is also derived.

5.1.1 FALLING HEAD TEST: CASED HOLE BELOW G.W.T.

The following assumptions are made:

(a) The medium is homogenious
(b) Flow from the cavity is hemispherical Fig. 5.1
(c) Darcy's law holds
(d) Test is carried out below the groundwater table.

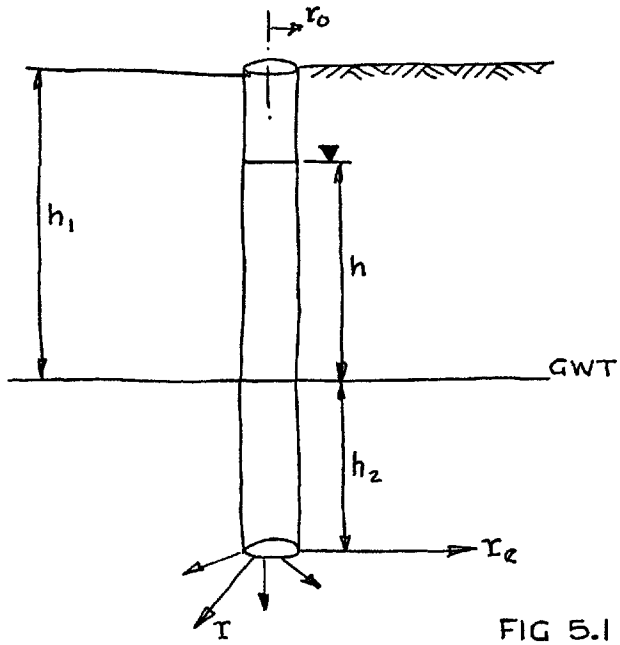


FIG 5.1

If we assume hemispherical flow and use Darcy's law at a distance and from the bottom

$$Q = -2\pi r^2 K \frac{dh}{dr}$$

$$\therefore \frac{dh}{dr} = -\frac{Q}{2\pi r^2 K}$$

$$\int_0^h dh = -\int_{r_o}^{r_e} \frac{Q}{2\pi r^2 K} \qquad \therefore h = \frac{Q}{2\pi r_o K} - \frac{Q}{2\pi r_e K} = \frac{Q}{2\pi K}\left[\frac{1}{r_o} - \frac{1}{r_e}\right]$$

Rate of change of water level in the hole

$$Q = \pi r_o^2 \frac{dh}{dt}$$

$$\therefore h = \frac{\pi r_o^2}{2\pi K}\frac{dh}{dt}\left[\frac{1}{r_o} - \frac{1}{r_e}\right] \qquad \int_{h_1}^{h_2} \frac{dh}{h} = \frac{2\pi K}{\pi r_o^2}\left[\frac{r_o r_e}{r_e - r_o}\right]\int_{t_1}^{t_2} dt$$

$$\log_e\left(\frac{h_2}{h_1}\right) = \frac{2K}{r_o}\left[\frac{r_e}{r_e - r_o}\right](t_2 - t_1) = \frac{2K}{r_o}\left[\frac{1}{1 - \frac{r_o}{r_e}}\right](t_2 - t_1)$$

5.I.2 Falling head test carried out when test section is below the groundwater table.

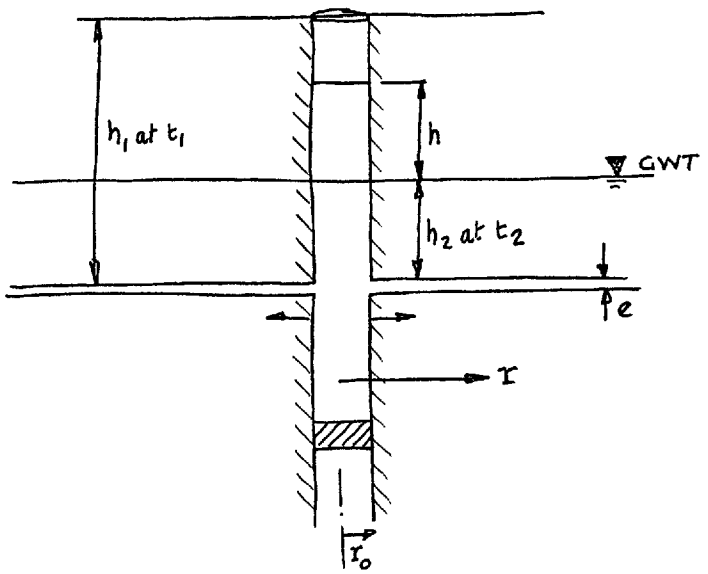


FIG 5.2

If we assume radial flow in the fracture and we use Darcy's law at a distance r

$$Q = -2\pi r e K_J \frac{dh}{dr}$$

$$\therefore \int_0^h dh = -\frac{Q}{2\pi e K_J} \int_{r_o}^{r_e} \frac{dr}{r}$$

$$h = \frac{Q}{2\pi e K_J} \log_e \left(r_o/r_e\right)$$

$$h = \frac{Q}{2\pi e K_J} \log_e \left(r_e/r_o\right)$$

Kg = joint conductivity

$= \frac{e^2 g}{12\upsilon}$

e = mean aperture of the fissure

rate of change of water level in the hole = $Q = \pi r_o^2 \frac{dh}{dt}$

$$\therefore \quad h = \frac{\pi r_o^2}{2\pi e K_J} \frac{dh}{dt} \log_e \left(r_e/r_o\right)$$

$$\int_{h_1}^{h_2} \frac{dh}{h} = \frac{2\pi e K_J}{\pi r_o^2} \log_e \left(\frac{r_o}{r_e}\right) \int_{t_1}^{t_2} dt$$

$$\log \left(\frac{h_1}{h_2}\right) = \frac{2 e K_J}{r_o^2} \log_e \left(\frac{r_o}{r_e}\right) (t_2 - t_1)$$

$$\frac{\log \left(h_1/h_2\right)}{t_2 - t_1} = \frac{2 e K_J}{r_o^2 \log_e \left(r_e/r_o\right)} = \frac{2 e^3 g}{12\upsilon r_o^2 \log_e \left(\frac{r_e}{r_o}\right)} = \frac{e^3 g}{6\upsilon r_o^2 \log_e \left(\frac{r_e}{r_o}\right)}$$

5.2.0 EQUATIONS FOR A FALLING HEAD TEST IN AN UNSATURATED FISSURED MEDIA:

Assumptions:

(a) Fissure is unsaturated, ie. above the groundwater table.
(b) Linear flow-pressure relationship.
(c) Axsymmetric flow.
(d) Homogenious and isotropic fissures.
(e) Kinetic energy is small.
(f) Infinite aquifer.
(g) It is assumed that there is no significant flow in the fissure while the borehole is filled with water.
(h) Viscous flow.

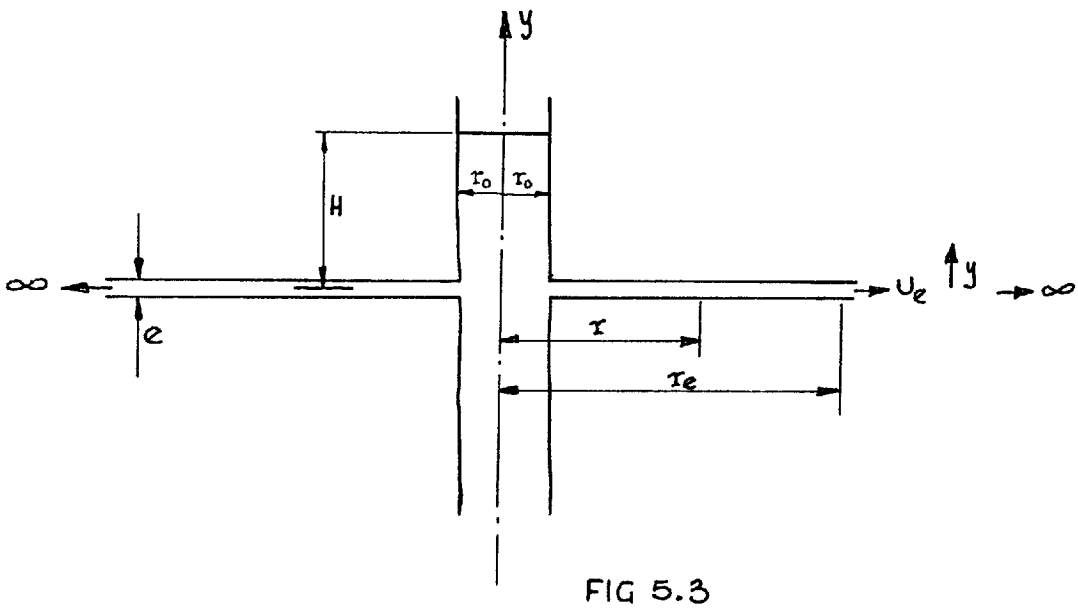


FIG 5.3

5.2.1 DERIVATION OF PERMEABILITY FROM RELATIONSHIP BETWEEN PRESSURE AND TIME

From the general equilibrium equation

$$\frac{\partial \sigma_r}{\partial r} + \frac{1}{r}\frac{\partial \tau_{r\theta}}{\partial \theta} + \frac{\partial \tau_{yr}}{\partial y} + \frac{\sigma_r - \sigma_\theta}{r} = 0$$

for radial flow : $\frac{\partial}{\partial \theta} = 0$; $\sigma_r = \sigma_\theta = p$, say

$$\therefore \quad \frac{\partial \sigma_r}{\partial r} + \frac{\partial \tau_{yr}}{\partial y} = 0 \qquad (1)$$

for viscous flow $\tau_{yr} = -\mu \frac{\partial u}{\partial y}$ where μ viscosity, τ drag, u velocity

$$\therefore \quad \frac{\partial \tau y}{\partial y} = \mu \frac{\partial^2 u}{\partial y^2}$$

$$\therefore \quad \frac{\partial \sigma_r}{\partial r} - \mu \frac{\partial^2 u}{\partial y^2} = 0$$

$$\text{or} \quad \frac{\partial P}{\partial r} = \mu \frac{\partial^2 u}{\partial y^2}$$

Integrate $u = \frac{y^2}{2\mu} \frac{\partial P}{\partial r} + By + C$ where B & C are consrants of integration

$B = 0$ since $\frac{du}{dy} = 0$

Boundary Conditions

$$y = \pm e/2 \; ; \; u = 0$$

$$\therefore \quad C = -\frac{1}{2\mu} \frac{\partial P}{\partial r} \left(\frac{e^2}{4}\right)$$

$$\therefore \quad u = -\frac{1}{2\mu} \frac{\partial P}{\partial r} \left[\frac{e^2}{4} - y^2\right] \qquad (3)$$

$\therefore$ Velocity distribution parabolic

Rate of flow, $Q = 2\pi r \int_{e/2}^{e/2} u\,dy = -\frac{\pi r e^3}{6\mu} \cdot \frac{\partial P}{\partial r}$

$$\therefore \quad \frac{\partial P}{\partial r} = -\frac{6\mu Q}{\pi e^3} \cdot \frac{1}{r}$$

Integrating $p = -\frac{6\mu Q}{\pi e^3} \times \left[\log r + \text{constant}\right]$

when $r = r_e$ outer radius of fissure $p = 0$

when $r = r_o$ at borehole, $p = \gamma H$, γ specific wt. of water

$$\therefore \quad 0 = -\frac{6\mu Q}{\pi e^3} \left[\log r_e + \text{constant}\right]$$

$$\gamma H = -\frac{6\mu Q}{\pi e^3} \left[\log r_o + \text{constant}\right]$$

$$\therefore \quad \gamma H = \frac{6\mu Q}{\pi e^3} \log \left(\frac{r_e}{r_o}\right) \qquad (4)$$

Initial conditions

$$H = H_o \; , \; r_e = r_o$$

When head drops to any other value, H

Volume of water displaced = $(H_o - H)\pi r_o^2$

also $\pi (r_e^2 - r_o^2) e$

$$\therefore \left(\frac{r_e}{r_o}\right) = \left[1 + \frac{H_o - H}{e}\right]^{\frac{1}{2}} \qquad (5)$$

Also $$Q = -\pi r_o^2 \frac{dH}{dt} \qquad (6)$$

Substitute (5) and (6) into (4)

$$\gamma H = -\frac{3\mu r_o^2}{e^3} \log \left(1 + \frac{H_o - H}{e}\right)^{\frac{1}{2}} \frac{dH}{dt} \qquad (7)$$

Integrating in time t = $\int dt$

$$= \int \left(-\frac{3\mu r_o^2}{e^3}\right) \cdot \frac{\log \left(1 + \frac{H_o - H}{e}\right)^{\frac{1}{2}} dH}{H} \qquad (8)$$

If this can be evaluated we have related $H \rightarrow t$ for the case of flow from a borehole into a fissure of infinite radius.

Noting that the aperture e is small compared with (Ho-H) except when the hole is full we can rewrite (7)

$$\frac{1}{2} \log \left[H_o - H\right] = \frac{1}{2} \log e - \frac{\gamma e^3}{3\mu r_o^2} \cdot \frac{H}{\left(\frac{dH}{dt}\right)} \qquad (9)$$

$\therefore$ plot $\log \left[H_o - H\right]$ vs $\frac{H}{\left(\frac{dH}{dt}\right)}$ should be straight line

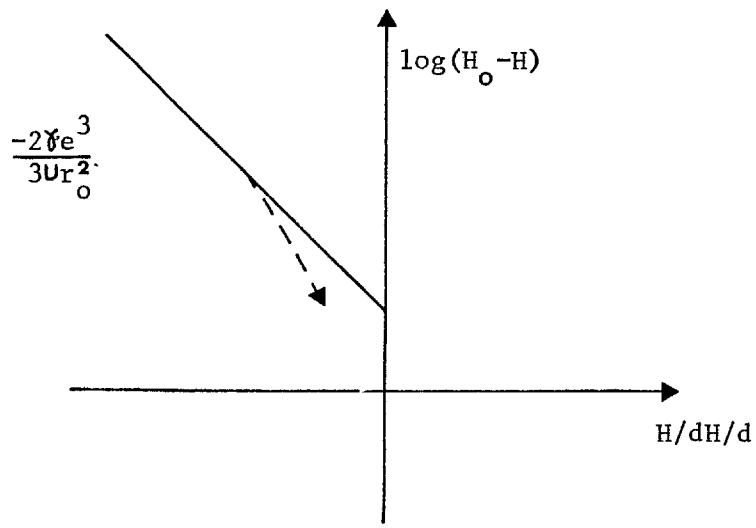


FIG 5.4

At the beginning of the test, H = Ho $\log (H_o - H) \to -\infty$

This is not given by straight line plot because

(a) Eqn (9) we assumed e negligible compared with (Ho-H)

(b) Ignored the kinetic energy.

Hence there will be a departure from the straight line as indicated in Fig. 5.4.

5.3.0 LABORATORY TESTS

The model described in section 4.2.1 part II was used to test some of the equations which have been derived in the previous sections.

The equation in section 5.1.2 describes the result of a falling head test carried out below the water table. The test simulation of this consisted of maintaining constant input into the model until steady state was achieved. The input was then turned off and the change in level of water in the tube was monitored with respect to time, and can be seen in Fig. 5.5.

For such a test from section 5.1.2

$$\frac{\log\left(\frac{h_1}{h_2}\right)}{t_2 - t_1} = \frac{e^3 g}{6U r_o^2 \log\left(\frac{r_e}{r_o}\right)}$$

$r_e = 12.5$ cms

$r_o = 1.25$ cms

$U = 1.15 \times 10^{-2}$

If the data in Fig. 5.5 is replotted on a semilogarithmic scale the result is a straight line, Fig. 5.6 as predicted by theory.

$$\therefore \text{the slope in fig 5.6} = \frac{\log (h_1/h_2)}{t_2 - t_1} = \frac{1}{190}$$

$$\therefore \quad e^3 = \frac{6 \times 1.15 \times 10^{-2} \times 1.55 \times 2.3}{980 \times 190} = 1.33 \times 10^{-6} \text{ cm}^3$$

$$\therefore \quad e = 0.011 \text{ cms.}$$

From section 4.2.1 for the same model and test set up the value of e = 0.015 cms.

5.3.1 The case of flow from a borehole into a fissure of infinite radial extent can be modeled if the viscosity of the liquid is increased in which case the fluid front moves slowly through the model and allows sufficient observations before reaching the boundary. For this test an oil of known viscosity was used. The test began with

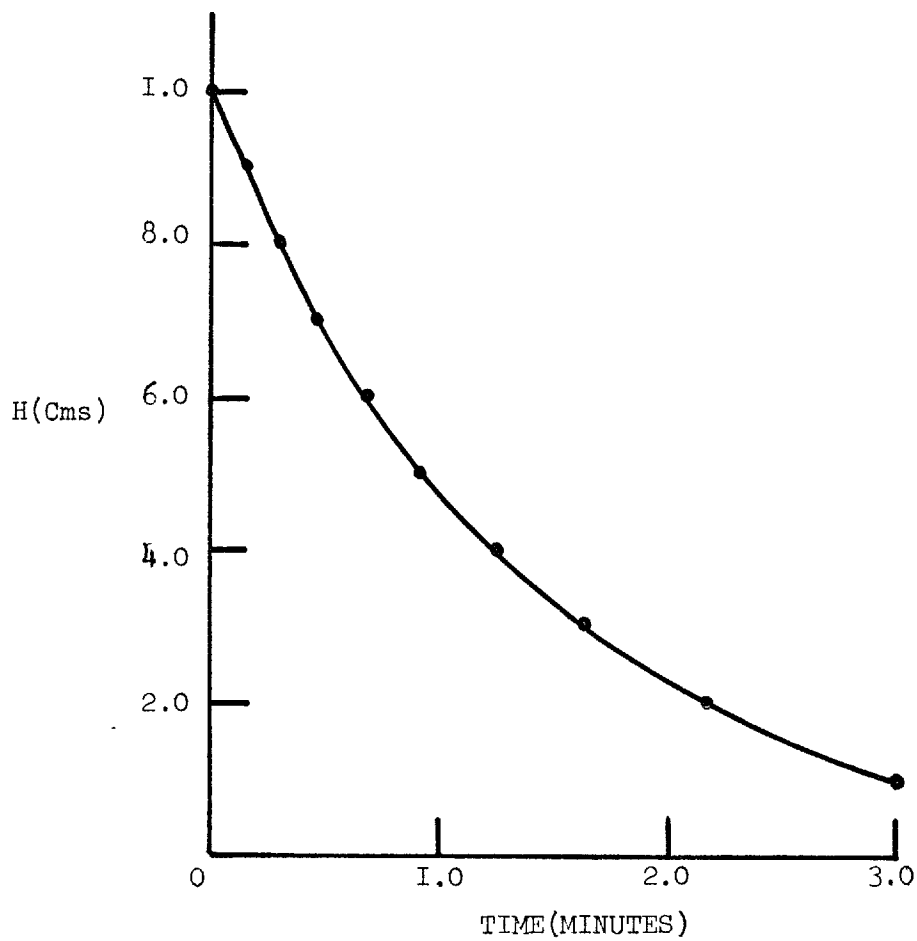


FIG 5.5

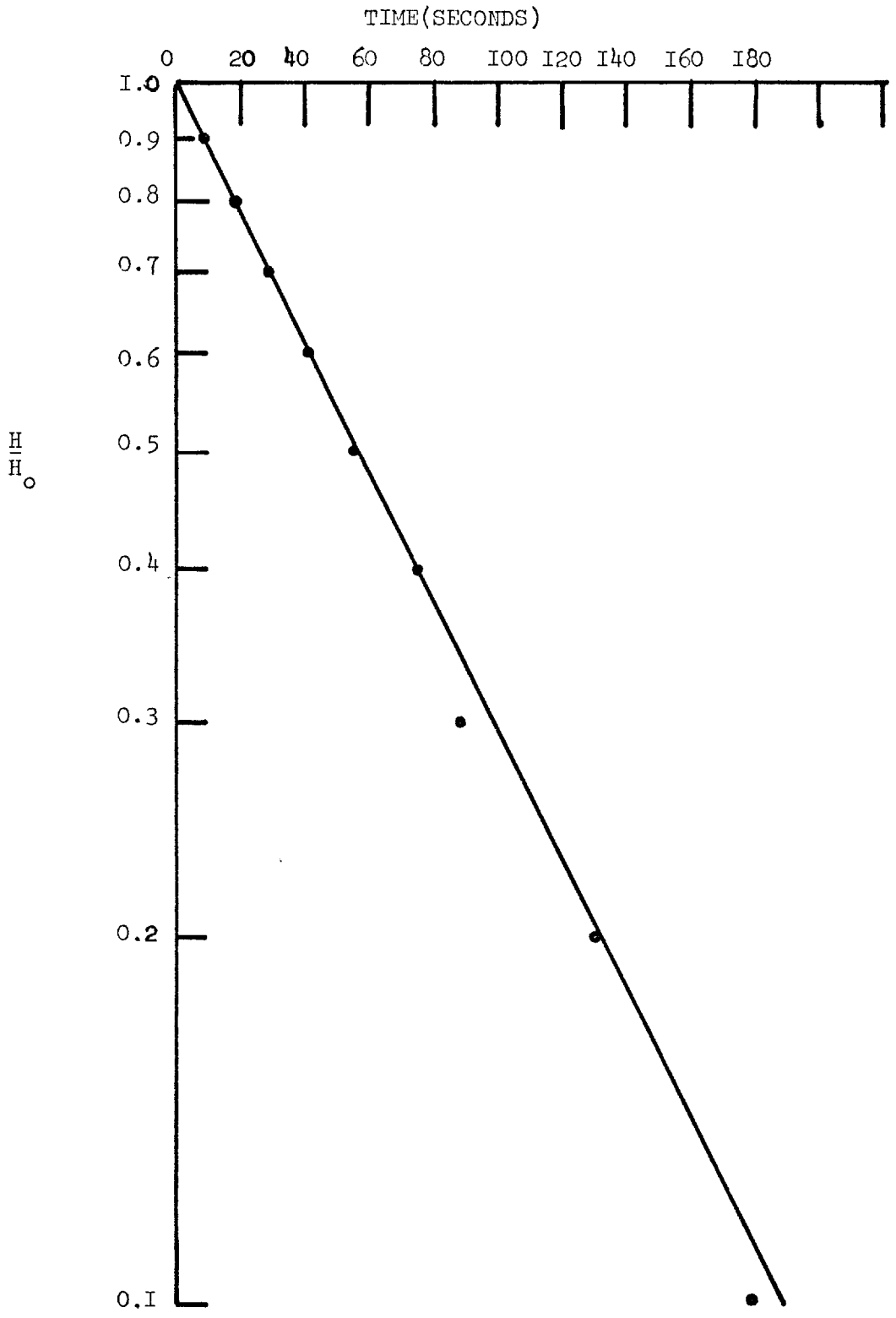

TIME(SECONDS)
0
20
40
60
80
I00
I20
I40
I60
I80
I.0
0.9
0.8
0.7
0.6
0.5
0.4
0.3
0.2
0.I
H/H_o

FIG 5.6

the fissure unsaturated. Fig. 5.7 illustrates the change of oil level in the borehole with time. If Equation 9 section 5.2.1 is used to calculate the aperture of the fissure the relationship is graphically demonstrated by Fig. 5.8. This is very similar to the predicted shape as in Fig. 5.4 where it was shown that for low values of $H/\frac{dh}{dt}$ the experimental curve should deviate from the theoretical curve.

From Fig. 5.8 the aperture can be calculated from the slope of the straight line.

$$\frac{2\gamma e^3}{3\mu r_0^2} = \frac{0.58}{290}$$

$$\therefore \quad e^3 = \frac{3 \times 0.58 \times 1.55 \times \mu}{290 \times \gamma \times 2}$$

$$= \frac{3 \times 0.58 \times 1.55 \times 0.6}{290 \times \gamma \times 2}$$

$$\therefore \quad e^3 = \frac{1}{2} \times 5.75 \times 10^{-6}.$$

$$\therefore \quad e = 1.42 \times 10^{-2} = 0.0142 \text{ cms.}$$

This value agrees fairly well with a constant pressure test value of $e = 0.0158$ cms, see section 4.2.2 part II.

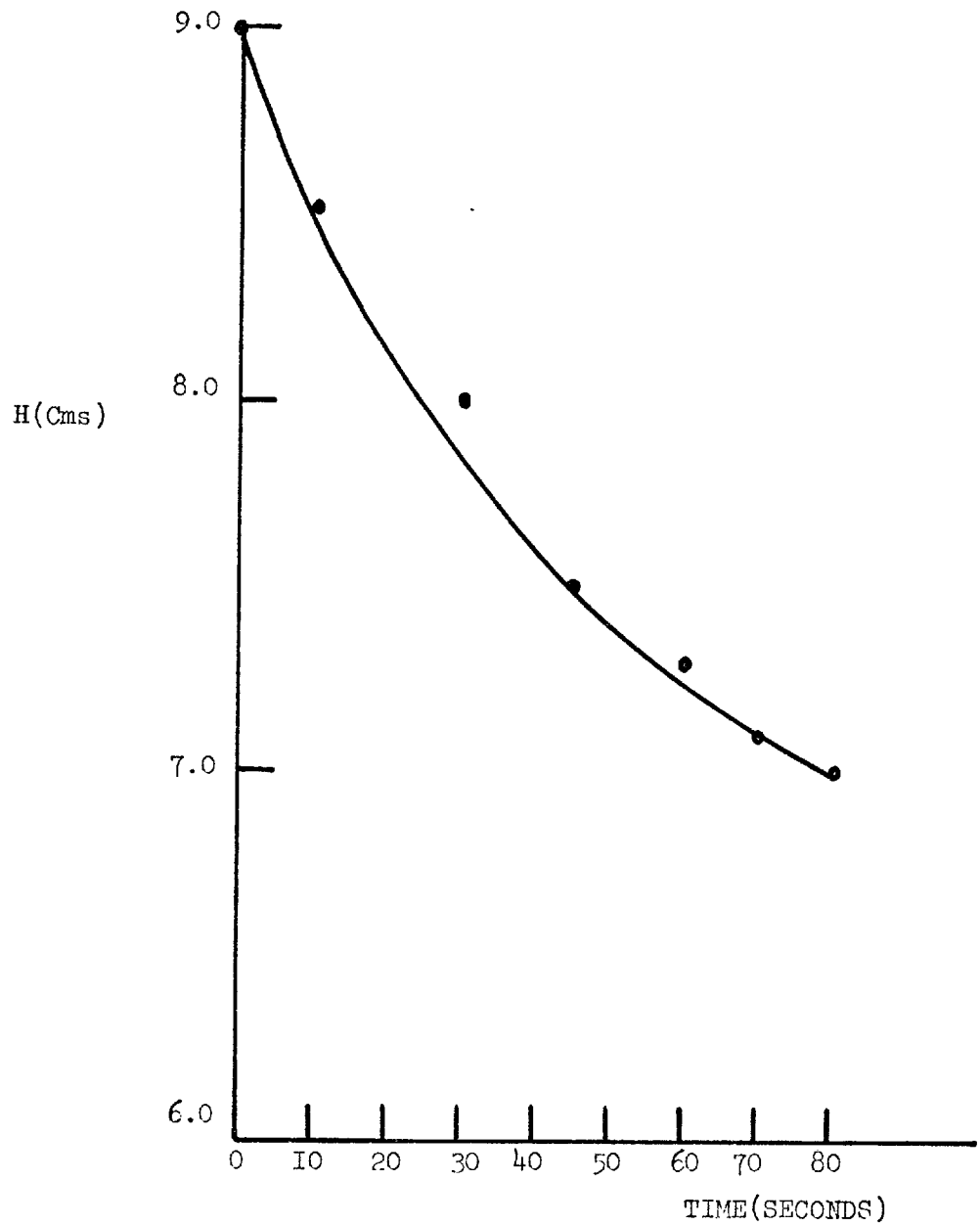


FIG 5.7

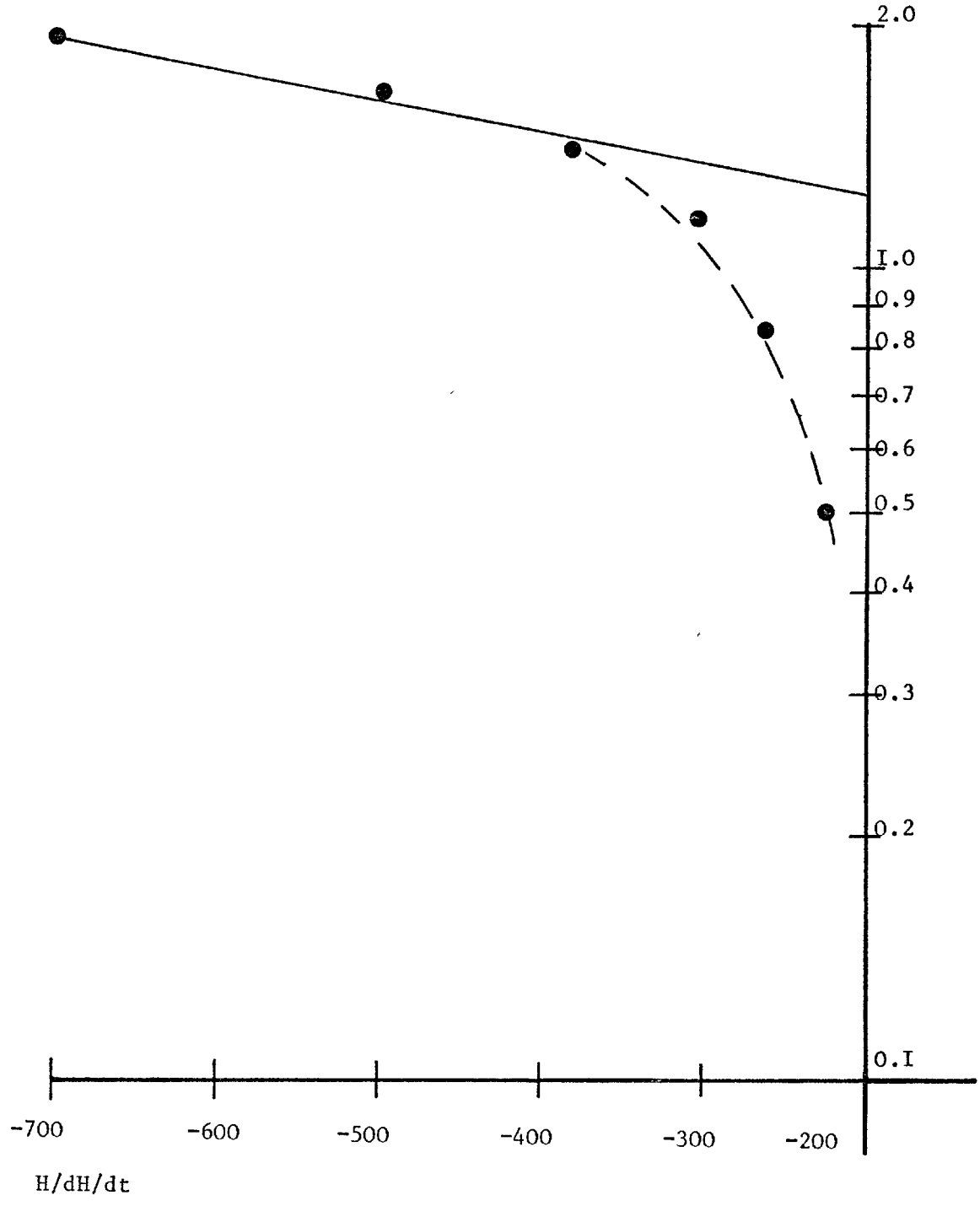


FIG 5.8

CONCLUSIONS

It has been shown how the mean aperture or permeability of a fissure can be evaluated from a falling head test for the case of a finite-boundary and also the infinite boundary. The mathematical derivation has been verified for the two cases by model tests. Besides practical reasons it is felt that this approach to the determination of permeability is a very sensitive one since an additional variable "time" is used in the test, thereby giving more information than the steady state methods. By looking at the changes in the pressure-time relationship the existance of permeable and impermeable boundaries in the radial direction can possibly be observed. A parametric study could be conducted with different systems to see the relationship between pressure and time. A preliminary attempt is made in part III to do this and it is hoped that this line of research is further pursued.

PART 3

FIELD EVALUATION

SYNOPSIS

In order to estimate the in-situ hydraulic parameter in fissured rock it is essential to have a clear understanding of the fracture pattern in as much detail as possible. Once the orientation of the major fissures becomes apparent it is then possible to decide the test layout in terms of borehole orientation. The next step is to obtain the frequency distribution of the fissures so that the tests are carried out on the correct scale relative to both the rock mass and the structures, i.e. dam or slope under consideration. Having established a "map" it is then possible to carry out pumping tests in the various boreholes on the basis of the analysis presented in Part II.

It was not possible to obtain pressure-test data from commercial projects in fissured rock which satisfied the above limitations and therefore it was decided to find a suitable site where the various ideas which are developed in this thesis could be tested. A sedimentary environment was chosen for ease of geological and fracture mapping.

The field evaluation by the author consisted of an initial fracture mapping and subsequent drilling of holes in suitable directions. This was followed by core logging and examination of the holes with a Borehole Television Camera. The modified Lugeon testing and Tracer equipment was designed for execution in this field project.

Part III deals with the design of equipment, geological investigation of the area where in-situ hydraulic tests were carried out and results of the field measurements based on the theory developed in Part II.

INSTRUMENTATION

1.1.0 INTRODUCTION

In this section the outlay of the test apparatus will be described together with the details of the essential components. It is felt that the inclusion of such details is very important for two reasons:

(a) so that a researcher can critically examine the test set-up and use it as a basis for future improvement and perhaps not make the same mistakes.

(b) it is easier for the practising engineers to improve his present set up on the basis of the equipment described.

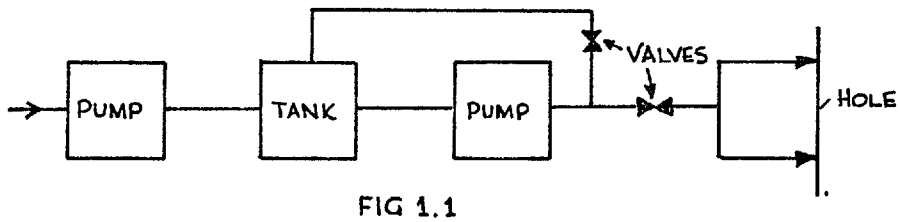


FIG 1.1

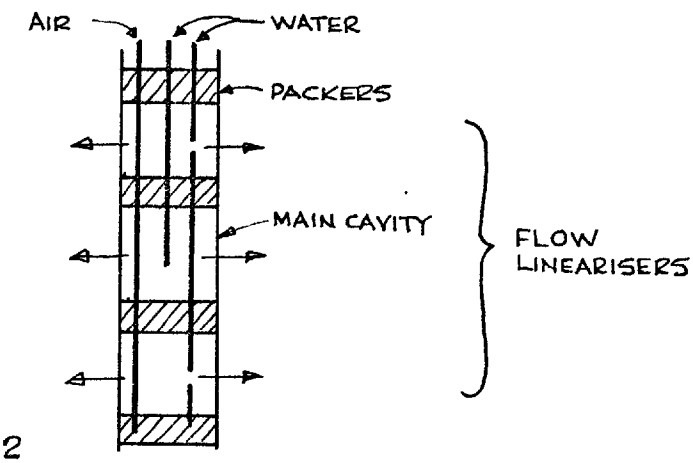
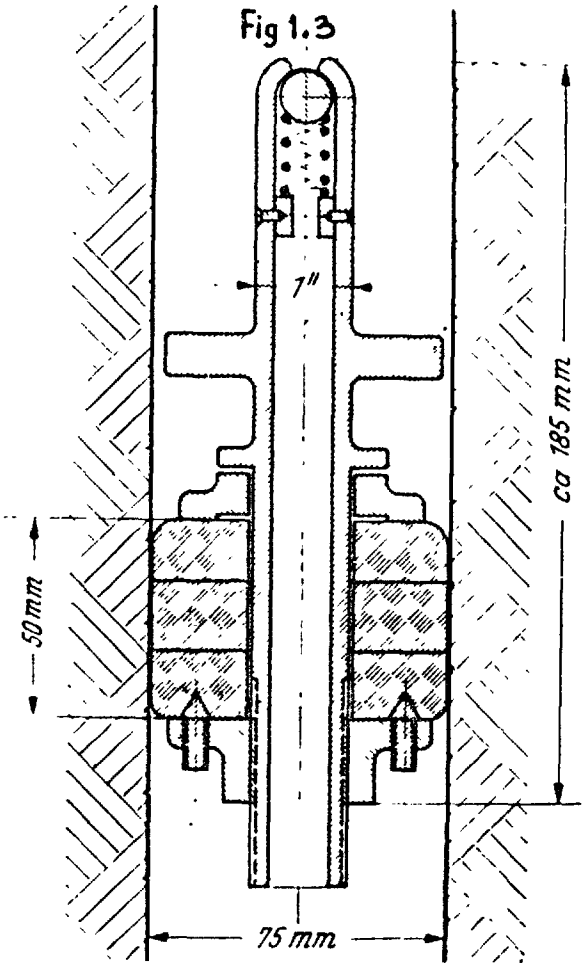


FIG 1.2

Fig. 1.1 and 1.2 are a schematic outlay of the test as it was carried out at a quarry in South Wales. Owing to the extreme shortage of water on the site, the constant flow tests had to be run for as short a period as possible. On an average day (10 hours) approximately 2000 gallons were used up in testing in one hole.

The electrical equipment was designed so that it could be operated on an alternating current at 50cps and 250 volts.

Fig 1.3


1"
ca 185 mm
50 mm
75 mm

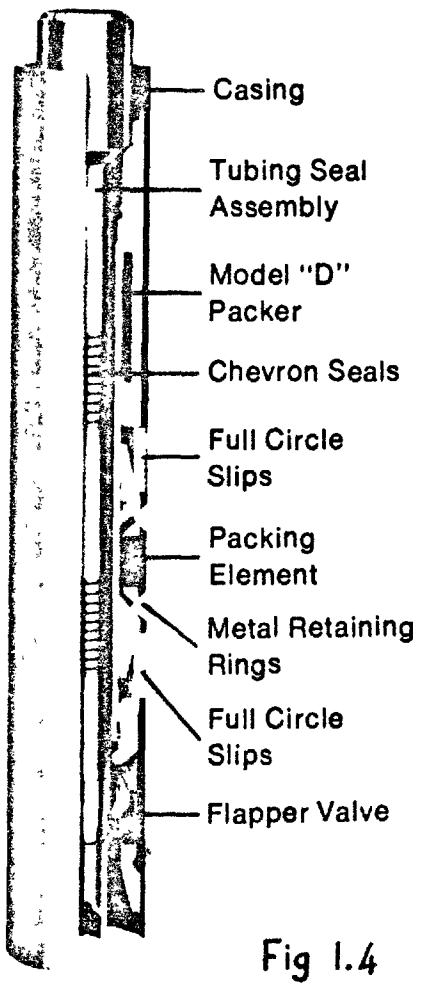

Casing
Tubing Seal Assembly
Model "D" Packer
Chevron Seals
Full Circle Slips
Packing Element
Metal Retaining Rings
Full Circle Slips
Flapper Valve

Fig 1.4

1.2.0 DETAILS OF THE APPARATUS USED IN THE FIELD

1.2.1 PACKERS

Packers are used in the constant and falling head water pressure test so that certain zones of interest in a borehole can be hydraulically sealed. By supplying water in such a zone at a known flowrate and pressure, the permeability of the medium can be estimated. In spite of the extensive use of packers in the civil engineering and petroleum industry little is written on their design. A large variety of packers exists on the market; but they are generally designed for specific jobs. There are basically three types of packers which exist:

(a) Permanent (b) Manual (c) Pneumatic.

(a) Permanent: This merely consists of a grout or cement plug which permanently isolates given zones. In fact, piezometers may be classed in this group in that they can be used for pumping tests. However, they are generally only a few installations per hole and thus permeability determination is restricted to those areas.

(b) Manual: This type is quite often used in civil engineering practice and is illustrated in Fig.1.3. The two rubber plugs are separated by a perforated pipe (test cavity). The packers are lowered on drilling rods and by suitably rotating them a torque is applied on the rubber plugs. This results in an axial compression and hence a bulge in the rubber which isolates the test cavity hydraulically from the rest of the hole. This type of packer is limited in its use, because of the difficulty of applying torque at great depth. Further it is also very cumbersome in terms of weight.

(c) Pneumatic: This is by far the most popular type of packer in current practice. A large variety of commercial packers are available, such as in Fig.1.4 which is used in the Petroleum industry. During this field trip none of the commercially available packers were used because of the system, that was going to be used.

As can be seen in Fig.1.1 three pipes go down the hole. The first one carries water to the main test cavity. The second pipe carries water to the flow linearisers and the third pipe is an air line which is common to all four packers. With this arrangement it was essential to have a packer which would allow three tubes through it. A packer was designed to oversome this problem. The entire construction of the packer and associated tubing was in p.v.c. and all the different air tight and water tight joints were made by using a p.v.c. glue.

This had an advantage over the conventional metal system in that it was (a) light, and (b) complicated machining of "O" ring recesses was avoided. The inflatable part of the packer consisted of rubber tubing. Fig.1.5 illustrates the packer as a finished product. Incidentally, the diagram illustrates the problems associated with a down hole tool in that one is severely restricted in space. The diameter of the hole is 3 inches and the tool is approximately $2\frac{3}{4}$" in diameter. Within this radius one has to provide pipes which are capable of delivering as much as 20 gallons per minute for the test section and the same amount for the flow linearisers.

The length of the packers was chosen at a minimum of 18". Most commercial packers are only 6" or so and it was felt with such a small packer leakage could occur past the packer, i.e. a short circuit between the test cavity and the rest of the hole. In theory packer length should be related to the mean distance between fissures. However, in practice this would cost a great deal. From model tests in fissures it seems that the majority (80%) of pressure drop occurs within a radial distance of 4 x diameter and therefore a packer longer than that value should stop the majority of the likely short circuiting (See Fig.1.6).

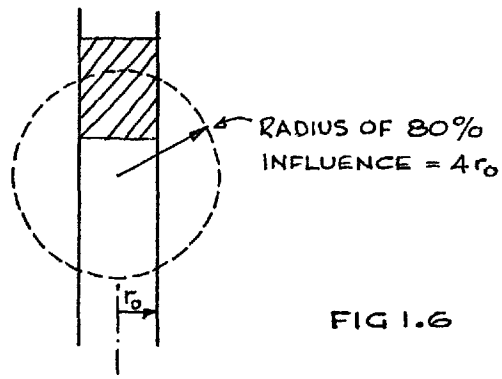


FIG 1.6

With the programme provided in the appendix and from Chapter 3.2.1 it is possible to numerically model this problem packer length for a variety of fissure spacings.

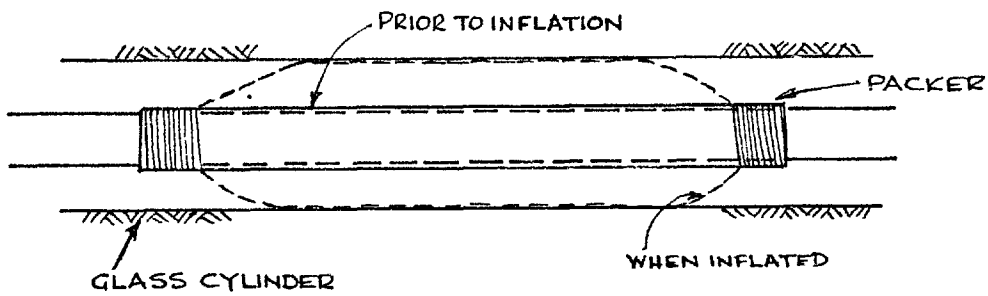


FIG 1.7

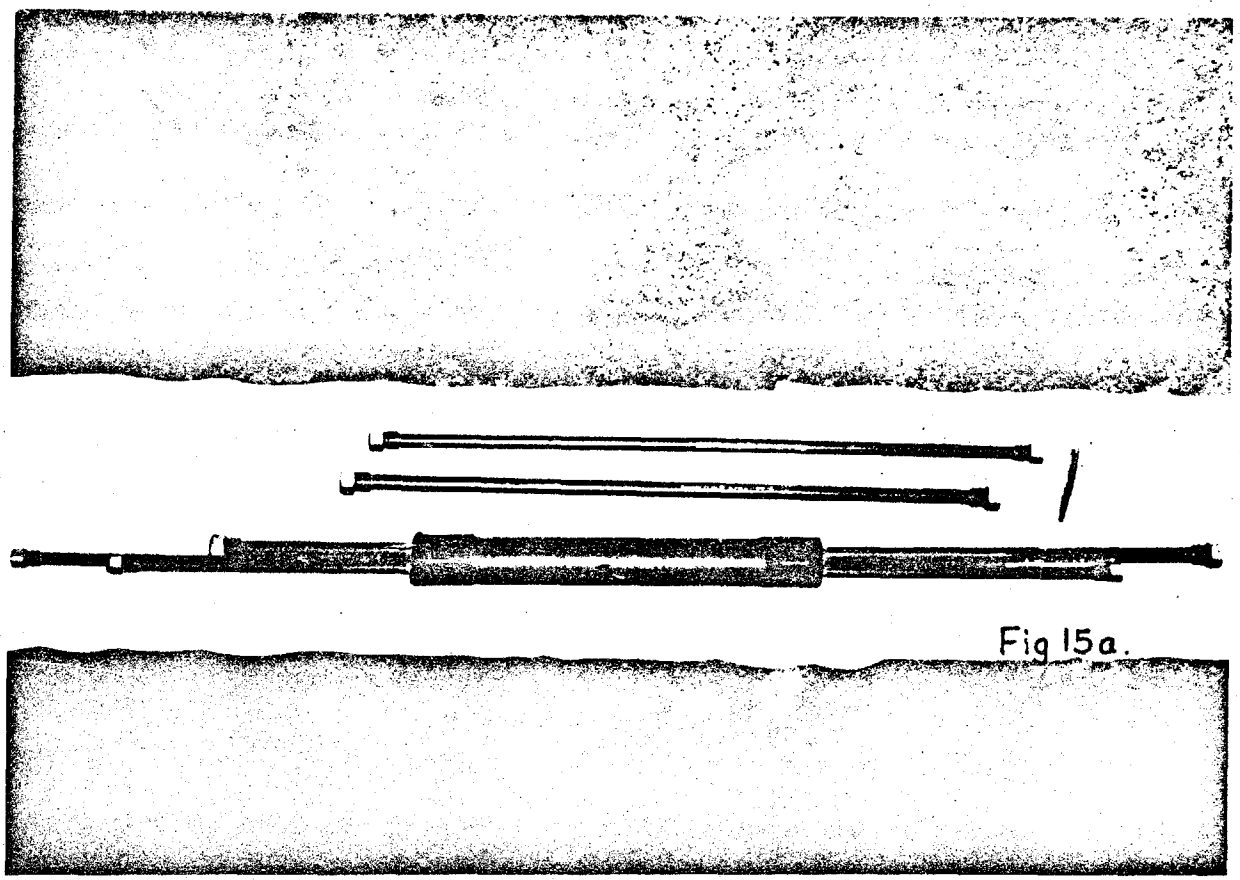


Fig 15a.

Fig. 1.7 demonstrates schematically the testing of the packer in the laboratory. The packer was placed in a glass tube and inflated. This was done to see if a seal could be obtained and also if there was any excessive strain on the inflated rubber sleeve. These tests in the laboratory were successful and illustrated that the technique could work.

In the field this packer was subjected to a very much more rugged environment than had been anticipated. The most serious problem was that the extreme changes in atmospheric temperature caused the partial breakdown of the glue and hence the leakage of air. This meant that the packer could not be kept blown up indefinitely. During some early tests this caused the leakage of water past the packer. All the leakages and cavities in the packers were subsequently filled up with liquid araldite which set hard in approximately 24 hours. The presence of three separate tubes down the hole made the aligning of the tubes leading to the packer very difficult and cumbersome. It is suggested that in any future design this connection between the packer and the pipes must be a very simple one - something along the lines of a bayonet mechanism. P.V.C. has tremendoes advantages in terms of economy, ease of machining, sealing and portability. However, it sadly lacks rigidity and also behaves badly under variations in temperature conditions.

The packers were blown up with compressed air or Nitrogen cylinders with regulators. During the test it is very important to monitor the airline pressure, this aspect will be discussed in a further section on the evaluation of the test. The amount of pressure used depends on the depth of the instrument relative to the water table and the pressure as a result of inflow into the cavity.

1.2.2 MEASUREMENT OF FLUID PRESSURE

In conventional pumping tests, the fluid pressure is measured, as water leaves the pump, by a Bourdon-type gauge. This is a mechanical gauge very often mounted on to the pump outlet. It was felt that this method was extremely crude and that the pressure gauge ought to fulfill the following requirements:

(a) During a pumping in test it is the excess pressure at the hole which is required to compute permeability. A Bourdon-type of gauge only gives total pressure at the exit point of the pump. In a fissured rock mass the pressure distribution with depth may not be linear and therefore during such a test it is essential to estimate the natural pressure in the packed off section prior to pumping.

Since this estimation is a static determination of pressure the most convenient way to do this is to have some sort of a pressure gauge which is directly connected to the packed off section that does not need a steady flow of water to function.

(b) A reasonable degree of accuracy, in these experiments an accuracy of about 1% for a range of 0-100 psi. This is generally not possible with mechanical gauges unless a few with a smaller ranges are used; range 0-10 psi, 0-20 psi, 0-50 psi, 0-100 psi.

(c) A record of pressure with respect to time - this necessitates the use of a chart recorder connected to the gauge. A history of pressure build up and fall off is extremely invaluable in determining the state of the fissures in the test zone.

(d) Measure pressure directly in the cavity between the packers. The mechanical pressure gauge is fixed at the outlet of the pump, an estimate of pressure losses down the pipe, past elbows and numerous junctions is not only cumbersome, but prone to inaccuracies. The errors are introduced during tests because the losses are a function of flowrate and the geometry of the system which in the course of a test may vary.

(e) In the falling head test the test cavity is filled with water and so is the tube bringing this liquid. Having established the required head, the flow is turned off and from then on a record of pressure vs time is required in order to calculate permeability. The Bourdon-type gauge relies on a steady supply of water under pressure for it to work.

(f) Leakage past a packer during a test is a very common problem (15,21) which leads to substantially high permeability values. This leakage is difficult to estimate and there are no papers on the topic which indicate the magnitude or control. A Bourdon-type gauge fitted to the outlet would be rather slow in reacting to the packer air pressure changes. The changes in fluid pressure could well be confused with the variations in pump performance or non attainment of steady state conditions.

In view of the above problems outlined it was felt that the mechanical gauge ought to be discarded and an electric transducer used instead. The transducer has some very important and distinct advantages. The size of the unit and its capability of sending pressure signals, via a cable makes it possible to use it down the hole, close to the zone which is being pressurised. Fig. 1.8A illustrates the transducer.

The signal which indicates the pressure down the hole is coupled to a chart recorder via a flexible cable. Fig. 1.8B is the field unit with the associated plumbing. The transducer is placed in a water tight compartment and the cavity pressure communicates with the transducer via a hollow pipe as indicated.

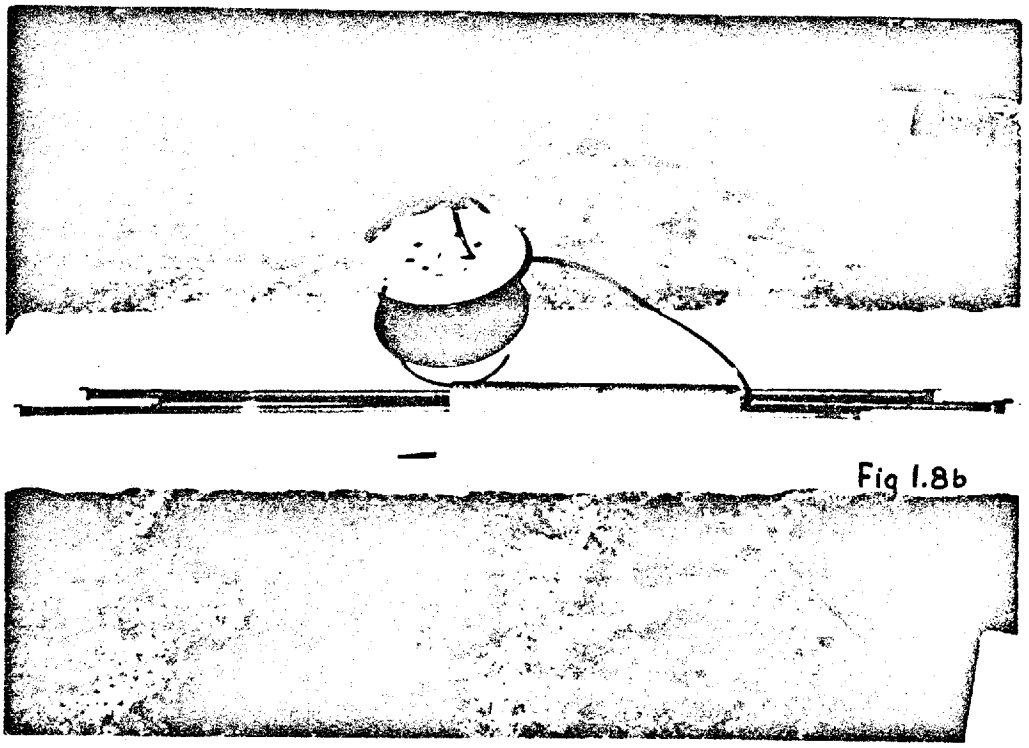


Fig 1.8b

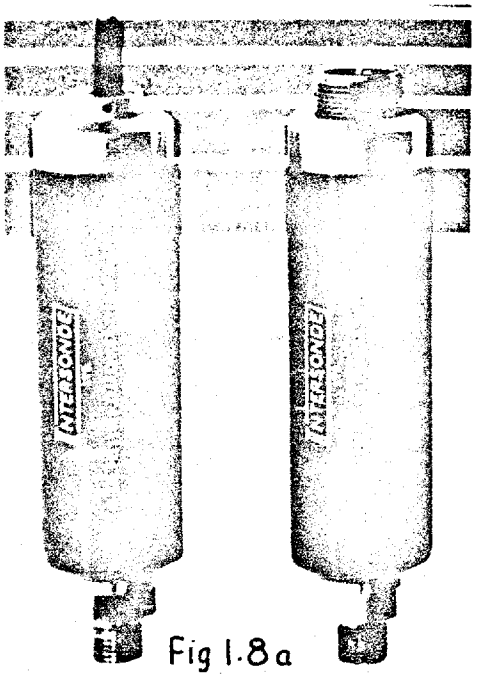


Fig 1.8a

CALIBRATION CERTIFICATE

HIGH OUTPUT PRESSURE TRANSDUCER

TYPE No. [illegible]17-350 DATE 20th. October, 1970.

RANGE 0-100 P.S.I. ~~KG/cm²~~ SERIAL No. 323

The following output parameters were determined using the circuit of fig. 2 and with an excitation voltage of 20 volts d.c. ± 0.1%.

FULL RANGE SENSITIVITY (F.R.S.) 1.044 V (open circuit)

ZERO PRESSURE OUTPUT [illegible] mV (open circuit)

COMBINED NON-LINEARITY & HYSTERESIS ± 0.9 % of F.R.S.

MAXIMUM LOAD CURRENT 1.0 mA.

OUTPUT RESISTANCE [illegible] ohms

CALIBRATION CHECK POINT: With a resistor of value [illegible] ohms ± 0.1%, connected across the green (C) and blue (D) leads (pins), the change in output voltage is equal to 30.7 % of F.R.S.

ELECTRICAL CONNECTIONS: The coding applicable to transducers with a cable or plug and socket termination is shown in fig. 2.

DEFINITION OF TERMS: See fig. 1.

This transducer was calibrated at a laboratory temperature of 20°C.

SIGNED [signature]

Calibration Engineer

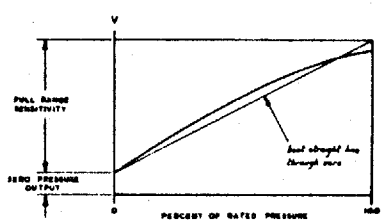


fig.1

Fig 1.8c

This type of gauge fulfills all the requirements which are listed above. The accuracy is well within 1% of 0-100 psi. Full scale deflection is obtained on the chart recorder by simply altering the scale knob (details in further section). Having selected a suitable speed on the chart recorder the pressure build-up and fall-off can be observed during pumping in and when the flow is stopped. Since the pressure is measured close to the cavity there is no need to correct the pressure for losses in the pipes, etc. An outstanding advantage of such a gauge is that it measures the insitu pressure between the packed off section prior to any test. This determination in a fissured rock mass where the pressure may not be hydrostatic with depth can be extremely cumbersome. As soon as the packers are inflated the transducer gives a value of the fluid pressure within the cavity. Once this pressure is known inflow of water is begun into the cavity at a steady rate and the new pressure is automatically recorded.

During a pumping test it is very important to make certain that the packer is sufficiently well sealed to avoid any leakage past it. With a Bourdon gauge it is difficult and time consuming to test for leakage. Since the transducer is so near the test section any change in conditions within the cavity is reflected almost instantaneously at the surface via an electrical signal.

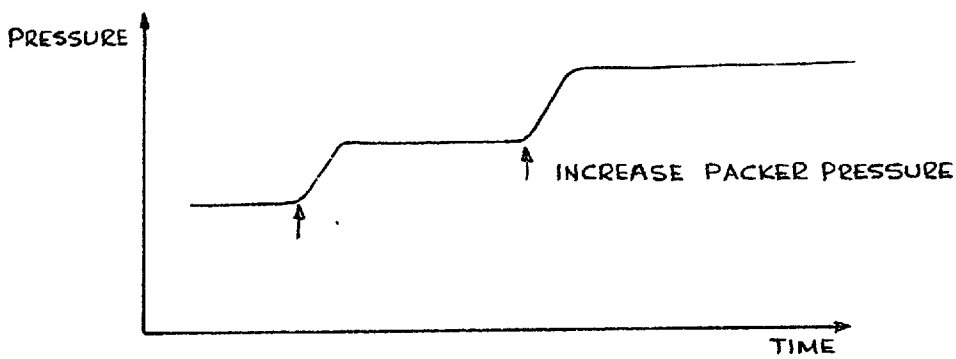


FIG 1.9

For example if there is leakage past the packers an increase in packer pressure will produce an increase in cavity pressure and a decrease in flowrate, as in Fig.1.9. Leakage obviously occurs when the permeability of the fissures is low and the input volume of water is too high for the fissures to transport at that pressure.

If the pneumatic pressure is not high enough to maintain a seal with the borehole, water will leak past it. This adjusting procedure of increasing packer pressure is carried out until no further changes take place in the cavity pressure or the input flowrate. An indication of a good seal is when a temporary increase in packer pressure produces a surge, as in Fig.1.10 indicating a momentary or transient pressure in the cavity owing to the incompressibility of water.

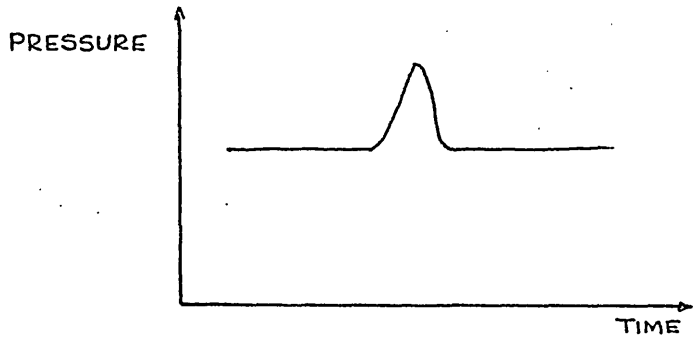


FIG 1.10

During a falling head test the hole is pressurised to a known level and then the water supply cut off. The transducer gives a continuous signal as the pressure drops. Traditionally this test has been carried out very crudely by dropping a piece of cable down the hole, when the two terminals of the cable meet the top of the water column a signal is given in the form of a light or a bleep. Unfortunately, the contacts get damp and tend to give false readings. Further the recording of such data is very cumbersome and discontinuous. Since the gauge is so near the test cavity any increase in the packer pressure produces a temporary test cavity pressure surge plus, if there is leakage, a rise in pressure and a drop in the flowrate. After a series of adjustments a stage is reached where an increase in the packer pressure makes no difference to the test cavity pressure. This indicates that the packer is sealed.

At the end of the field tests the transducer proved its worth beyond all expectations, especially because all the field data during a test could be recorded on the chart recorder, thus providing neat and readily understood data. In view of the fact that a lot of practising engineers are not likely to go over to electrical systems, also a Bourdon-type gauge was used and comments on the efficiency etc., will be made when the individual tests are evaluated. In brief it can be stated that the mechanical pressure gauge gave only approximate pressure values as would be required for calculating permeability; but it failed to satisfy the requirements (a) to (f).

1.2.3 FLOW MEASUREMENT

The criteria for a flow measuring device are as follows:

(a) Ease of operation and portability

(b) Accuracy of 1% for a range of 0-20 gallons per minute

(c) Automatic recording

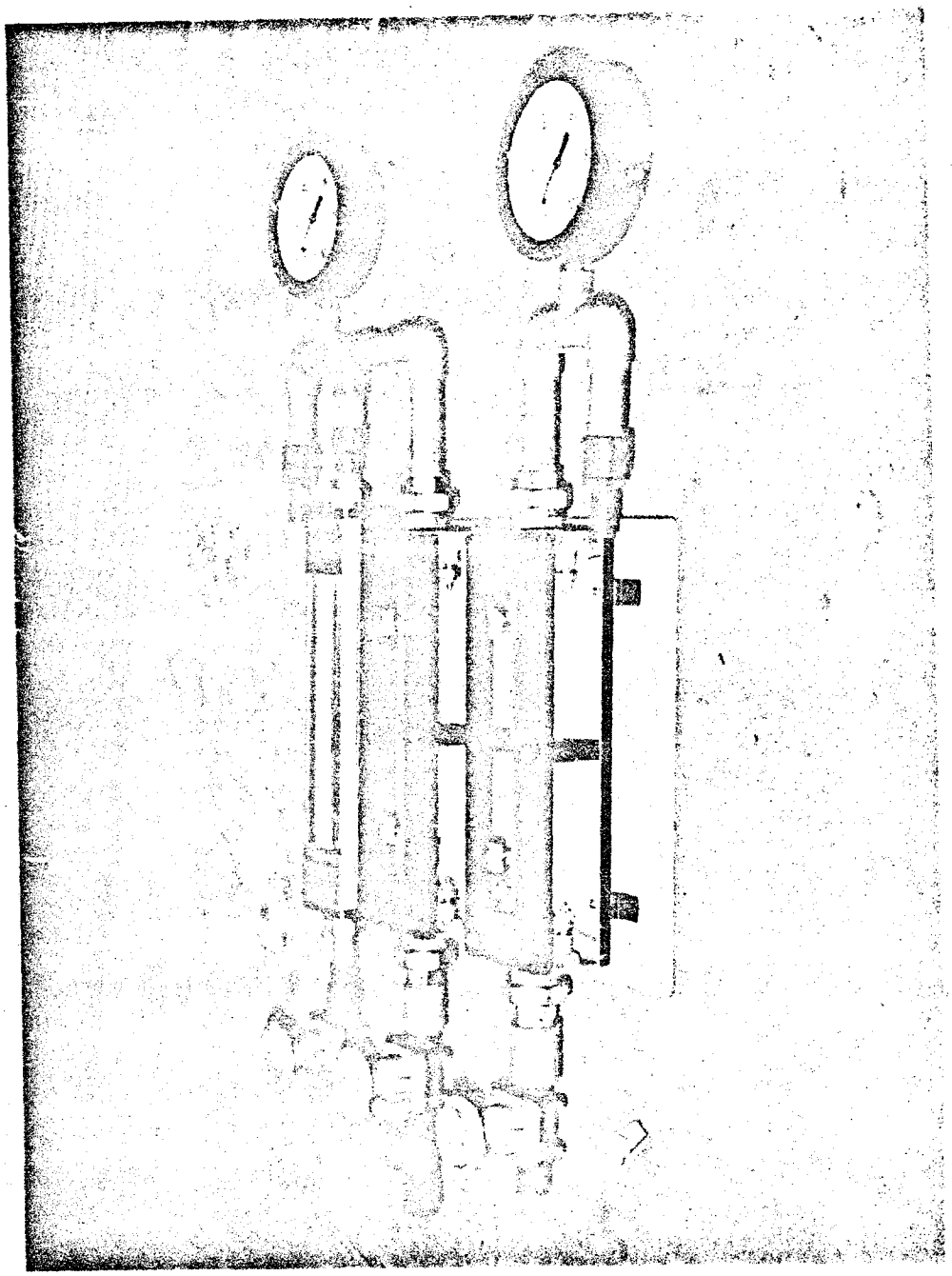


FIG. 1.11.

A large variety of flow measurement devices were considered from the electric turbine to the simple float. Although the electric turbine provided automatic recording of flowrate, the accuracy over such a large range could not be coped with unless a few different turbines were used. The extremely high cost of the unit plus its constant need of service and calibration ruled it out. Instead a simple float type device was used (Fig.1.11). For the main cavity two flowmeters were used so that maximum efficiency could be obtained. One of them gave a range of 0-5 litres/min. and the other one 5-50 litres/min. Unfortunately the option for automatic recording had to be left out. During the tests the flowrates were recorded namually on the chart in front of the respective pressure.

1.2.4 VALVES

All valves were p.v.c. types. A parallel type of arrangement with different diameter tubes provided the necessary control of the flowrate. Also, use was made of a by-pass system from the pump to provide the first stage of control. Further manipulation was carried out by altering the values at the flowmeter end.

1.2.5 PUMP

Once again very little information is available on the types of pumps that are used in pumping tests. In view of the large variation of permeability that was anticipated from the structural examination of the area a pump had to be selected which provided low and high delivery without too much loss of efficiency. This is an extremely difficult criteria, and after a lot of searching, a vortex type of pump was selected (Fig.1.12).

This pump is in theory relatively free of surge; but since there is always some vibration the outlet and inlet tubes to the pump were of flexible p.v.c. tubing. Owing to the great shortage of water on the site the entire operation of pumping water became extremely hazardous and time consuming. The choice of pump, in retrospect, could be improved to one with a steadier output. Also the metal casing of the pump was unable to take the extremes in the weather (i.e. freezing) and consequently cracked.

1.3.0 ASSEMBLY

The entire unit could be assembled very quickly and without too much manual assistance since the entire unit was constructed in lightweight p.v.c. The total weight of an 80ft. assembly with three sets of pipes, packers, transducers did not weigh more than 35 pounds.

Various options were provided for in that pipes could be of different lengths. Also since the pipes in the packer have to be rigidly mounted to be air tight the attachments have to be such that for greatest ease the pipes are not rotated. Fig.1.13 shows how this can be achieved using special unions.

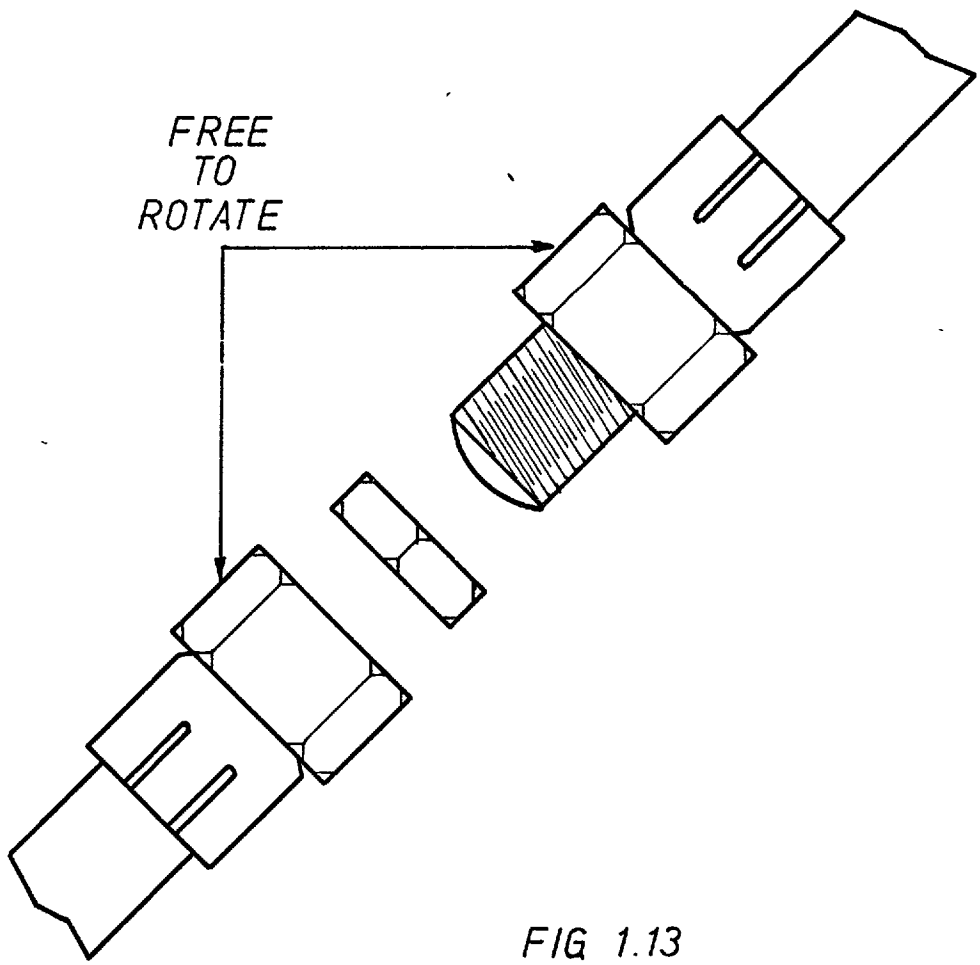
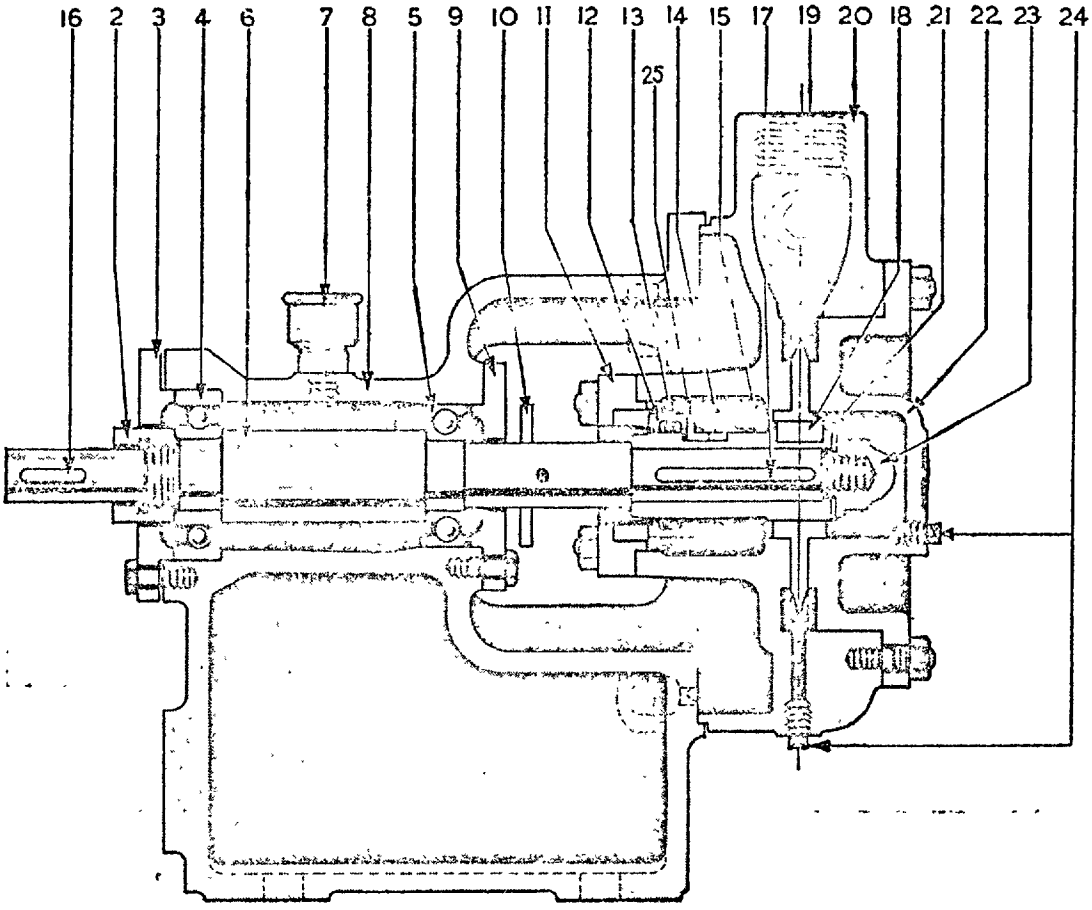


FIG 1.13

TYPE "T" VORTEX PUMPS



Ref.	Name of Part	Ref.	Name of Part	Ref.	Name of Part
2	Bearing Locknut	11	Seal Cover and Face	20	Pump Casing
3	Outer Bearing Cover	12	Seal Ring (Metal)	21	Shaft Sleeve
4	Thrust Bearing	13	Seal Ring (Rubber)	22	Pump Cover
5	Journal Bearing	14	Seal Spring	23	Sleeve Nut and Washer
6	Pump Shaft	15	Spring Seat	24	Drain Plugs
7	Stauffer Lubricator	16	Feather for Coupling	25	Seal Key
8	Driving Head	17	Feather for Sleeve		
9	Inner Bearing Cover	18	Feather for Impeller		
10	Water Thrower	19	Impeller		

N.B. When ordering spares, the pump number should be quoted together with the number and name of part required.

FIG 1.12

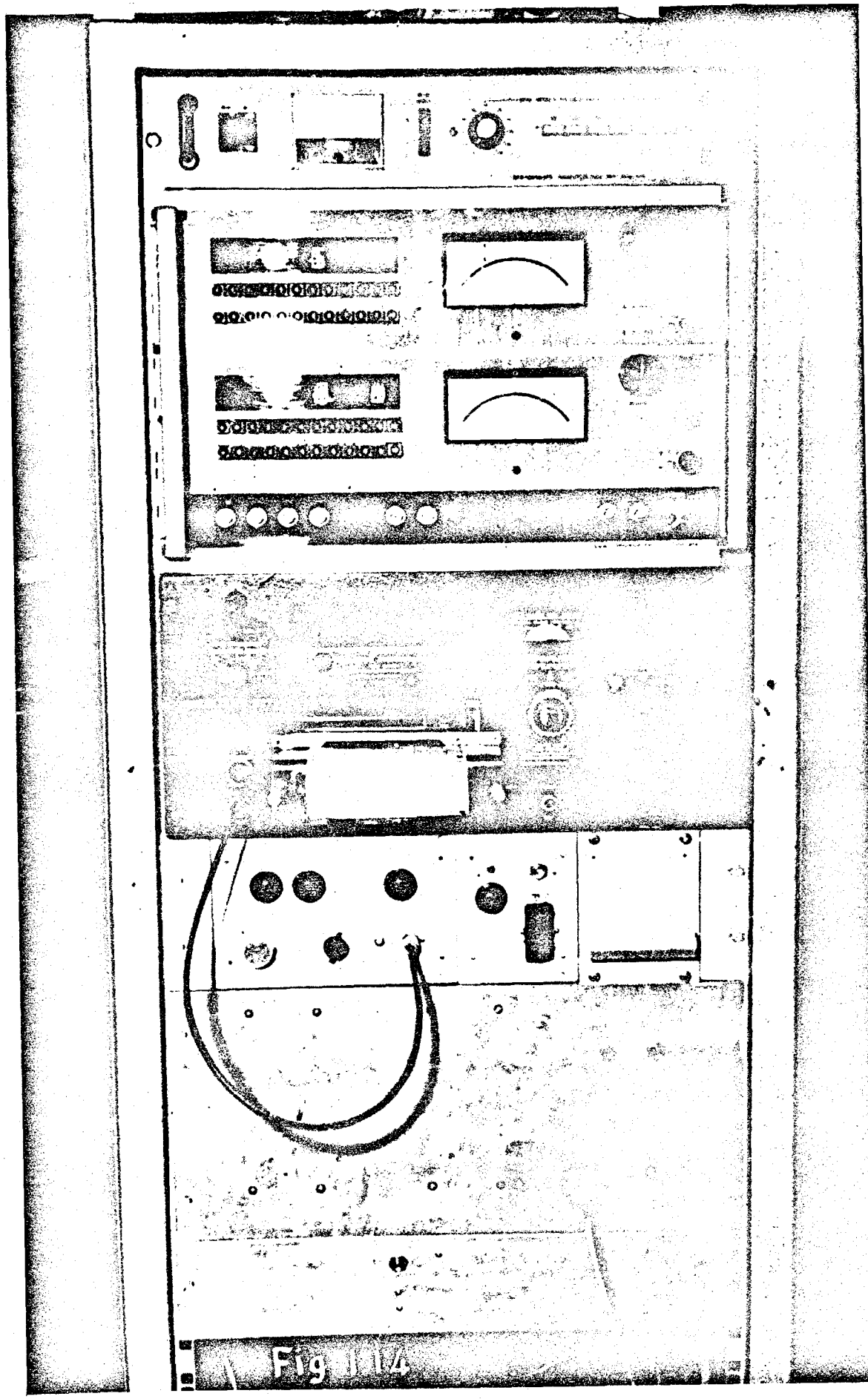


Fig I 14

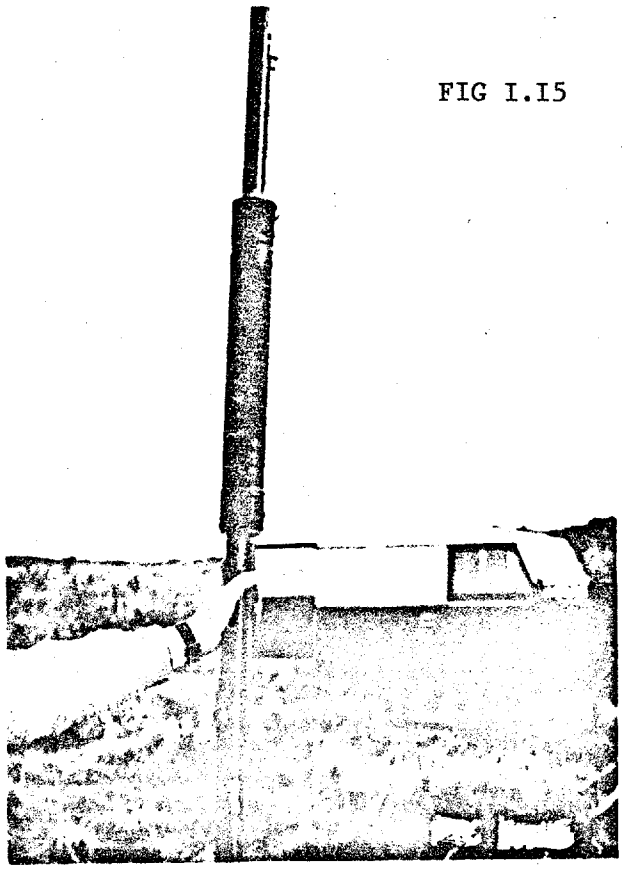


FIG I.I5

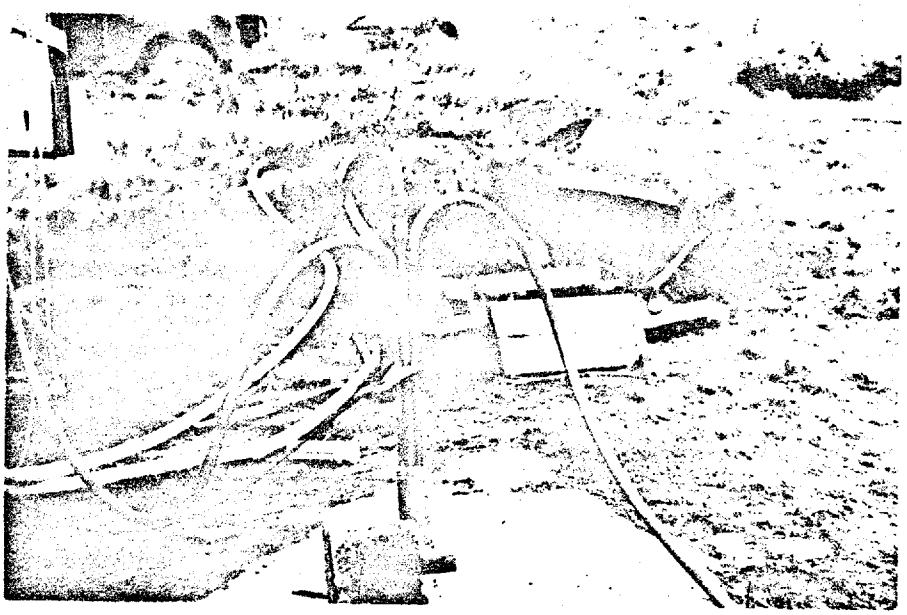


FIG I.I6

1.3.1 CONTROLS

At the top of the hole the electronic control box looks as in Fig. 1.14.

As far as the pressure tests were concerned readings of pressure could be made directly on an Avometer or on to a chart recorder. For full scale deflection of the chart recorder four different pressure options were available; 0-5 psi, 0-20 psi, 0-50 psi, and 0-100 psi. The chart recorder was extremely sophisticated and had a wide variety of speeds. The rest of the instrumentation is for tracing and it will be described elsewhere. Fig.1.15 indicates the final assembly which is being lowered into the hole and Fig. 1.16 shows it during a test.

CONCLUSIONS

In this chapter the design of the equipment that was used in the field has been described. Unfortunately no commercial projects were under way where these tests could have been carried out during the period of study and therefore most of the equipment had to be designed and built in the college workshop. The pressure probe and the four packer system have never been used before and consequently a large number of practical problems had to be solved. The use of a pressure probe in the test cavity as opposed to pressure measurements at the output of the pump proved its worth in terms of reliable and accurate measurements. The test set up was designed for research purposes where economics and speed of construction had to be optimized. In that the choice of equipment proved its worth. From the experience obtained in these tests, any equipment for commercial or repeated application should be designed on a much more rugged basis.

The equipment should be such that it presents the user in the field a minimum amount of headache so that attention can be given to the execution of the tests. For example, it would be extremely useful not only to have a continuous recording of pressure but also a flowrate so that at any time during the test history it is possible to have an idea of pressure and flowrate. If possible the direct link up of the test cavity to a pump should be aboided and a constant head tank used instead of the input end. The author had enormous difficulty maintaining a constant supply of water free of surge. The design of the packer could be improved for application where the excess pressure in the cavity is to be greater than 40 p.s.i. The improvement could be either in the choice of a thicker rubber with better seals to fix it to the probe or a completely different packer system. One possibility is the use of a hydraulic piston which would compress a solid cylinder of rubber causing it to bulge. This piston could be activated by a servo-motor coupled to a system of gears. Finally the degree of sophistication of the entire equipment depends largely on the economic importance of the problem under consideration.

ALLTWEN QUARRY

Synopsis

After a brief description of the geology of the area attention is given to the mapping of the major fissures in the quarry where in-situ hydraulic tests are to be carried out. Mapping consists of determining the mean orientation of the sets of fissures together with frequency counts of fissures in areas where the tests are to be carried out. Determination of fissure frequency is made from scaled photographs of the quarry face, corelogging and the borehole television camera. Global anisotropy of the system is described in terms of the frequency counts of fissures in different directions. At different depths in the borehole localised anisotropy will depend on the water intake during pumping tests and it will be discussed in a further section.

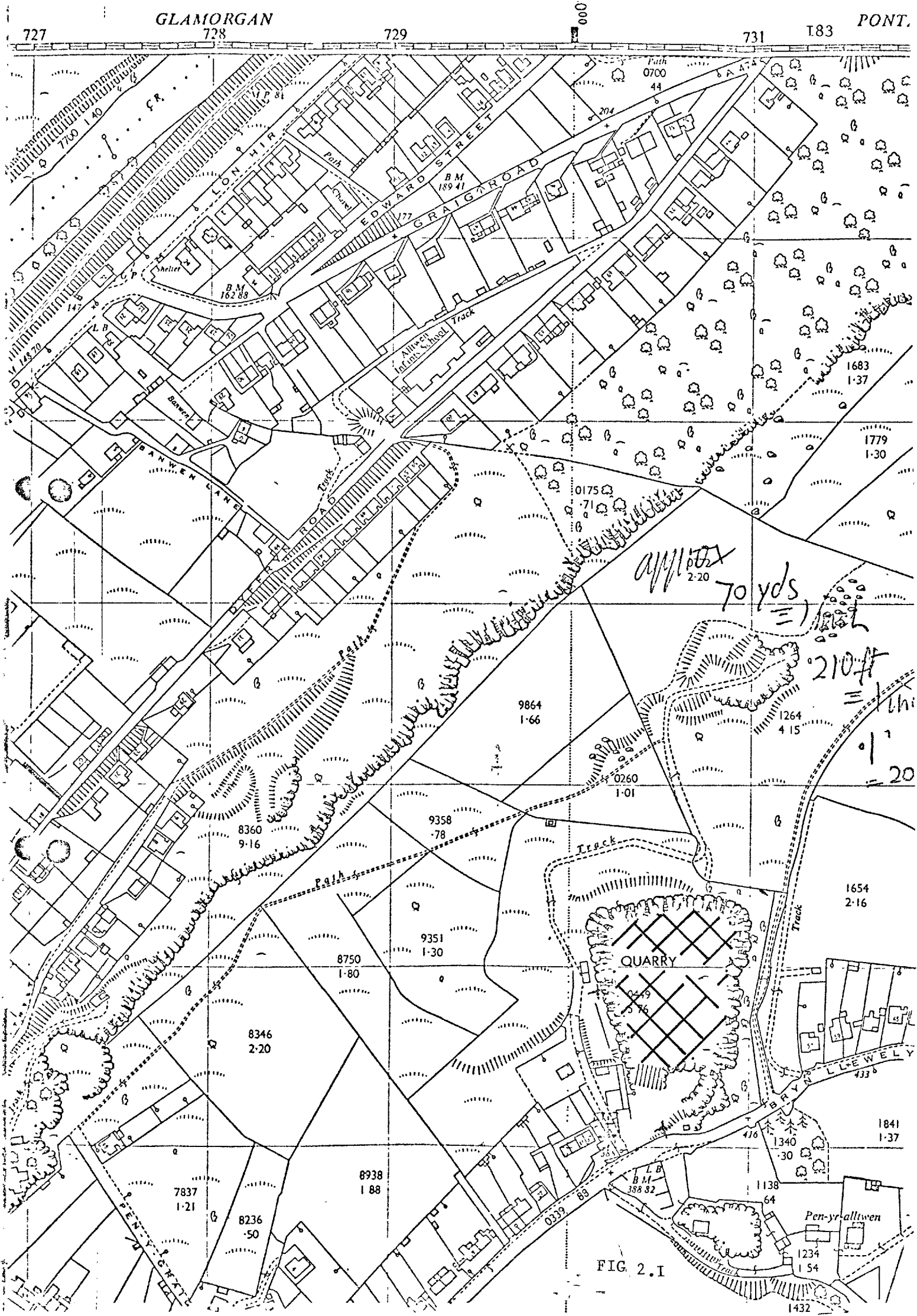

GLAMORGAN
PONT.
727
728
729
731
183
EDWARD STREET
GRAIG ROAD
LON HIR
Path
Shelter
BM 189 41
BM 162 88
Allwen Infants School
Track
BANWEN LANE
Banwen
ROAD
Track
Path
Path
Track
Track
QUARRY
BRYN LLEWELY
Pen-yr-alltwen
PEN Y GRAIG
0700
44
0175
·71
2·20
70 yds
9864
1·66
1264
4·15
0260
1·01
9358
·78
8360
9·16
9351
1·30
8750
1·80
8346
2·20
8938
1·88
7837
1·21
8236
·50
1683
1·37
1779
1·30
1654
2·16
1841
1·37
1340
·30
1138
64
1234
1·54
1432
433
416
389
0339
L B
BM 388 82

FIG 2.1

2.1.0 GENERAL

Alltwen, Glamorgan is a small village in South Wales with the following grid reference:

It has an elevation of 417ft. above the ordnance datum. The village is well above the Pontardawe valley and river. The general surface dip in the village is towards the south. Fig.2.1 is an extract from the 6 inch ordnance map. The shaded area indicates the area of the quarry. A line which runs NE-SW north of the quarry is an escarpment approximately 500ft. above the level of the river.

2.2.0 REGIONAL GEOLOGY

The tectonic structures in this area lies in the coal measures on the northern limb of the major South Wales syncline. According to Trotter (22) earth movements which have affected this area can be divided into three episodes. The first one was a force from the South giving rise to N-NW tear faults. The second episode was tension during which a second N-NW system was developed. In the last stage the structures of the past two episodes were moved latterally by the NE Tawe Valley tear fault. This can be very clearly seen from the top of the escarpment indicated in Fig.2.3 which is from Trotter (22).

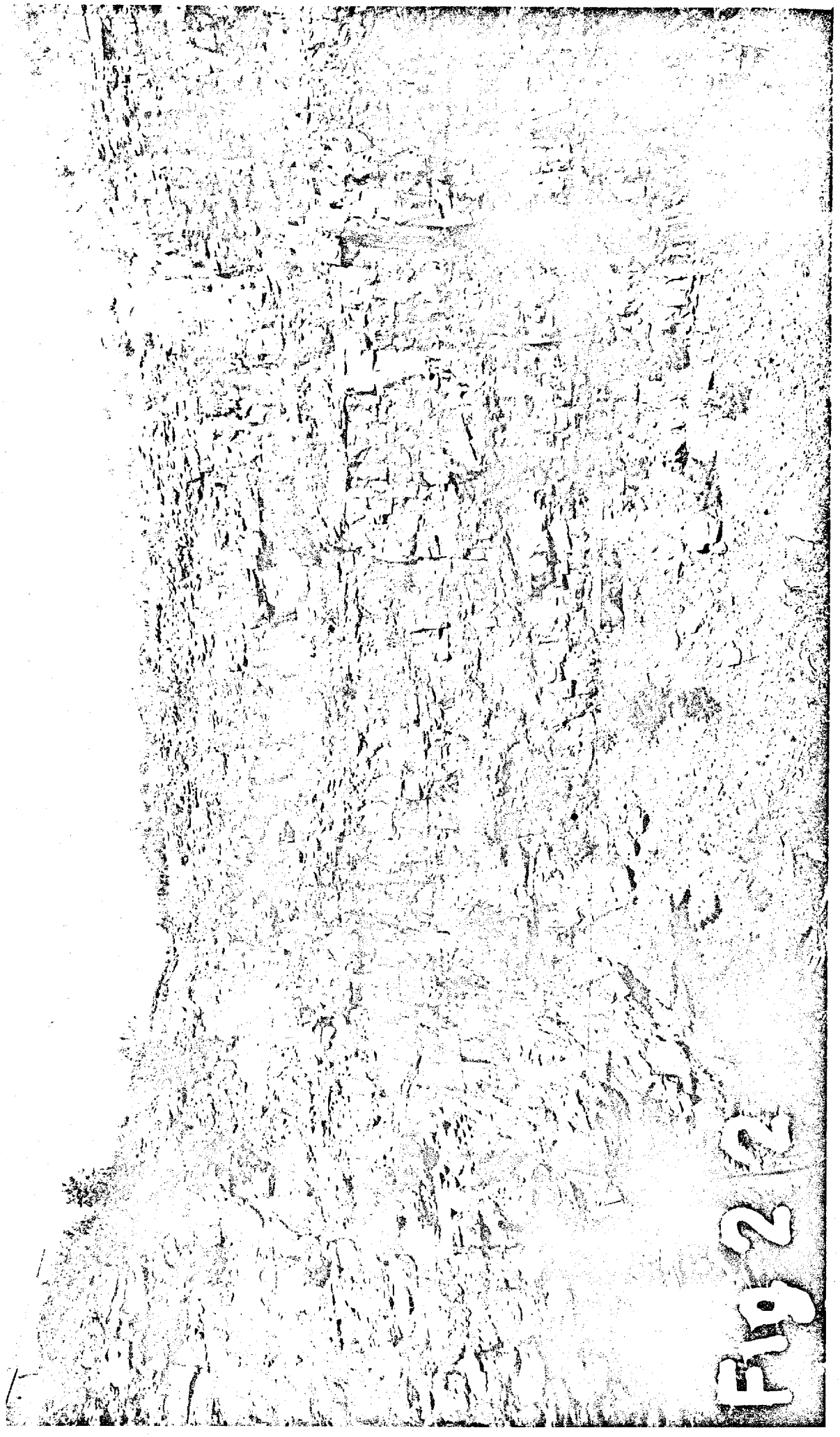
The principal rivers that drain into the area are the rivers Tawe and Loughor. Outside the river valley the chief topographical feature is the broad upland formed by the Pennant Sandstone, which slopes towards the south. To the east of the Tawe it rises to 1371ft. and to the west 1221ft. above O.D.

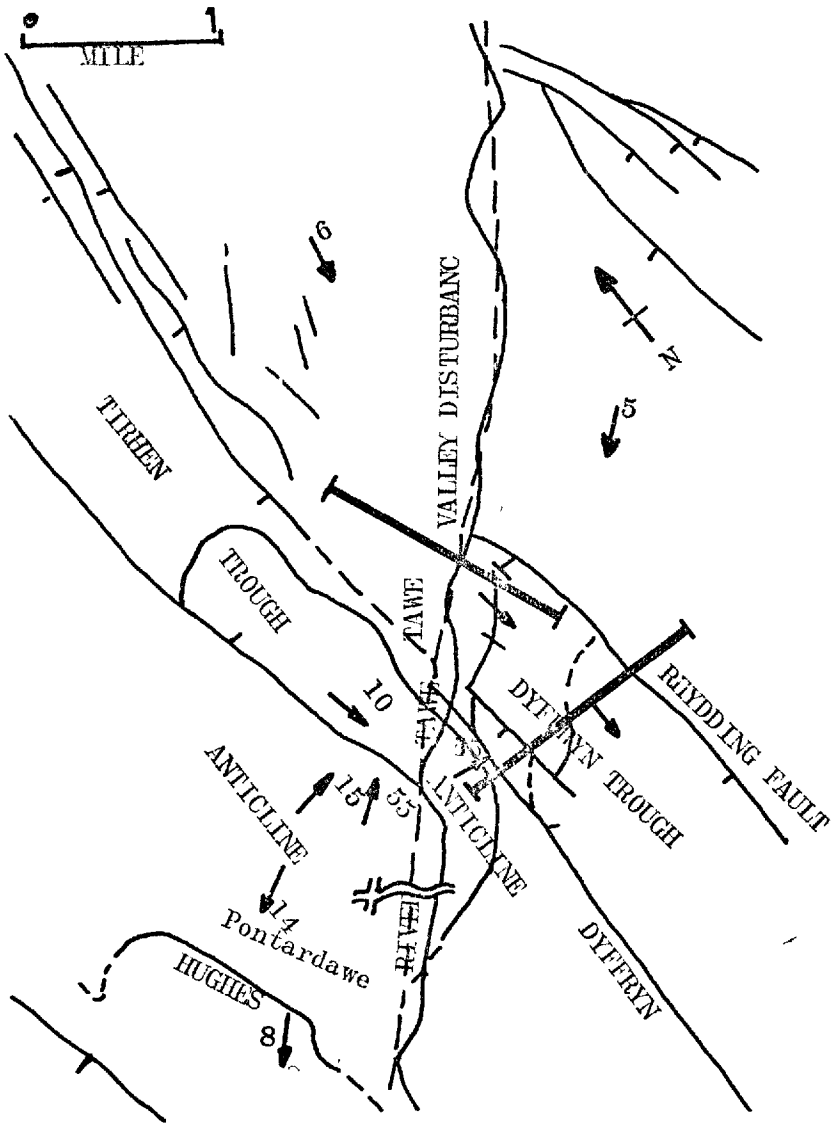
2.2.1 THE GEOLOGY OF ALLTWEN QUARRY

This quarry was chosen as the test site for its apparently simple geology so that the theories developed for testing could be tried out under conditions which were well understood. However, a more detailed examination showed that the geological structure was not as simple as had been anticipated. Fig.2.2 shows the north face of the quarry in which the bedding and vertical joint systems are very clearly shown. On closer examination the bedding is a bit confused by the cross-bedding.

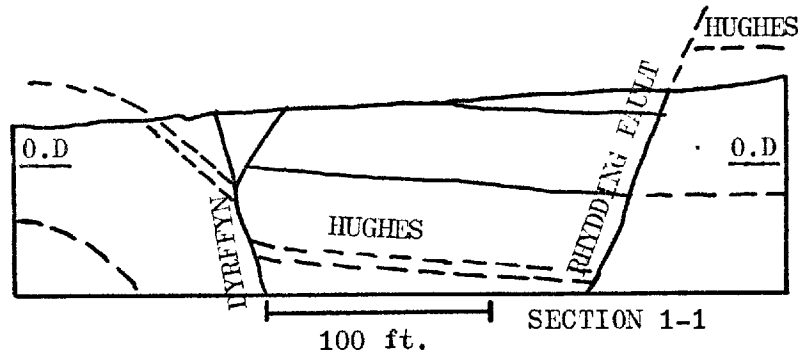
2.2.2 ORIENTATION

In order to identify the main fissure systems many readings were taken with an inclinometer. A sterio plot is the simplest and clearest way of visualising the different systems and for measuring average directions.


FIG 2



SECTION ACROSS THE TROUGH AT ALTWEN



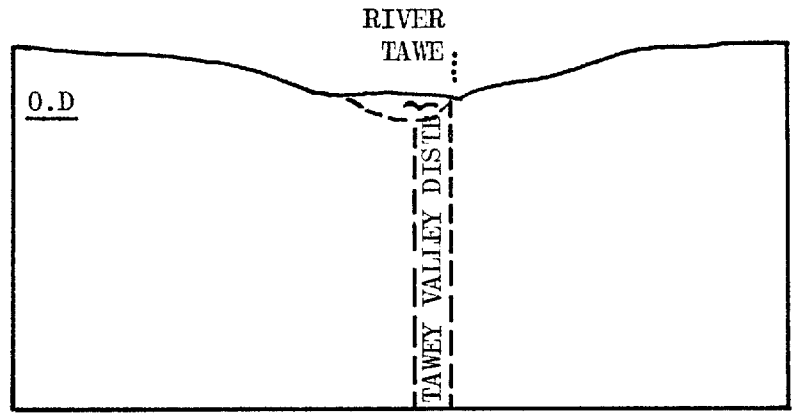


FIG 2·3

Fig.2.4 demonstrates this at Alltwen. The spread is extremely small by practical standards. From this Wulf net three main features stand out and they are:

(a) the bedding which is shallow at 18deg. dipping towards south

(b) Trend 1 dipping 80deg. west, a set of fissures running north-south

(c) Trend 2 a near enough vertical set 297deg. - 117deg.- these trends are averaged and indicated in Fig.2.4

In order to check the continuity of this system readings were taken at the small quarry and escarpment and a wulf net as in Fig.2.5 is plotted. There is a remarkable degree of agreement between these plots indicating that the fissure sets belong to the same family. Since the exposure in this quarry and the surrounding area is so good no corrections had to be made. For sites where this is not possible, the reader is referred to the paper by R. Terzaghi (23). Having established the orientation of the main sets of fissures it was decided to drill holes orthogonal to them so that permeability could be measured in the plane of the fissures. Provided the orientation of the holes is correct permeability can be evaluated in the principal directions with ease, see section 3.1.0 Part 3.

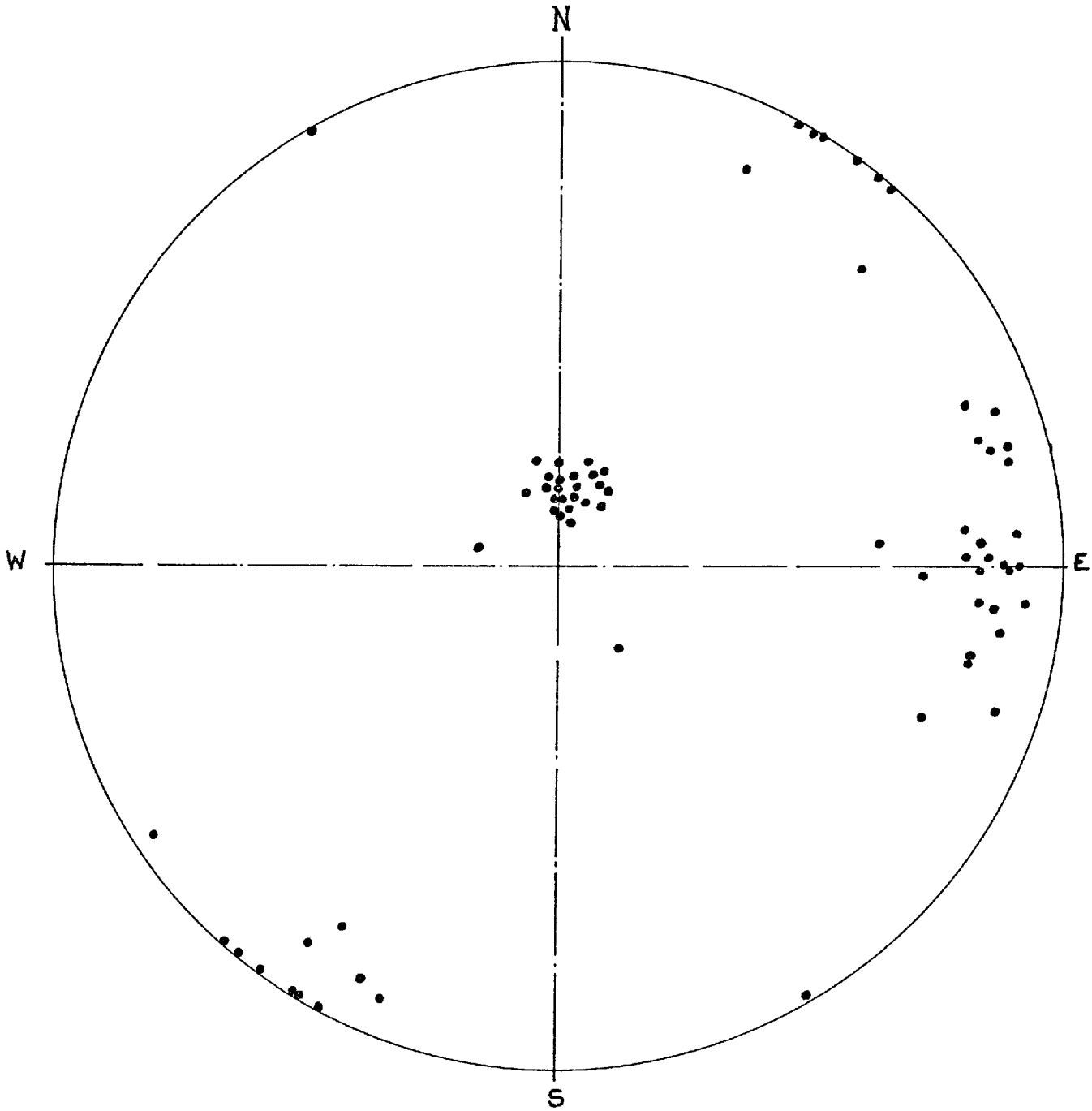
Having established the first important parameter, i.e. orientation of major fissures the next detail that has to be described is the fissure frequency in different directions.

2.2.3 DETERMINATION OF FRACTURE FREQUENCY

In order to do this there are several options. The simplest approach is to identify the main sets and use a measuring tape stretched across any two points. By counting the number of fissures an idea of frequency can be obtained. However, this simple approach does not always work because in a slope accessibility it is very often difficult and dangerous, thereby leaving the engineer to measure frequency in only a few places. In this way it is difficult to obtain a reasonable average value.

(a) Large Scale Overlay Method

In order to overcome this difficulty, it was decided that a photographic approach would be tried. Photogrammetric techniques exist for joint surveys; but these were considered as cumbersome and expensive for the quality of information they yielded.

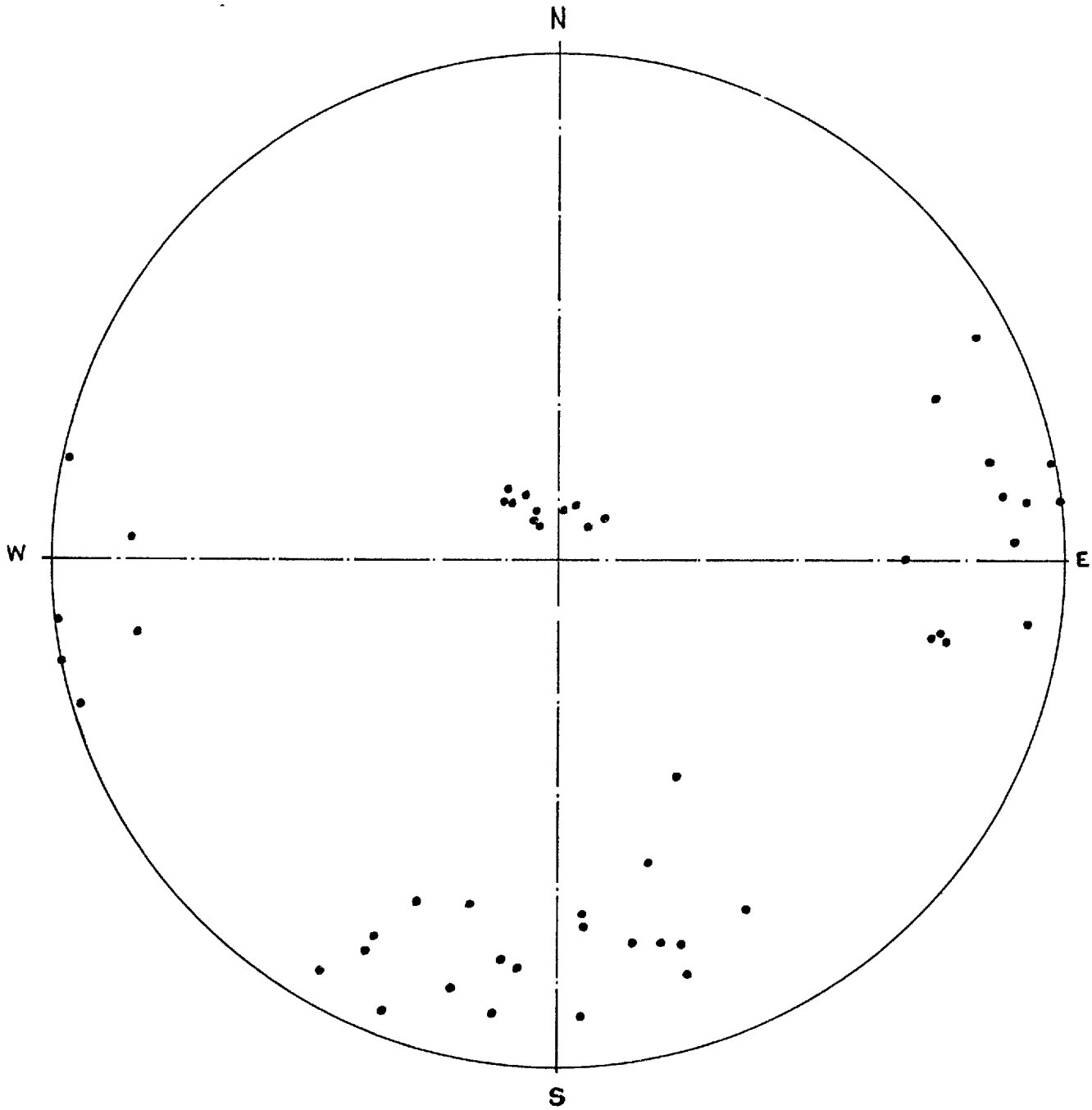


MAIN QUARRY ALLTWEN

WULF NET

Lower hemispherical projection

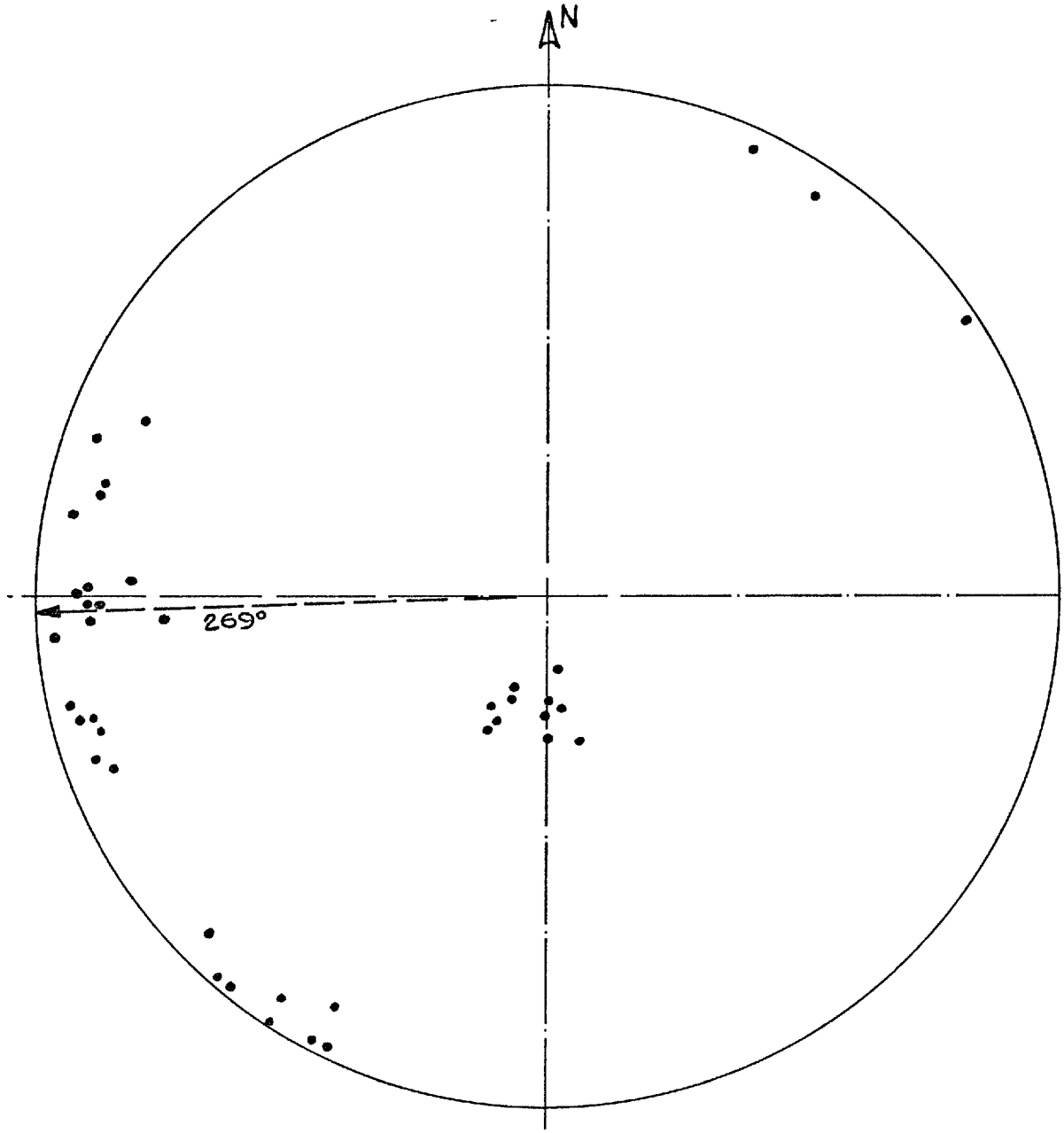
FIG 2.4



SMALL QUARRY ALLTWEN

Lower hemispherical projection

FIG 2.5



	Dip direction	Dip
Bedding	188°	18°
Joint set 1	213°	90°
Joint set 2	269°	82°

POLAR DIAGRAM

Main Quarry

FIG 2.6

Therefore a much simpler alternative was sought and this consisted of simple surveying combined with photographs using a standard 35mm. camera from the survey stations.

Fig.2.7 shows the quarry with large white crosses which were marked at the top and bottom of the face. It also shows a typical station from which a survey was conducted to fix the coordinates of the various crosses.

Fig.2.8 shows the result of such a survey. Points 1-4 from the baseline quadrilateral and points L1 to L12 are crosses on the bottom of the quarry while points T1 to T11 are at the top of the face. Photographs of all three facies were taken from stations 1-4. In this way a scale is obtained for the photographs so that frequency counts can be made directly.

This method is used to give an overall indication of the ratio of principal permeabilities based on fissure frequencies in different directions. The primary source of information of frequency as far as the water test is concerned remains the core log and the borehole television pictures. This overlay technique which involves placing a transparency over the exposure photograph and following the fractures with a pen gives some measure of continuity of fissures. It can be thus very useful for making a numerical model based on discrete fissures, or groups of fissures.

RESULTS

The success of this method depends on two factors:

(1) The clarity of the exposure. An exposure may be large and clear to observe, but quantification becomes difficult when it is attempted. This is generally due to the weathering that takes place. An exposed face is liable to corrode with the influence of air and water. The first feature that is effected is the fissure system. This was observed at Alltwen. Although it is easy to see the orientation of the main features, i.e. the fissure systems, it is extremely difficult to count them.

(2) The clarity of the picture is very important. However, this is only worth pursuing if the exposure is not badly weathered. Fig.2.9 is the mean of anisotropy ratios from four different sections within the vicinity of the hole. The histogram is broken into three steps because these depths seem to be the zones where the frequency of bedding changes, and also a 30 ft. radius seems a reasonable size with respect to the test cavity in a water test which is 5ft. Between the 30-60 ft. mark there is an abrupt change of frequency in bedding and jointing and this is due possibly to the lithological change in the rock mass. From 60ft onwards the vertical fissuring increases in number and this is indicated by the anisotropy ratio being less than 1.

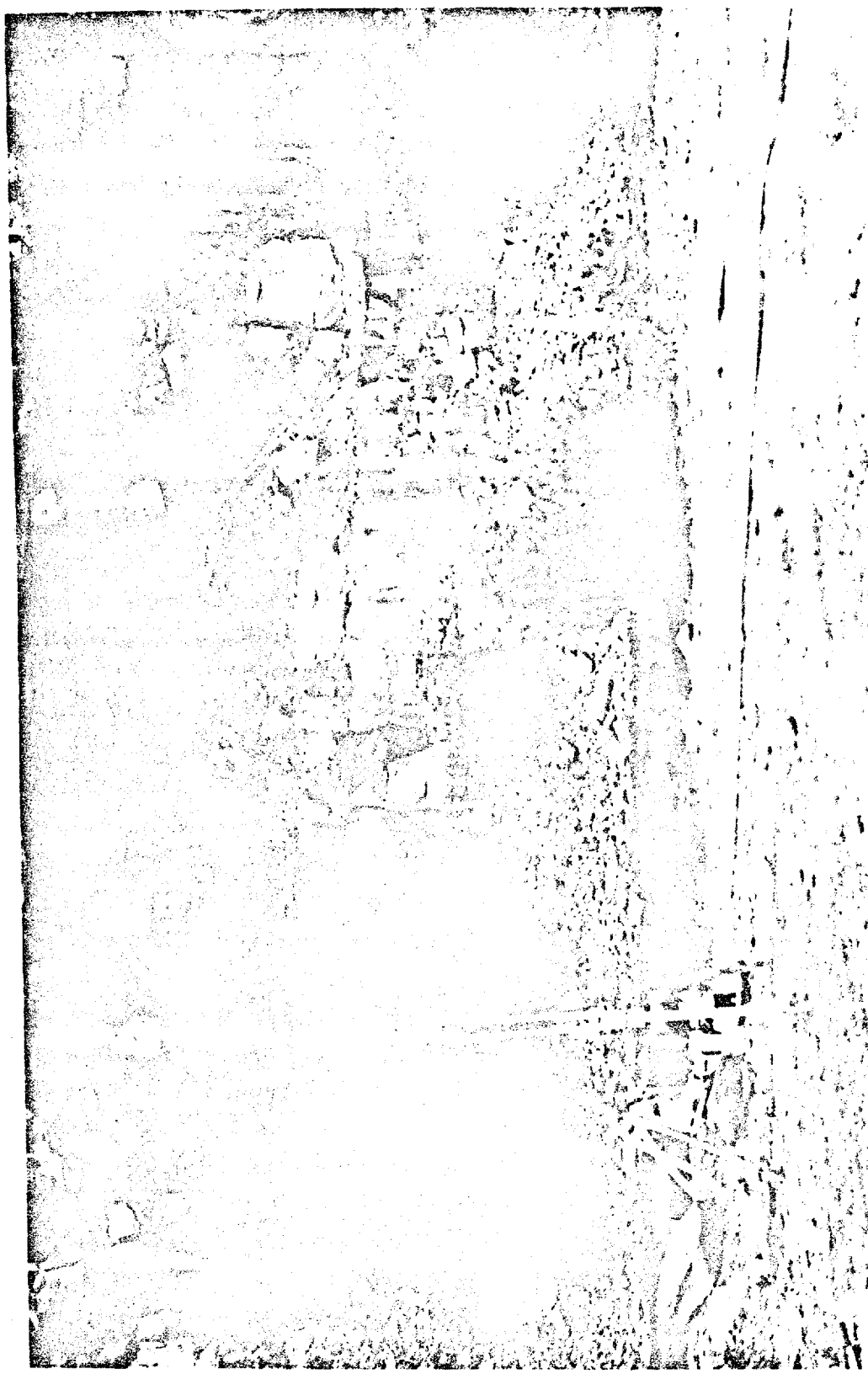


FIG. 2.7

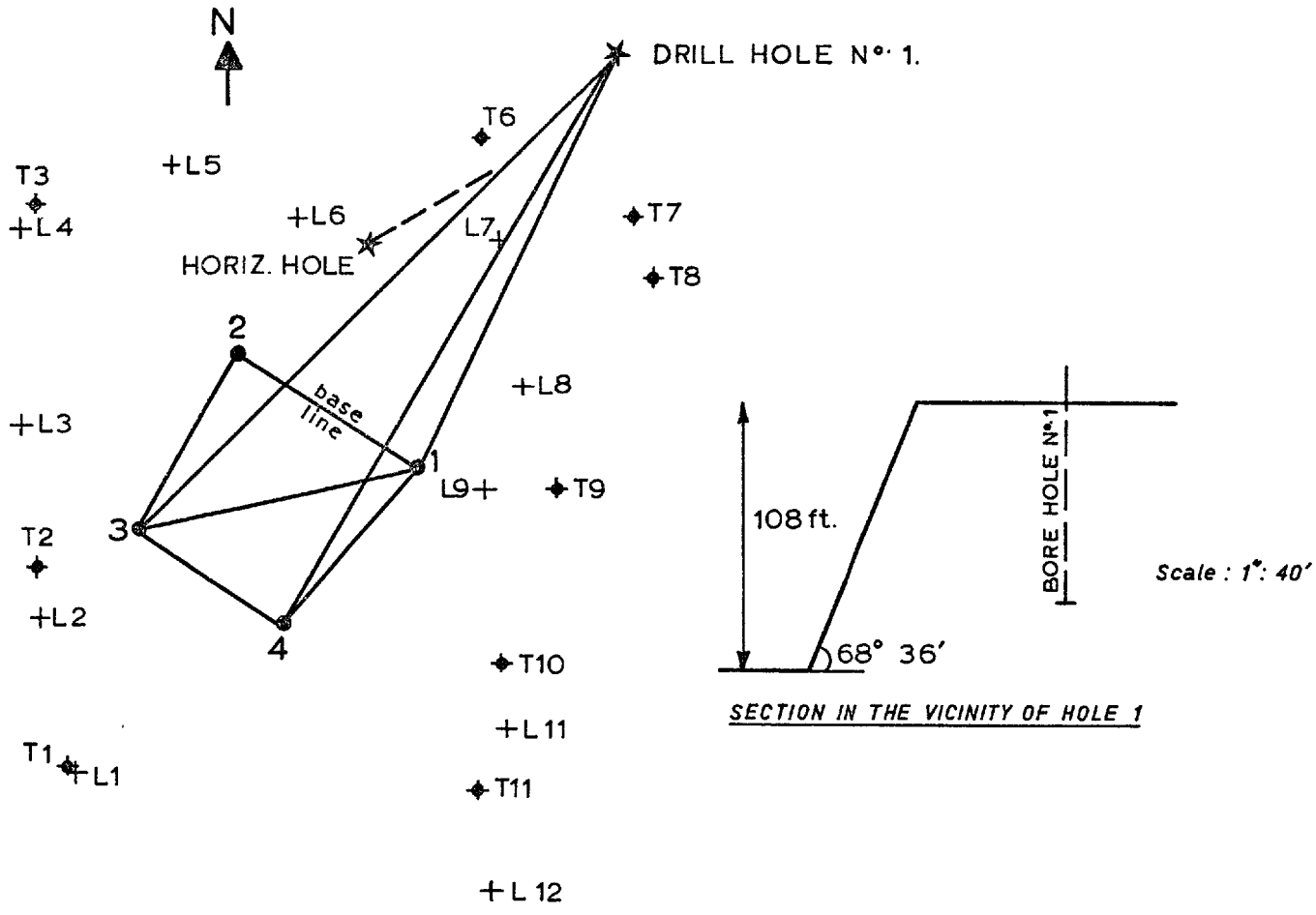
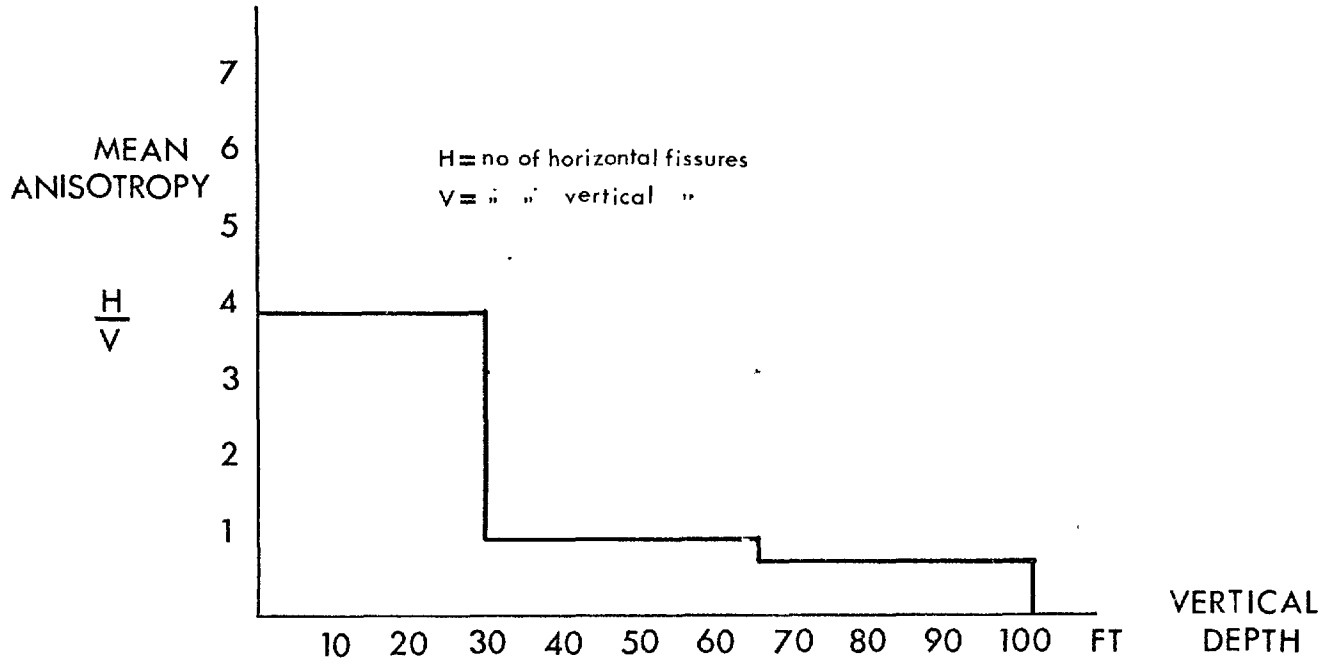

N
DRILL HOLE N°. 1.
T6
+L5
T3
+L4
+L6
L7
T7
HORIZ. HOLE
T8
2
base line
+L8
+L3
1
L9
T9
3
T2
+L2
4
T10
+L11
T1
+L1
T11
+L 12
108 ft.
BORE HOLE N°1
Scale : 1": 40'
68° 36'
SECTION IN THE VICINITY OF HOLE 1

FIG. 2.8.



ANISOTROPY FROM DIRECT OBSERVATION

FIG 2·9

(3) Degree of fissuration at the face of a slope due to blasting and stress relief.

(b) Detailed Evaluation Using Core Logging and Borehole T.V. Techniques.

The influence of fracture frequency within the test cavity of a water test is of extreme importance (section 2.1.1). A reasonable estimate of this frequency is a prerequisite to a meaningful test. The majority of tests that are carried out in practice are in exploratory holes, therefore, there is no record of the fissures. Snow (7) postulates a model where the water bearing fractures occur randomly along the boreholes and may be characterized by a Poisson distribution. The mean of this distribution is the average number of water bearing fractures. However, in a large number of problems the distribution is not randomly distributed, such environments as sedimentary rocks, and further the apparent randomness could be a function due to a sampling technique. By this is meant that fissure frequency counts are made in a hole without sorting out the orientation of the fissures. It is therefore proposed that it is by far simpler and safer to log these fissures. For this purpose two methods were tried out.

For example in a rock mass such as in Alltwen where there are very thin horizons (either shale or coal) which are weaker than the intact rock, fracture occurs during drilling and it is difficult to distinguish these from natural fissures. Further when a disintegrated shaley mess is withdrawn from the corebarrel, it is important to decide, via the test model whether this represents a highly porous void or an impermeable plug which has been shattered by drilling.

The first method was to look at the core, which came out in an excellent condition (98%) recovery. From this a fracture log was constructed. Direct observation and the stereonet was used to augment further knowledge of the different discontinuities that intersected the hole.

Fig.2.10 (A,B,C) shows the fracture logs of the three holes which were to be water-tested. Fig.2.10A is the log of the hole which intersects the bedding normally. The horizontal lines indicate the bedding while the inclined lines are the other joint sets as indicated in the stereonet. Holes A,C were specially drilled so as to intersect one set at a time while Hole B was drilled so as to interect the fissure system in an arbitrary fashion. It can be seen how in Hole A initially there is a very high density of fractures, it then dies out and increases again. This is a type of phenomenon which occurs quite often in sedimentary environments and is believed to be due to the influence of different lithologies on the jointing phenomenon (24). Since this area is associated with coal measures, thin coal bands were seen by using the borehole television camera all along the borehole walls. In many places the material was disintegrated, probably due to weathering. The majority of the bedding planes were stained brown indicating that they possibly transmitted water.

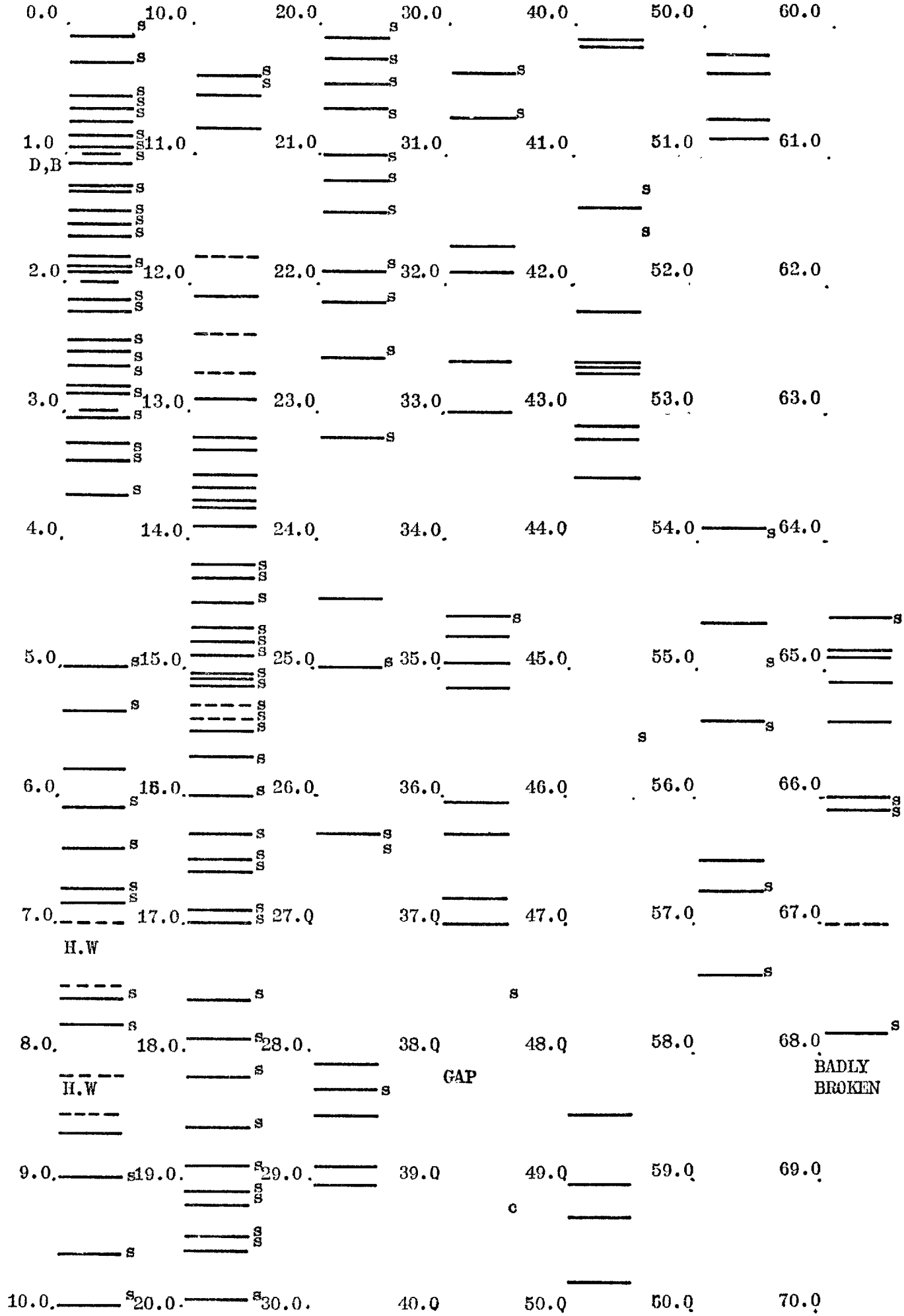

VERTICAL HOLE
0.0
10.0
20.0
30.0
40.0
50.0
60.0
1.0
11.0
21.0
31.0
41.0
51.0
61.0
D,B
2.0
12.0
22.0
32.0
42.0
52.0
62.0
3.0
13.0
23.0
33.0
43.0
53.0
63.0
4.0
14.0
24.0
34.0
44.0
54.0
64.0
5.0
15.0
25.0
35.0
45.0
55.0
65.0
6.0
16.0
26.0
36.0
46.0
56.0
66.0
7.0
17.0
27.0
37.0
47.0
57.0
67.0
H.W
8.0
18.0
28.0
38.0
48.0
58.0
68.0
H.W
GAP
BADLY
BROKEN
9.0
19.0
29.0
39.0
49.0
59.0
69.0
10.0
20.0
30.0
40.0
50.0
60.0
70.0

FIG 2.10

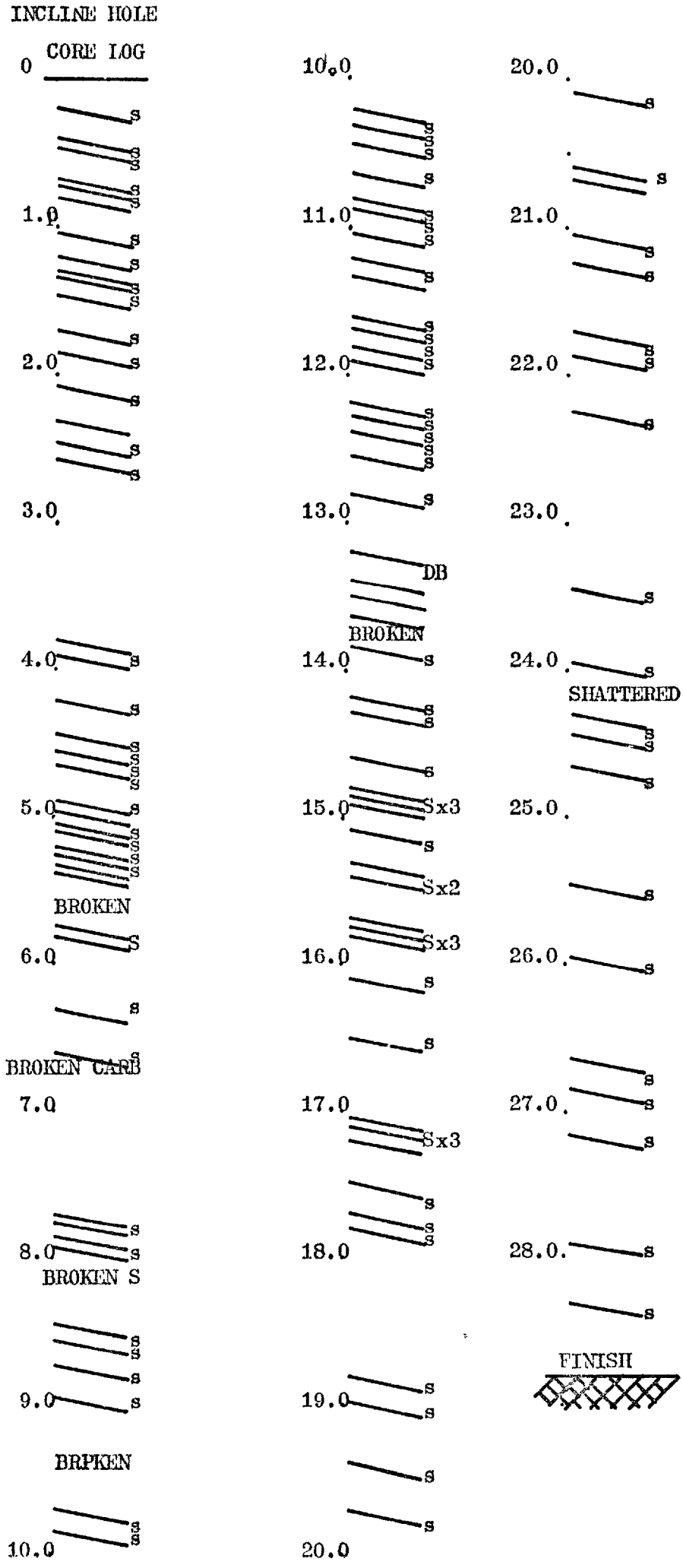
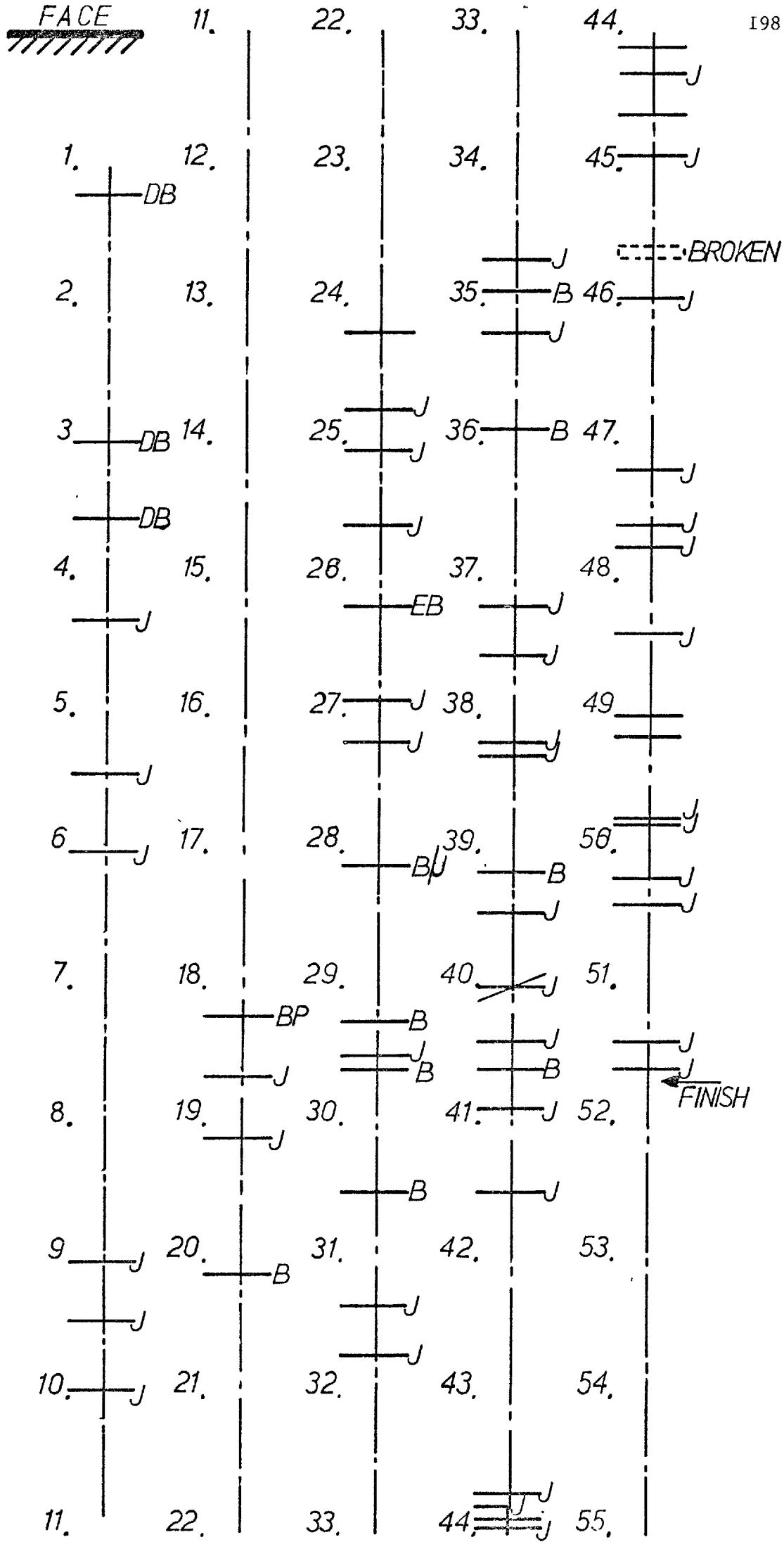

INCLINE HOLE
CORE LOG
0
1.0
2.0
3.0
4.0
5.0
BROKEN
6.0
BROKEN CARB
7.0
8.0
BROKEN S
9.0
BRPKEN
10.0
10.0
11.0
12.0
13.0
DB
BROKEN
14.0
15.0
Sx3
Sx2
16.0
Sx3
17.0
Sx3
18.0
19.0
20.0
20.0
21.0
22.0
23.0
24.0
SHATTERED
25.0
26.0
27.0
28.0.
FINISH

FIG 2.10


FACE
1.
DB
2.
3
DB
DB
4.
J
5.
J
6
J
7.
8.
9
J
J
10.
J
11.
11.
12.
13.
14.
15.
16.
17.
18.
BP
J
19.
J
20.
B
21.
22.
22.
23.
24.
J
25.
J
J
26.
EB
27.
J
J
28.
B
J
29.
B
J
B
30.
B
31.
J
J
32.
33.
33.
34.
J
35.
B
J
36.
B
37.
J
J
38.
J
J
39.
B
J
40
J
41.
J
B
42.
J
43.
J
J
44.
J
J
44.
45.
J
BROKEN
46.
J
47.
J
J
J
48.
J
49
J
J
J
FINISH
51.
J
J
52.
53.
54.
55.

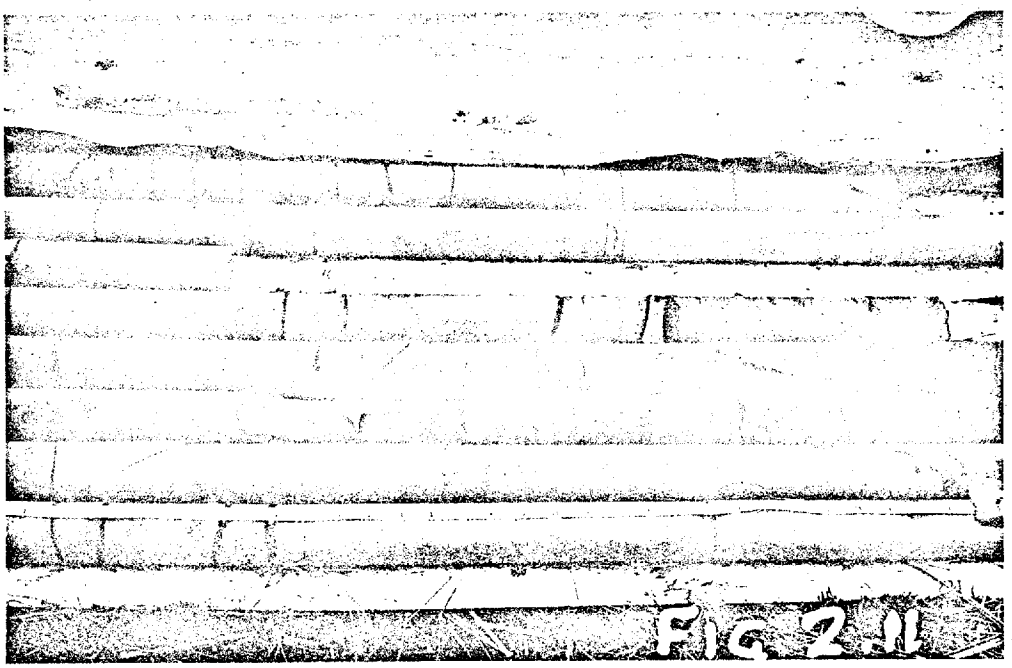


FIG 2.11

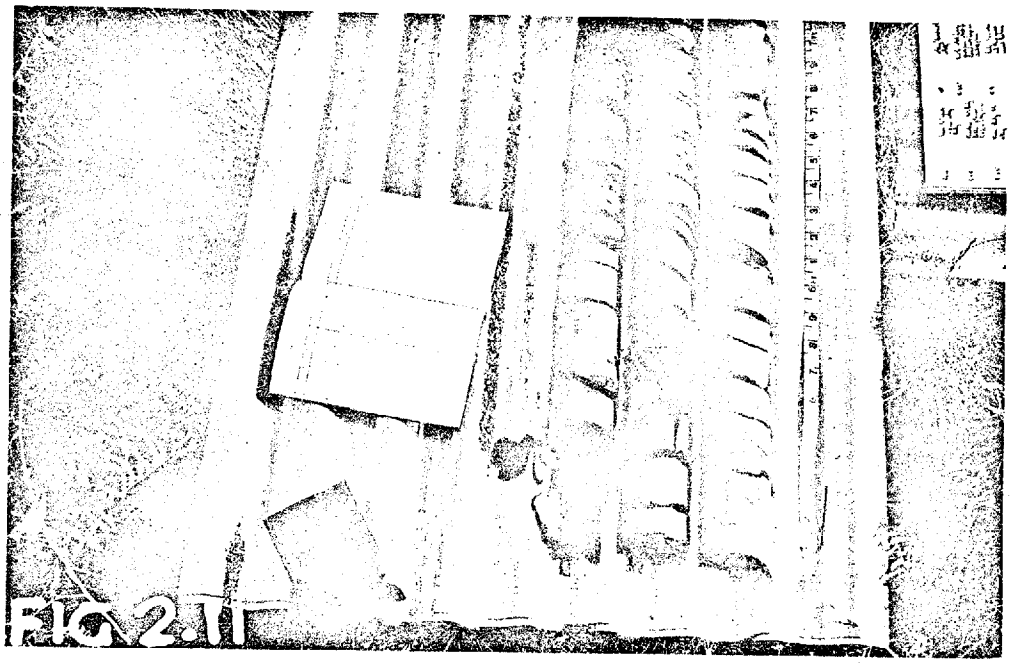


FIG 2.11

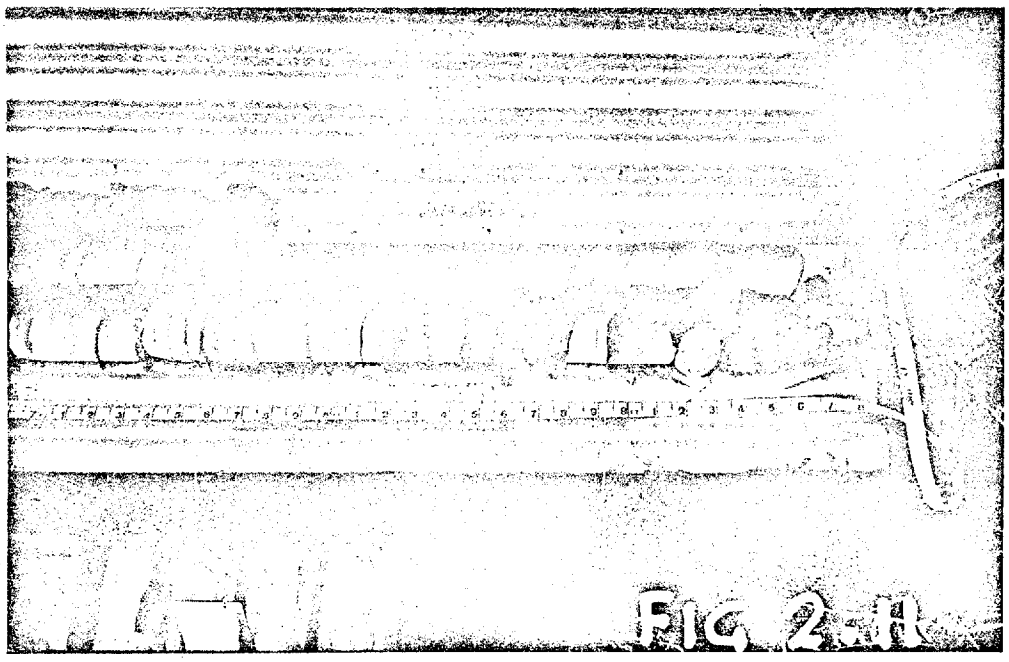
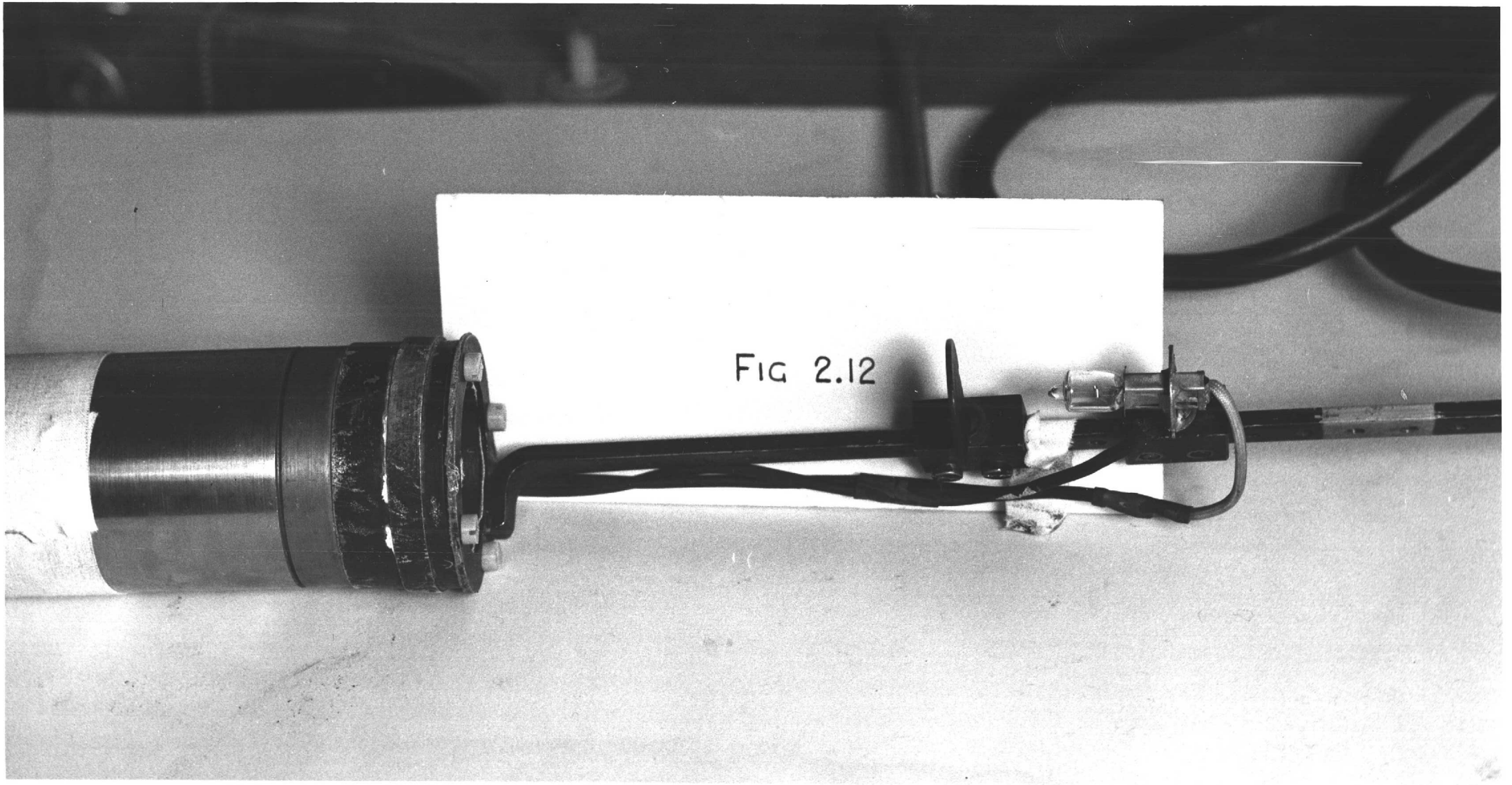


FIG 2.11


FIG 2.12

The inclination of the bedding agreed very closely with measurements made on the exposures.

Fig.2.11 is a series of photographs which indicates the quality of the recovery and also the fissure spacing and orientation. Details of the location and hole are indicated on the diagram.

In spite of the reasonable core recovery as shown by the photographs, it was felt that certain errors could creep into the model as a result of drilling. Use was made of a borehole television camera for two reasons: (i) to improve or substantiate the information obtained from a core; (ii) to see if a camera log on its own could produce data which could be of engineering significance (20,26). Previous work on the use of the T.V. camera has so far been qualitative and therefore, it is difficult to assess its practical usefulness.

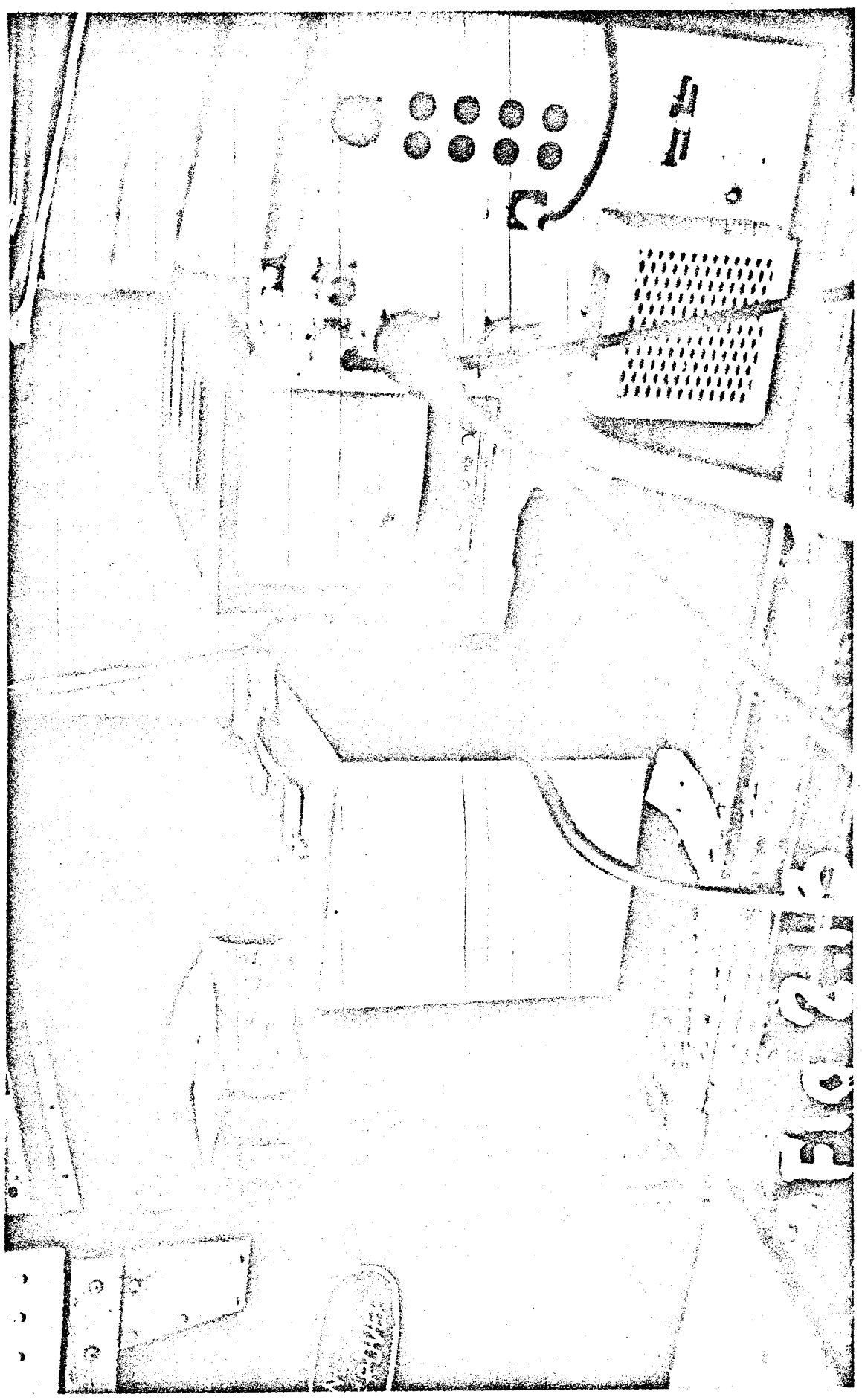
BOREHOLE CAMERA

A Pye closed-circuit television set was used for this evaluation. The camera of $2\frac{3}{4}$in. diameter is equipped with an axial viewing lense (Fig.2.12). Lighting and focus controls are remote (Fig.2.13). Maximum focussing distance is 50"

The picture is received on a monitor screen which is approximately 10sq.ins. It is possible to connect the T.V. camera to a video tape; but unfortunately, this could not be arranged in the time available for this particular field trip and therefore the camera had to be lowered slowly while manual readings were taken. The lowering device is illustrated in Fig.2.14. The cable break and depth measuring techniques were temporary; but they served their purpose very well. Three surveying tapes were attached to a lead weight and lowered down the hole (See Fig.2.14). With this type of arrangement it was possible (a) to see the depth of the camera head below ground level on the monitor; and (b) to estimate the orientation of the fissures, as the three tape method was rigid and did not twist down the hole. By placing one of the tapes on the north wall of the B/H it was possible to orientate the fissures that appeared in the field of view.

Fig.2.15 illustrates the log obtained from a camera survey. While it was very easy to see what appeared in the core as "shattered zones" the problem arose as to the distinction between fissures and thin coal bands. In most cases it was possible to tell because the coal bands were shining as the light intensity was increased, while fissures appeared to have sharp edges.

Fig.2.16 illustrates the different locations as seen on the T.V. monitor. The clarity of the pictures is extremely good. It is interesting to observe points where water is flowing into the borehole. These elevations correspond to the face seepage quite well. However, the flowrate is so small and does not substantially alter the water level in the hole.



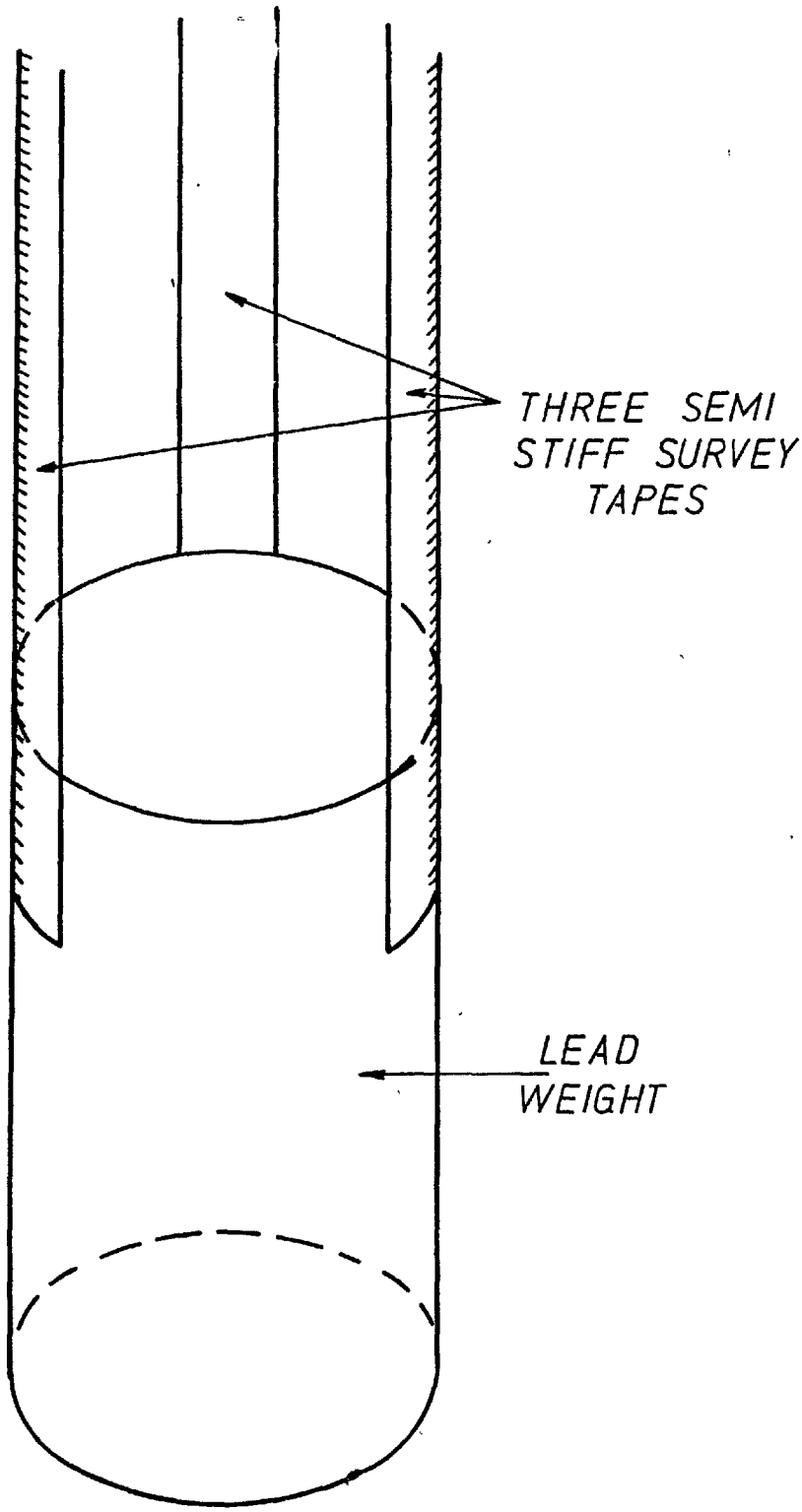
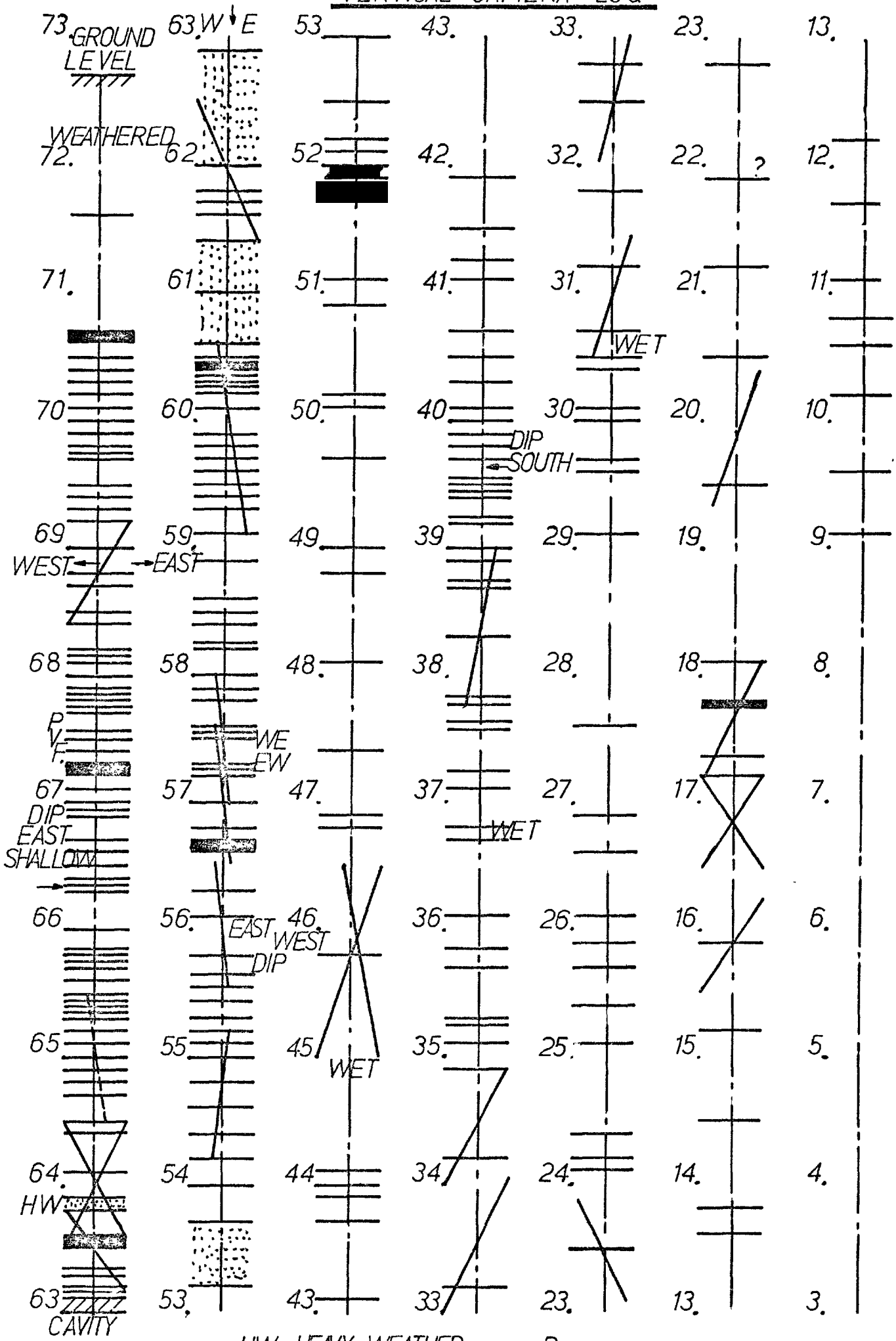


FIG 2.14

VERTICAL CAMERA LOG

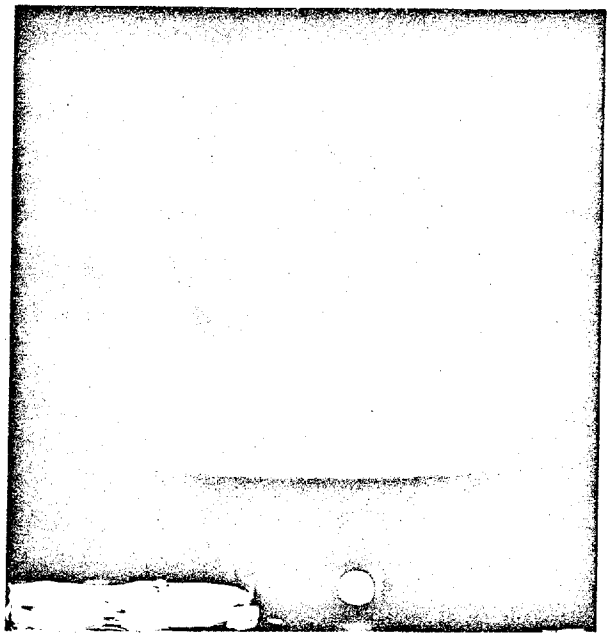


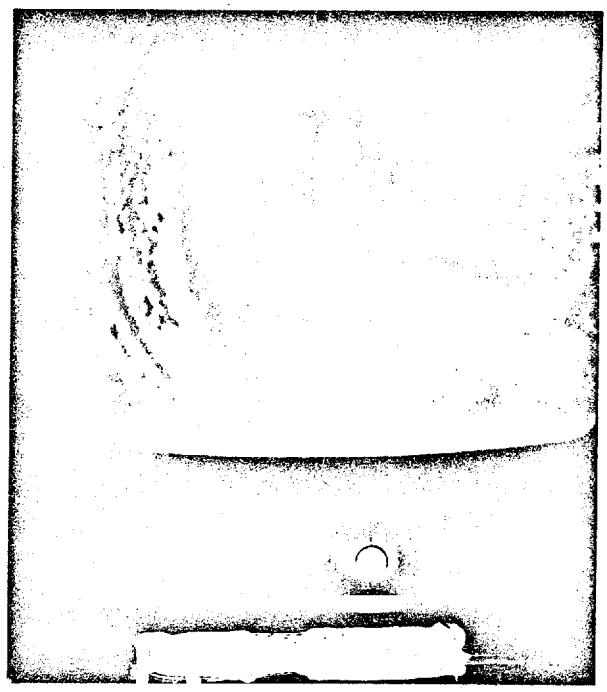
WE.= WEST EAST

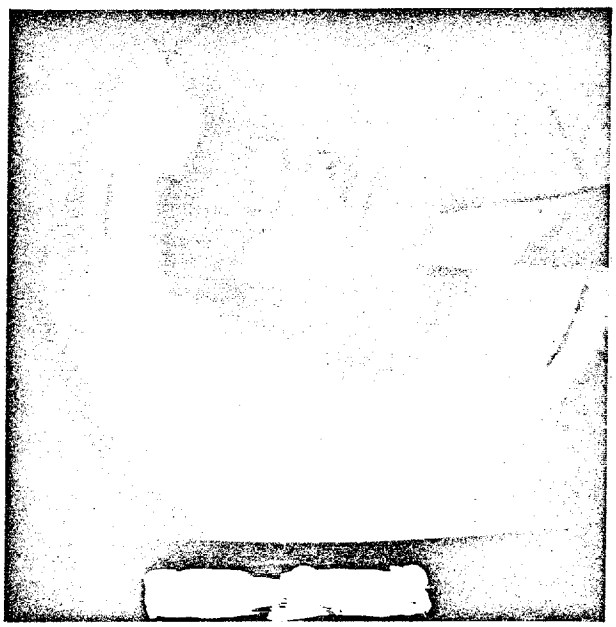
H.W =HEAVY WEATHED
EW.= EAST WEST

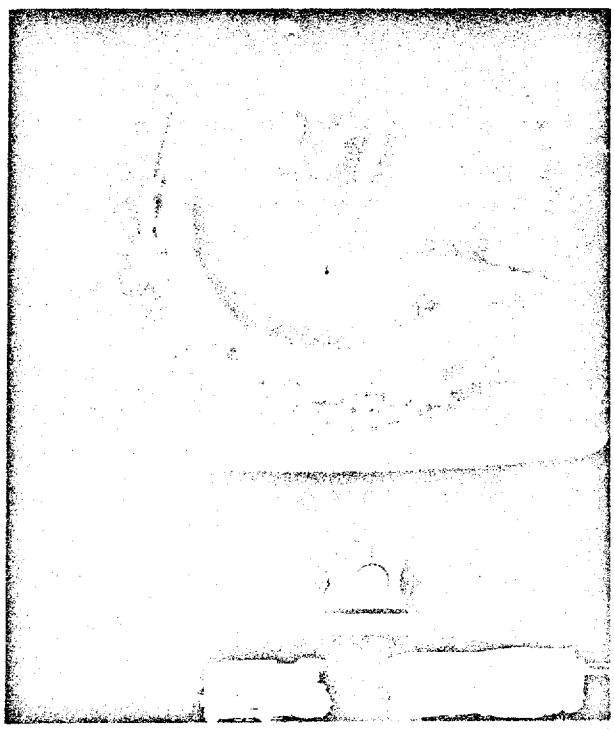
P
V
F.= POSSIBLE VIRTICAL FRACTURE

FIG 2 15









In order to get a clearer idea of the frequency distributions the results from the core log are replotted as number of fissures per 5ft. vs depth. Fig.2.19 shows the results for all the fractures that were stained and therefore water conductors. In the vertical hole the total number of fissures is high to begin with and then decreases rapidly and rises again. The inclined hole was only 30ft. deep and the frequency drops as would be expected if there is continuity between the two holes.

In Fig.2.20 the horizontal and vertical fissures are plotted separately to (a) make certain that the majority of the fissures are orthogonal to the vertical hole and (b) the fissures that intersect the inclined hole are arbitrary. Fig.2.20 shows that very few inclined fissures intersect the vertical hole while in the inclined hole the spread of the two systems is fairly wide. These diagrams are extremely useful in identifying the types of zones where the water test is being carried out in terms of high or low fissure frequency. Further it gives the ratio of stained to unstained fractures at any depth.

Fig.2.21 is the histogram of frequency vs depth as obtained from a camera survey. In general they are very similar in shape; but the ordinates differ in areas where it is difficult to give fissure distributions in the core due to damage or loss. The histogram of total number of horizontal fractures is very much closer to the camera log than to the number of water conducting fractures. This does suggest that it is difficult to distinguish between the water conductors and the impermeable discontinuities. Obviously, this illustrates this type of problem perhaps at its worst, since discontinuities in a fissured rock mass are usually open. The use of colour T.V. would undoubtedly give better differentiation. If we assume that the water bearing horizontal fractures are stained (although there is no direct proof) then a camera survey would lead to a difference infrequency of 42% as compared to 26% if all the fractures in the core were assumed to be conducting. These are not absolute values since in the estimate of stained fissures a few must be lost in drilling. In the absence of staining the estimate would be reasonable if there were no impermeable discontinuities such as coal seams then this estimate could be improved. On the basis of a camera survey in this particular example the answer is rather poor. It is further emphasised that no account is taken of errors introduced by the observer. This example illustrates the difficulty of data aquisition and interpretation. Further research into the errors introduced by the different techniques and observers in predicting geological information is well warranted.

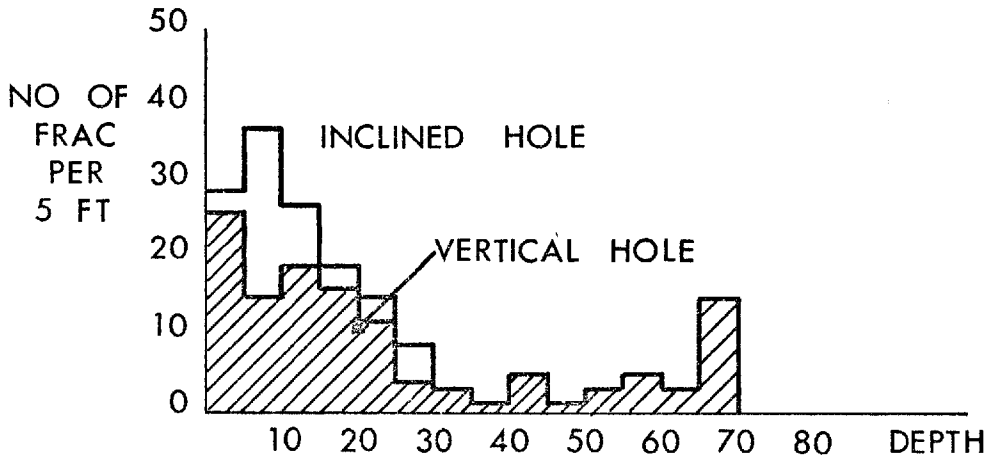


FIG 2·17

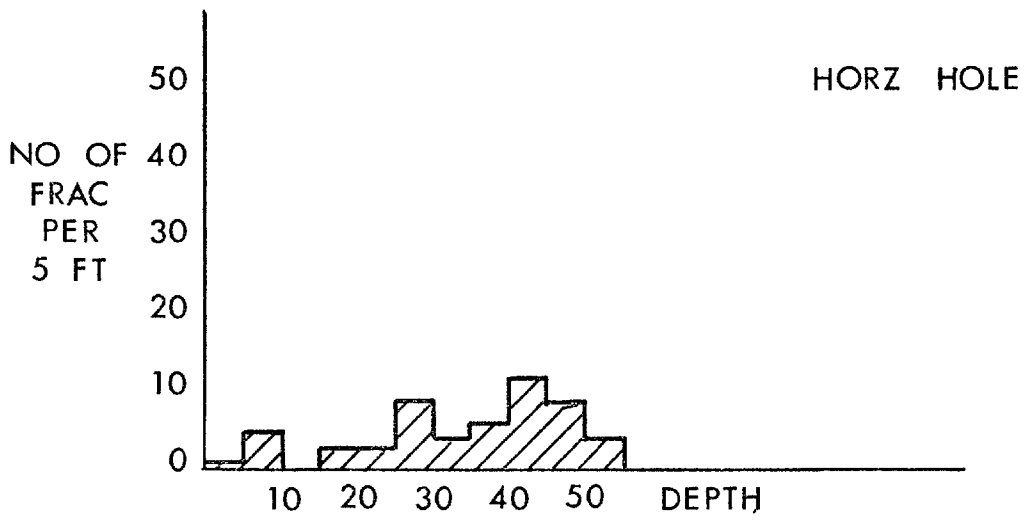


FIG 2·18

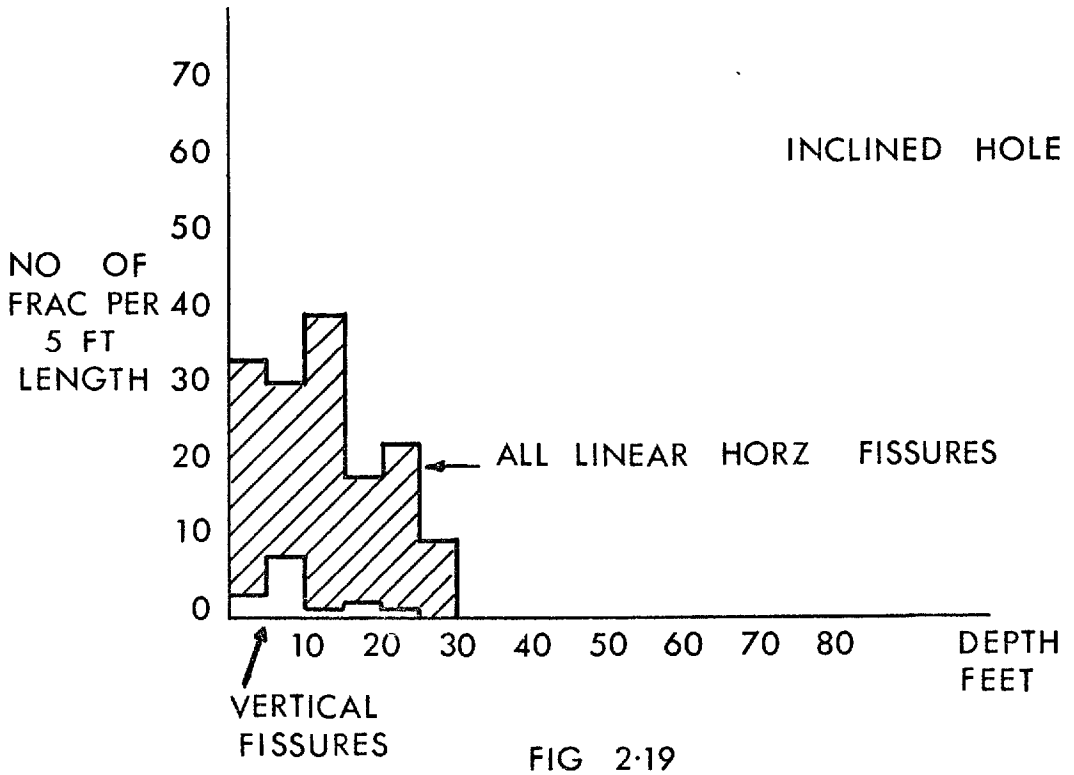


FIG 2·19

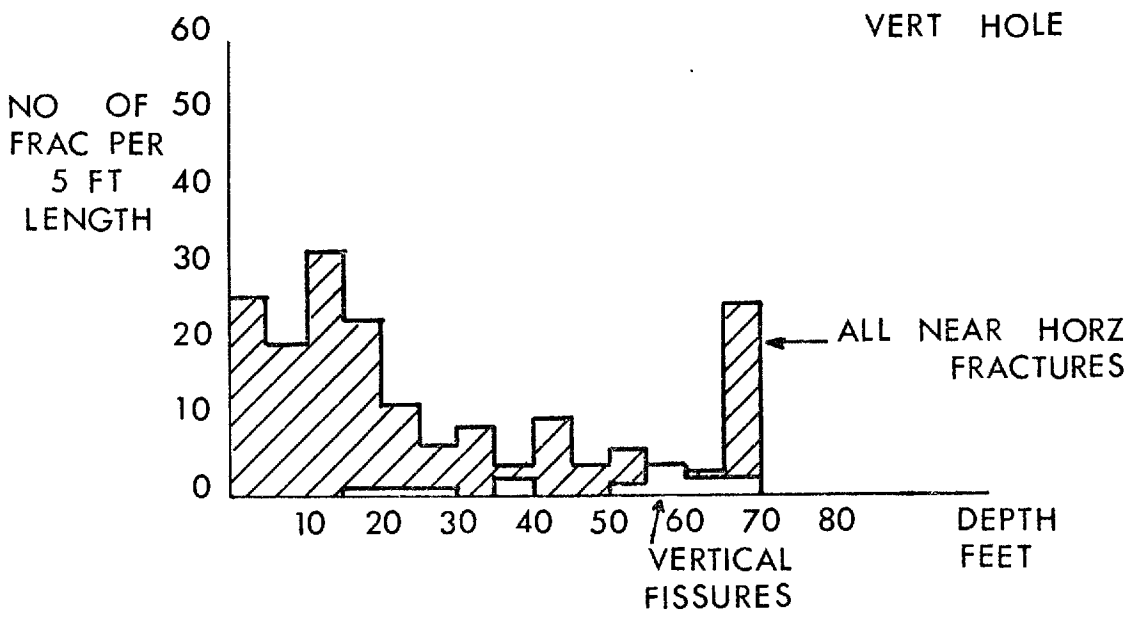


FIG 2·20

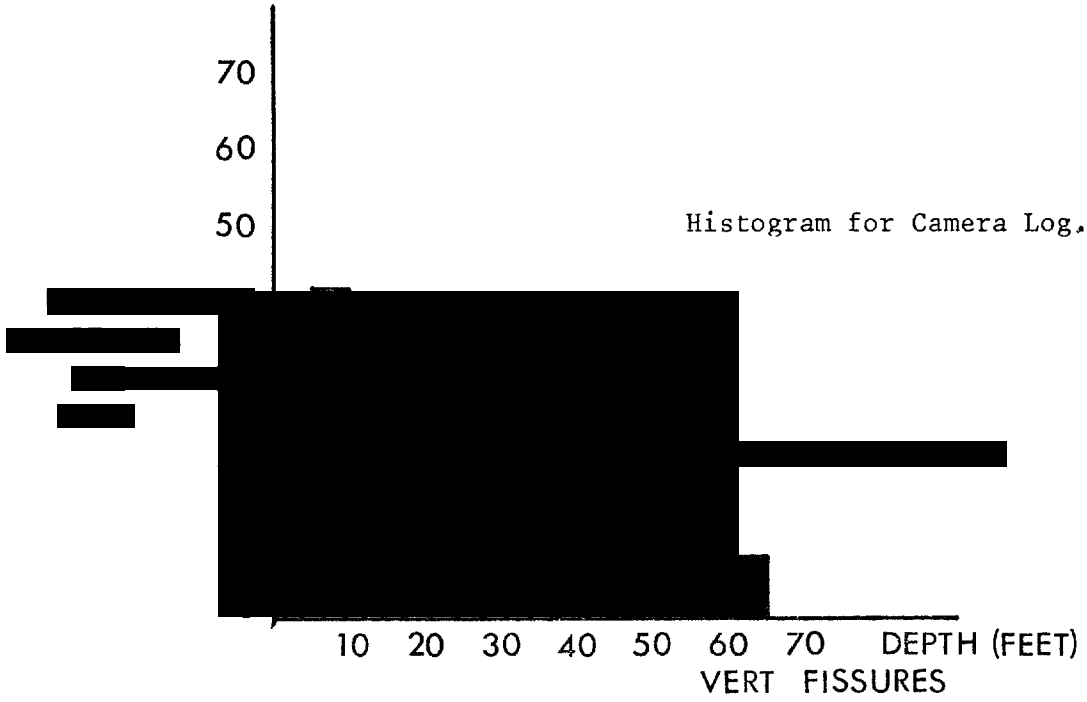


FIG 2·21

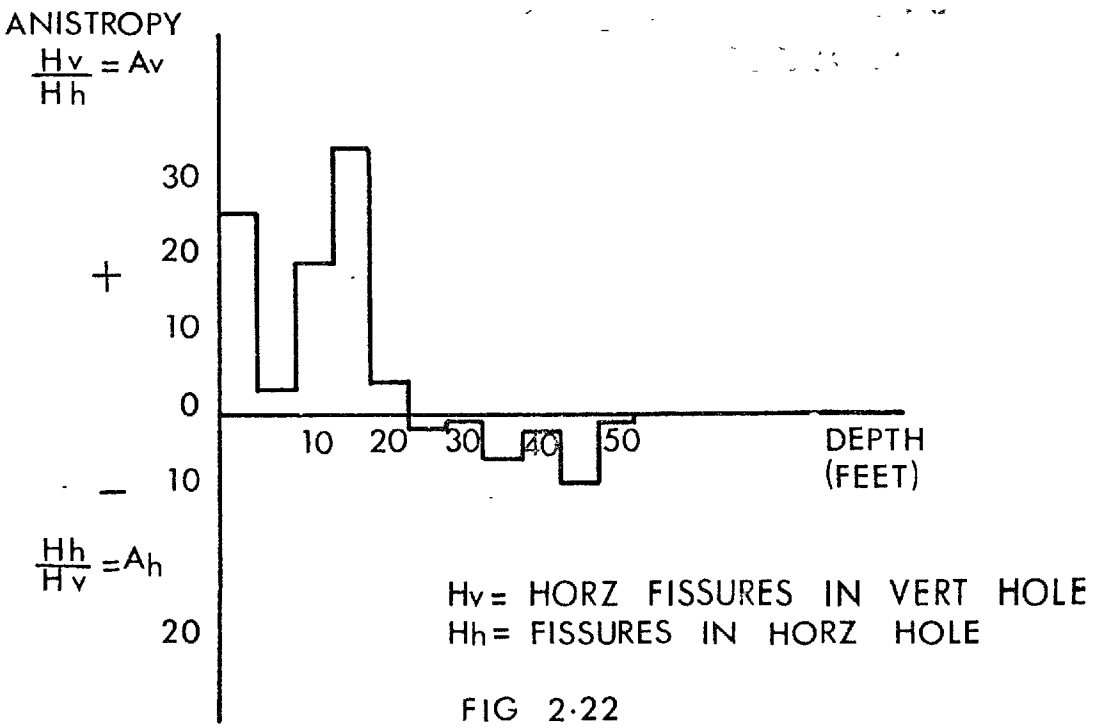


FIG 2·22

2.2.4 ANISOTROPY

The important role of anisotropy has been outlined in section 2.1.6 and 3.2.3 and this briefly is that the entire flow field is altered. If global permeability was estimated on the basis of isotropy the errors in computing pressure distributions and flow quantities would be so large as to question the validity of the test. By plotting the ratio of principal permeabilities it is possible to classify the different zones of permeability so that tests are carried out in those zones alone and are not overlapped. If however, permeability is to be evaluated on the basis of conductivity of fissures then the anisotropy diagram helps to build numerical models.

Fig.2.22 is an "anisotropy diagram" of the ratio of principal permeabilities if the apertures are equal on the basis of frequency counts in the two holes, one vertical and the other horizontal. An implicit assumption in this method is that the vertical fractures which intersect the horizontal hole are continuous and occur from the top to the bottom of the quarry. Comparison of Fig.2.22 with Fig.2.9 shows the large discrepancy between the numerical values, although qualitatively they agree. These discrepancies are believed to be largely due to the weathering of the face which does not permit high count of the closely fractured rock. The closely fractured rock does give a much lower value because of its inherent weakness it weathers quickly and appears from a distance to be smooth and planar. This is obviously a very important area of research where a degree of confidence must be placed on the frequency counts. In view of the importance of such a count to the flow model the topic ought to be studied in more depth. It is clear that this sort of a count is more difficult in a systematic joint, than for example the fracture. In orientation a heavily fractured rock with no apparent clear systems, statistical methods can possibly be used such as those proposed by Snow.

Use will be made of these anisotropy plots in the analysis of the results from pumping tests.

CONCLUSION

In a sedimentary environment such as Alltwen with no complex history in terms of folding and faulting within the quarry, the identification of different sets and orientation of the fissures was not a major problem. However, difficulties do arise when the fracture frequency is to be determined. Here localised phenomenon can lead to differing answers, but it was felt that the core log and the T.V. camera provided sufficient information. In the absence of core logging it is recommended that photographs of exposures are used to estimate global anisotropy. The description of the structure as in this chapter is the first step to identifying the material in which the water tests are to be carried out. This is the first stage tie up between the structural detail in the field and the mechanics of fluid flow through a discontinuum. Owing to the very complex nature of the problem it is a first stage and it is recommended many more such investigations are carried out in different rock types so that experience can be gained into how much of geological information can be quantified for use in numerical models of discontinua. Obviously, logging techniques such as those used in the petroleum industry would be a great asset in such investigation. Zemanek (51) for example, has described how the "Borehole Teviewer" can automatically record the orientation and position of fractures thereby reducing the time involved in producing a map of the discontinuities and further increasing the reliability of the results. Such a device would not only give an accurate picture of the discontinuities in a rock mass, but would considerably speed up the process of water testing. Effort must be chanelled into the determination of frequency distribution of fissures in a borehole as it is vital in the determination of permeability of a rock mass.

DETERMINATION OF IN-SITU HYDRAULIC PARAMETERS

SYNOPSIS

The main purpose of carrying out water tests at the Altwen Quarry was to assess the theoretical approach discussed in Part I and Chapter 1 and 2 in Part II in terms of a real situation in the field. The integration of the geological information and the mechanics of flow in fissured rock is a complex problem. These two aspects cannot be developed separately with the hope of combinging them at some final stage. Theoretical models have been postulated for a fissured rock mass and the sensitivity of various parameters on the 'pressure-flowrate' relationship studied. In order to do this it is very important to have a detailed set of points on the pressure-flowrate curve during a pumping test. Existing data from the field has at the most 2 or 3 points on the curve (10, 21, 32) and therefore the best curve has to be fitted to these few points. Further, the scant data that is available makes no mention of whether the packers have been checked for hydraulic short circuiting (7). It is therefore difficult to use such data for analysis. It is exactly with all this in mind, field tests have been carried out. The result and comparisons to the theoretical model are described in Chapter 3. It is hoped that a close examination of the results will help to improve the existing models and act as a guide to further theoretical developments in areas which have not received much attention.

Both steady state and falling head tests were carried out in Altwen in three holes to determine the permeability of the fissured rock mass at different depths. As has been described in a previous section the first hole was orthogonal to the bedding, the horizontal hole was orthogonal to one of the vertical fissure sets and the inclined hole was at an arbitrary angle so that it intersected the bedding and the two vertical sets. By carrying out computations in detail it is proposed to show how permeability of different fissure systems can be measured in the field and how different factors influence the accuracy of the answer. To begin with the linear and non-linear pressure-flowrate curves will be established and each permeability will be discussed with reference to a continuum and a discontinuum model. Reasons will be given which could lead to the non-linearity of the relationship. Finally the scale and spatial effects between the cavity and the fissure system will be described.

Subsequent to this it is proposed to show the permeability profile as measured over the entire length of all three holes. This description is the first step in building any numerical model to solve problems of drainage and uplift pressures. It was originally

envisaged that tracer tests would be carried out on this site and permeability results of the pumping tests compared with values obtained from tracer tests. Unfortunately, the extreme shortage of water during the vital period of the tests made this impossible. Only one very brief tracer test was possible and this will be reported separately in Part IV. The author considers this comparison extremely important and it is hoped that it will be carried out in the near future by other research workers.

3.1.0 LINEAR PRESSURE-FLOW RELATIONSHIP

It is proposed to consider in detail one of the many tests carried out in the vertical hole. The 'pressure-flowrate' curve obtained as a result of the test is linear indicating negligible secondary phenomenon. The following assumptions have been made in this test:

(a) Aquifer of infinite extent; this assumption is based on the geological observation of the area surrounding the test section. From Chapter 2 it is clear that the fissures have approximately the same orientation within a radius of at least 500 metres and therefore they are likely to be continuous. The aquifer is not bounded by impermeable zones and thus there is no danger of pressure building up within the test area causing unsteady state conditions.

(b) Radial flow takes place during the test. Unfortunately it was not possible to check this with two observation holes as suggested in Chapter 2. Only geological evidence was used which suggested that there had been no movement of the fissure and therefore the fissures were unlikely to have lineations. The observation of core samples of fissure surfaces and exposures did not indicate any strong lineations within the fissure planes.

(c) Negligible effect of secondary fissures, ie. those parallel to the borehole axis. In general the fissure openings were less than 0.5 mm at Altwent and therefore more than 80% of the pressure crop will have occurred within 6-9 inches from the borehole. The mean fissure spacing in a direction parallel to the borehole axis in the area of the vertical hole was approximately 2'5" (see Fig. 2.17, Chapter 2). It is on such a basis that it is assumed that near vertical fissures do not play much part in the pressure-flow relationship of the horizontal fissures.

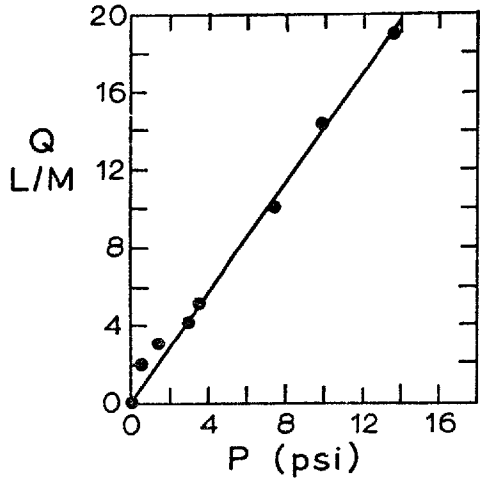


FIG. 3.1.

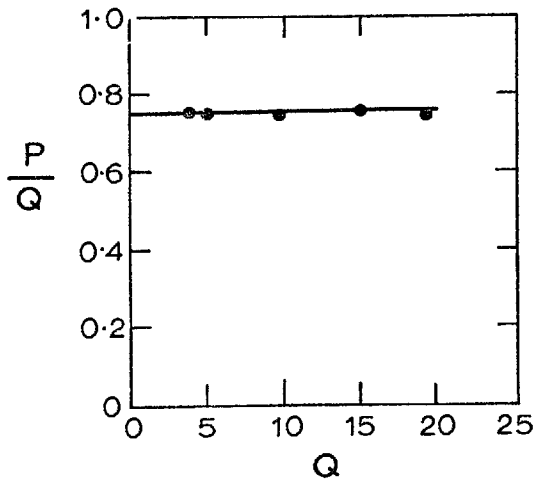


FIG. 3.2.

For flowrates corresponding to pressure see Fig 3.I

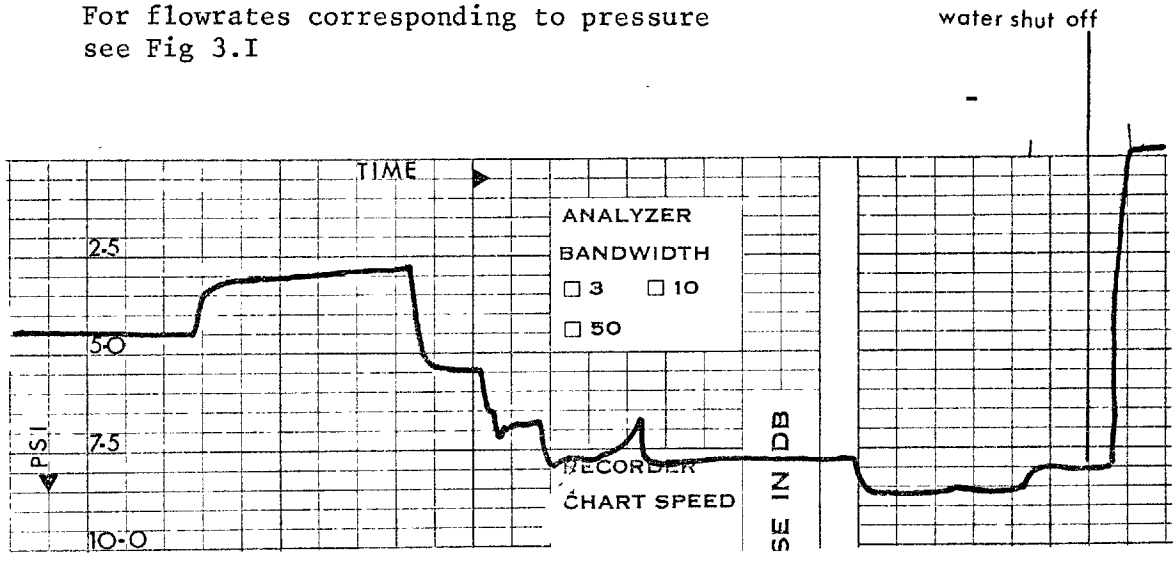


FIG 3-3 TYPICAL TEST DATA

It is proposed to derive the permeability value from this test based both on the continuum and discontinuum approach.

From section 2.1.2 in Part IIA, the pressure and flow can be equated in a general way.

$$P = AQ + BQ^2$$

In this equation, A represents the pressure drop as a result of friction, while B represents kinetic energy losses, expansion of the joint under fluid stress or any other cause for non-linearity. A curve of Q vs P as in Fig. 3.1 is a common way of representing the relationship between the flow and pressure. However, this curve is generally not sufficient in pin-pointing side effects which occur during the test. The above equation can be rewritten as

$$\frac{P}{Q} = A + BQ$$

A curve of P/Q vs Q provides the different constants. However, if secondary phenomenon do not play an important part, this curve is in the form of a horizontal line provided the flow law is linear, ie. B = 0. Fig. 3.2. A detailed evaluation will be carried out to illustrate the above points.

Location: Hole A, packed off section 13.3-18.8 ft below ground level.

Packing space = 5.5 ft.

Plotting P/Q vs Q gives a horizontal line (as in Fig. 3.2) thus indicating that the non-linear effects are negligible.

Continuum Approach

From section 2.1.2

$$P_e - P_o = \frac{Q/L}{2 K_s} \log_e \left[{}^{r_e}/_{r_o} \right]$$

P_o pressure at the hole

P_e pressure at radius r_e

r_e large dist. from test = 200 ft.

r_o radius of B/H = 1.5 inches

L packer spacing

K_s system permeability

From Fig. 3.1

$$Q/P = 20/14 \qquad \left[\frac{L/M}{P.S.I.}\right]$$

$$\therefore K_s = \frac{20}{14} \times \frac{0.236}{2\pi} \times 6.6 \times 10^{-3} \qquad (0.236 \times 10^{-3} \text{ (conversion factor)})$$

$$= 0.35 \times 10^{-3} \text{ cm/sec}$$

Permeability based on the continuum approach, or Lugeon type of test

0.35×10^{-3} cm/sec

Discontinuum

Using equations for a discontinuum; section 2.1.2

$$P - P_o = \frac{Q}{2\ neK_J} \log_e \left\{ r/r_o \right\}$$

n = No. of Fissures

e = Effective opening of fracture (cms)

K_J = Fissure conductivity (cm/sec)

From fracture log n = 15, assume fissures are identical in aperture and from fracture log it can be seen that they are evently spaced.

$$\therefore eK_J = \frac{Q}{(P_o - P)2\ n} \log_e \left\{ r/r_o \right\}$$

$$= \frac{20}{14} \times 0.236 \times \frac{1}{2} \times \frac{1}{15} \times 6.6$$

$$= 0.024 = 2.4 \times 10^{-2} \text{ cm}^2/\text{sec}$$

Effective opening of fissures = e

For a parallel plate model, $K_J = \frac{e^2 g}{12V}$ REF(8)

g = gravitational acceleration

V = kinematic viscosity

$= 1.45 \times 10^{-2}$ poise

$$\therefore \frac{e^3 g}{12V} = 2.4 \times 10^{-2}$$

$$\therefore e^3 = 4.3 \times 10^{-6}$$

$$\therefore e = 1.62 \times 10^{-2} \text{cms} = 0.162 \text{ mm}$$

$$\therefore K_J = 1.5 \text{ cm/sec}$$

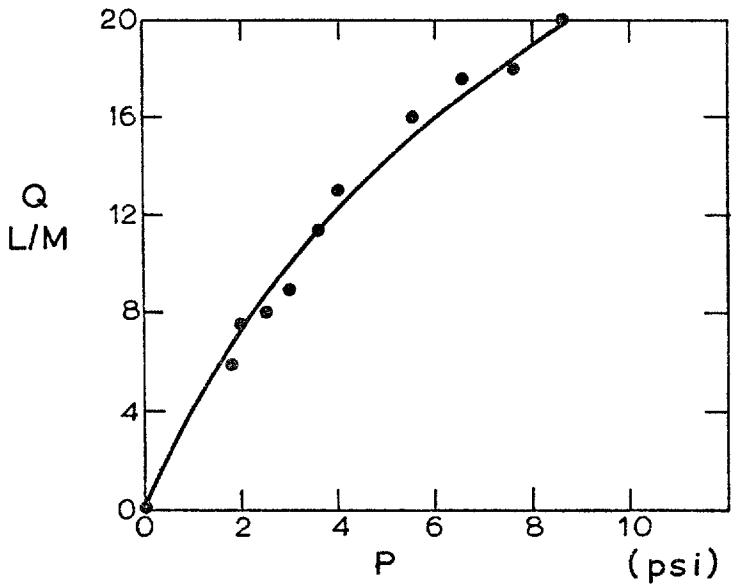
Fissure permeability:

	CONTINUUM	DISCONTINUUM
PERMEABILITY	0.35×10^{-3} cm/sec	1.5 cm/sec

Why is it necessary to compute permeability in two different ways? The answer really lies in the use that is going to be made of the results. If, for example, it is important to calculate transit time of water from one point to another in a fissured media, eg. pollution by some form of contamination, it is clearly important which concept is used. Transit time is calculated from a flow law such as Darcy's Law and by using the two different values discussed above, two completely different answers would appear for the seepage velocity, a difference of three orders of magnitude. Often Continuum permeability values are obtained as mean values and applied in computations of pressures and discharges in dams and slopes. If fissure frequency changes within a rock mass extrapolation on the basis of a continuum theory is invalid whereas permeability on the basis of discrete model could be extrapolated with reference to fissure frequency with slightly greater confidence. This extrapolation will be discussed in a further section.

3.1.1 NON-LINEAR PRESSURE-FLOW RELATIONSHIP

The case of non-linear pressure-flow relationship has recently received considerable interest in the field of fluid flow through fissured media (10, 13, 19, 21). This non-linearity is an extremely complex problem and can be attributed to (a) Kinetic Energy effects (b) non-linear pressure-flow laws within the fissures (c) Leakage past packers (d) fissures opening up. In principle there is no reason why these effects do not act individually or in a combination. The last factor is a very much more difficult problem to analyse. It is proposed that it is dealt with separately because it influences both the linear and the non-linear case. The available technology is far from pinpointing the side effects; but hypotheses can be made and checked on the basis of simplified models. Pressure-flow non-linearity is an extremely important phenomenon because it is on such a basis discharges and pressure distributions are calculated in a rock mass. If the non-linearity is a result of the test then grossly inadequate results will follow from any computation. Alternatively, failure to reccgnise non-linearity in a fissure system will lead to disastrous results.



6·0 – 11·5 ft. below ground level Hole A packer spacing 5·5 ft.

FIG. 3.4.

(a) Kinetic Energy Effects

The possibility of secondary phenomenon such as kinetic energy losses as a result of the fluid accelerating as it leaves the hole must be evaluated at the outset; section 2.1.2 & 2.1.4. If these are negligible and the relationship between pressure and flowrate is non-linear, it is then necessary to apply non-linear flow laws to the analysis of the results. Let us consider a field example to illustrate the point.

Location: Hole A, packed off section 6.0-11.5 ft below ground level

Packer Spacing = 5.5 ft.

Consider Fig. 3.4 which is a non-linear pressure-flowrate curve. From this curve it is possible to calculate the component of pressure drop due to the changes in kinetic energy. From this it will be possible to see if the non-linearity is a result of K.E. changes due to acceleration of the fluid.

$$eK_J = \frac{Q}{(P_o - P)2\ n} \log_e \left\{ r/r_o \right\}$$

Using the linear portion of Fig. 3.4

$$eK_J = 0.084\ cm^2/sec$$

Let us assume a parallel plate model for the fissures.

$$K_J = \frac{e^2 g}{12V}$$

$$\therefore \quad e^3 = 1.46 \times 10^{-5}$$

$$\therefore \quad \underline{e = 2.44 \times 10^{-2} \text{ cms}}$$

The frictional component of the pressure drop at a flow of 20 litres/min

$$P = \frac{\log_e\{r_1/r_o\}\, Q}{2\pi e n K_J} = \frac{233 \times 6.7}{2\pi \times 15 \times 0.084} = \underline{280 \text{ cms head of water}}$$

The K.E component of pressure: EQ 2.15

$$P_{Kn} = \frac{3Q^2}{20\pi^2 e^2 n g} \left[\frac{1}{r_1^2} - \frac{1}{r_o^2}\right]$$

$$= \frac{3 \times 333 \times 333}{20\pi^2 \times (2.44 \times 10^{-2})^2 \times 15^2 \times 980 \times (1.5 \times 2.54)^2}$$

$$= \underline{0.89 \text{ cms head of water}}$$

This indicates that the kinetic energy losses as a result of the fluid acceleration as it leaves the hole is negligible. It is interesting to note that at a flowrate of 20 litres/min the pressure change was 9.5 psi - approximately 680 cms. This loss is not indicated if we accept the linear pressure-flowrate law. The extra energy to provide a flow of 20 litres/sec is presumably lost in overcoming friction within the fissure.

(b) Non-linear pressure-flowrate laws within the fissure system

In section 2.1.3 the use of a non-linear 'pressure-flowrate' law has been discussed. Two laws, ie. those by Forchheimer and Miesbach describe non-linear phenomena of fluid flow adequately (13). Although the Forchheimer law is more general (13) it was decided that there would be no loss in generality if the Miesbach law was used. A further advantage of the Miesbach law is the ease with which data can be handled. The procedure involves plotting log P vs log Q and from the slope and intercept it is possible to determine all the constants in Equation 2.2.0. The Forchheimer law applying the n^{th} power needs a cumbersome process to separate the various constants.

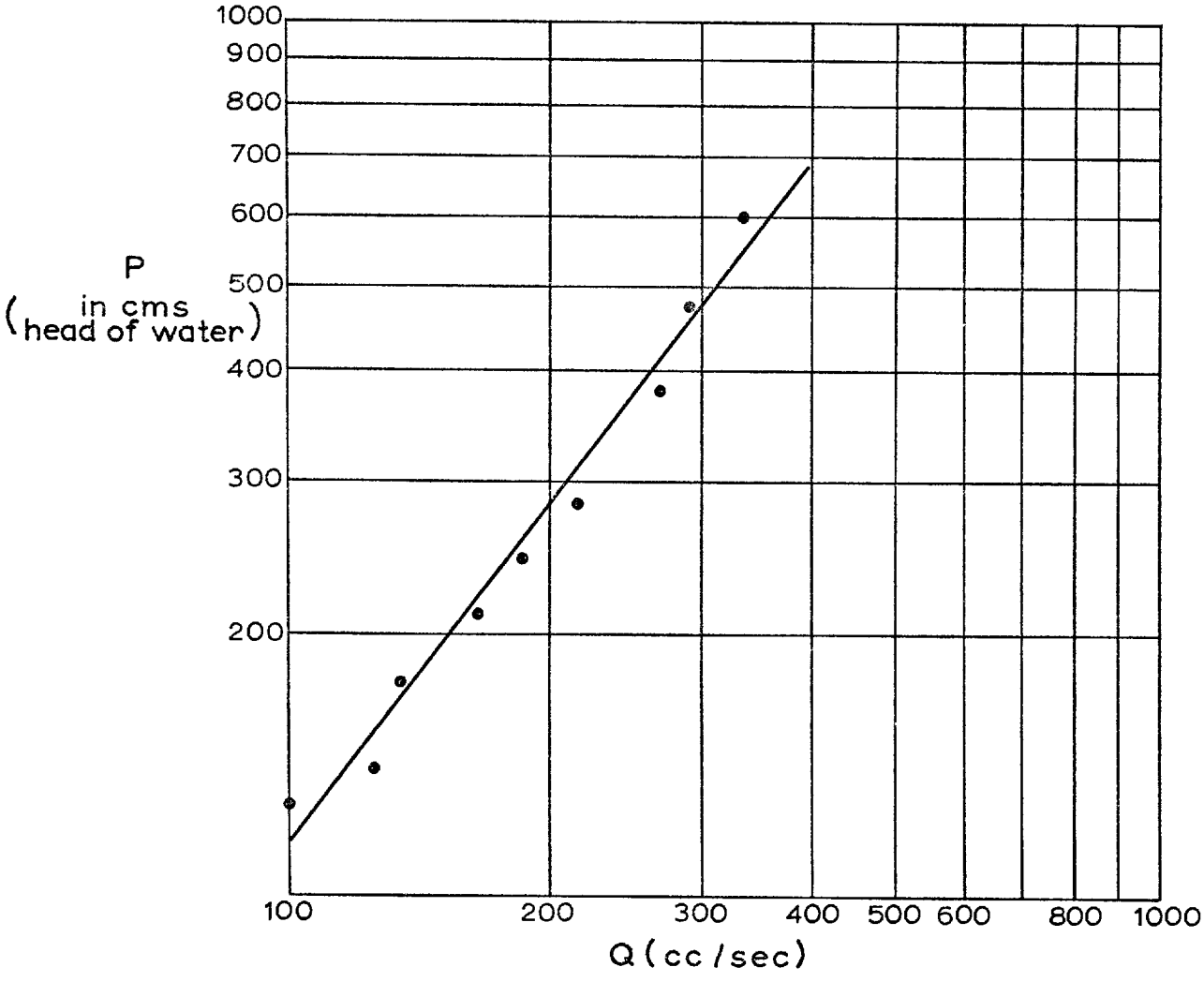

1000
900
800
700
600
500
400
300
200
P
in cms
head of water
100
200
300
400
500
600
800
1000
Q (cc/sec)

FIG. 3.5.

A very large number of tests at Altwen gave a non-linear 'pressure-flowrate' relationship. It was very carefully decided at the outset that not very high excess pressures would be used in the tests because this was theoretically one of the conditions for causing non-linearity. However, this was not always the case as non-linearity occurred for both high and low flowrates and pressures.

It is proposed to deal with one of the results in detail to show the non-linearity and also calculate the various parameters which describe flow. A demonstration of this nature should highlight the various problems and also give an understanding of how to use the permeability function for computations of discharge and pressure distribution.

Location: Hole A, packed off section 6.0-11.5 ft below G.L.

Packer spacing 5.5 ft

The data from the test has been plotted in Fig. 3.4 and it shows the non-linearity between pressure and flowrate. A large number of observations makes it possible to draw a smooth curve and thus avoid errors which creep into the existing standardised data which consists of 3 measurements per test (9). If the data from Fig. 3.4 is replotted as log Q vs log P the result is a straight line with very little scatter, as in Fig. 3.5.

Equation 2.19 and 2.20 describe the conditions for non-linear radial flow from or towards a cavity.

$$n\log Q + \log E = \log(P_o - P_1)$$

n = degree of non-linearity

$$E = {}^{1}/_{c(2\pi e)^n} \left(\frac{r_o^{n-1} \times r_1^{n-1}}{r_1^{n-1} - r_o^{n-1}} \right)^{(1-n)}$$

where:

P_o is pressure at B/H

P_1 is pressure at distance r_1 from B.H.

Q is the flowrate from the cavity

e is aperture of the fissures

r_o radius of borehole

r_1 distance from B.H.

c is a constant for a particular fissure - or system - and is dependent on the geometry of the fissure and the viscosity of the fluid

From Fig. 3.8, the slope of the curve gives the degree of non-linearity.

$$ce^{1.3} = \frac{1}{71} \frac{3.8^{0.3} - 1000^{0.3}}{3.8^{0.3} \times 1000^{0.3}} \times \frac{1}{2\pi^{1.3}} \times \frac{1}{0.3}$$

$$\simeq \frac{1}{71} \times \frac{1}{1.58} \times \frac{1}{11} \times \frac{1}{0.3}$$

$$= 2.7 \times 10^{-3} \text{ cms}^3/\text{sec.}$$

Since C is dependent on fissure topography and viscosity, it is only possible to determine it in the laboratory. In the field it is not essential to determine the value of C as there is no loss in generality in using Ce 1.3. This term will now be referred to as the permeability function. For calculations of seepage and pressure distribution this value can be directly used in Equation 2.17 (Chapter 2)

$$(Vm)^n = C \frac{\partial P}{\partial r} \quad \ldots \quad \text{Equn. 2.17}$$

or alternatively, flowrate per unit width of a fissure with aperture e is given by

$$\left(\frac{Q}{e.1}\right)^n = CJ$$

J hydraulic gradient $= \frac{\partial P}{\partial r}$

$$\therefore \quad \underline{Q^n = ce^n J}$$

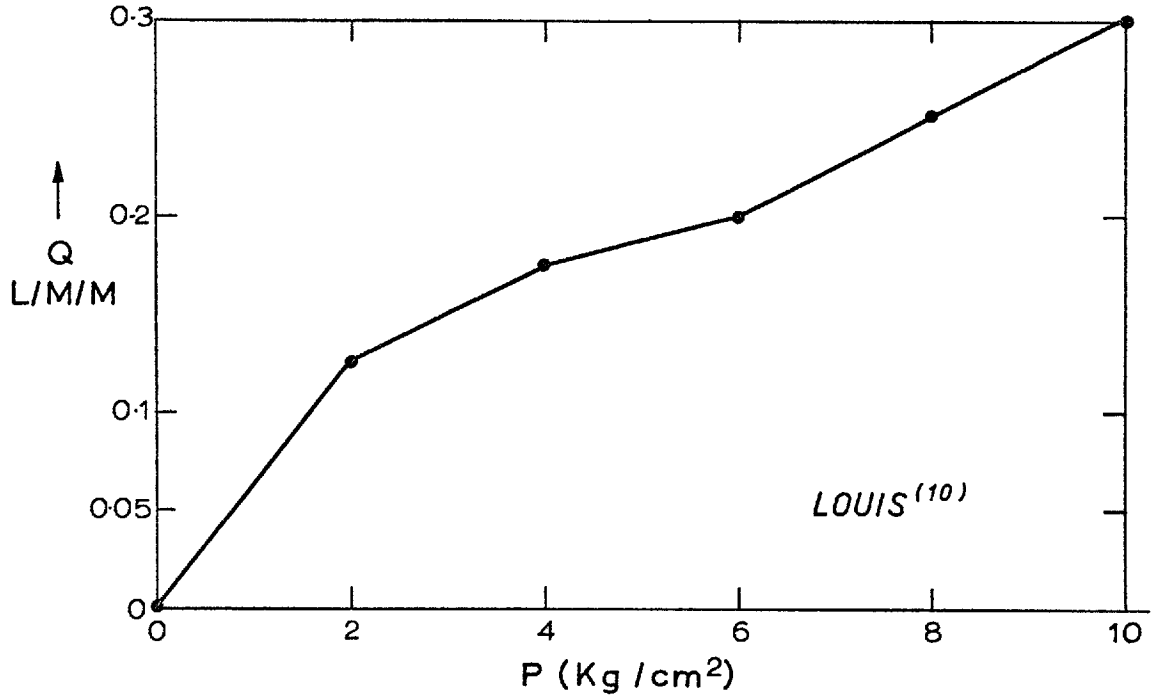


FIG. 3.6.

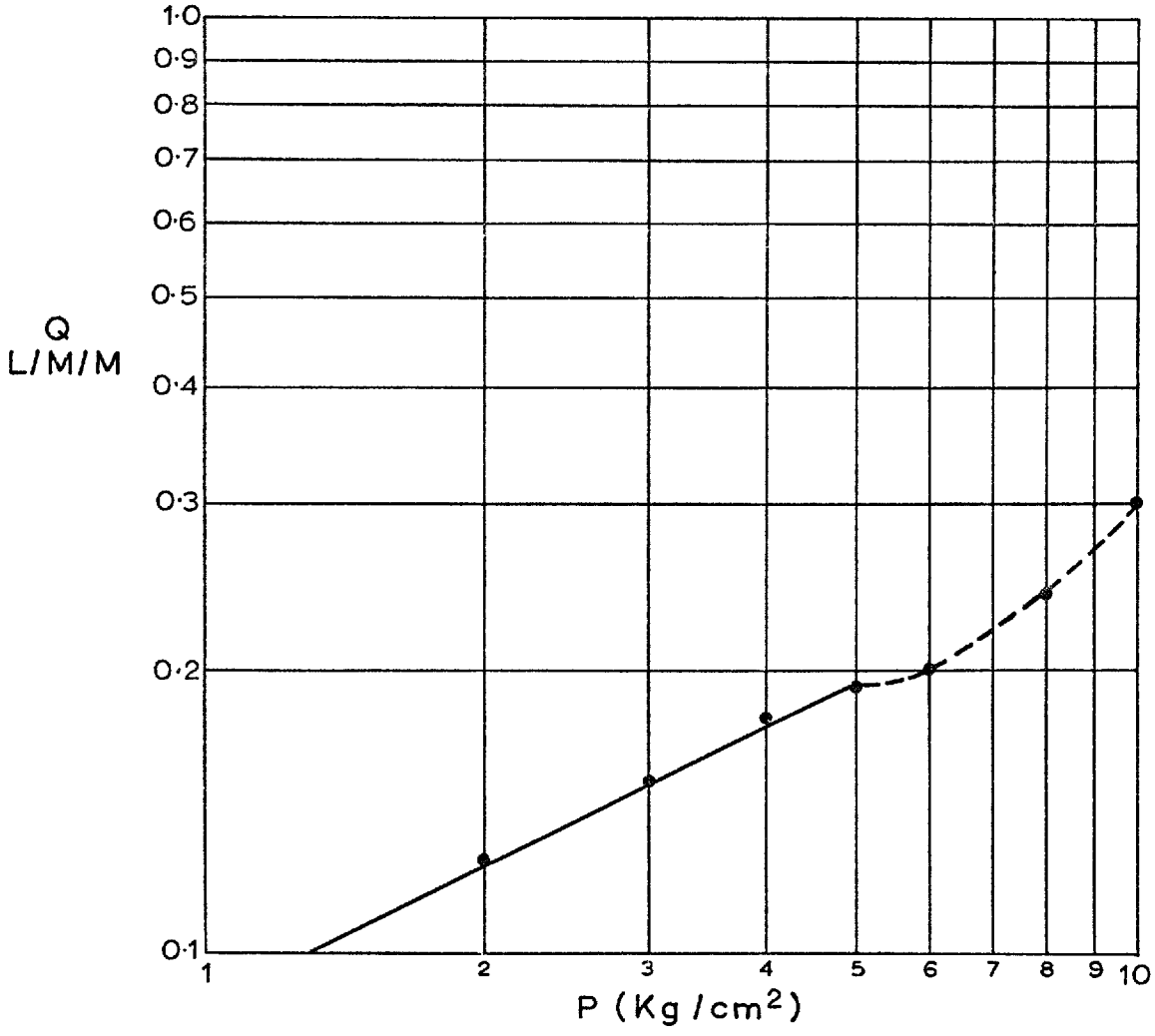


FIG. 3.7.

This non-linear test refers to a situation where there is a high flowrate although it is interesting to note that the applied pressure was not too high. Obviously this represents a situation where the Reynolds number is fairly high. A test carried out by Louis (10) is reanalysed because it represents the other extreme of conditions, ie. very high pressure and low flowrate. Fig. 3.6 is the test data published by Louis. The results were replotted on a log-log scale, Fig. 3.7. The set of experimental points fit a straight line well up to a pressure of 6 Kgm/cms^2 after which it seems as if the fissures are beginning to dilate. The slope of the curve or the degree of non-linearity is given by n = 1.75. This, together with other data from Altwen indicates a higher degree of non-linearity with increased applied gradient; obviously the permeability of the fissure enters the relationship. This is what is predicted by the non-linear model in Part I, where the permeability changes with the applied "Pressure-Field".

The non-linear 'pressure-flowrate' relationship obviously poses problems. The field determination of the 'pressure-flowrate' curve becomes more difficult and time consuming as a lot more readings are required to describe the relationship adequately. This process should not be difficult if a system such as used by the author is used. Extrapolation becomes more difficult and it is therefore very important to carry out the water test within the 'pressure-field' that is to be encountered in the problem under consideration. Application of non-linear laws for computations of pressure distributions or discharges is very difficult, but not impossible with the availability of numerical methods (8, 9, 19).

(b) Leakage Past Packers

This is a problem which has dogged many workers in the field of fluid flow. Both Snow (15) and Nonveiller (21) state that packer leakage is a very commong phenomenon resulting in values of permeability far in excess of the truth. Nonveiller (21) quotes several examples where supposedly good packers leaked at pressures of 10 Kgm/Cm^2 which is the recommended Lugeon test pressure as in Fig. 3.9. The petroleum industry realised the importance of good packers and a wide variety of tools are available on the market which are extremely expensive owing to the degree of complexity that must be involved in providing a system which seals effectively. Van Pollen (30) and McAllister et al (31) provide an excellent review of the tools required.

A 'built-in' transducer in the test section is an excellent way of checking leakage past packers. It is also a good way of providing the excess pressure, ie. it gives an indication of the in-situ pressure as the packers are inflated, isolating a given area of the rock mass. The response in the transducer was instantaneous if any changes of packer pressure were made. The usual procedure adopted by the author for the test is to commence

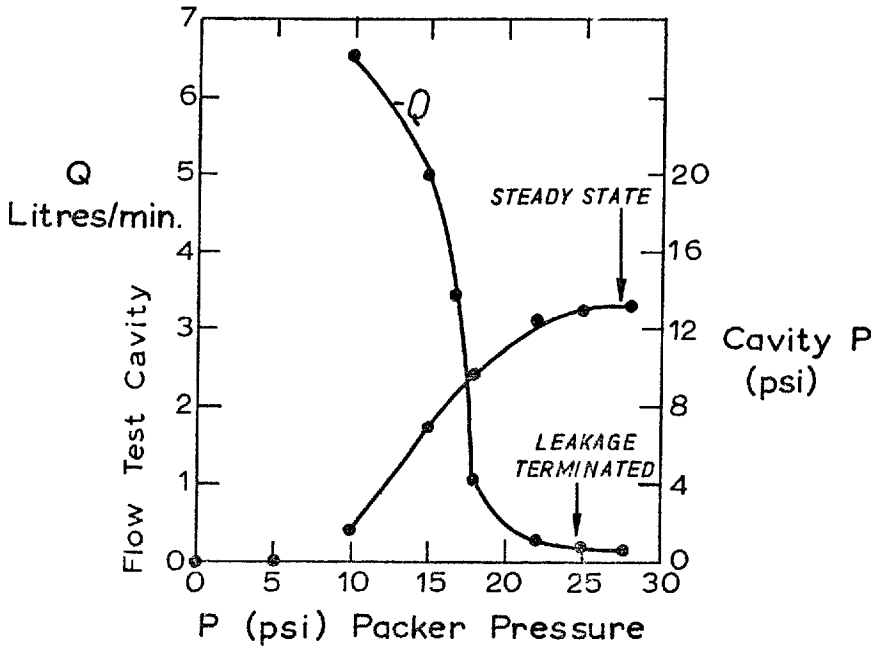

Q
Litres/min.
Flow Test Cavity
Q
STEADY STATE
LEAKAGE
TERMINATED
Cavity P
(psi)
P (psi) Packer Pressure
0
1
2
3
4
5
6
7
0
4
8
12
16
20
0
5
10
15
20
25
30

FIG. 3.8.

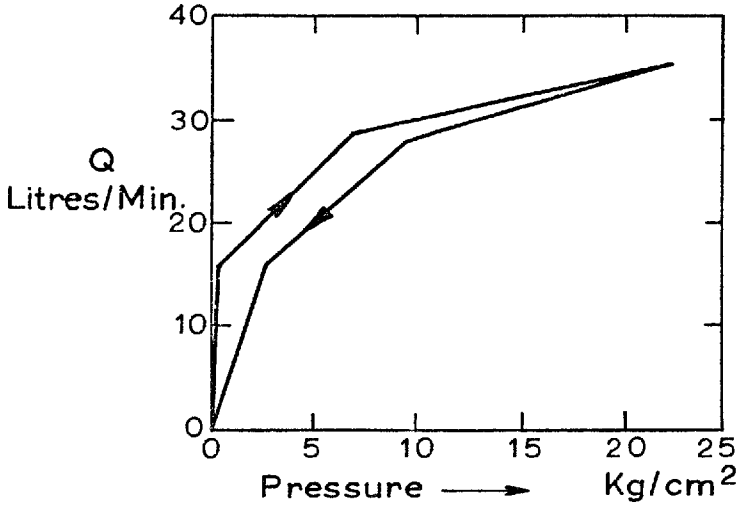


FIG. 3.9. Nonveiller-Fissured/Bedded Sandstone

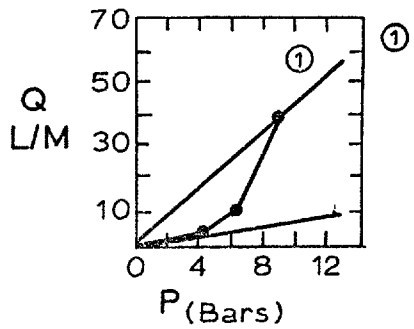


FIG. 3.10. Sabarly

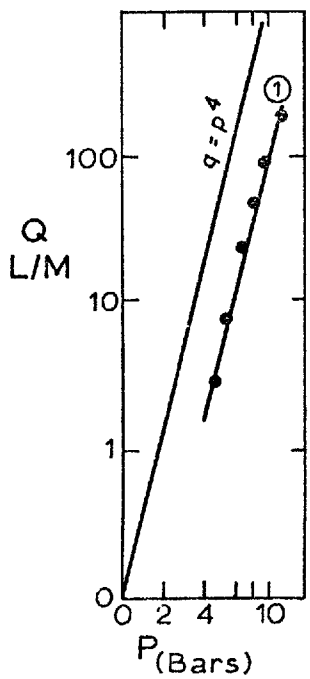


FIG. 3.11. Sabarly

inflow into the system and then gradually apply packer pressure. In this way large airpockets within the test cavity are avoided. With increased packer pressure, the in-situ cavity pressure increases and the flow rate decreases. Thus indicating a convergence towards hydraulic sealing. After a certain value of packer pressure there is no increase in the test cavity conditions except for a slight peak at the instant of packer pressure increase indicating a small compression of the fluid body. This effect is a dynamic one and soon settles to the steady state value of in-situ pressure.

Tests carried out a depth of 58·3→63·8 ft. below ground level in vertical hole.

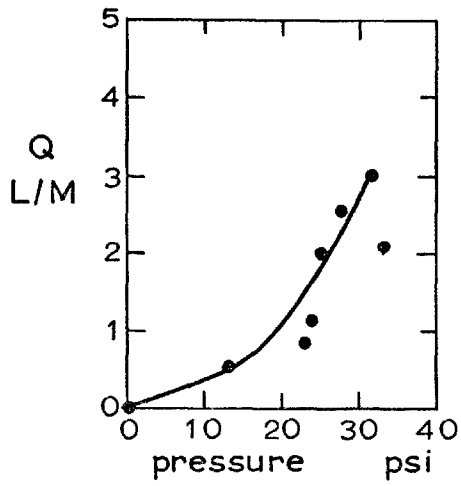


FIG. 3.12.

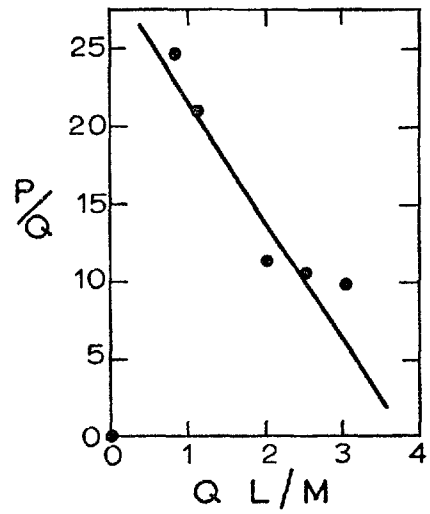


FIG. 3.13.

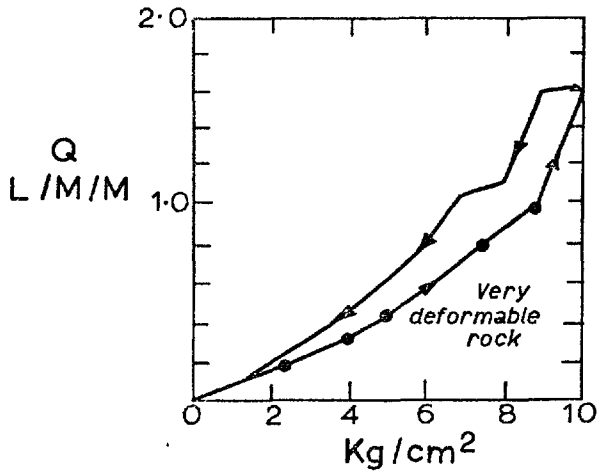


FIG. 3.14. Louis

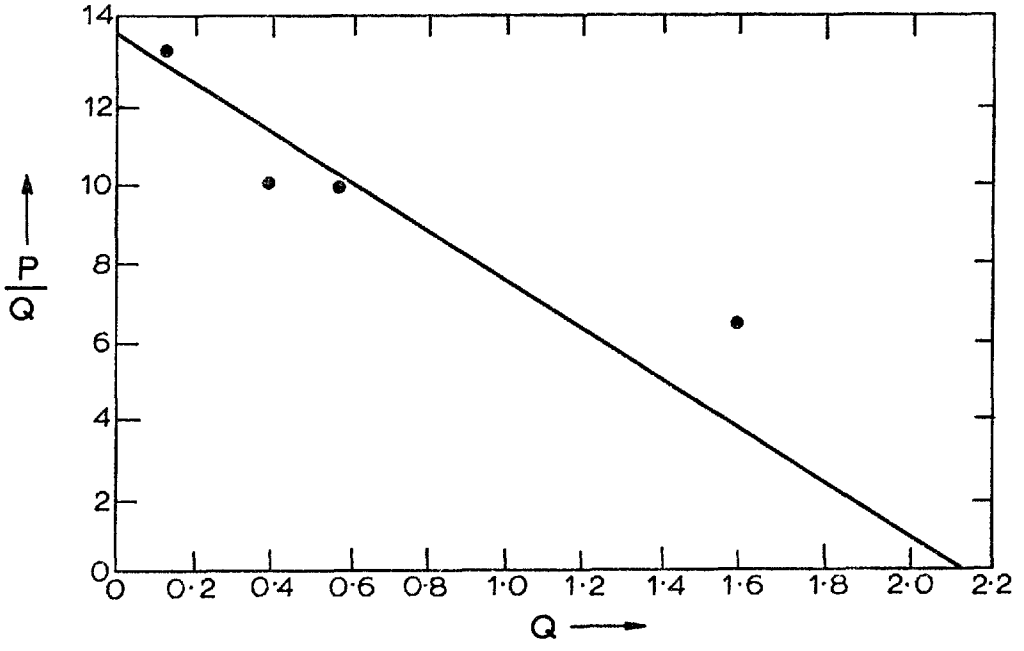


FIG. 3.15. Louis as Interpreted by Maini

A constant pressure test was carried out at depth 27.6-33.1 ft below G.L. in Hole A. Fig. 3.8 shows this process of sealing. Leakage is terminated at approximately 28 psi packer pressure. As would be expected towards the end the flow rate and pressure steadies relatively quickly. This procedure is adopted for all tests to make certain that there is no leakage during the tests. This method was checked during tests in the horizontal hole by observing leakage out of the hole and it proved beyond any doubt that it worked. At certain depths this sealing procedure unfortunately could not be achieved because the packer design did not permit application of an excess pressure of 30 psi. In effect, this limitation on design was a blessing in disguise because it brought out the importance of carrying out tests at low cavity pressures in terms of non-linearity. If the test is being carried out in unsaturated media at say 80 ft depth, a constant pressure test even before it attains steady state applies approximately 40 psi pressure to the fissures. This, in a further section will show to cause deformation of fissures. In situations where curves such as Fig. 3.8 were not possible a falling head test was carried out with a very much smaller applied head. A leaky packer can give results of permeability up to many orders of magnitude in error. Therefore it is proposed that in all tests the procedure outlined above is used, otherwise this leakage factor cannot be eliminated and its subsequent effect on the pressure-flowrate relationship cannot even be estimated.

(c) Fissures Opening Up

INTRODUCTION

In section 2.1.8 it was demonstrated how during a pumping test the fluid pressures open up a fissure. The so-called interaction between the fluid and the solid body stresses is an extremely complex phenomenon. In Part I this problem has been discussed with reference to rock mass. Coupled stress-flow numerical methods indicate the mechanics of the problem. Evidence of such a phenomenon in the field was presented by Sabarly (32) and subsequently by Louis (10) and Nonveiller (20). Snow (33) discussed this problem with special reference to earthquakes.

Sabarly (32) presents his analysis in a very simplified manner assuming a Boussinesq deformation at the centre of a circle. His analysis is carried out to highlight the orders of magnitude that are involved in the problem. Fig. 3.10 is a typical result from the field reported by Sabarly which indicates the hysteresis loop that is obtained in a pumping-in test which causes permanent deformation. Prior to damage the permeability is 3 Lugeons, increasing to 9.2 Lugeons at the end of the test. By plotting the results on a log-log paper the relationship between pressure-flowrate during a test is given by:

$q = Ap^4$ (See Fig. 3.11)

Unfortunately, Sabarly's curves (although all four of them have the same slope) cannot be considered as a generalised conclusion. The main reason being that there is an interaction between the fluid stresses and solid body stresses which causes the non-linearity in the pressure flowrate relationship. The degree of non-linearity depends on the individual stress levels of the two components. The author plotted out of interest all the field results from Altwen on log-log scales and discovered no such universal law. However, Sabarly's results are important since they indicate the non-linearity of the pressure-flow relationship. In a more recent publication Nonveiller has published the result of a pressure test in fissured/bedded sandstone (see Fig. 3.9). Once again the trend is similar to that in Sabarly's tests in that the relationship P-Q is nonlinear. Both writers conclude that in essence the most important thing in a pressure test is to decide the 'pressure level' that the final structure is going to be subjected to and then carry out tests within those limits. The Lugeon criteria as a generalised criteria for fissured media is incorrect for the above reasons and this is the conclusion reached by Louis (10) and the author.

3.1.2 TEST TO DEMONSTRATE FRACTURE BREATHING

The test carried out at a depth of 58 ft below the surface demonstrates the jacking influence of fluid stress. Fig. 3.12 is the result of the test as fluid is pumped into the hole at different pressures. Clearly the relationship is a nonlinear one, and if it is plotted as suggested in section 2.1.8 as P/Q vs Q the fissure breathing mechanism becomes apparent. Fig. 3.13 shows that as the flowrate is increased the kinetic energy drops and this is only possible if the fracture opens up, thus decreasing the flow velocity (velocity = flowrate = AREA OF APERTURE). In this particular test the leakage past the packer was checked as previously suggested in Part (B). A similar phenomenon is observed in the data published by Louis, Fig. 3.14 and 3.15.

It is clearly instructive at this stage to look at the solid-body stress level. Fig. 3.16 is a non dimensional stress plot from Cundall (34). At the depth where the test was carried out the stress is given by:

$$\sigma_v \doteq 24 \text{ psi}$$

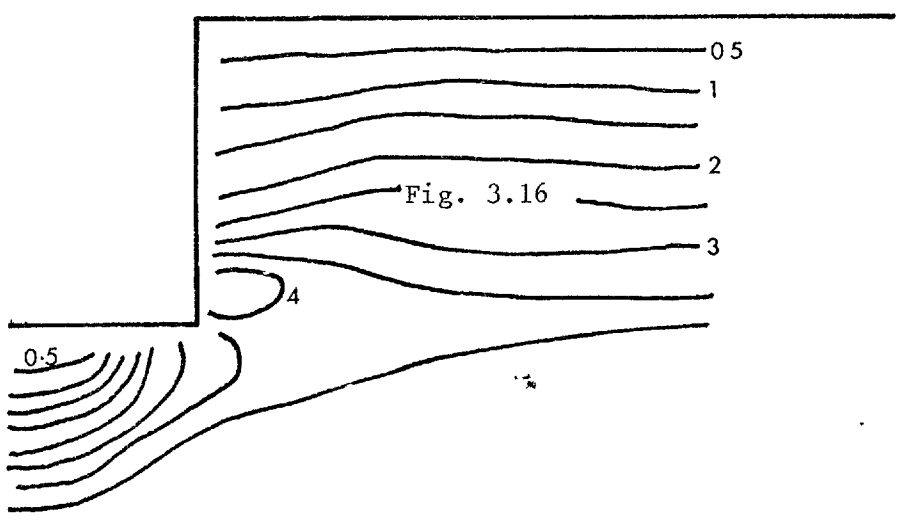


Fig. 3.16

This analysis (although approximate and simplified) illustrates that the fluid stresses are well within the stress level of the rock mass. The normal stiffness of a fissure (35) is in range of 1/10th that of the solid mass and this means that the deformation of the fissure as a reuslt of pressure testing is very likely. A very much more sophisticated analysis of the type of situation is under consideration using an interaction numerical model, the result of which is described in Part I.

3.2.0 CHANGING GEOMETRY OF THE TEST SECTION

3.2.1 INTRODUCTION

By changing geometry of the test section is meant the complex interaction that takes place between the fissure frequency and the potential field. As was mentioned in Section 2.1.1, Part II the value of permeability is more meaningful if it is based on the fissure distribution rather than an arbitrary length which may be practical from the point of view of carrying out the test. In the numerical section it was shown how the flow per unit length increases with fissure frequency until a stage is reached where the increased test section length makes no difference on Q/L. Obviously, such an idealised model could never be found in nature; but the principle will be demonstrated. It must be remembered that scale effects are important when bulk parameters are used, or conversely a test should be carried out to see if bulk parameters can be used. For example in a highly fissured and structurally random system (15) it is possible to use directional bulk or global parameters whereas as in a sedimentary environment where the orientation of the fissures is systematic in spite of folding and faulting and the degree of fissuration depends on the lithology, it is important to measure permeability on a fissure set basis. Obviously, the same reasoning applies to faults which occur more distinctly and are fairly well spaced relative to the diameter of the borehole.

3.2.2 INFLUENCE OF 'END EFFECTS' IN A WATER TEST

In section 3.3.2 Part II the influence of end effects in a water test was discussed. While it is theoretically possible to eliminate end effects by having a long test section the practical usefulness of this method is limited because of the changing frequency/unit length of the fissures. The method could only be tested within certain limited zones where the fissure frequency was constant. The best results were obtained in the horizontal hole because the fissures there have a fairly constant effective aperture.

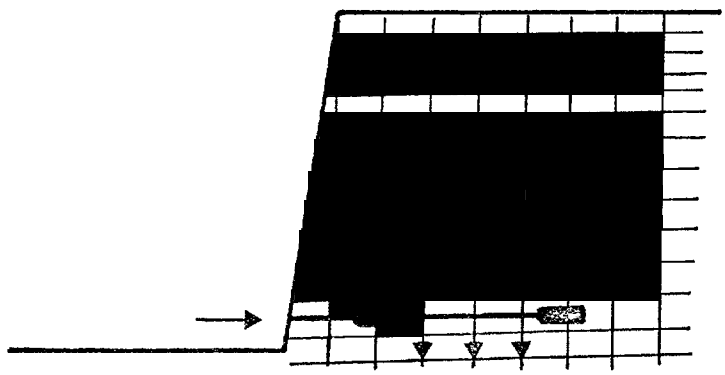


FIG 3-17

Fig. 3.17 illustrates schematically the test carried out in the near horizontal hole. The majority of fissures that intersect this hole are near vertical (see Chapter 2). A pumping-in test into this hole would involve the transport of fluid in the near vertical fractures and some to the horizontal fissures. Two tests were carried out between 21.2-31.9 ft from the face of the slope with a packer spacing of 5.5 ft. The values of permeability obtained were as follows

Test 1. $eK_J = 2.25 \times 10^{-3}$ $cm^2/sec.$ number of fissures: 7

Test 2. $eK_J = 1.67 \times 10^{-3}$ $cm^2/sec.$ number of fissures: 6

Thus indicating that the fissures are almost identical. Subsequently a test was carried out from 27.3-38.0 ft with an increased packer spacing of 10.7 ft. The value of permeability was as follows:

Test 3. $eK_J = 6.2 \times 10^{-4}$ $cm^2/sec.$ number of fissures: 13

This decrease in permeability could be due to the increased test cavity size which leads to a dominance of cylindrical flow. In general the permeability of the horizontal fissures is much higher than the vertical fissures and thus a dominance of flow in the vertical fissures should lead to a smaller value in permeability orthogonal to the borehole axis. A more practical approach than increasing cavity size to eliminating end effects is described in the next section.

3.3.0 TRIPLE PACKER PROBE

3.3.1 INTRODUCTION

In section 1.2.0 the details of the packer and the test equipment are described. Fig. 3.20 illustrates the triple packer system. All the details of the equipment remain unchanged except that there are three cavities where fluid is injected from ground level.

Louis (36) described this system as an obvious and simple way of correcting the end effects during a pumping-in test. The end effects essentially constitute flow in a hemispherical fashion resulting in the motion of the fluid in a direction at right angles and along the axis of a borehole. If the system is anisotropic hemispherical flow could lead to rather distorted answers in the determination of permeability. Fig. 3.21 is self-explanatory and describes the test in a schematic manner. Sharp (9) has performed calculations for such an arrangement with varying cavity sizes. The results are essentially applicable only to a porous medium. For such a method to work in jointed rock, the degree of fissuration has to be intense, ie. the fissure spacings is comparable to the diameter of the hole. In a fracture system where the fissuration is in the order of a few feet upwards, the method does not apply, since flow is essentially axisymmetric within the fissures intersecting the borehole rather than two dimensional. This is largely due to the severe pressure drop near the hole leaving very little excess pressure to cause a dominantly two-dimensional flow. Tests were carried out at Altwen to assess the new method to see if better answers could be obtained - by isolating the influence of the fissures parallel to the borehole axis.

3.3.2 FIELD TESTS

In view of the fact that the analysis for this type of method is based on a continuum model tests were only carried out in areas where the fracture frequency is high.

Louis (36) and Sharp (9) recommend using equal pressures in the sub-cavities. Failing this, Sharp recommends increasing the sub-cavity pressure, so that flow within the main test cavity can be confined. This practice was not adopted since it was felt that

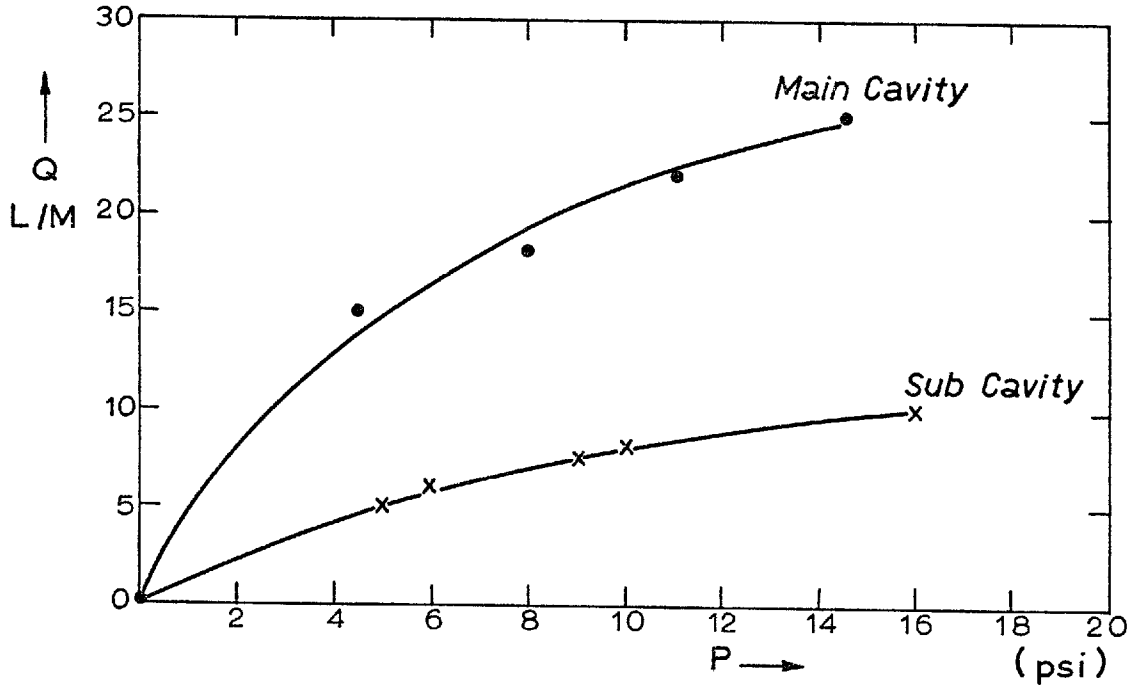


FIG. 3.18. Location: Hole A, Depth approx. 10·0-15·5ft.

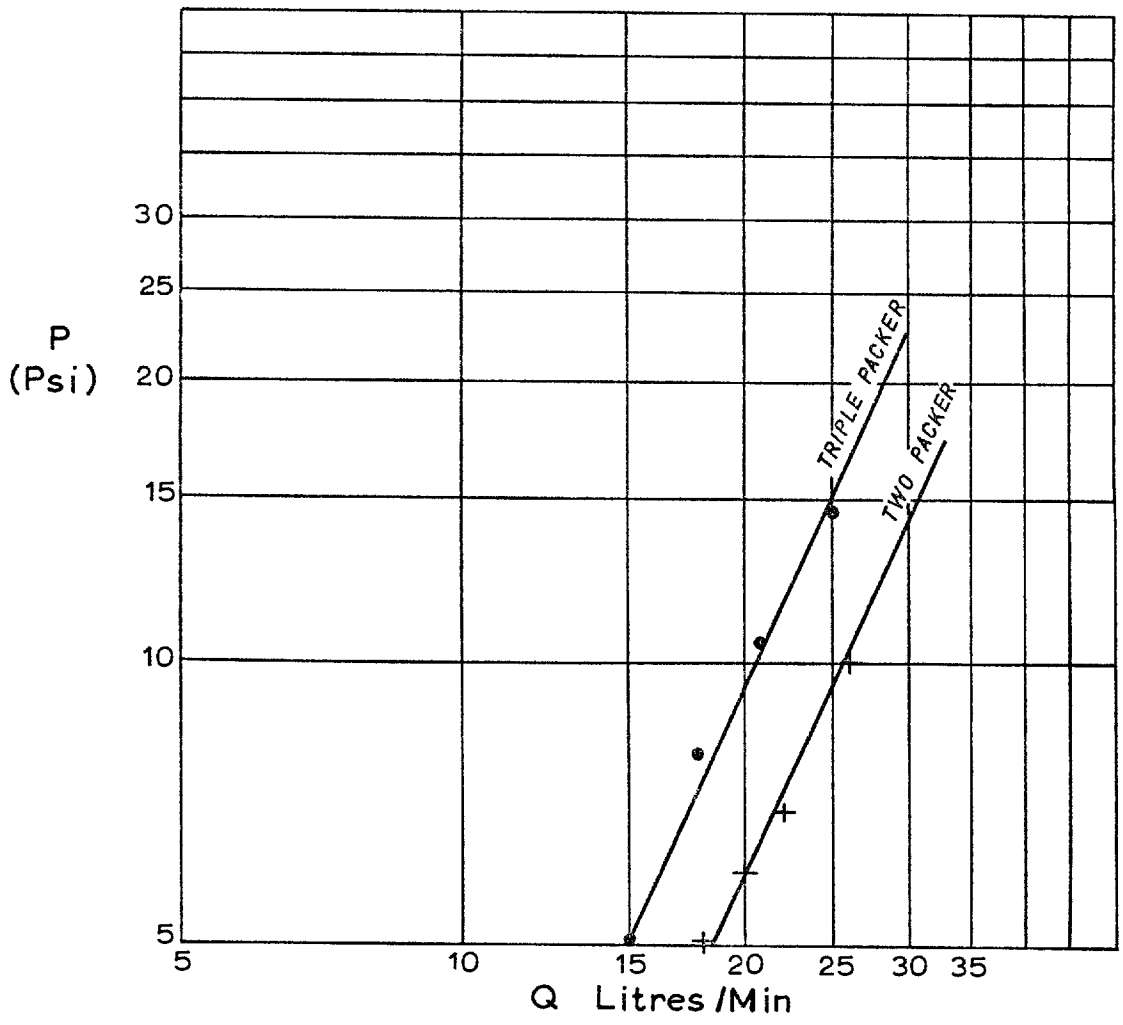

P
(Psi)
30
25
20
15
10
5
5
10
15
20
25
30
35
Q Litres/Min
TRIPLE PACKER
TWO PACKER

FIG. 3.19

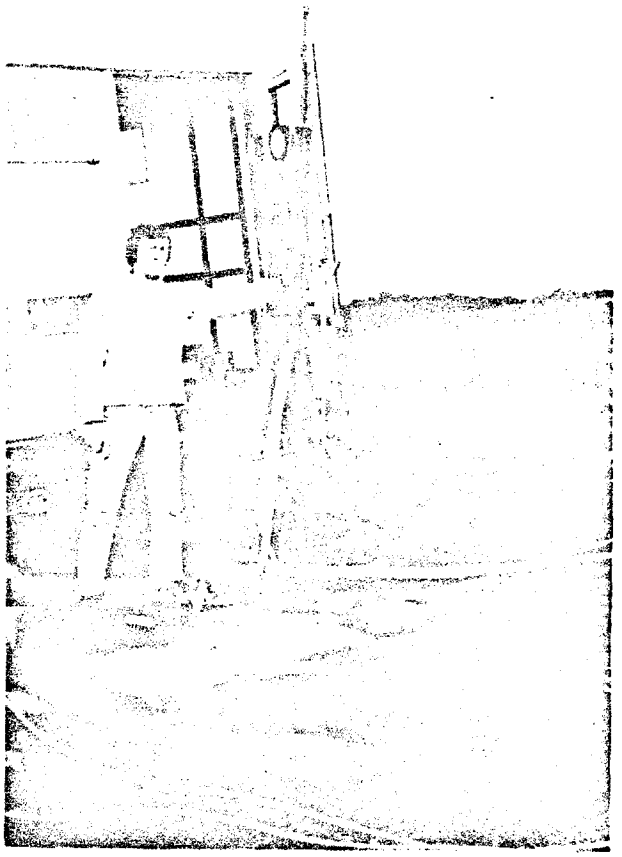


FIG. 3.20.

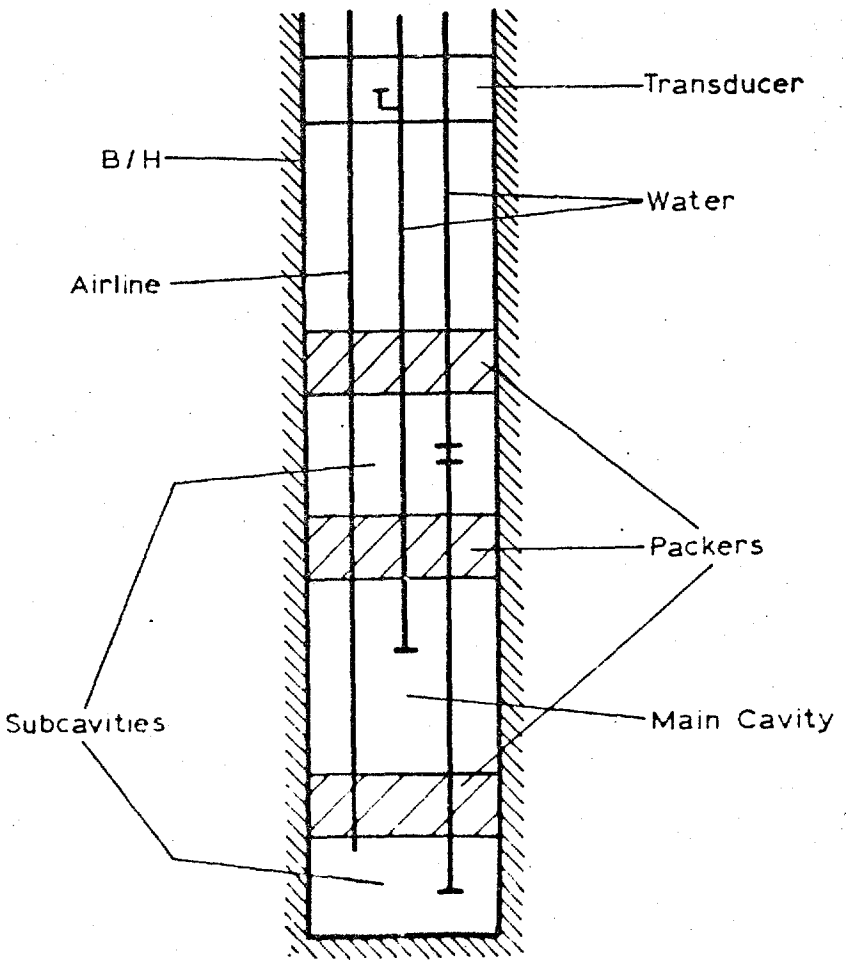


FIG 3.21. Schematic Drawing.

the influence of higher sub-cavity pressures would be to distort the potential field and that short circuiting would occur from the sub-cavity to the main cavity. Owing to the variation in permeability with depth, the supply to the sub-cavities was commenced first and also the potential was maintained at a lower value than the main cavity since this is easier to achieve than equal pressure in all three cavities. This sub-cavity potential was still above the in-situ potential and therefore, it provided a saturated zone above and below the main cavity. In this way any external influences on the main cavity flow were minimised. The flowrate within the flow lineariser was altered $\pm$ 20% and it made no significant difference to the pressure-flow relationship in the main cavity.

Fig.3.18 illustrates the test result of a triple packer probe. The 'pressure-flowrate' relationship in both the cavities is non-linear. If the results for the main cavity are plotted on log-log paper the points lie fairly well on a straight line, see Fig.3.19. Also plotted on the same diagram are the results from a two packer test at the same depth. The degree of non-linearity is approximately the same in both the tests and equal to 2 indicating that flow is fully turbulent. The difference in the non-linear permeability functions is about 25%. This difference is certainly not substantial; but it indicates that the flow-linerisers could be providing a constant potential flow zone above and below the test cavity and isolating some of the vertical fissures in the vicinity of the borehole thereby cutting down the output from the test cavity into fissures parallel to the axis of the B.H. Water is forced to flow in a direction orthogonal to the borehole and therefore at a given value of borehole pressure the flowrate in the triple packer system is less than in the two packer system. Obviously this change of conditions depends on the ratio of the permeabilities of the two fissure systems. Other tests with the triple probe did not show a dramatic change in the value of permeability. Many more field investigations should be carried out to further assess this method.

3.4.0 SCALE EFFECT IN A TEST

Scale effect is the influence of variation in n the number of fissures per given length on the value of permeability. In section 3.3.4 Part II the theoretical aspects of scale effects were discussed and it was shown how with increasing number of fissures per given length the continuum value of permeability goes up while the discontinuum value goes down. In theory, if the number of fissures is increased indefinately the discontinuum value of permeability approached the continuum value. This can be seen by examining the expressions for permeability based on the two approaches;

Equation 2.3 Part II

$$eK_J = \frac{Q \log_e \left(r_1/r_o\right)}{2\pi(P_o - P_1)n}$$

(All symbols defined in Part II or nomeneliture)

Equation 1.1 Part II

$$K_s = \frac{Q \log_e \left(r_1/r_o\right)}{2\pi(P_o - P_1)L}$$

where $K_J = \frac{e^2 g}{12U}$ for a parallel plate model

L above is the spacing between the packers and if it remains constant for a given water test $K_s \ll K_J$ if n is small. If n is increased the value of K_J decreases and approaches that of K_s. This phenomenon will now be demonstrated to exist in the field. Obviously other factors influence the value of permeability such as the variation in aperture of the fissures, orientation, applied pressure field during a water test, different fissure families intersecting the borehole etc.

In Part I, section 1.2.0 the rock mass is described in terms of the fissure frequency or order of heterogeneity. Fig. 1.1 in the same section describes the concept graphically.

Let us consider the fractures in the vertical hole for instance (Fig. 2.2 0) for the first twenty feet below ground level the mean spacing of the fissures is approximately 1.3 cms. On Fig. 1.1 Part I this point lies at the border of second and third order heterogeneity, consequently a sample test would be in the 'inhomogeneous media class'. However, a massive test would fall in the homogeneous region as long as the distance between the packers was greater than 10 ft. In terms of a water test this implies that if the packer spacing was increased within this region, the flowrate per unit test section length would not change substantially. This in fact was the case in the highly fissured zone (spacing 1.3 cms and less) at Altwen (see Chapter 3 Part III).

From 30-50ft below ground level in the vertical hole the mean spacing between fractures is approximately 22 cms. On Fig. 1.1 Part I this corresponds to a massif test where the packer spacing is of the order of 100 ft before the test gives a value of permeability of an equivalent homogenous media. Once again this is the correct order of magnitude, as can be seen in Chapter 3 Part III that the system permeability varies substantially for packer spacing of 5.5 ft and 10 ft thus indicating that at this scale the system appears to be heterogeneous; but when the number of fractures is approximately 100 the permeability of the

inclined hole is the same as that of the vertical hole, Fig. 2.25 and 2.26. This result shows that when the test section is large enough the medium behaves as if it were homogeneous. It must be realised that neither these results are exact nor in the theory rigorous, but it throws some light on what is an extremely complex phenomenon.

3.4.1 FIELD RESULTS ON THE INFLUENCE OF FRACTURE FREQUENCY ON THE VALUE OF PERMEABILITY

Fig. 3.22 is a plot of the discontinuum value of permeability eK_J plotted vs the number of fractures for tests carried out in the horizontal hole. The most important outcome of this set of results is that the value of eK_J falls with increasing fracture density per unit volume. This is exactly what was predicted by theory. Further the points lie fairly close to a straight line. Results from the inclined hole fit the relationship, Fig. 3.23 and so do the permeability values from the vertical hole, Fig. 3.24. In the latter set of results it is interesting to note that there is a cluster of points away from the straight line relating permeability and fracture density. These points all belong to a set of fissures where the lithology has changed. In Chapter 2 it was shown how the lithology changes with depth and presumably the characteristics of the fissures change as depicted by their conductivity in Fig. 3.24. If we accept the relationship between log eK_J and log n as being linear it should be possible to predict the permeability orthogonal to the borehole provided the fracture density was known. With a relationship such as this it is then possible to compute leakage under a dam or in a rock slope with a greater degree of confidence. For example in Fig. if we start increasing the fracture density the value of permeability decreases, and at n = 126 which is the total number of fractures in the vertical hole, the projected straight line from tests carried out on fewer fissures lies extremely close to the value from the water test carried out on the entire hole. These results justify not only the extrapolation of eK_J values but they simplify the application of numerical models to predict the behaviour of a rock mass. On the basis of this study an hypothesis is proposed on the basis of the numerical modelling and field results that if the assumptions outlined hold true, such as the fissures belonging to the same family, tests carried out within the same pressure field etc, then $eK_J = An^{-B}$ where A, B are constants which depend on the properties of the rock mass of the fluid. It is suggested that in any field application this procedure of carrying out the water test with changing frequency is established to see if extrapolation based on frequency distribution is possible. The method obviously relies on the availability of data on fracture density and the degree of confidence that can be placed on the continuity of the fissures in terms of fluid transport.

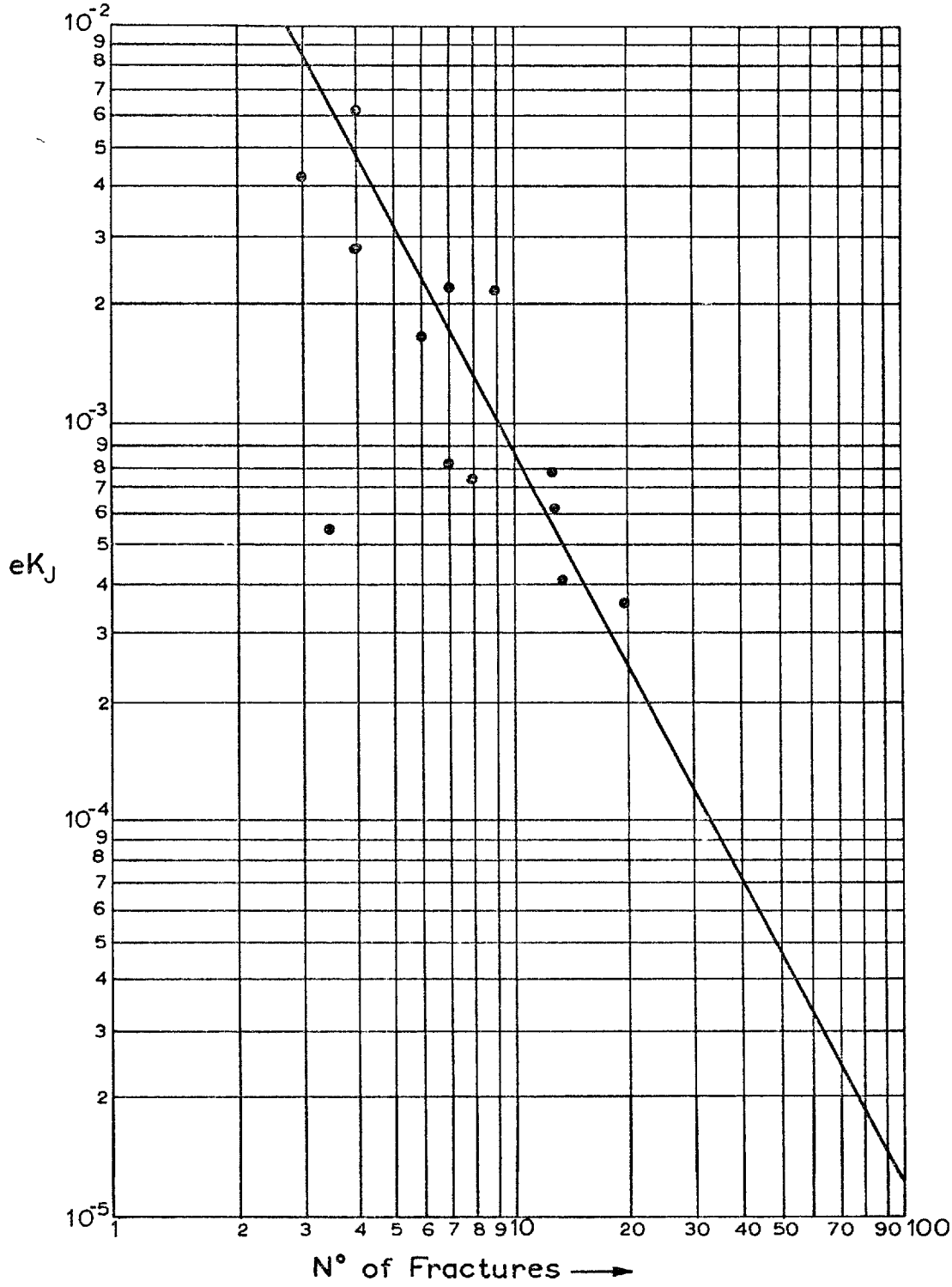


FIG.3.22 Horizontal Hole

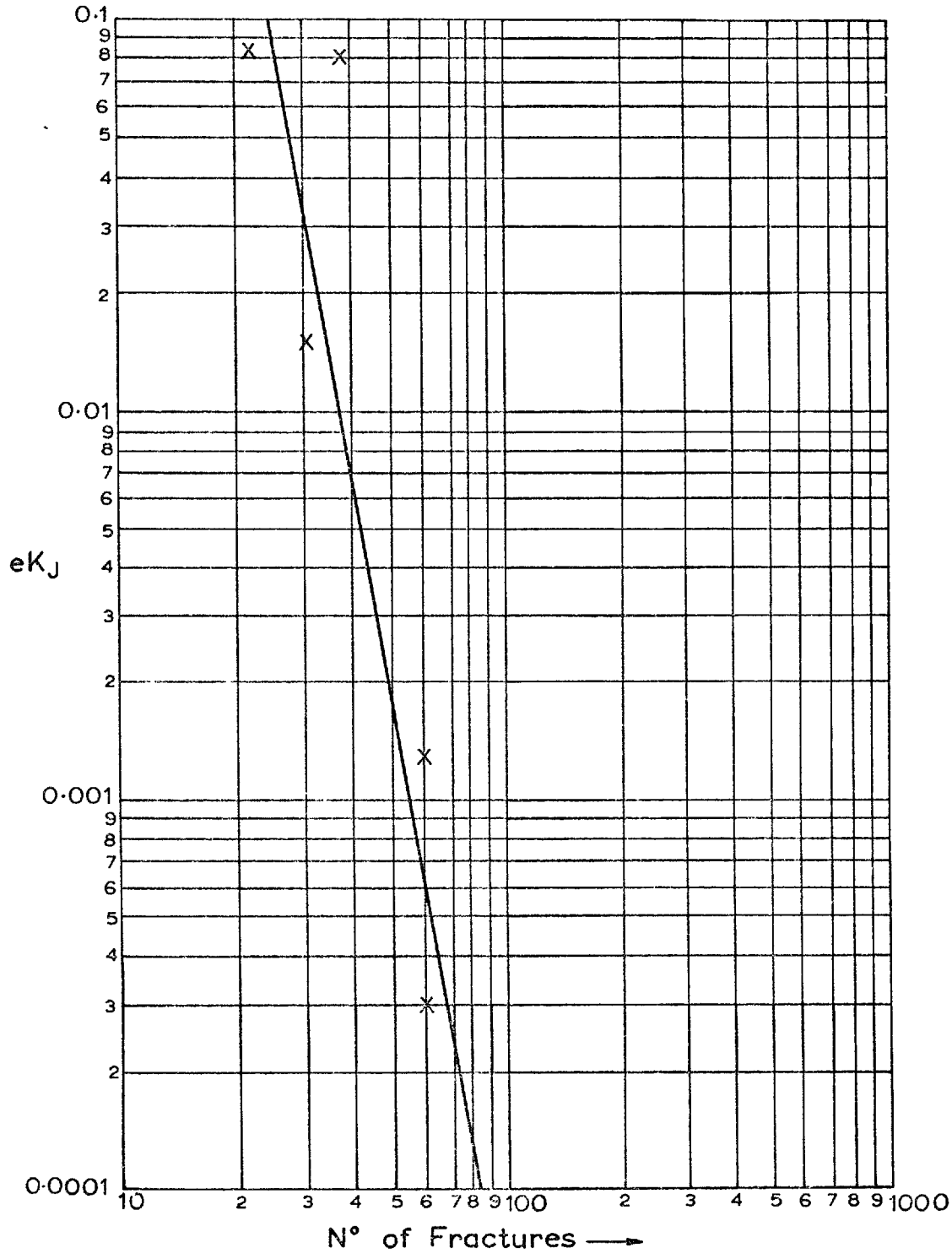


FIG.3.23 Inclined Hole

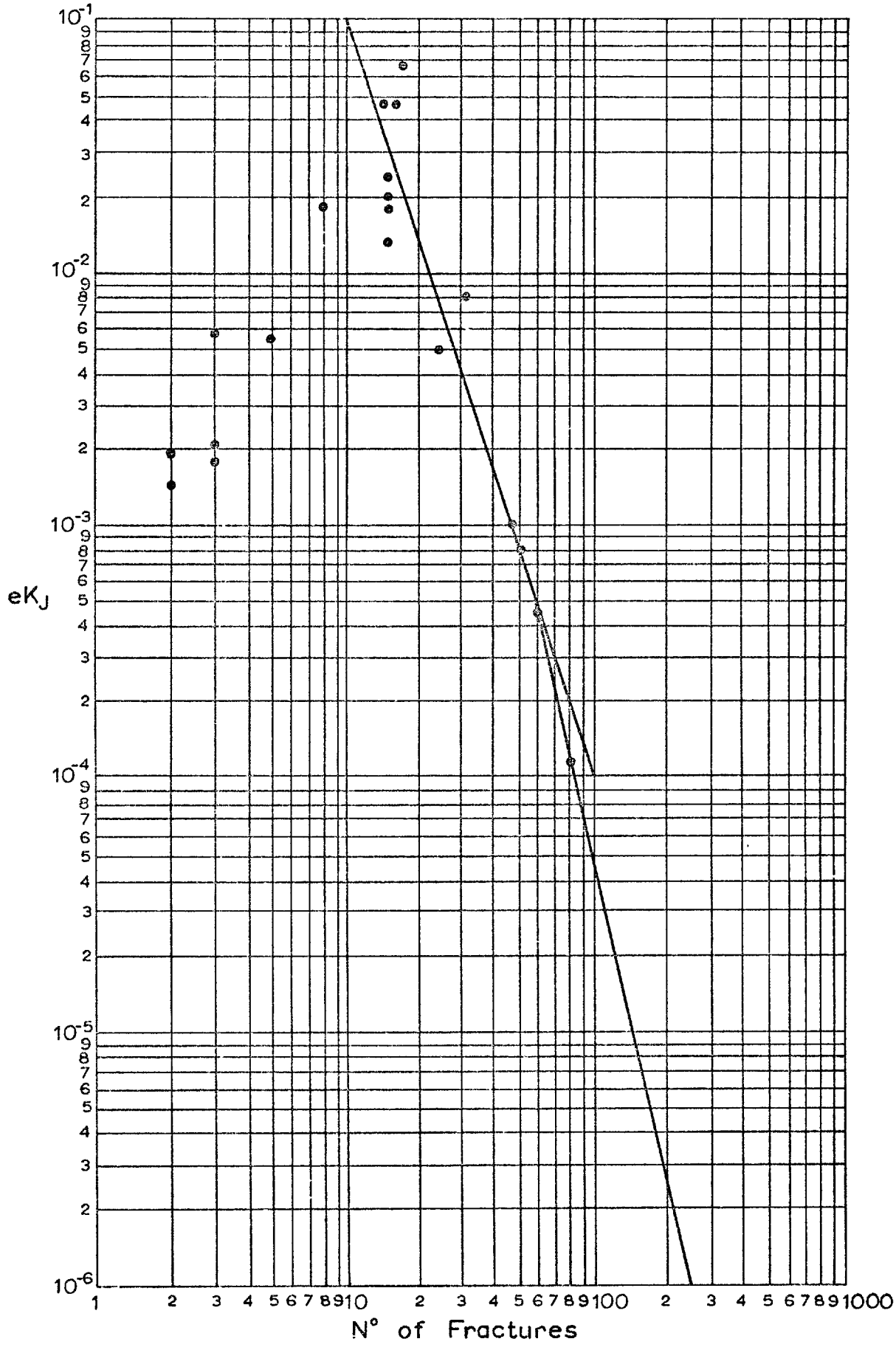


FIG. 3.24 . Vertical Hole

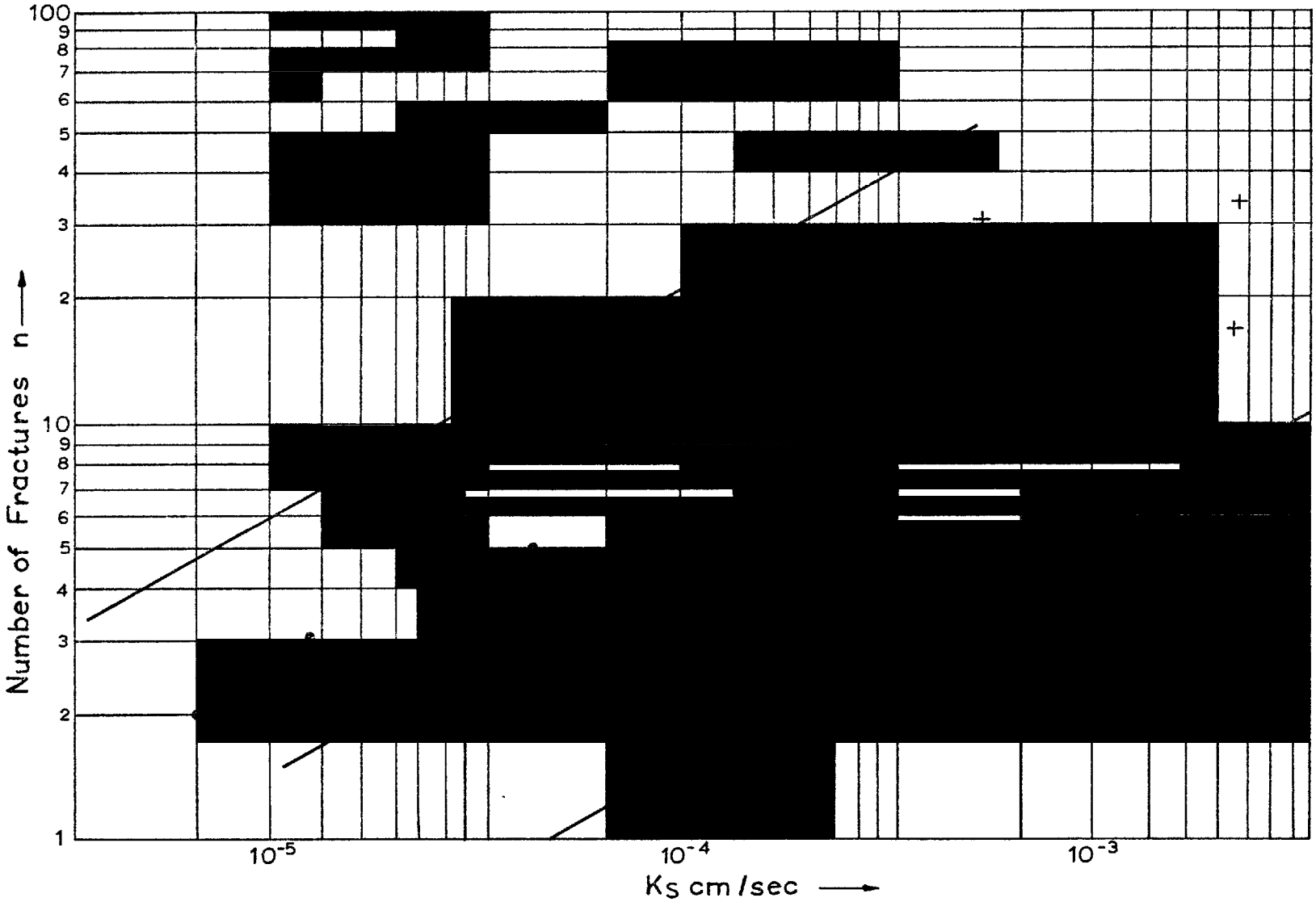


FIG. 3.25. Influence of Increasing Number of Conductors on System Permeability.

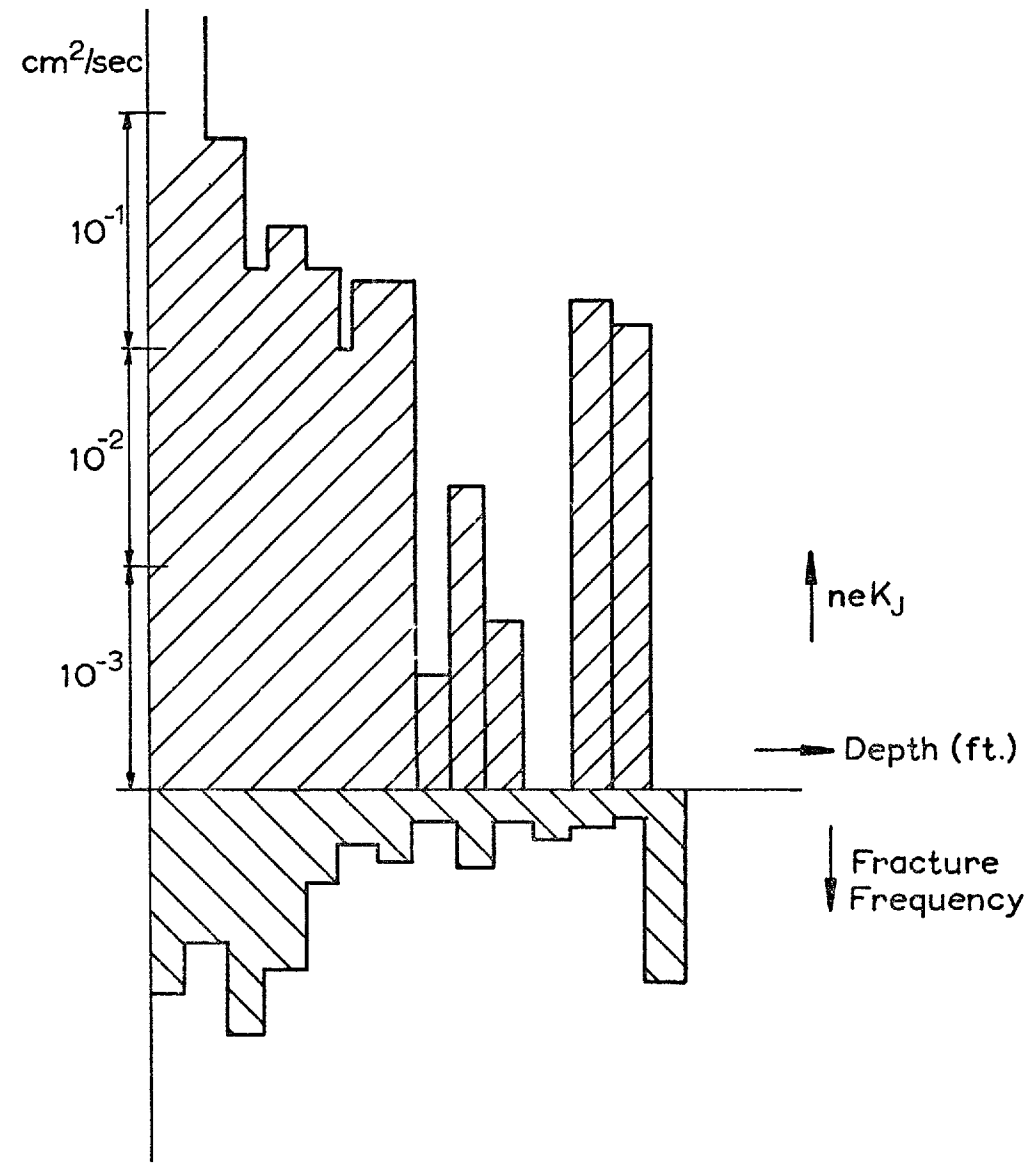


FIG. 3.26.

The system permeability K_s has been plotted vs number of conductors as in Fig.3.25. Once again as predicted the value of permeability K_s increases with increasing fracture density. However, the scatter in values is much higher because this system in its evaluation of K_s takes no account of the fissures frequency and the value of permeability K_s is based on a fixed length L between the packers.

3.4.2 CORRELATION OF FREQUENCY OF FISSURES AND WATER ABSORPTION

The term neK_J is an indication of the water absorption of a mass of fissured rock (Chapter I, Part II). This quantity correlates extremely well with fracture frequency as can be seen in Fig. 3.26. This in general suggests that the absorption of the fluid is highest where the fracture frequency is the densest; once again the assumption that the fissures belong to the same family must hold. A graphical comparison such as this is extremely useful in seeing rapidly if there is any correlation between permeability fracture density and/or depth.

3.5.0 INFLUENCE OF BOREHOLE ORIENTATION ON PERMEABILITY VALUES

In section 2.1.7 Part IIA, the importance of making certain that the borehole intersects one fissure set orthogonally was outlined. This in principle, allows the determination of permeability of one fissure set at a time. Field tests were carried out to demonstrate this and the table below shows quite remarkable results. The inclined hole is at approximately 25 deg. and it consequently intersects both the horizontal and vertical fractures. The value of permeability as obtained from the inclined hole lies between the permeability of the horizontal and vertical fissures, clearly suggesting that in the first and third tests flow is confined to one set of fissures only while in the second test it is free to flow in both sets of fissures.

	HOLE	DEPTH	Ks cm/sec	$neK_J cm^2/sec$	n
(1)	Vertical Hole	38.2-19.3	$2x10^{-3}$	$3x10^{-1}$	15
(2)	Inclined Hole	13.0-18.5	$1x10^{-4}$	$1x10^{-2}$	22
(3)	Horizontal Hole	38.2-48.9	$2x10^{-5}$	$6x10^{-3}$	20

Very often fissures are not horizontal or vertical but may be inclined in almost any position. In general boreholes are drilled vertically downwards for Lugeon testing. This, in effect, results

in values which are somewhere between the true values of individual fissures. If the individual values of permeability are vastly different, very large errors could creep into calculations of seepage volume if the test hole was not orientated correctly with respect to the fissures system under investigation.

3.6.0 ANISOTROPY OF THE FISSURE SYSTEM

The method proposed by Snow is not used to determine the ratio of principal permeabilities because the fissure system is not considered random. Since the fracture system is fairly well defined it is proposed that an ideal anisotropy is best obtained from tests in two orthogonal directions. Also the method described in section 3.3.3 based on the numerical approach will be used to see if it gives a reasonable answer. As was pointed out in the section the method proposed is extremely ideal and only gives an idea as to how the system behaves. It is assumed that in an anisotropic system the ratio of principal permeabilities adequately describes the anisotropy of the system.

3.6.1 APPROXIMATE DETERMINATION OF PRINCIPAL PERMEABILITIES FROM TESTS IN ONE HOLE

The method described in section 3.3.3 Part II is applicable to data obtained from the horizontal hole.

In general, $Q = AneK_J H$

$$\therefore \frac{Q}{Q_c} = \frac{n_1 eK_J}{n_2(eK_J)} = \frac{13 \times 6.2 \times 10^{-4}}{80 \times 6 \times 10}$$

$$= 0.168$$

Q_c = flowrate assuming cylindrical flow
A = constant
eK_J = permeability x e
H = Excess pressure
n_1 = No. of fractures with packer spacing 5.5 ft
n_2 = No. of fractures for entire hole.

Let us consider that complete cylindrical flow is obtained when NH = 50 ft.

$$\therefore \frac{NL}{NH} = \frac{2.25}{50} = 0.045 \qquad 2NL = \text{packer spacing}$$

$$\therefore \frac{Q}{Q_c} \frac{NH}{NL} = \frac{0.168}{0.045} = 3.75$$

From Fig. 3.18 Part II

$$\frac{KY}{KX} = 3$$

In this case since the hole is horizontal, y is in the horizontal direction; and therefore the ratio;

$$\frac{KY}{KX} = \frac{\text{PRINCIPAL HORIZONTAL PERMEABILITY}}{\text{PRINCIPAL VERTICAL PERMEABILITY}} = 3$$

3.6.2 RATIO OF PRINCIPAL PERMEABILITIES AS OBTAINED FROM WATER TESTS IN ORTHOGONAL DIRECTIONS

In view of the large variation in the horizontal permeability the test results are divided into three zones and the ratio of principal permeabilities is as follows

Depth	Ratio of principal permeabilities
(a) 10'-30'	10
(b) 30'-50'	1
(c) 55'-65'	10

Obviously these values are substantially more accurate within the specified zones than the value obtained in section 3.7.1. The value obtained in section 3.7.1 is more of an indication than a precise determination as was pointed out earlier. However, it is encouraging that it gives an answer in the right direction. Also the answer in section 3.7.1 is of a Global nature rather than localised as would be the case of a two borehole test.

Another method that can be used to get an idea of the ratio of principal permeabilities is to use the ratio of the number of fissures in the two orthogonal directions. This method however, relies on the apertures being equal and can therefore be grossly inaccurate since permeability is related to the cube of the aperture.

Summary of Results

Vertical Depth	Principal Horizontal Permeability / Principal Vertical Permeability		
FEET	One Hole Test	Two Hole Test	Fissure Frequency Method
10-30	3	10	20
30-50	3	1	0.2
55-65	3	10	0.1

CONCLUSIONS

In this chapter some of the results of the tests carried out in Altwen are reported. They reflect the in-situ hydraulic measurements made with the geological structure in mind. The capacity to absorb water has been observed to be related to the fracture frequency and orientation. An outcome of such an approach is a decision as to which concept of permeability should be used to define the hydraulic characteristics of a fissured rock mass. As predicted by theory the discontinuum value of permeability converges towards the continuum value as the number of fractures per unit length increases. For purposes of extrapolation of such data in a large scale problem it is suggested that the discontinuum concept is used if the scale of the structure, i.e. dam or slope, is comparable to that of the size of the heterogeneity. In practical terms on the basis of a continuum concept this would imply very little change in permeability with different lengths of test cavity.

In order to calculate seepage pressures and performance of drainage holes the directional value of permeability is an important parameter. In a sedimentary environment for example the principal directions of permeability may be aligned with the structure, e.g. bedding. If the ratio of principal permeabilities in such a system is large a test carried out in an arbitrary direction would lend to a value of permeability which has no directional significance. It is therefore suggested that the test holes are drilled orthogonal to the fissure system which is to be examined. In Altwen this hypothesis was checked. Three holes were drilled, two orthogonal to the fissure systems under examination and the third was at an arbitrary angle so that approximately equal number of both the fissures were intersected. The permeability measurements from the inclined hole were approximately equal to the mean of the other two measurements indicating the directional significance of the test.

The simplified computer simulation of an anisotropic fissure system was used to obtain the ratio of principle permeabilities from a single hole test. The results are within an order of magnitude of the field measurements in two separate, but orthogonal holes thus showing that a certain amount of practical information can be gained from parametric studies if carefully used.

The presence of a nonlinear pressure-flowrate relationship which has aroused a lot of speculation was observed in the field. However, these results had to be carefully examined because very often the nonlinearity was introduced by the test procedure. The nonlinearity was observed at both low and high flowrates and pressures. The practical implications of a nonlinear relationship are obviously important and it is therefore suggested that in an evaluation care is taken to make sure that the correct test is carried out at a pressure which the rock mass is likely to undergo.

An important outcome in evaluating the results of the experiments described in this chapter is that during the tests pressures at an observation hole should have been monitored. In this way it is possible to observe the anisotropy in three dimensions. Further it would give an extremely good idea of the radius of influence of the test. Since this has been shown to be very small (Part II) it would be essential to have the observation hole very near the test area, otherwise the changes in the observation hole would be too small to be used with any degree of confidence. Unfortunately, the shortage of time did not permit this at Altwen. Since the observation hole in a Lugeon test is not customary it is suggested that tests should be carried out to evaluate its importance.

Eventhough the size of area tested in Altwen was so small a large variation in permeability was observed. The changes would be apparently random if careful observation was not made of the fissures. The zone of influence of a single hole test is small and therefore its value is of some doubt unless it is carried out in conjunction with an observation hole. The equipment and services required for a constant pressure test are quite substantial. For measurement of permeability below the groundwater table if it is not possible to carry out a two hole test it is suggested that the falling head test with two packers is used (see Chapter 4) because its requirements in terms of logistics are not as great.

The triple packer test which was carried out to elliminate the end effects in a borehole test proved to be practically very difficult because of limitations in size and complexity of test set up. The value of permeability obtained as compared to a two packer test showed that the end effects were slightly reduced, but in practical terms the answer was not widely different. However, this system would be useful if the ratio of principal permeabilities was very high.

UNSTEADY STATE TESTS TO DETERMINE PERMEABILITY

Snopsis

Falling head tests with a packer system were carried out at Alltwen to determine the permeability of the fissure systems. The practical advantages of such a field test were enormous and it is proposed to demonstrate in this chapter how the test was carried out to obtain permeability as described in Chapter 5 Part 3.

By using a packer system it was possible to measure the permeability of the fissure system all the way down the hole. From such a test if the results are going to be used for comparison of the different zones it is possible to assign a time constant to a test. Alternatively, the conventional approach of calculating permeability can be adopted.

4.1.0 TEST SET UP

The test set up used is as in a conventional pumping or Lugeon test. Two packers were lowered down the borehole to a suitable depth and the packers were inflated. The test cavity is then suddenly filled with water to a given pressure depending on the depth of test section below ground level and the permeability of the fissure system. Obviously in a falling head test it is not necessary to fill up the water input pipe all the way up to the ground level.

At Altwen the same arrangement for the falling head test was used as in the constant pressure test. A tranducer was mounted immediately above the packers as in fig 4.I

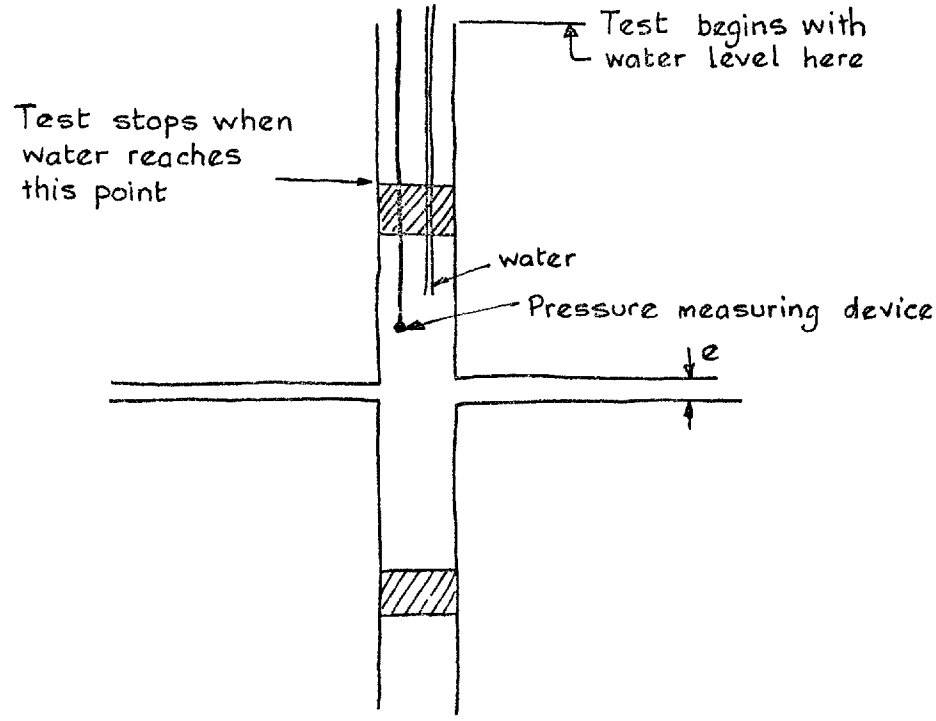


FIG 4.I

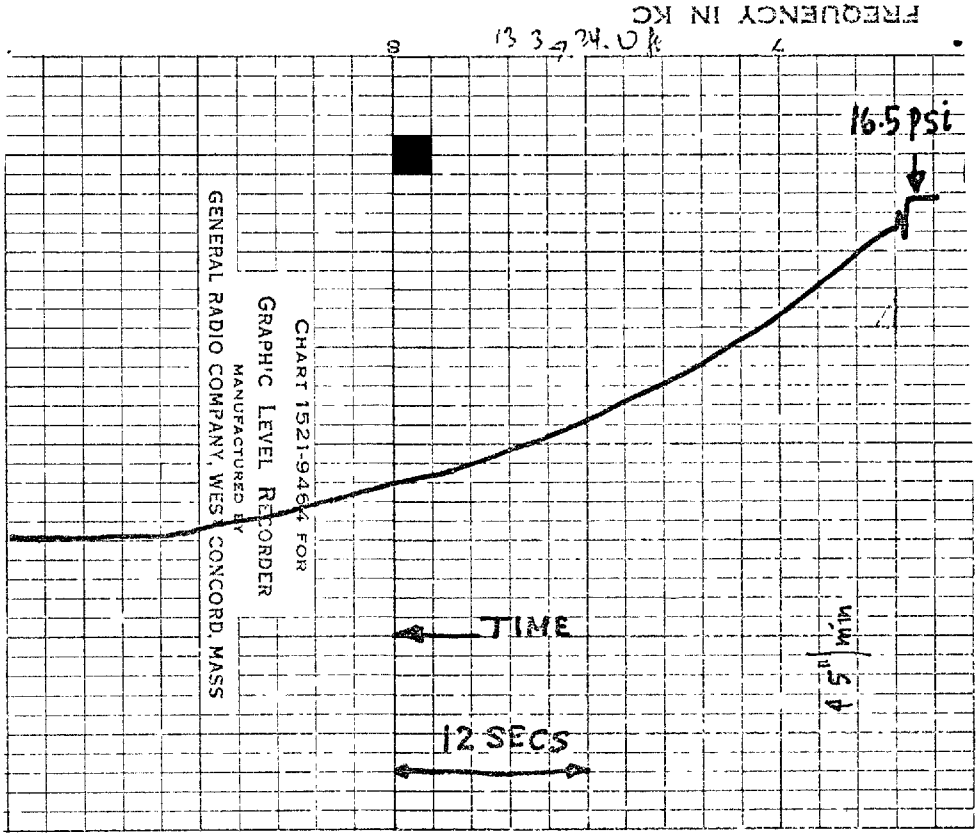


FIG 4.2 Typical test data.

4.2.0 DETERMINATION OF PERMEABILITY USING THE FALLING HEAD TEST

For those tests carried out above the water table in the field it was difficult to decide whether to analyze the results as if the test began in an unsaturated fissure system of infinite radial extent or to use the case where the horizontal fissures are of known radial dimension in which case they become saturated for that part and the rest of the unsaturated fissure system has such a large storage and permeability that it can be assumed that at

$r = re, \quad p = o$

Fig.4.3 shows a typical test result carried out in the unsaturated zone at a depth of 24.5ft. below ground level. If the results are replotted on the basis of the theory in section 5.21 Part III, i.e. the fissures are unsaturated and of infinite extent a curve as in Fig.4.4 is obtained. The data although it fits a straight line well is in the opposite direction to that predicted by theory. It is therefore evident that the assumption regarding the model is incorrect.

An interesting observation was made when carrying out model tests described in Chapter 5 Part III. Where oil was used to test the theory of flow from a cavity in an unsaturated media another falling head test was carried out, but this time the test began subsequent to steady state test. The falling head was monitored with respect to time and gave a result as in Fig.4.5. Replotted on the basis of an infinite aquifer the slope of the graph is opposite to that predicted by theory, Fig.4.6. Infact this leads us to the second type of model where at:

$r = re, \quad p = o$

4.2.1 CALCULATION OF PERMEABILITY FROM THE H-t CURVE

Fig.4.7 represents the data from a falling head test carried out in the unsaturated zone at a depth of 17.8' - 28.5' below the ground level. If we use the analysis in section 5.1.2 Part III by plotting log P/PO vs time it is possible to calculate the permeability of the system from Fig.4.7 and 4.8.

$$e^3 = \frac{6U r_o^2 \log_e (r_e/r_o)}{g} \times \frac{\log_e (P_1/P_o)}{t_2 - t_1}$$

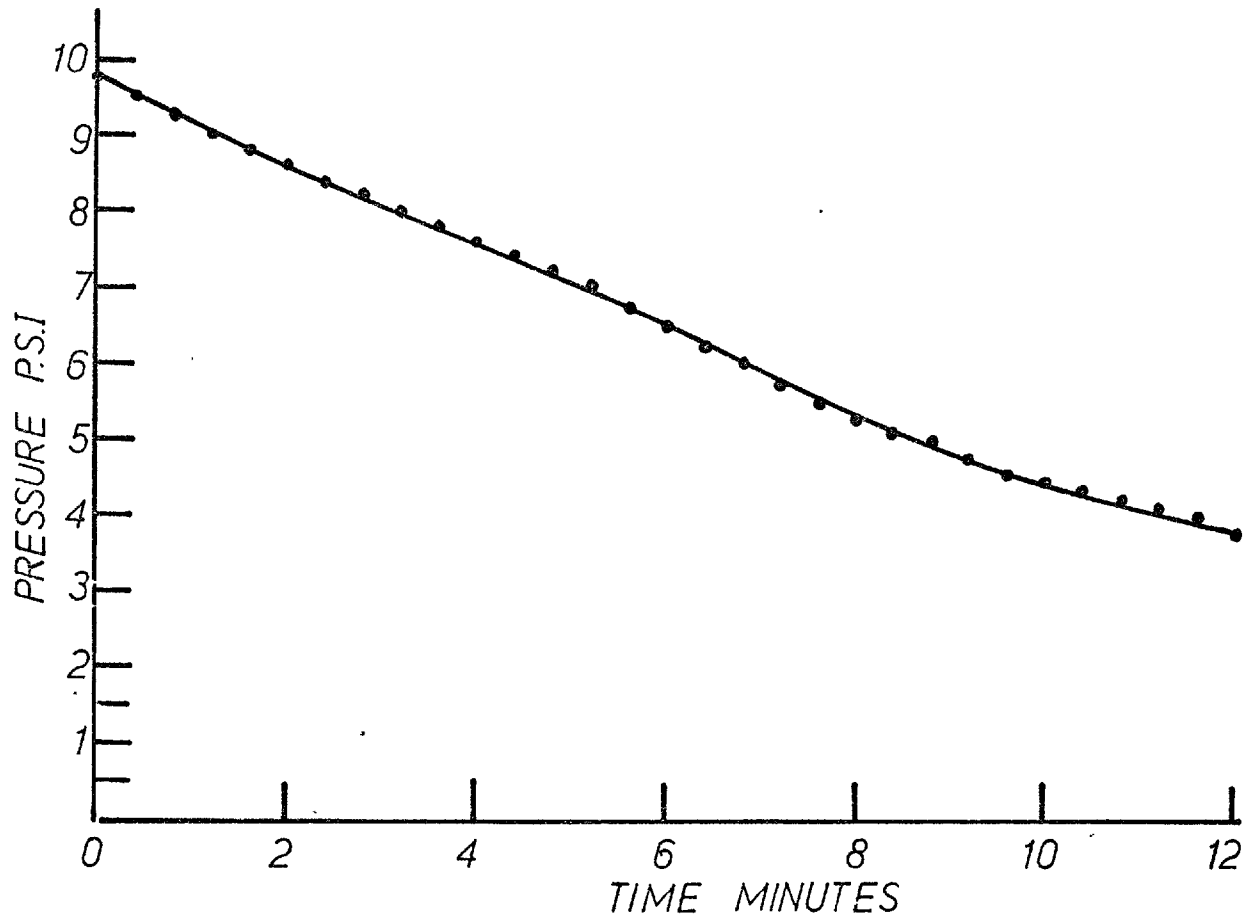


FIG 4.3

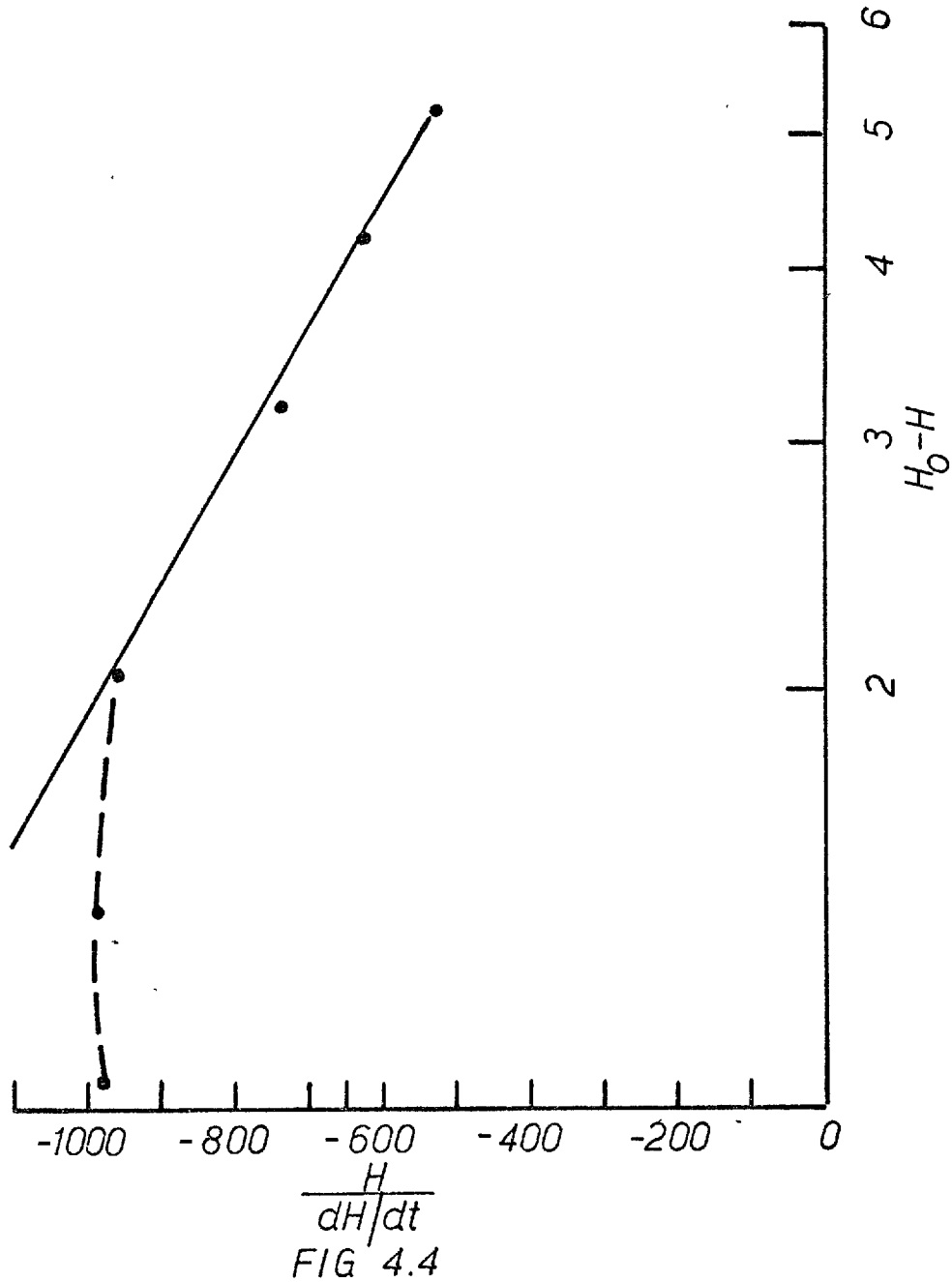


FIG 4.4

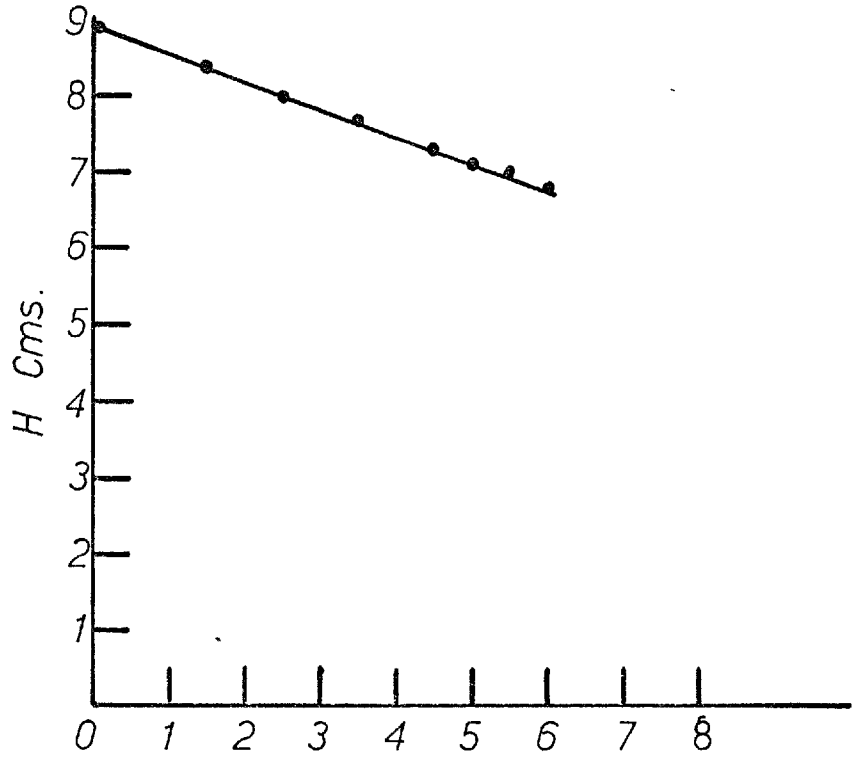


FIG 4-5

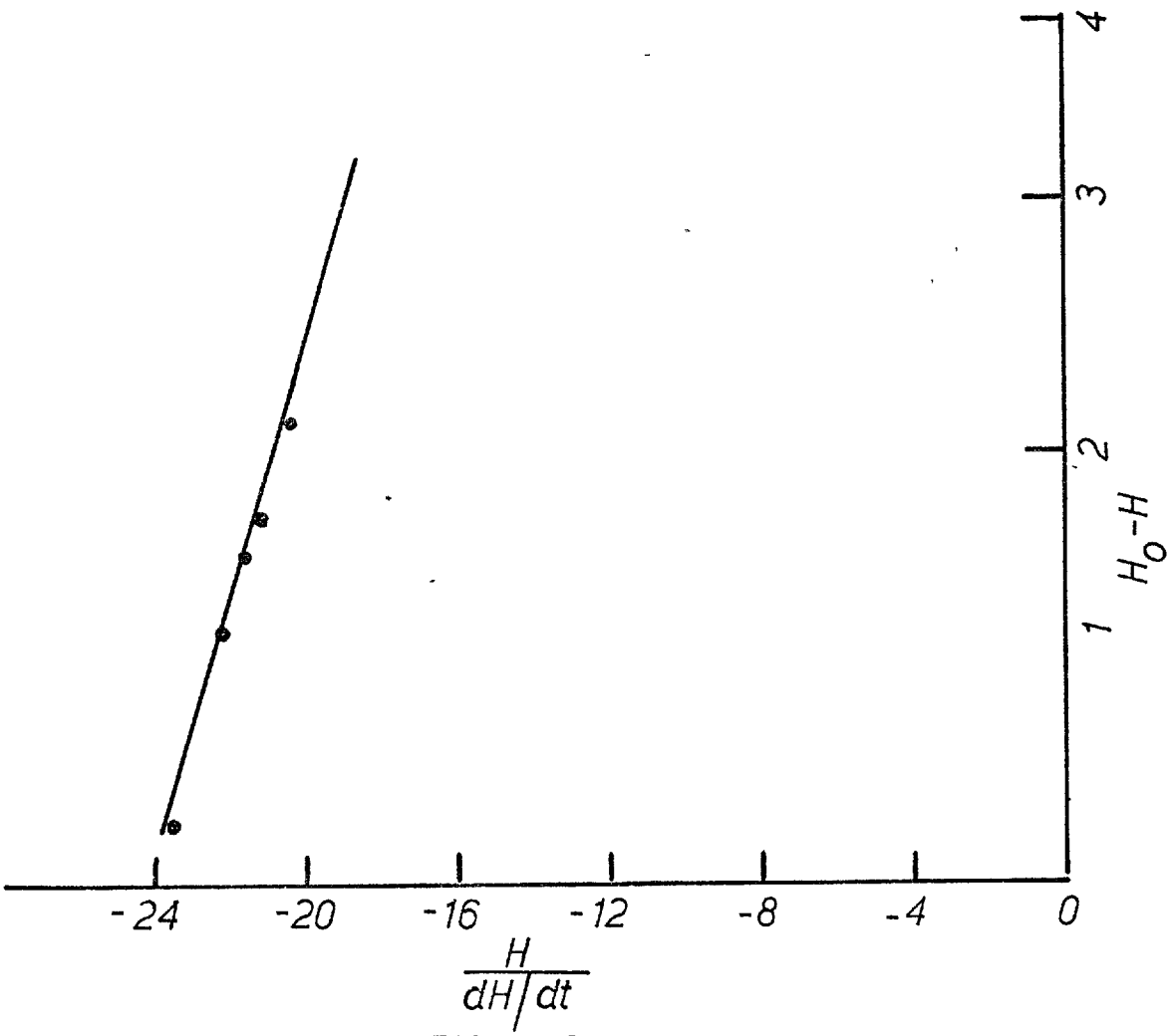


FIG 4.6

If n = number of fractures = 25
e = aperture
U = kinematic viscosity
re = radius at which vertical fissures intercept the horizontal fissures = 12″
r_o = radius of hole

Also $eK_J = \frac{e^3 g}{12U}$ K_J = Fissure conductivity

Substituting in the above:

$$eK_J = \frac{6 \times (1.5 \times 2.54)^2 \times 2.1}{12 \times 25 \times 136} = 4.45 \times 10^{-3} \text{ cm}^2/\text{sec}$$

This is the value of permeability as defined in section 2.1.0 Part II.

At the same location a constant pressure test was carried out, the results of which are given in Fig.4.9.

$$eK_J = \frac{Q}{P} \times \frac{1}{2\pi n} \times \log_e (r_e/r_o) \times \text{conversion factor}$$

$$= \frac{1}{2} \times \frac{1}{2\pi} \times \frac{1}{25} \times 6.7 \times 0.236$$

$$= 5.05 \times 10^{-3} \text{ cm}^2/\text{sec}$$

The two results agree with each other and are well within an order of magnitude. The constant pressure test gives a slightly higher value and this could be due to the higher pressures used in the latter test.

4.2.2 PRACTICAL ADVANTAGES OF THE FALLING HEAD TEST

The falling head test has numerous practical advantages over the constant pressure or Lugeon type of test. The Lugeon type of test relies upon a large amount of plant being available to carry out a test, e.g. pumps, valves and water supply. The latter adding up to a vast quantity if the rock is permeabile. The high pressures imposed by the constant pressure test, as would be the case if the test zone was a long way down the hole and a constant head would have to be applied to maintain constant flowrate, would open up the fractures to give a false value of permeability. Whereas with a falling head test very little water is required and the level can be arbitrary as long as it is above the top packer and is sufficient to give a reasonable H-t curve. The low applied fluid pressure also in such a test would be less likely to cause inertia effects which once again give a false value of permeability.

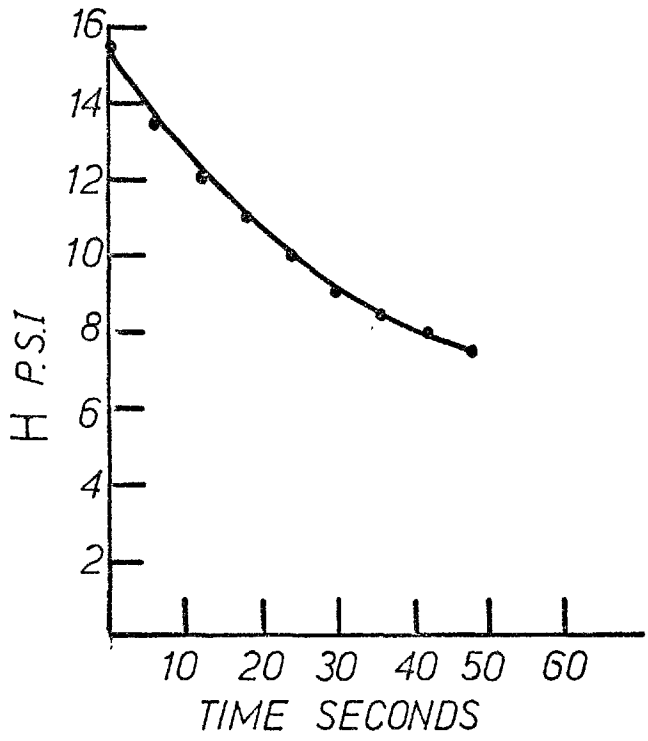


Fig 4.7

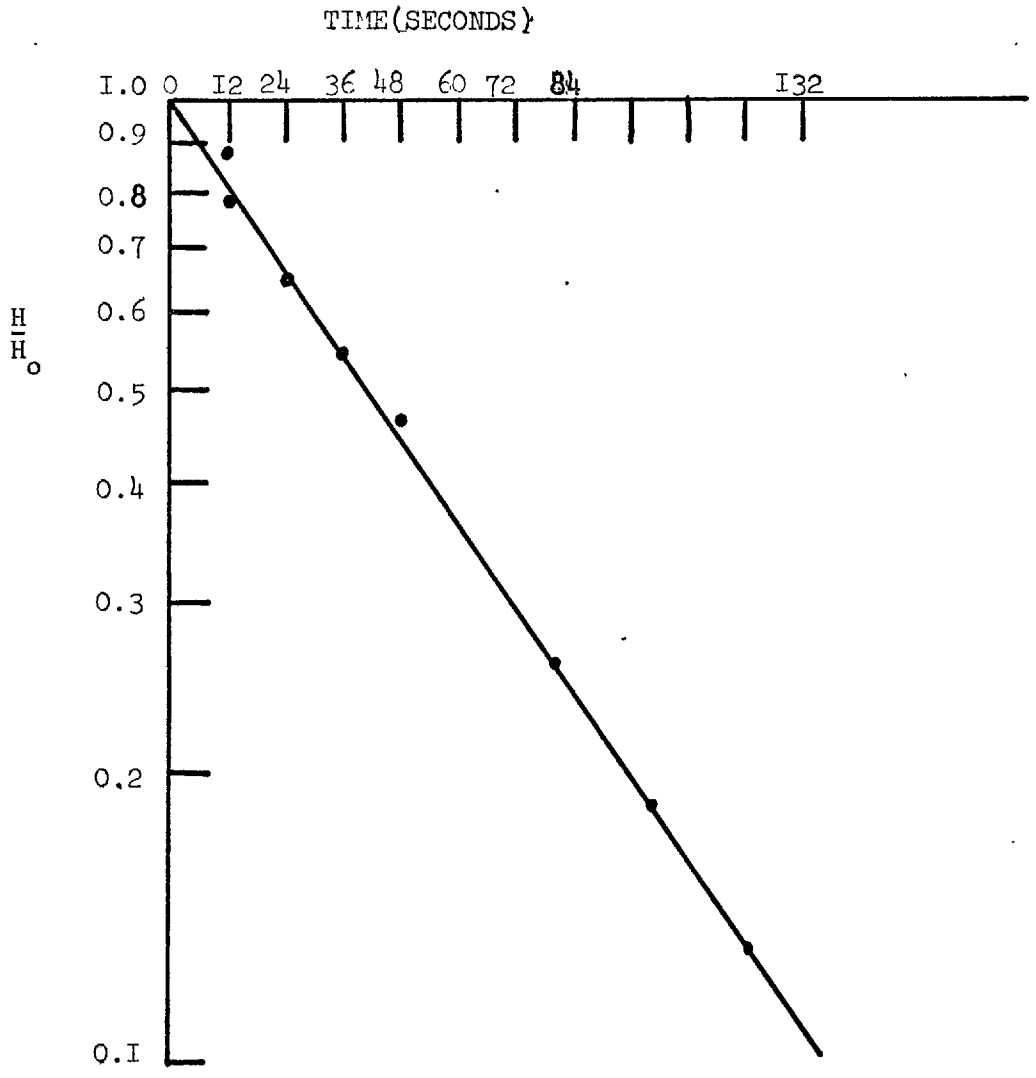

TIME (SECONDS)
I.0
0.9
0.8
0.7
0.6
0.5
0.4
0.3
0.2
0.I
H/H_o
0
I2
24
36
48
60
72
84
I32

FIG 4.8

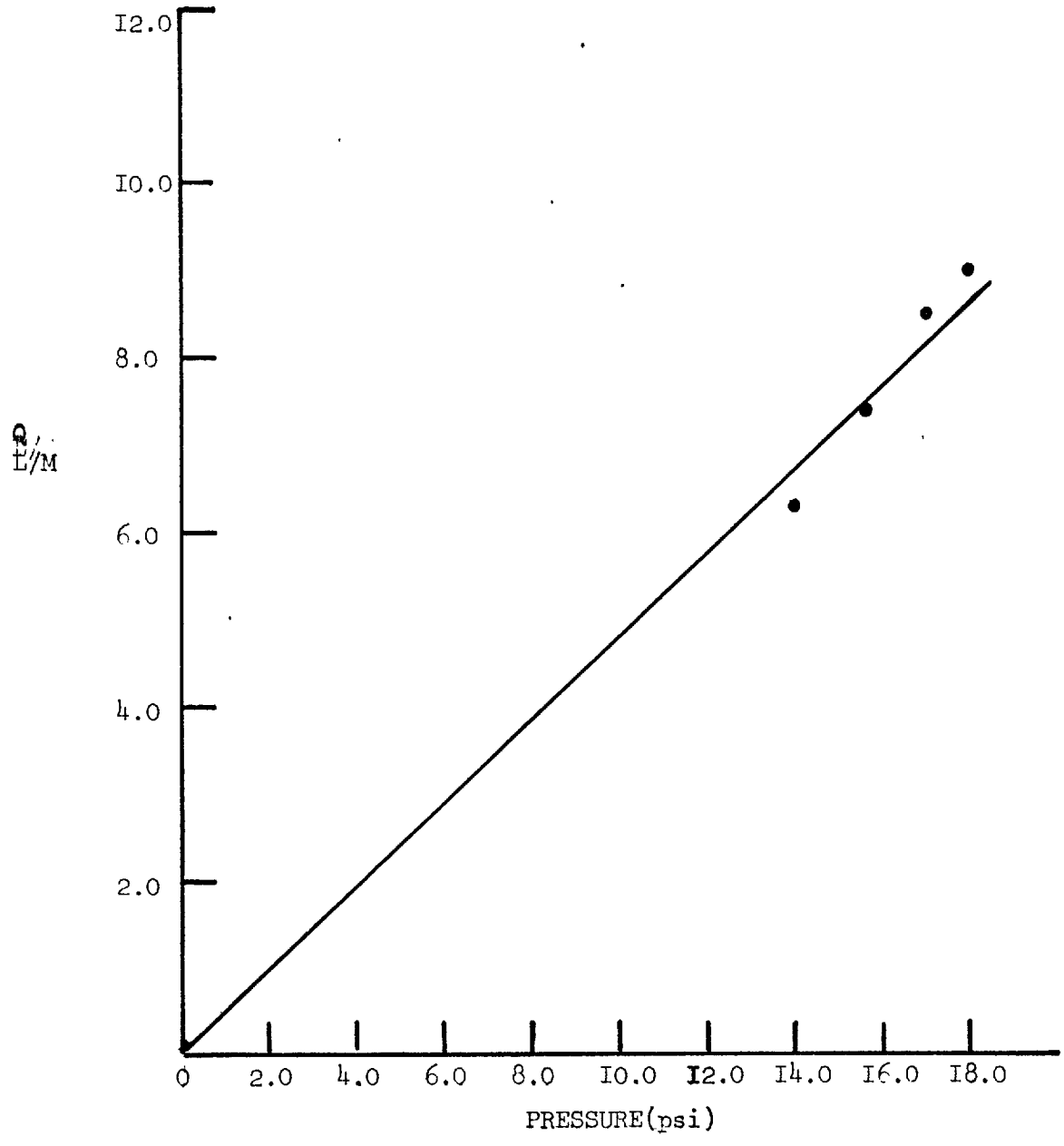

I2.0
I0.0
8.0
6.0
4.0
2.0
Q
L/M
0
2.0
4.0
6.0
8.0
I0.0
I2.0
I4.0
I6.0
I8.0
PRESSURE(psi)

FIG 4.9

CONCLUSIONS

It has been demonstrated in this chapter how a falling head test can be used in a fractured media to give a value of permeability. The use of the falling head test below the groundwater level presents no difficulty but if tests are to be carried out in the unsaturated region it is important to decide if the medium can be treated as if it were of infinite radial extent or alternatively the value of re can be assumed or established such that during the test the region between the borehole and re is always saturated. A practical way to satisfy this condition is to run water into the hole and hence the fissure system for somewhile before testing. The test result which compares the value of permeability from a falling head test to that using a constant pressure shows that in spite of the assumptions that were made there is a close agreement between the answers. The higher value of permeability using the constant pressure test possibly indicates that the fractures are opening up as a result of the applied pressure.

PART 4

INTRODUCTION

Tracing has played a very important part in hydrological investigations. However, its application in Mining and Civil Engineering problems has been far from satisfactory. The use of radio active isotopes for tracing, together with the detection of natural tritium in water has helped to advance state of knowledge and technology in groundwater tracing (37).

Groundwater tracing generally involves the introduction of an inert solution in the flow field. This inert solution acts as a label making it possible for the observer to follow the flow path of the contaminated fluid. The choice of tracer is a complex matter depending on many factors. They are best summarised by Clayton and Smith (38) as:

(a) Dye adsorption properties of the tracer

(b) Stability and solubility in water

(c) Life of the tracer

(d) Types and energy of emitted signal

(e) Maximum permissible level in drinking water

(f) Maximum specific activity available

(g) The cost of the tracer

(h) Its availability

After an exhaustive survey by the author it was decided that although radioactive isotopes were probably the best tracers in general, factors, e,g,h, completely ruled out their use. The best alternative which satisfies all the above points is some form of Fluorometric technique. This will be discussed in Chapter 5.

Introduction and detection of the tracer can influence the hydrodynamic field and it is this factor that must be given careful attention when evaluating the aquifer or formation characteristics.

Natural chemicals and tritum exist in groundwater and in some cases it is possible to evaluate groundwater parameters on such a basis. Geochemical analysis has been carried out on two field problems and these will be reported in a further section.

TRANSIT TIME TRACING

SNOPSIS

Methods are described whereby seepage velocity can be determined directly from the transit time of a tracer between two points which are at a fixed distance apart. Seepage is considered both under a natural gradient and under an applied field. These methods are discussed on the basis of a discontinuum model and where possible laboratory tests are carried out to test the methods. Finally a case study is reanalyzed on the basis of a discontinuum to show that large errors in seepage velocity and hence transit time can occur if a fractured rock mass is considered as homogeneous and isotropic with respect to flow.

2.1.0 "TRANSIT-TIME" TRACING

By this is meant that a given volume of tracer is injected at a constant rate or as a pulse. It is then picked up elsewhere and the concentration measured. The method of introduction and pick up of the tracer in the flow field is an important part of the test and controls the method by which the formation characteristics are evaluated.

SINGLE WELL TEST

This is probably by far the easiest of the cases where the tracer is introduced upstream of the borehole or well. Assuming steady state conditions, the tracer mixes well with the entire ground water regime and flows towards the hole under a natural gradient. Fig.2.1 illustrates the method schematically.

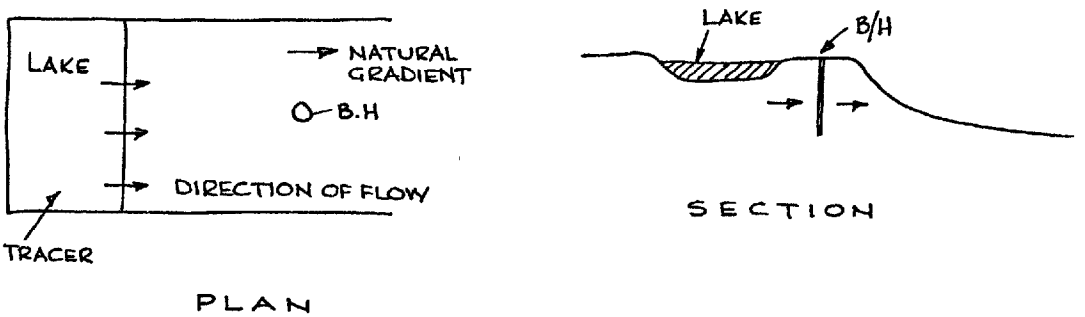


FIG 2.1

This problem illustrates for example, the case of a lake in a sedimentary environment where the majority of water is conducted in the bedding planes. Since the hole is in the natural flow field, the level of water in it will reflect the pressure within the field at that position. The hydrodynamic influence of the hole is minimal in this case and is shown in Fig.2.2. This is a computer solution for equipotentials, assuming an isotropic and homogeneous fissure. If it can be assumed that the bedding plane can be represented by a parallel plate model (7) it is possible to calculate the permeability or average aperture of the fissures by directly using Darcy's law V=KJ, where V is given by the time taken for the tracer front to travel from the lake to the hole. J is the hydraulic gradient and is given by

$$J = \frac{\text{Difference in elevation between lake water level to hole water level}}{\text{Distance between the lake to the hole}}$$

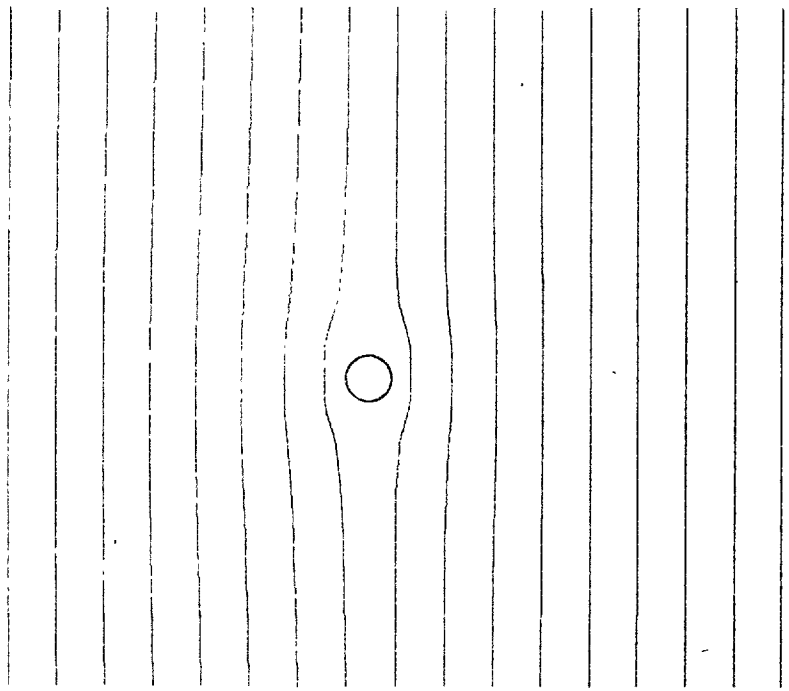


FIG. 2.2.

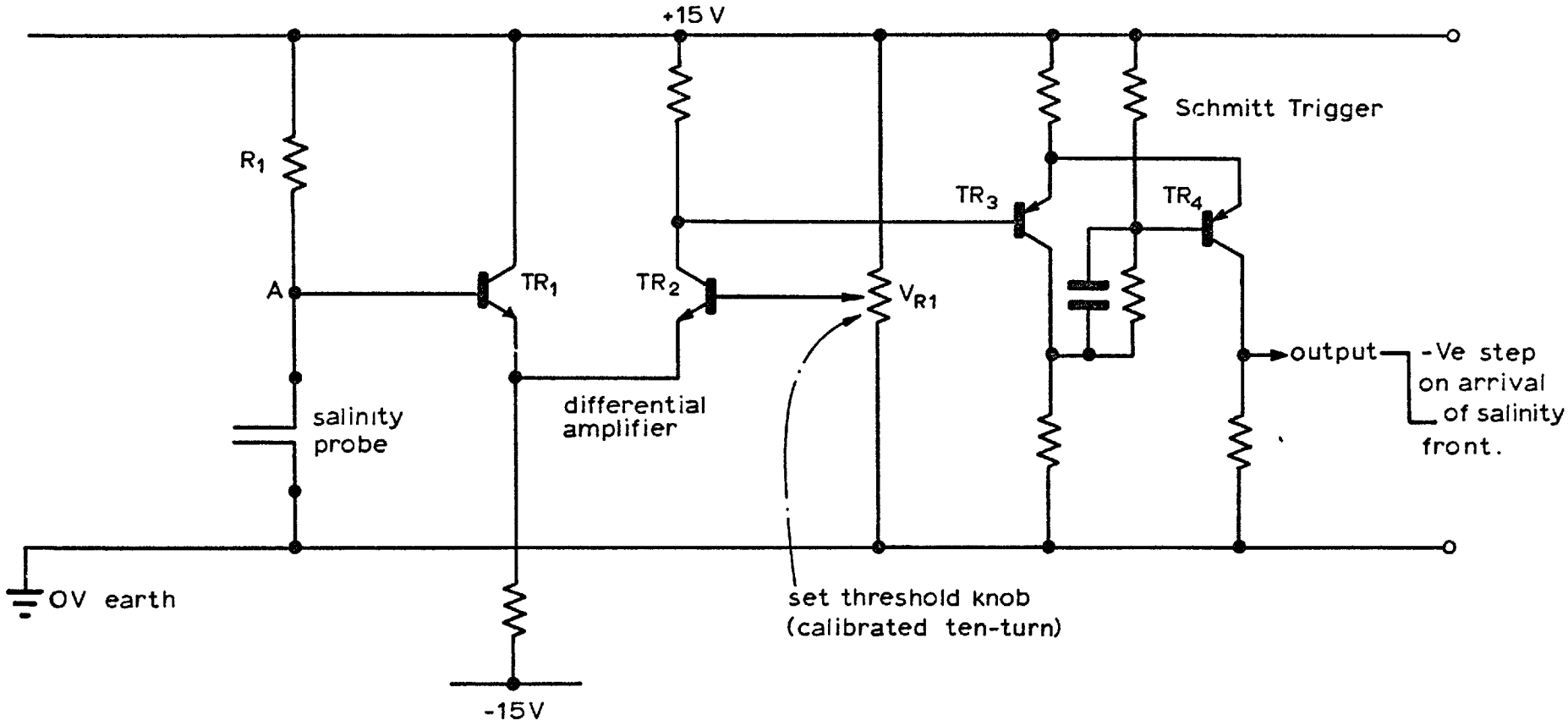


FIG.2.3 Variable Threshold Salinity Front Trigger. *Circuit of one channel shown.*

LABORATORY EVALUATION

It is assumed that in fissure flow the velocity of flow is so high that there is virtually no dispersion of the dye or tracer. For example if a tracer such as salt is injected into a stagnant pool of water the ionic activity is such that the tracer spreads out in all directions, and given enough time contaminates the entire pool, provided the active life of the tracer is greater than the dispersion time.

If a tracer is introduced into a reservoir of water and it mixes well and then enters the groundwater regime, a device which gives the arrival of the front as a sharp pulse is essential. The tracer used in the laboratory tests was salt (NaCl) which is highly conducting when in solution. Fig.2.3 illustrates the essential circuit required for such a device. As the front arrives at the 1st observation point a sharp pulse is released and the same happens at point 2. From the time taken to travel from (1) to (2) the seepage velocity vector can be calculated.

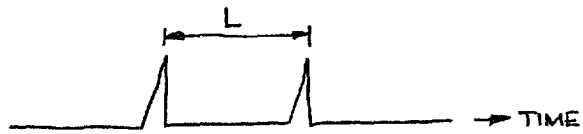


FIG 2.4

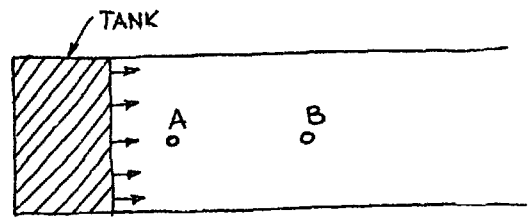


FIG 2.5 Brick model — plan view

Tests were carried out on the brick model, Fig.2.5 which described in detail in part 1. The observation holes A, B are at a fixed distance apart and the time taken to travel this distance by the tracer front is the velocity in the fissure. From the chart recorder result Fig.2.6, the transit time is given as: t = 3 seconds

the distance from A to B; L = 4 x 4 x 2.54 cms.

∴ Mean seepage velocity in the fissures;

$$Vm = \frac{L}{t} = \frac{4 \times 4 \times 2.54}{3} = 13.5 \text{ cm/sec.}$$

From pressure measurements; the hydraulic gradient is;

$$J = \frac{\Delta P}{L} = {}^{9}/_{4 \times 4 \times 2.54}$$

using Darcy's Law;

$$Vm = K_J \frac{\Delta P}{L}$$; where K_J is average fissure permeability = 33.0 cm/sec. part 1

$$\therefore \quad Vm = \frac{33 \times 9}{16 \times 2.54} = 7.3 \text{ cm/sec.}$$

The above two answers are in fair agreement, considering that in the second one the value of permeability is based on the mean value of the aperture, which is obtained from a histogram of the aperture distribution.

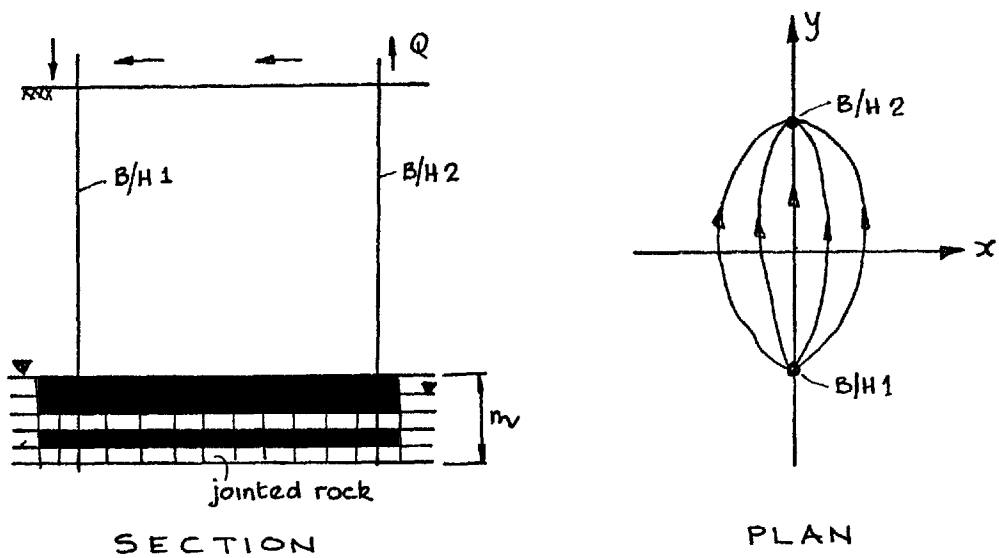


FIG 2.7

If in a fissure media a hydraulic gradient is applied by pumping water out from one well and returning it to another, steady state is achieved after a certain period of time. In an infinite homogeneous aquifer this is equivalent to a source and sink problem (see Fig.2.7). Several solutions exist for the case of a homogeneous aquifer and the one by Muskat (46) and Webster (47) gives the following relationship for the mean transit time between two wells

$$t_{ao} = \frac{1}{3} EM \frac{\pi L^2}{g_o} \qquad (2\text{-}1)$$

where g_o average pumping flow rate

L is distance between wells

E is the porosity

m is thickness of aquifer

This value of transit time is for the streamlines which travel directly from B/H1 to B/H2, i.e. the shortest path.

Similarly, the transit time for the general streamline in equation 8 can be expressed as a ratio to the shortest transit time in equation 2.1.

$$\frac{ta}{tao} = 3 \frac{1 - \psi \cot \psi}{\sin 2\psi} \qquad (2\text{-}2)$$

ta transit time for general streamline

ψ angle at which streamline leaves injection well or enter discharge well measured from the line joining the two wells.

The above equations apply for the case of non dispersed flow.

The injection of the tracer can be in the form of a pulse as described in section 2.2.1 or it can be a steady discharge of the tracer for a short period of time. Details of injection and pickup of the tracer concentration are detected in detail in Webster (47) and therefore will not be discussed.

If we assume that the two wells are connected by continuous conductors from B/H1 to B/H2 e.g. bedding or alternatively anisotropic fissure system where the permeability is much greater in the horizontal direction than the vertical direction then analytical techniques can be used to form simplified models.

Let us assume a model where the fracturing is dominantly horizontal from B/H1 to B/H2. Equn.2.1. is modified to:

$$t_{ao} = \frac{1}{3} \text{Ene } \frac{\pi L^2}{g_o} \qquad (2\text{-}3)$$

where n = number of fractures

e = effective opening of fissures

In a fissure system the porosity of the system is given by:

$$E = \frac{e}{b} \qquad (2\text{-}4)$$

where e is the aperture
b is the spacing between fissures

2.3.1 CASE STUDY OF A TWO-CELL TRACER TEST

It is proposed to recalculate the results published by Webster et al (47) on the basis that fluid flow takes place throught a discontinuum rather than a homogeneous porous media.

Webster et al (47) describes a two well tracer test which was carried out in fractured crystalline rock. A pulse injection of tritium was made into the fractured rock mass 1,000ft below the surface. The two wells were 1,765ft. apart and the duration of the test was 2 years. "The theoretical curve was developed and the only unknowns were (a) the transit time for non dispersed flow along a line joining the two wells and (b) the characteristic dispersion length in the medium. These two values were obtained by curve fitting. The results of the tracer test agree with computations based on the assumption that flow was through a homogeneous medium consisting of numerous intersecting fractures".

However, examination of the data shows firstly, a recovery of 33% of the injected tracer. Secondly Fig.5 in the paper (47) shows that the tracer begins to appear at the monitoring borehole at 50 days; although the non-dispersed flow arrives at 400 days. This latter valve is assumed to be the mean transit time. Several things could have happened in this test: (a) the flow is anisotropic and this would explain the 33% recovery since the rest could have travelled in a direction not parallel to the applied gradient (7); (b) Figure of 50 days might suggest that the model is not necessarily equivalent to a homogeneous porous media.

It would be useful to carry out an excercise based on the flow through a discontinuum. However, to use the discontinuum approach an estimate of flow conductors is required if from a given value of porosity we wish to calculate the mean aperture. Let us assume that there is a conducting fracture every two feet.

From Eqn.2.4

e = Eb we are given that E = 0.08% (not unrealistic Ref.(44)).

L = 1765 ft.

m = 250 ft.

$$= \frac{0.08}{100} \times \frac{1}{500} \times 12 \times 2.54$$

$$= 1.22 \times 10^{-2} \text{ cms} \simeq 1/10\text{mm}.$$

A thickness of approximately 1/10mm for a fracture is not unlikely. Darcy's Law for a parallel plate model:

$$V = \frac{e^2 g}{12U} I$$

substituting the above values I = 120/1765

V = 0.11 cm/sec.
= 325 ft/day.

This approach immediately illustrates that the velocity of flow in a fissure system is much higher than that in a porous media. The previous calculation is not an exact analysis; but it illustrates how the velocities can be fairly high. Obviously in a real situation the fissures will not be continuous and this would reduce the seepage velocity, but not too seriously.

CONCLUSIONS

This chapter has outlined very simple methods which can be used to predict the overall behaviour of the fractured mass. These techniques are useful and very cheap compared to other tests where the transit times are required between two points in the field. However, they are not suitable for detailed permeability evaluation of a rock mass for pressure distribution analysis. Further it is important to decide if the field situation approximates to a discontinuum or a porous media. This decision should be based on the degree of fissuration and the recovery of the tracer. Perhaps monitoring the tracer concentration in a direction at right angles to the applied gradient would be useful in deciding the criteria for a flow model.

CHAPTER 3

THE DILUTION METHOD

SNOPSIS

Where natural groundwater flow occurs as a result of a field gradient it is proposed that a borehole tracer dilution method is used to determine seepage velocity and permeability. This method has been very successfully applied to a porous media (11). Lewis et al (48) has applied the technique to determine the hydraulic conductivity of fractured rock. However, in estimating the permeability, flow was assumed to occur in a porous and homogeneous media. In this chapter the relationship between seepage velocity and the rate of dilution is derived from first principles. The validity of the equation is subsequently checked with a physical model. The predicted values of seepage velocity agree extremely well with the measured velocities. Field equipment was designed as a result of the above experience. Unfortunately, owing to the shortage of time and the unusually low water table encountered during the field trip prevented the author from carrying out field trials.

DILUTION METHOD: THEORY OF THE PROPOSED METHOD

If a borehole intersects a system of fractures below the groundwater table and there is groundwater flow as a result of a natural gradient, it is possible to obtain seepage velocity and subsequently permeability by the dilution method. Very simply the borehole dilution method consists of injecting a tracer in the borehole and mixing it adequately and then observing the change in concentration of the tracer as a result of flow into the borehole.

The choice of tracer has been outlined in Chapter 1 and for the purpose in mind it was decided to use dilute hydrochloric acid (HCl) as it fulfilled all the conditions laid out in Chapter 1.

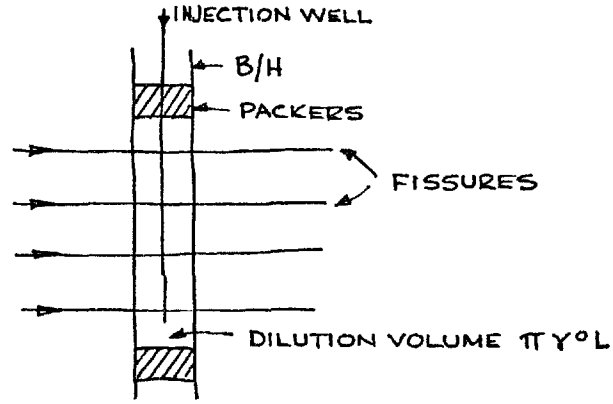
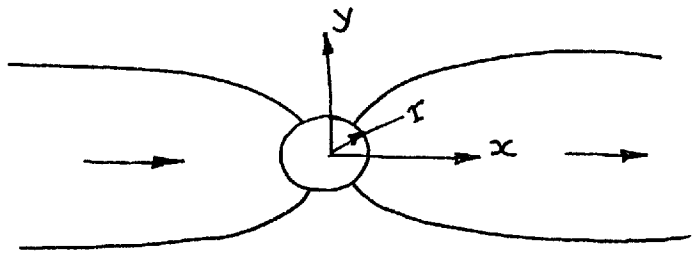


FIG 3.1

Fig.3.1 is a schematic diagram illustrating the field application of the method. For the analytical solution of this problem it will be assumed that the majority of the flow occurs in horizontal fractures; which can be represented by a parallel plate model.

MATHEMATICAL DERIVATION OF SEEPAGE VELOCITY IN TERMS OF THE DECAY OF SALT SOLUTION CONCENTRATION



PLAN VIEW

FIG 3.2

Fig.3.2 illustrates, in plan, a borehole and the flow into it. It is assumed that the hole has the same potential as the flow field at that point; but the flow lines are "pinched" in the vicinity of the hole as a result of the hydrodynamic effect of a circular potential field of radius r_o.

If the potential $\emptyset$ is constant in the direction which is orthogonal to the X-Y plane:

From Equation of continuity:

$$\text{div } (\gamma_w V) = \frac{\partial}{\partial x} (\gamma_w V_x) + \frac{\partial}{\partial y} (\gamma_w V_y) = 0$$

If we assume Darcy's Law to hold for flow through a fracture: $\emptyset$ is the potential and is equal to $- P_{/rh+}$

$$V_x = K \frac{\partial \emptyset}{\partial x}$$

$$V_y = K \frac{\partial \emptyset}{\partial y}$$

substitute Eq. 3. in Eq.3.

$$\frac{\partial^2 \emptyset}{\partial x^2} + \frac{\partial^2 \emptyset}{\partial y^2} = 0$$

This however, is the familiar Laplace Equation.
Converting the above to a system of polar coordinates;

$$\frac{1}{r}\frac{\partial}{\partial r}\left(r\frac{\partial \phi}{\partial r}\right) + \frac{1}{r^2}\left(\frac{\partial^2 \phi}{\partial \theta^2}\right) = 0 \qquad (3.4)$$

Equation (3.) is a common equation in problems involving groundwater flow and heat conduction. However, the case of the dilution process involves boundary conditions which are not commonly met elsewhere. Suppose the solution to Eq.3.4 is given by:

$\phi = F_1(\theta)\, F_2(r)$ Equn. 3. where F_1 and F_2 and functions

substitute Eq.3. in Eq. 3.

$$\frac{F_1(\theta)}{r}\frac{\partial}{\partial r}\left(r\frac{\partial F_2}{\partial r}\right) + \frac{F_2(r)}{r^2}\frac{\partial F_1(\theta)}{\partial \theta^2} = 0$$

Multiply by r^2 and dividing by $F_1\, F_2$

$$\frac{1}{F}\left[r^2\frac{d^2F_2}{dr^2} + r\frac{dF_2}{dr}\right] = -\frac{1}{F}\left[\frac{d^2F_1}{d\theta^2}\right] = n^2 \qquad (3.5)$$

where n is a constant and called the degree of Harmonics.
Equn.3. can be solved by:

$$\frac{d^2F_1}{d\theta^2} + F_1 n^2 = 0 \qquad (3.6)$$

$$r^2\frac{d^2F_2}{dr^2} + r\frac{dF_2}{dr} - F_2 n^2 = 0 \qquad (3.7)$$

Equns.3.6 and 3.7 are standard equations: e.g. Equn. 3. is S.H.M.
Solutions for the above are:

$F_1 = A\cos n\theta + B\sin n\theta$ if $n \neq 0$

$F_2 = Cr^n + Dr^{-n}$

If $n = 0$

$F_1 = A_o\theta + B_o$

$F_2 = C_o \log r + D_o$

$\therefore$ the complete solutions to the equations 3. and 3. are;

$$\phi_o = (A_o\theta + B_o)(C_o \log r + D_o) \quad \text{Degree Zero} \qquad (3.8)$$

$$\phi_n = (A_n C\theta + B_n S\theta)(Cr^n + Dr^{-n}) \quad \text{Degree } n \qquad (3.9)$$

In all physical problems a function ϕ is usually a single valued function of θ i.e. if θ varies from $0 \to 2\pi$ we get different values of ϕ and after 2π they repeat themselves (Ref.49).

$$\phi_n (r, \theta + 2\pi) = \phi_n (r, \theta)$$

$\therefore$ It is essential for n to take integral values and a single valued solution is the sum of all values of n.

$$\therefore \quad \phi = a_o \log r + \sum_{n=1}^{\infty} r^n (a_n \cos n\theta + b_n \sin n\theta) + \sum_{n=1}^{\infty} \frac{1}{r^n} (q_n \cos n\theta + P_n \sin n\theta) + C \qquad (3.10)$$

Suppose that the applied field gradient is I_o :

$$I = -\text{grad}\ \phi = -\nabla\phi \qquad (3.11)$$

Original potential outside borehole

$$\phi_o = I_o r \cos\theta \qquad (3.12)$$

At infinity the effect of the B/H on the field vanishes. By symmetry the induced field is symmetrical about the X axis; hence it is an even function of n. The constant term = 0 without loosing generality.

$$\phi_i = \sum_{n=1}^{\infty} \frac{q_n}{r_n} \cos n\theta \qquad i \text{ inside the B/H.}$$

Total potential:

$$\phi_r = -I_o r \cos\theta + \sum_{n=1}^{\infty} \frac{q_n \cos n\theta}{r^n}$$

when r = a; $\phi = 0$

$$\therefore \quad 0 = -I_o r \cos\theta + \sum_{n=1}^{\infty} \frac{q_n \cos n\theta}{a_n}$$

$$\therefore \sum_{n=1}^{\infty} \frac{q_n}{a_n} \cos n\theta = I_o r \cos\theta$$

For n = 1; equation $\cos\theta$

$$\frac{q_1}{a} = I_o r$$

$$\therefore \quad \phi = -I_o r \cos = \frac{I_o a^2 \cos}{r}$$

alternatively $\phi = I_o a \cos\theta\left[\frac{a}{r} - \frac{r}{a}\right]$ (3.14)

Equation (3.2) $V = K\frac{\partial \phi}{\partial r}$

Substitute Eqn. (3.14) in Eqn. (3.2)

$$V = KI_o a \cos\theta \left(a/r^2 + 1/a \right) \quad (3.15)$$

Let us assume that the flow from the fissure into the hole = Q

$$\therefore \quad Q = \int_{\pi/2}^{3\pi/2} \left[V_r\right]_{r=a} . e . a . d\theta \quad (3.16)$$

where c is the fissure appendix
a is the radius of B/H

substitute Eq.3.15 in Eq.3.16

$Q = -4Vae$ (3.17)

V is the seepage velocity

At a given time T concentration $c = \frac{Vc}{Vo}$

Vo volume in B/H
Vc injection volume

$$\therefore \quad \frac{dc}{dt} = \frac{dVc/dt}{Vo}$$

But $\frac{dVc}{dt} = \frac{-CQ}{Vo}$ (3.18)

substitute Eq.3.17 in 3.18

$$\int_{c_o}^{c} \frac{dc}{C} = -\int_{o}^{t} \frac{Q\,dt}{Vo} = \int_{o}^{t} \frac{4Vae}{Vo}\, dt$$

$$\therefore \quad \log \frac{c}{c_o} = \frac{4Vae\ t}{Vo} \quad (3.19)$$

The volume of the cavity between the packers spaced h units; Fig.3.1

$$V_o = \pi a^2 h \qquad \therefore \log_e\left(\frac{c}{c_o}\right) = \frac{4Vaet}{\pi a^2 h} = \frac{4Vet}{\pi a h}$$

If d = diameter of hole:

$$V = \frac{\pi d h}{8et} \log_e\left(\frac{c}{c_o}\right) \qquad (3.20)$$

From Equation 3.20 it is obvious that in order to compute the seepage velocity V we have to know the aperture of the fissure. This is obviously not practical. In a porous media approach however, e is equivalent to h and therefore it is possible to determine the apparent velocity. In fissure flow equation 3.20 can be rearranged so that the flowrate per unit width is determined.

$$Q = Ve = \frac{\pi d h}{8t} \log_e\left(\frac{c}{c_o}\right) \qquad (3.21)$$

EXPERIMENTAL VERIFICATION OF THE MATHEMATICAL DERIVATION OF SEEPAGE VELOCITY

Having established the relationship between seepage velocity or flowrate per unit width of a fissure and the change of concentration with time of the tracer, Eq.3.21 it is proposed to test this hypothesis by carrying out model tests. The method relies on adequate mixing of the tracer so that the dilution process is a steady one. This mixing process has been studied and will be described.

Fig.3.3 is a schematic diagram of the test equipment with the different dimension marked on it. Fig.3.4 is a photograph illustrating the layout of the equipment.

The fissure model consists of two parallel perspex plates ½" thick separated from each other by strips accurately machined to 40/1000" or 1 mm. The borehole diameter is a tenth of the cross-section width of the fissure. Computer studies show that boundaries at that distance have no influence on the flow lines which converge towards the borehole (Fig.3.2). Input of water is from a constant head device via a control value which sets the value of velocity of flow. At the output end the stilling basin provides a constant back pressure.

Mixing of the solution is achieved by a magnetically coupled stirrer as shown in Fig.3.4 . The speed of the stirrer can be allowed to suit the flow conditions.

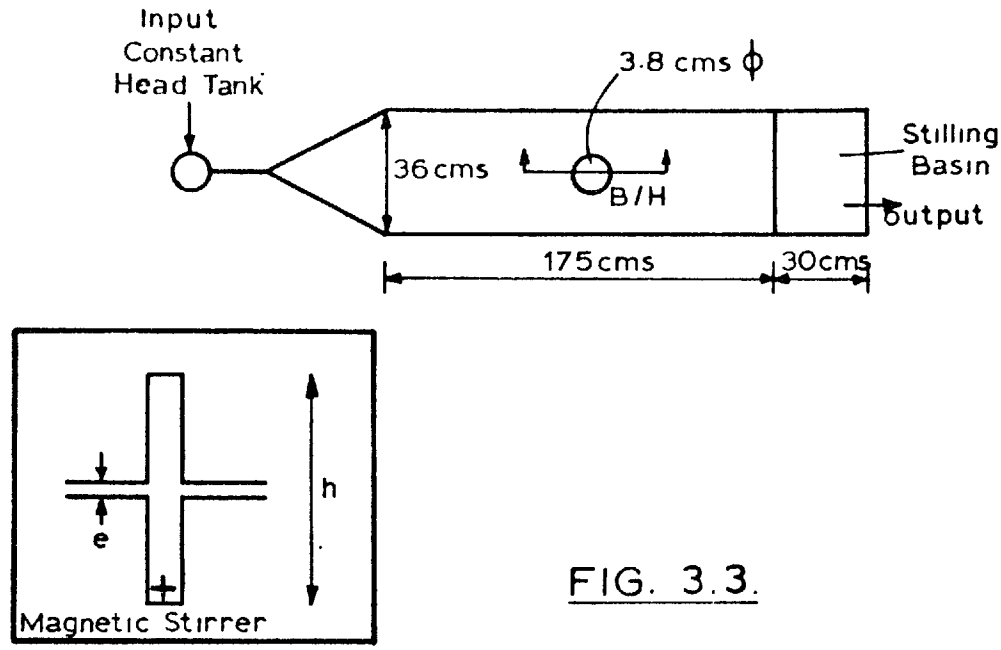

Input
Constant
Head Tank
3.8 cms ϕ
36 cms
B/H
Stilling
Basin
Output
175 cms
30 cms
h
e
Magnetic Stirrer

FIG. 3.3.

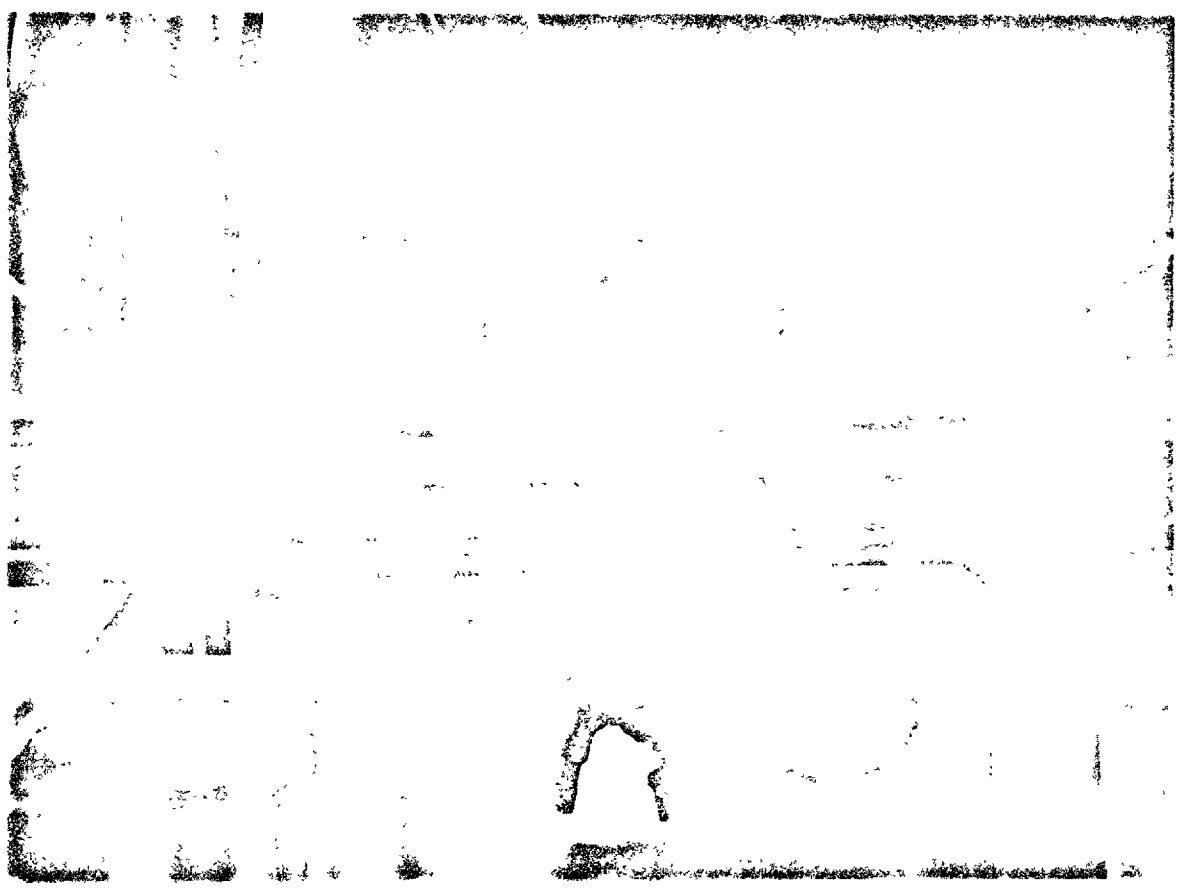


FIG 3 4.

This method relies on the accurate determination of tracer concentration with respect to time. Since hydrochloric acid solution was used in these experiments the conductivity of the solution had to be measured over a wide range and under continuously varying conditions. Normal P.H. measuring techniques are not accurate over such a wide range of conductivity values as were to be encountered in the experiment and also not stable under varying conditions. It was therefore decided to use a highly stable system employing an Alternating Current Bridge technique. Fig. 3.5 illustrates the equipment that was used.

In order to obtain continuous readings of concentration during the experiments the Wayne Kerr Bridge was connected to a chart recorder. This factor was important in speeding up the test operation and improving the accuracy of the data.

VERIFICATION OF THE "PINCHING EFFECT" OF A BOREHOLE

In section 3.1.1 it was stated that the presence of a borehole has a "pinching effect" on the flow field which would otherwise be linear. Fig.3.2 is a computer solution which verifies this. This effect was observed in the physical model when under conditions of natural flow coloured dye was injected upstream of the borehole. Fig.3.6 illustrates how the two injected dye lines begin as straight lines parallel to the applied gradient and then bend to converge towards the hole. The explanation for such an effect lies in the fact that within a radius of r/o within the borehole there exists a constant potential and a permeability value which tends to infinity.

DIFFUSION AND MIXING OF THE TRACER

It is important to have some idea of the diffusion of the tracer under "no-flow" conditions. If this diffusion is too slow mixing will have to be achieved under artificial conditions by using a stirrer. On the other hand if the diffusion is too rapid it could well be mistaken for seepage. Tests were carried out for both the static and dynamic case to study the speed of diffusion.

Fig.3.7 illustrates the increase in concentration as a result of a pulse injection of 5cc of dilute HCl (Ratio of Water to HCl of 20.1). The injection was carried out with the fissure and borehole full of water but with zero gradient. A, B, C are three separate injections of the tracer. It is evident from these tests that attaining steady state is a slow process without mixing and also very erratic. In all cases, however, the tracer finally mixes at times greater than five minutes.

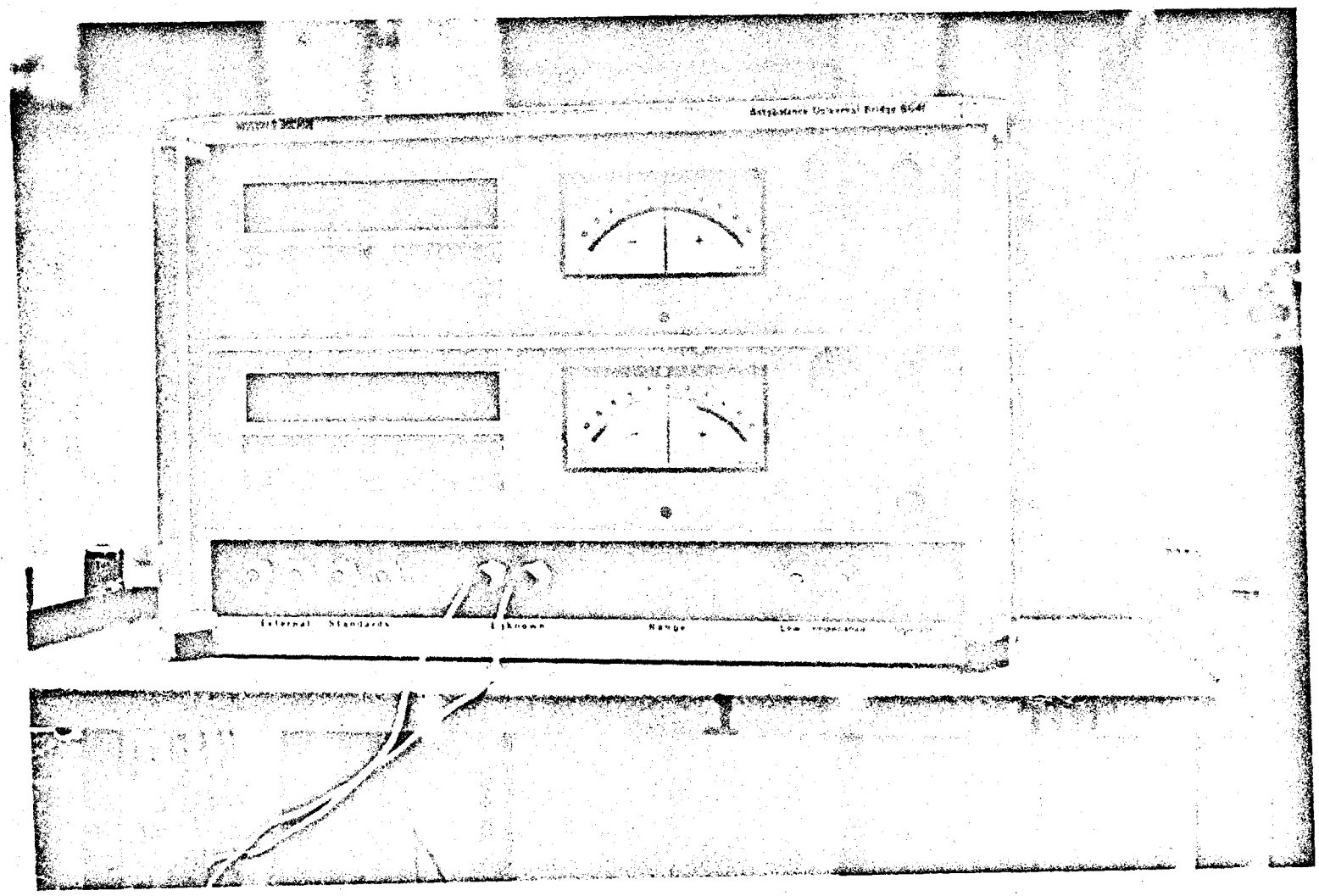


Fig 3.5

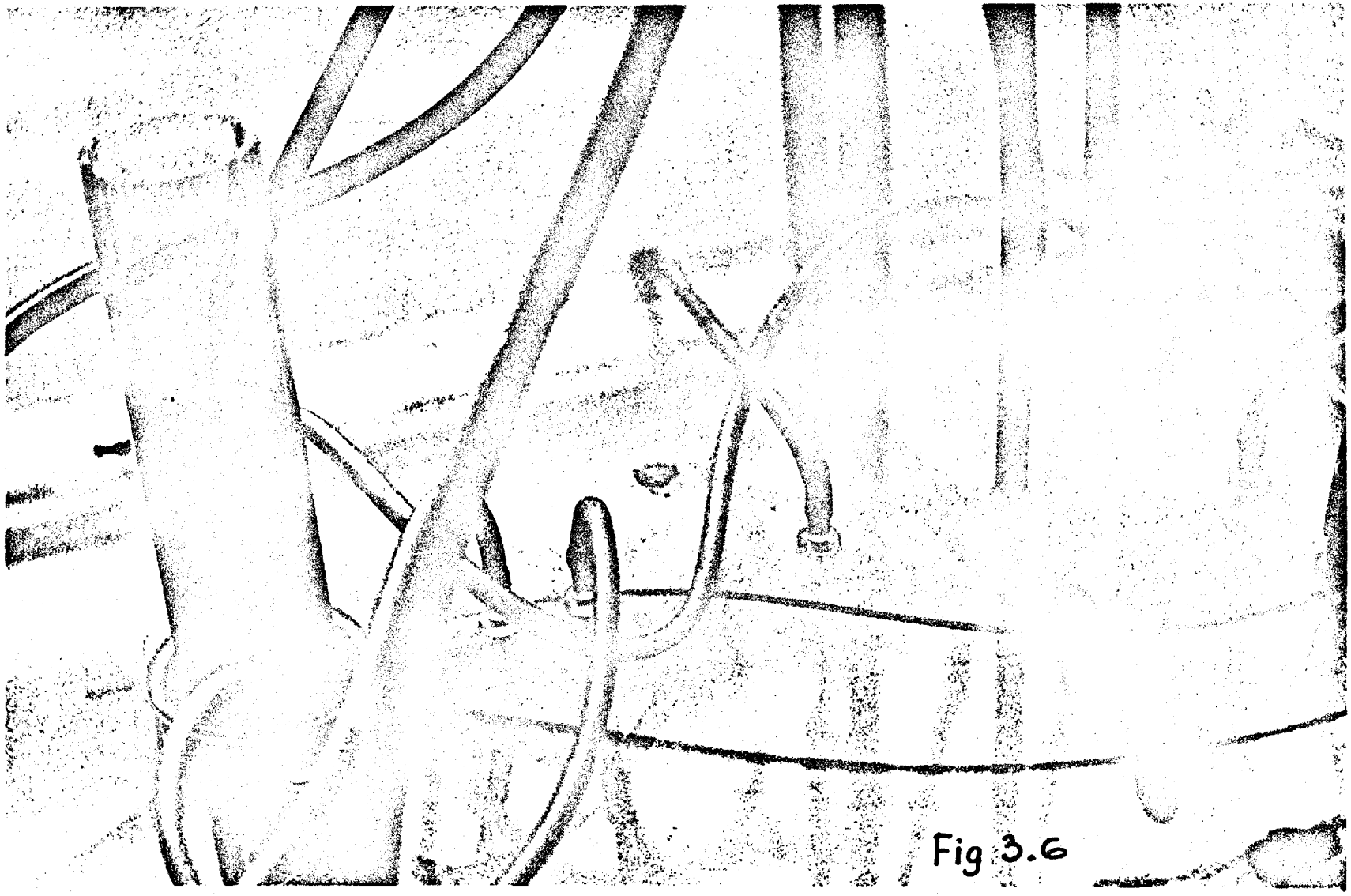


Fig 3.6

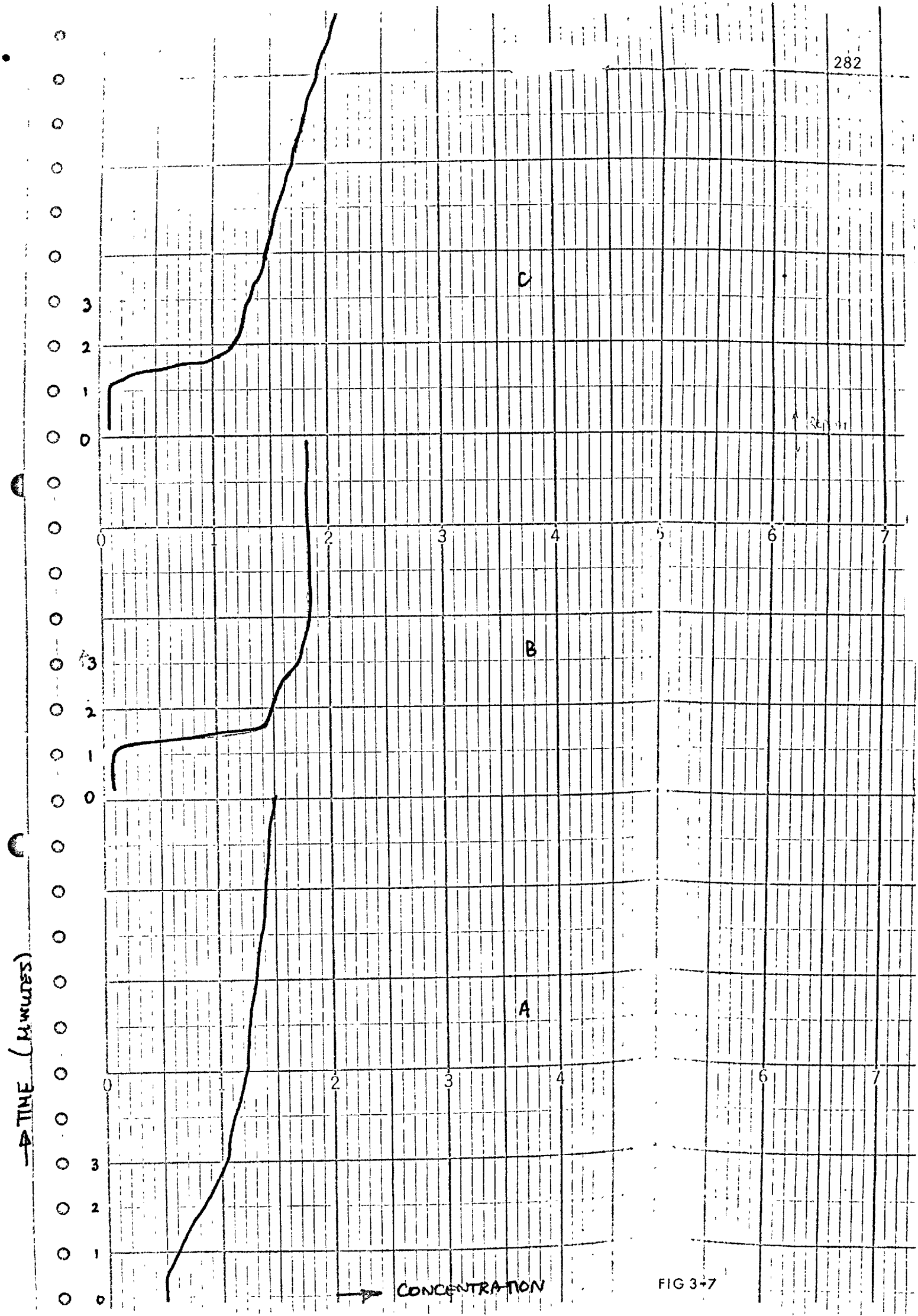


FIG 3-7

Once steady state was reached, there was no appreciable change in conductivity of the solution for at least eight hours. It cannot be envisaged that this method would be used in fissure flow studies where the seepage velocity is so low that the solution will have to remain stable for more than 8 hours; because by then most of the tracer will be washed away.

Now if under static conditions a stirrer is used, a pulse injection of the tracer mixes almost instantaneously as shown in four separate trials, Fig. 3.8 and remains absolutely steady thereafter.

Further tests were carried out to see how much difference there was in the decay of concentration of the tracer with the stirrer switched off and then on. Fig.3.9 shows how at a steady flow of 2000 cc/min. a pulse injection is detected and then it decays gradually with time. At exactly the same seepage velocity approximately the same amount of tracer was injected; but this time the stirrer was switched on, Fig.3.10 shows the decay in concentration with time. Although the maximum concentration indicated is not the same, this could be due to the volume of tracer injected, the change in concentration per unit change in time is different in both cases. The decay in the unstirred case is much slower and erratic due to inadequate mixing whereas constant stirring produces decay curves for the same seepage velocity which are identical. Tests were carried out with the stirrer revolving at 20, 40, 60, 80 c/s and in each case the decay curve was identical for a constant seepage velocity. This experiment was repeated at two other seepage rates. The result of this test is summarised in Fig.3.11 It can be concluded from this that if the stirring velocity is greater than 20 c/s adequate mixing will have been achieved.

DETERMINATION OF SEEPAGE VELOCITY USING THE DILUTION METHOD

Numerous tests were carried out under different input conditions to determine seepage velocity using the dilution method. Eq.3.20 and Eq.3.21 were then used to calculate the seepage velocity from the concentration decay curves. Results of seepage velocity are compared with direct measurements of flowrate using a bucket and stop watch. Since the cross section area of the flow model is known, it is possible to determine the mean seepage velocity from the measured flowrate.

Fig.3.12 is a plot of four tests (out of about 20) which were carried out at different velocities. A plot of log e C/co vs time is a straight line as predicted by Eq.3.20. One of the three tests is calculated in detail and the remaining results are tabulated.



FIG 3-8

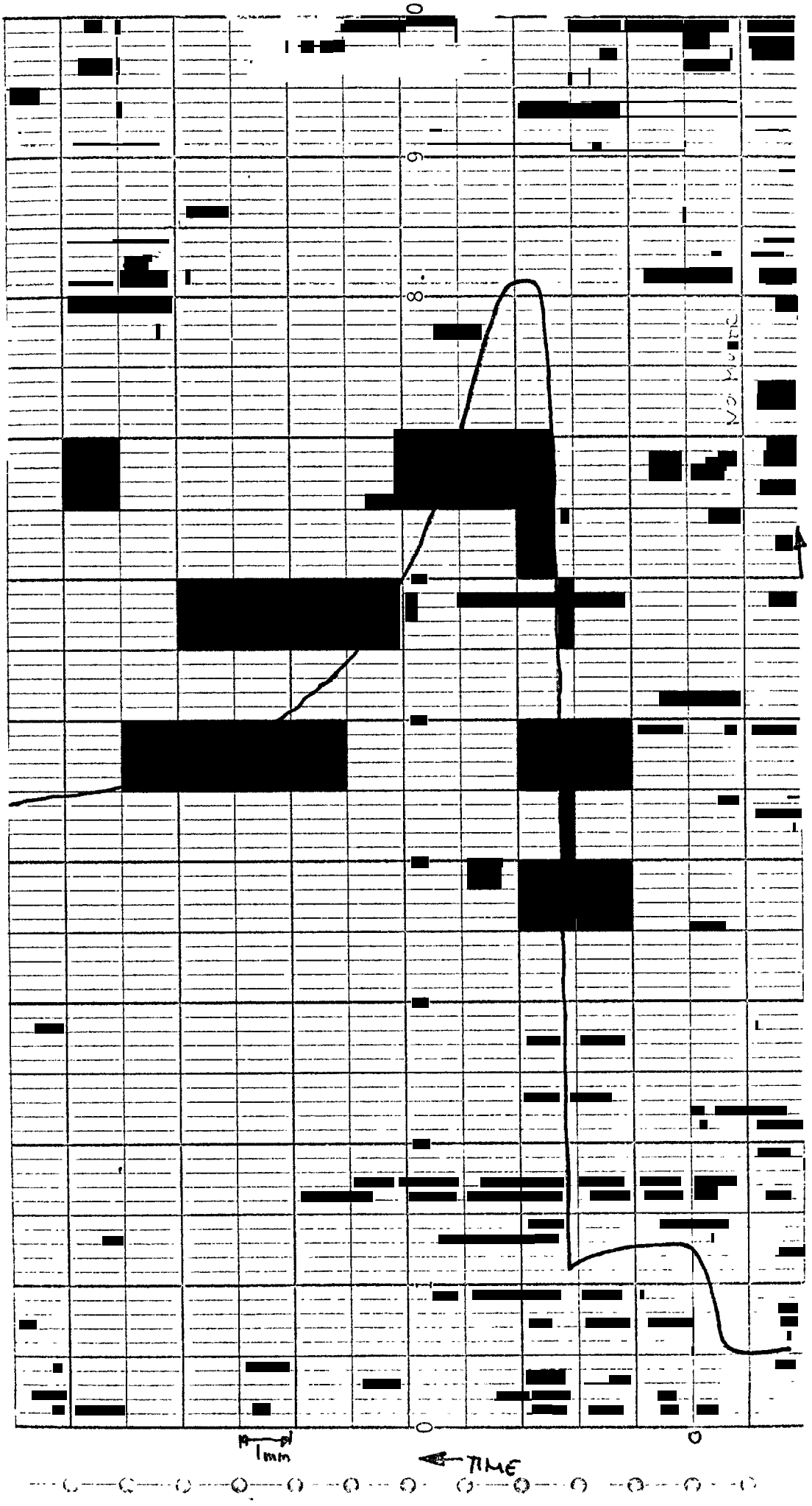


FIG 3-9

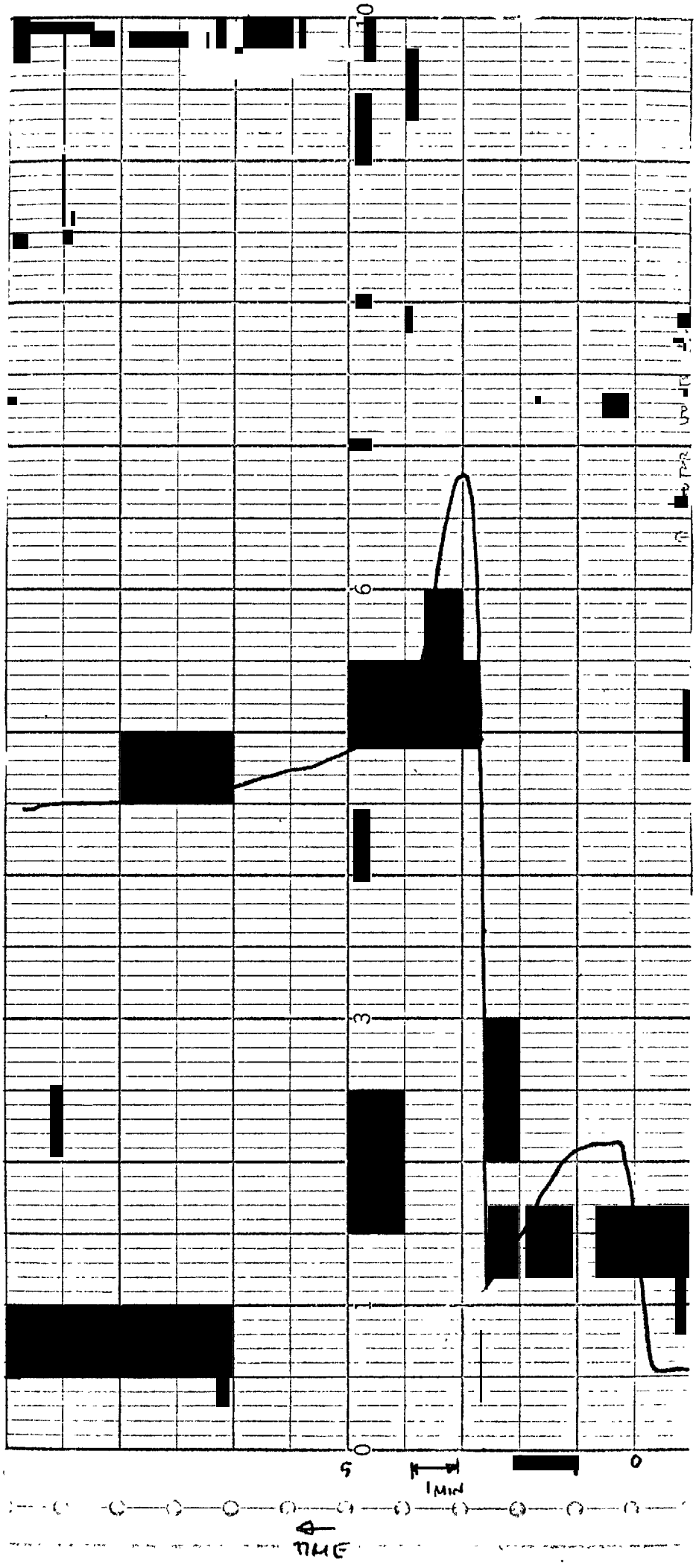


FIG3-10

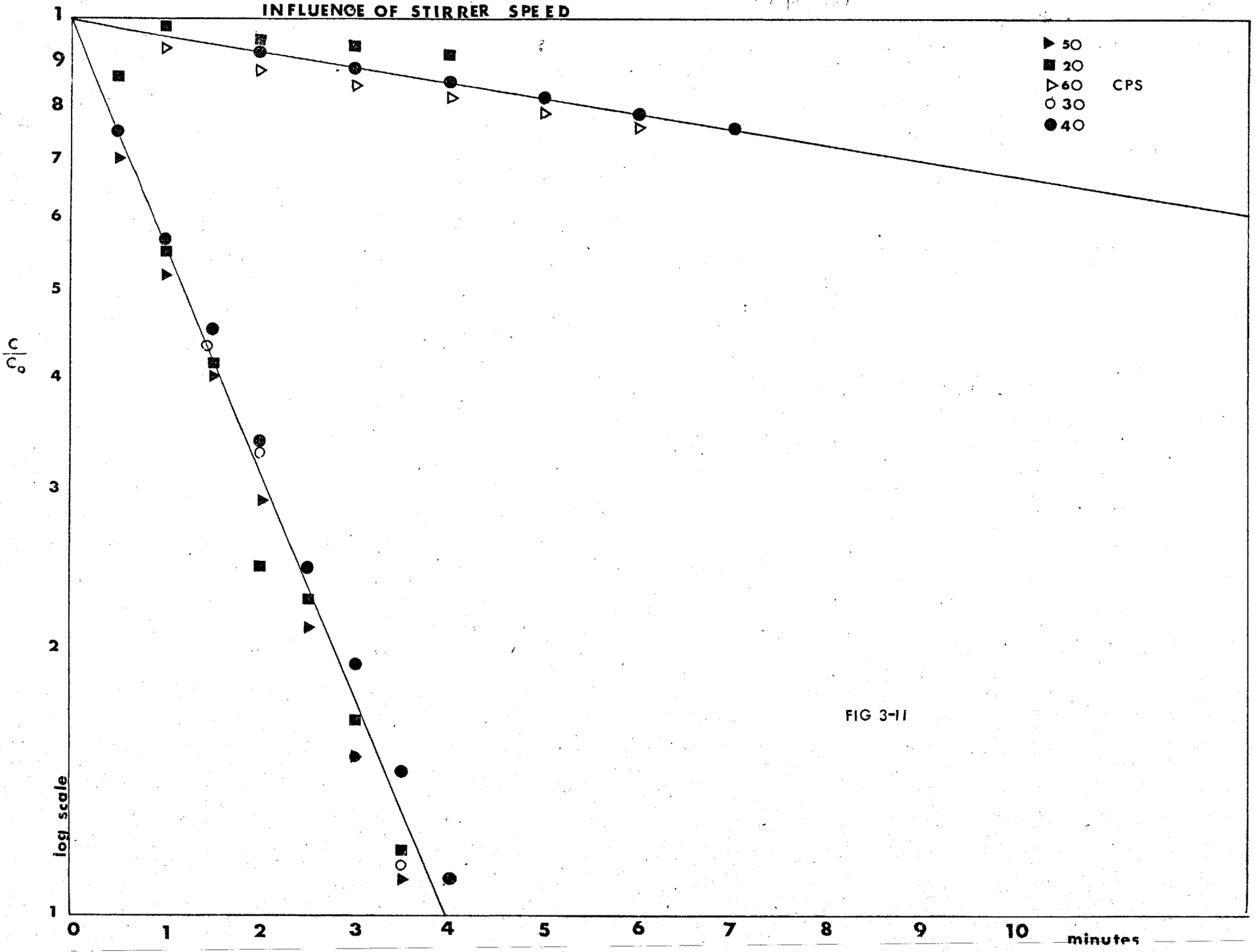

INFLUENCE OF STIRRER SPEED
50
20
60
30
40
CPS
C/Co
log scale
1
9
8
7
6
5
4
3
2
1
0
1
2
3
4
5
6
7
8
9
10
minutes

FIG 3-11

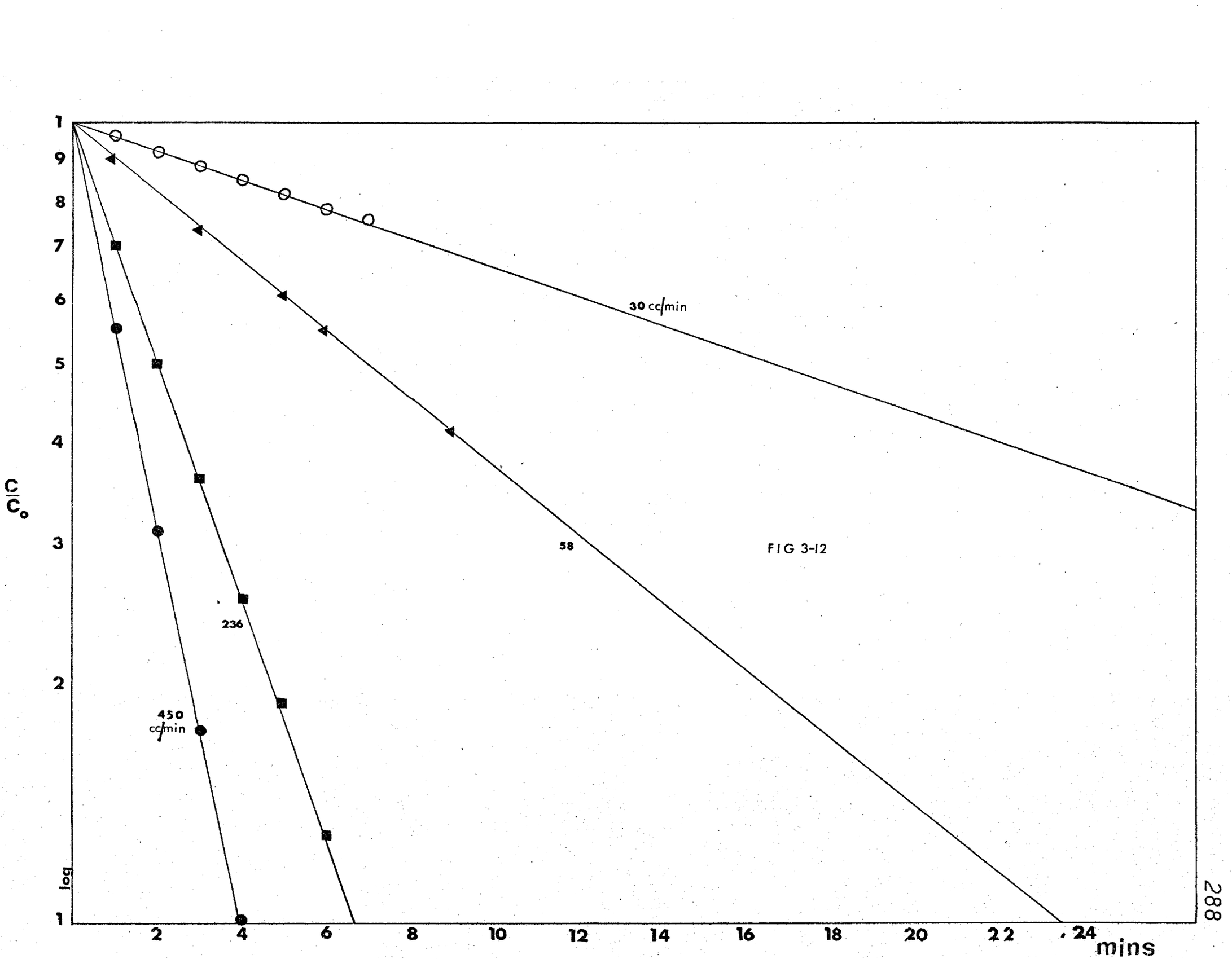

1
9
8
7
6
5
4
3
2
1
log
C/Co
30 cc/min
58
236
450 cc/min
2
4
6
8
10
12
14
16
18
20
22
24
mins

FIG 3-12

TEST 1

DIRECT METHOD

Measured Flowrate = 450 cc/min.

Cross sectional area of flow (Fig.3.) = 4.5 cms^2

$\therefore$ Mean velocity = $\frac{450}{4.5} \times 60$ = 1.67 cm/sec.

DILUTION METHOD

From Fig.3.12

$\log_{10} (c/co)/t = \frac{1}{4}$

$\therefore \log_e (c/co)/t = \frac{1}{4} \times 1/_{0.4346} \times {}^{1}/_{60}$

$= 0.0095$

substituting in Eq.3.

$V = \frac{\pi dh}{8e} \log_e (c/co)/t$

$= \frac{\pi \times 3.8 \times 15}{8 \times 0.125} \times 0.0095$

= 1.7 cm/sec.

The results are tabulated as follows:

	Direct Method	Dilution Method
	1.67 cm/sec.	1.7 cm/sec.
Seepage	0.875 "	1.04 "
Velocity	0.216 "	0.285 "
	0.110 "	0.130 "

FIELD EQUIPMENT

The encouraging laboratory results and the ease of operation of the equipment lead to the design of a field probe which was constructed for use in Altwen Quarry. Unfortunately the shortage of time did not permit extensive use of the dilution probe in the field.

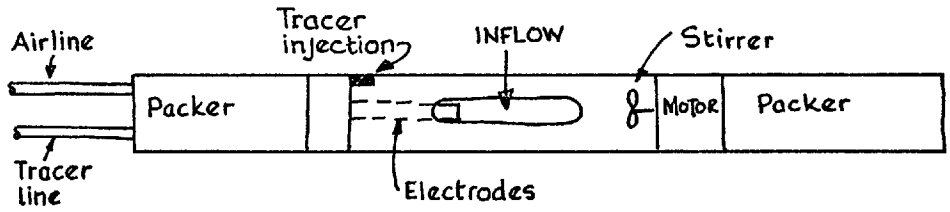


FIG 3.13

Fig.3.13 illustrates the dilution probe with packers at either end. The packers can be pneumatically inflated in the borehole to isolate the probe at any given depth in the borehole. A known volume of tracer solution is injected as a pulse from groundlevel via the tracer line. A magnetically driven stirrer is switched on and it mixes the injected tracer, i.e. salt solution or HCl, within the volume defined by the inflated packers. The probe is directly linked to a Wayne Kerr Bridge (described in section 3.2.0) and the output is in the form of a chart record.

As water flows into the confined volume the concentration of the "mixed" solution decreases with time. By using Equation 3.20 and the above information it is possible to determine the seepage velocity. The fully automated nature of the instrumentation makes the experiments very easy to carry out. The spacing between the packers can be varied to change the dilution volume so as to accommodate a large variety of problems. The probe was checked in the laboratory for construction and electrical stability in a glass tube and it performed extremely well. The signals from the electrodes to the bridge via 100ft. of cable were exceedingly stable. The magnetic stirrer mixed volumes up to 6ft. main cavity length with great ease.

This test was performed in the glass tube and instead of injecting HCl or salt solution, a solution of potassium per manganate was added. The stirrer caused enough disturbance to mix the solution within a few seconds.

It is porposed that for the field evaluation of permeability exactly the same equations and deductions are applied as in the experimental verification of the method (Section 3.2.0), due account being made for the number of fissures.

CONCLUSIONS

Although the probe has not been tested in the field at the time of writing this thesis the theoretical and laboratory evaluation of the method proves beyond any doubt its usefulness. Further its highly successful use in the field of continua by Moser (11) and Ogilvy (63) and in fracture media by Lewis et al (48) proves beyond doubt that the method is not only being used in practice; but that it has a very useful application in fluid flow through fissured rock masses.

This method has an outstanding advantage over pumping tests; that is very little equipment is required for field testing. The most important part of the equipment is a sensitive and accurate automatic bridge. In pumping tests the cost of testing is enormous due to (a) need to supply a large volume of water. This involves tanks, flexible piping etc., (b) cost of buying, running and maintenance of pumps, (c) personel involved at a minimum of two people, one to carry out the test and the other to look after the pumps and water supply.

The technical advantages of the dilution method are that (a) the natural hydrohynamic field is not disturbed,(b) no errors due to excess pressure causing deformation of fissures, turbulence, etc., (c) no assumptions have to be made regarding the extent of the fissure system, i.e. whether the test is being carried out in an infinite medium or a bounded reservoir, (d) no need to either estimate the pressure at a given distance during a test or the need for another borehole to measure this pressure change.

However, there are two clear disadvantages of the method:
(a) Tests can only be carried out below the groundwater level and provided there already exists natural groundwater seepage.
(b) Prior knowledge of the natural gradient is required for permeability determination.

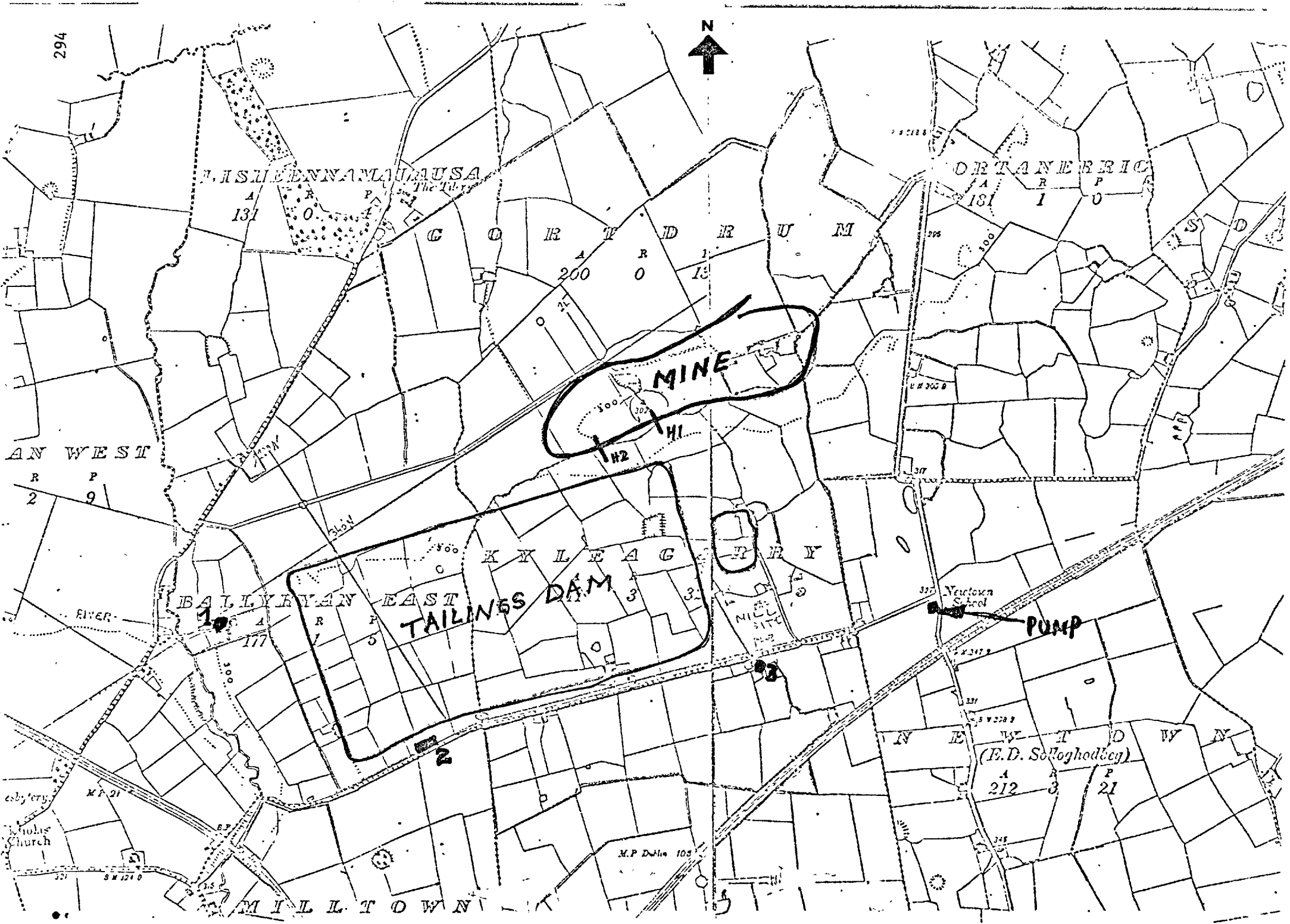
There is obviously further need for testing the dilution method in the field; but there is no reason why it should not be used for commercial application in determining seepage volumes and evaluation of permeability.

CHAPTER 4

GEOCHEMICAL ANALYSIS

SYNOPSIS

The chemistry of groundwater in conjunction with geology is a tool for hydrogeological studies for determining the zones and directions of flow. As groundwater flows through different rock types and soils the concentration of dissolved elements generally increases. By using a simple graphical technique it is possible to determine such movements. Two case studies illustrate the use of such a method for providing a reasonably quick insight into the flow patterns within a rock mass.


294
N
MINE
H1
H2
TAILINGS DAM
PUMP
1
2
3
Newtown School
(E.D. Softoghodbeg)
GORTADERRIC
GORTADERRIM
KILLEAGHY
BALLYKEAN EAST
BALLYKEAN WEST
MILLTOWN
RIVER
Church

INTRODUCTION

4.1.0 The method consists of collecting samples of water from a reasonable number of locations which can be identified on a map so that the appropriate geological sections can be studied for their chemical content. In general it is best to collect samples from areas where there is natural groundwater flow. Stagnant pools of water give rather inconsistent results because of local changes such as evaporation etc. Further the geochemical analysis yields better results in confined aquifers as opposed to unconfined aquifers because in the first case the fluid travels over a much greater distance and therefore has a much better chance of absorbing minerals. It is beyond the scope of this work to go into the chemistry of different rock and soil types. The interested reader is referred to (71-74).

4.1.1 SCHOELLER'S GRAPHICAL METHOD

Analysis of a large amount of data from many observation points can be bery tedious if care is not taken to present it adequately. After an examination of different methods it was decided that the Schoeller method (74) of graphical representation is by far the clearest. In this method semi logarithmic graph paper is used. On the logarithmic axis is plotted the concentration, in parts per million, of a given chemical. On the linear axis different elements are plotted and it is essential that the distance between the different elements is the same. The main advantages of the semi-logarithmic display are according to Schoeller:

(a) Values are absolute and not percentages
(b) It is possible to present a lot of data on one sheet
(c) It is easy to compare relative values of different elements i.e. the ratio of elements of a given type.
(d) On a lagarithmic scale if a straight line joins two points, i.e. elements A, B in one sample and is parallel to another line joining points A' B' (the same elements) in another sample the ratio of the elements A, B is unchanged in the two cases.
(e) In general flow from a lower to higher concentration gives the direction of movement of groundwater.

4.2.0 CASE STUDIES

4.2.1 Gortdrum Mine

Geochemical tests were carried out by the author at Gortdrum mine to assess the direction of groundwater flow in fissured sandstone and also to see if the Tailings Dam contributed anything to the aquifer. For reasons of economy and time only a few samples were taken for chemical analysis. Fig.4.1 is a plan view of the mine together with the tailings dam.

Hl and H2 refer to horizontal drill holes at the bottom of the mine which were installed as a dewatering measure. Fig.4.2 is a section showing how leakage from the tailings dam could possibly enter the sandstone aquifer.

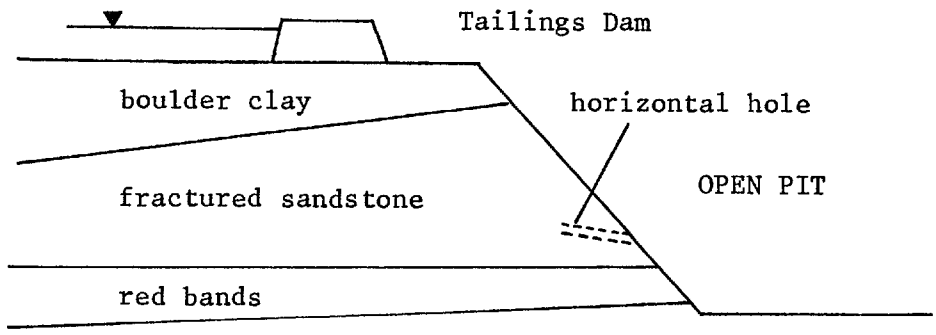


FIG 4.2

The geochemical analysis were carried out to supplement the piezometer investigation carried out by Sharp (75) to see if there was any connection between the tailings dam and the sandstone aquifer. Samples were taken from the tailings dam, the horizontal drains in the mine and the school pump. A Schoeller diagram of the values is presented in Fig.4.3. It is immediately apparent from Fig.4.3 that the sample from the slimes dam not only shows different absolute values; but also the ratios indicate that the samples are essentially different. The conclusion that the slimes dam did not contribute to the aquifer agreed with the piezometric observation made by Sharp (75). The remaining three samples however, indicate the same shape with relatively close absolute values. It is interesting to note that the absolute value of mineral content increases and so does the ratio Mg/Na from the school pump to the horizontal drains suggesting a flow in the aquifer from South to North.

Conductivity values of samples were taken at the mine at different locations and some of the values were as follows:

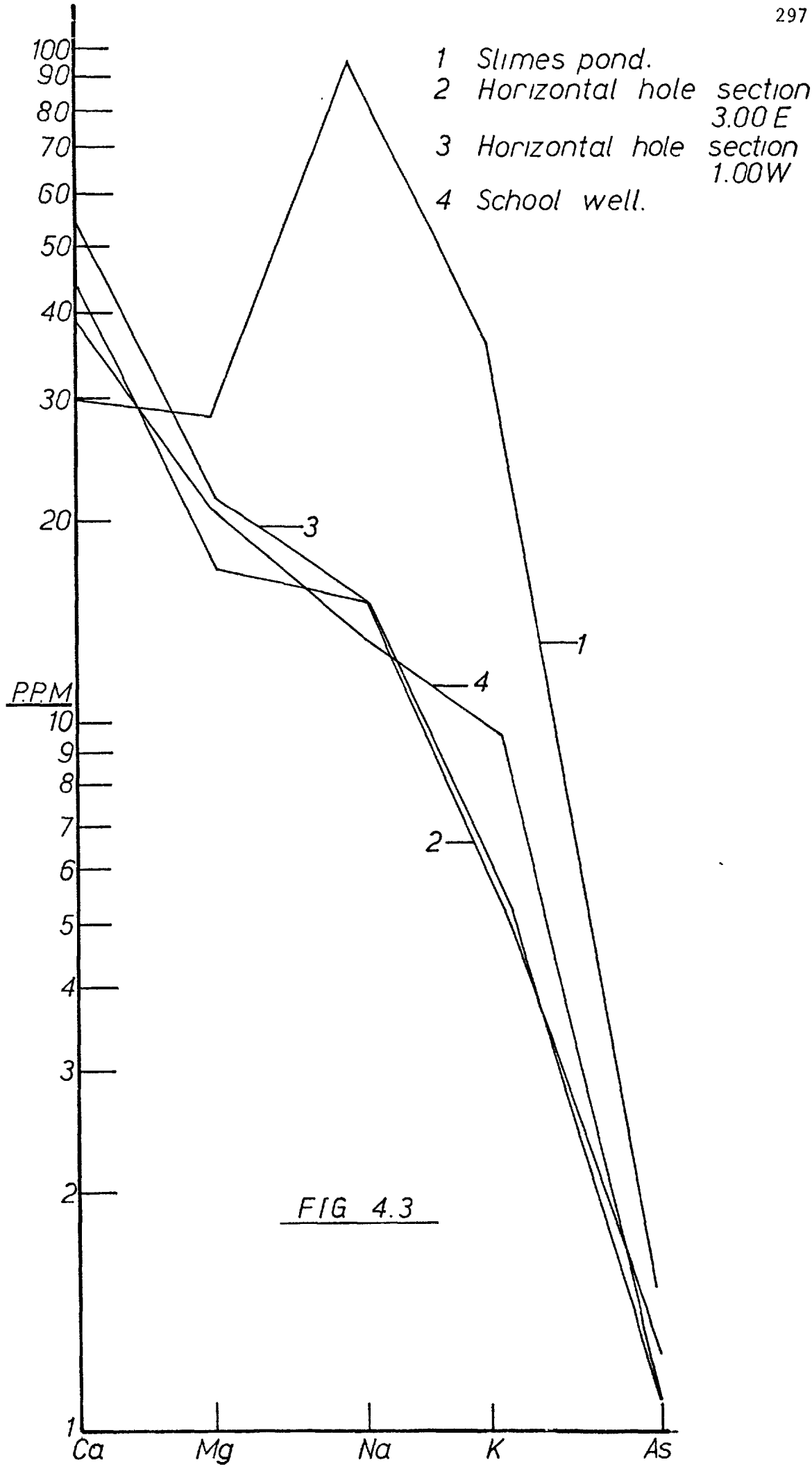

1 Slimes pond.
2 Horizontal hole section 3.00 E
3 Horizontal hole section 1.00W
4 School well.
100
90
80
70
60
50
40
30
20
PPM
10
9
8
7
6
5
4
3
2
1
Ca
Mg
Na
K
As

FIG 4.3

TABLE 1

School Well	355.4
Point 1	241.5
River Gate	298.4
Horizontal Drain 1	380.6
Horizontal Drain 2	343.6
Puddle at bottom of pit	425.0

The above table indicates that the conductivity of water has increased from South to North. This could be due to the increase in the mineral content (Fig.4.3) of water as it flows South-North.

4.2.2 SCAMMONDEN DAM

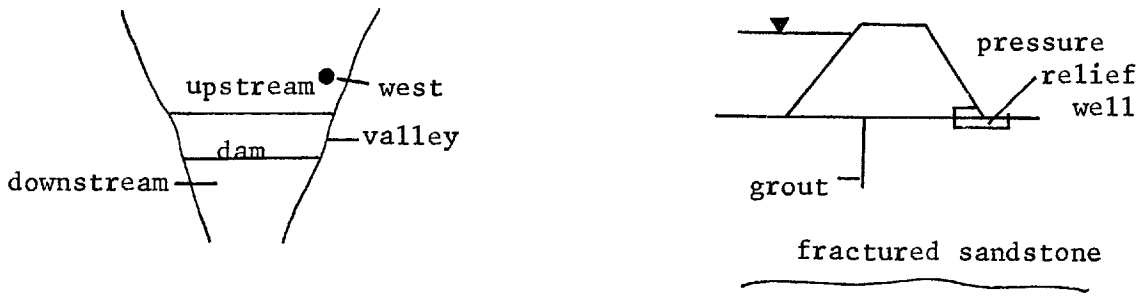


FIG 4.4

Fig.4.4 is a very simplified diagram of the dam site where samples were taken for the purpose of geochemical analysis. The output at the pressure relief well by far exceeds the expected value and it was proposed that this excess amount of water could come from the fractured sandstone, rather than the drainage system.

A sample of water was taken upstream of the dam and another from the pressure relief well. Fig.4.5 is a Schoeller diagram of the various elements from the two samples. There is a great deal of similarity in the two diagrams indicating that there is very little difference in absolute values of chemicals or alternatively, a change in the ratio of the elements and thus the two samples could belong to the same system.

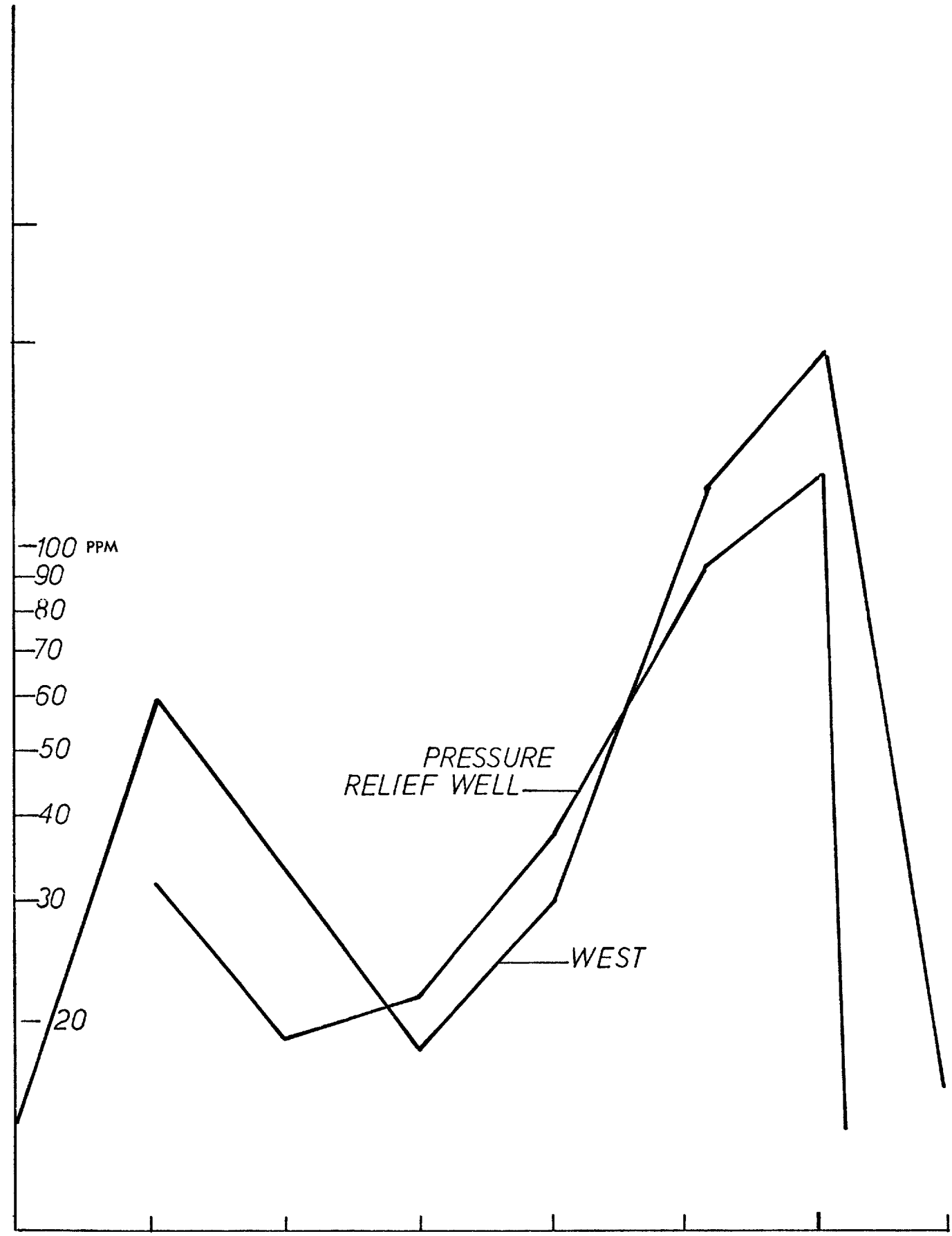

100 PPM
90
80
70
60
50
40
30
20
PRESSURE
RELIEF WELL
WEST
CO3
Ca
Mg
Na
Cl
SO4
HCO3
NO3

FIG 4.5

If water was to flow through the grout curtain a much higher value of Ca and HCO3 would be expected due to contamination and long transit time. Such a simple test although not conclusive gives a good idea as to areas where concentrated investigations should be made.

CONCLUSIONS

The purpose of this chapter is not to give a detailed explanation of how geochemical analysis ought to be carried out but to present two very brief but self instructive case histories. These two simple studies have shown how a simple test if correctly executed and analyzed can give insight into areas where further investigations should be carried out to determine in-situ hydraulic parameters. A great number of geochemical tests ought to be carried out in conjunction with inert tracer tests and/or pumping tests to assess the amount of confidence that can be placed in such methods.

FLUOROMETRY

SYNOPSIS

A lack of sensitive, accurate and easy to use tracing techniques lead to the development of fluorometric techniques. If the above criteria are not satisfied tracing becomes qualitative, subjective and cumbersome. After examining a multitude of tracing techniques and commercially available equipment it was decided to develop a field technique which would satisfy all the requirements specified in Chapter 1. In this chapter the phenomenon of fluoresence is explained prior to a discussion of the technique and construction of the tracing equipment. The final product of the research programme on tracing was a borehole device which could continuously monitor the presence of fluoresence and display the signal via a chart recorder. The borehole fluorimeter is capable of picking up 1 part in 100 million of fluoresin in clear water, or alternatively 1 gallon of 20% solution by weight in water can contaminate 100 million gallons of clear water.

This high degree of sensitivity permits a very sophisticated way of tracers to study groundwater seepage. Laboratory results of the calibration of the instrument for different fluorescent dyes are presented together with results of the field application.

5.1.0 INTRODUCTION

The use of fluorescein as a dye has been attempted by innumerable workers in the field of geohydrology. A large majority of this work has been of a qualitative nature where the detection of the dye has been with the naked eye. Very little data is available on quantitative measurements and what there is is usually based on discrete sampling where samples of water are taken to the laboratory for examination. The complex nature of fluid flow through fissured rock masses makes the qualatative approach not even worth attempting because prior to a test, little or nothing is known about the whereabouts of the feneral direction and velocity of flow. For example, in fissured rock the seepage velocity is very much higher than in a soil mass so the discharge of the dye could occur at some point away from the point of injection well before the observer has time to reach it. Further the detection of a dye with the naked eye is so subjective that it is liable to error unless vast amounts of traces are used to contaminate the flow system.

5.1.1 WHAT IS FLUORESCENCE

A brightly coloured dye is plainly obvious because it selectively absorbs light. A fluorescent material, however, upon absorbing light instantly emits light at a different wavelength. The emitted light is of a longer wavelength than the absorbed light. A material which absorbs ultra violet may emit a longer wavelength ultraviolet, blue, green, yellow or red light. Hercules (54) defines the process of fluorescence more rigorously as consisting of photon absorption by a molecule to go to an excited singlet state, relaxation from higher vibrational levels of that state to its lowest vibrational level, photon emission to a vibrationally excited level of the ground state, and again relaxation of the molecule to the lowest vibrational level of the ground state.

5.1.2 COMMONLY AVAILABLE DYES

A vast number of dyes exist which are used for tracing. Each dye has special properties (57) and therefore it is suggested that careful attention is paid to the selection of a dye in a given environment.

(a) Fluorecein: This is the most commonly available dye and is detectable at fairly low concentrations. According to Feuerstein and Selleck (55) it is the least ansorbed by sediment. Its properties do not vary significantly with temperature. At low levels toxicity is negligible and the dye is inexpensive. A serious disadvantage of this dye is that it decays rapidly in ordinary daylight.

(b) Rhodamin B: This dye is commonly available although slightly more expensive than Fluorescein. It is a dye which is used in hydrogeological studies (56) because it is fairly independent of pH value and also is not seriously affected during its passage through limestone or clay type materials. Further it does not decay in daylight.

(c) Rhodamin (WT): This dye is only available through Du Pont. It is claimed to be much more resillient than Rhodamin B in as far as absorption is concerned. Of the three dyes (a) - (c) tested in the laboratory for the properties already mentioned, Rhodamin (WT) gave the highest fluorescent emission and generally proved to be the best dye. Unfortunately, it is more expensive than (a) and (b).

5.2.0 BOREHOLE FLUOROMETER

An instrument for detecting and measuring fluorescence is called a fluorometer. The instrument was designed to fulfill the following specifications with a view to its use in geohydrological problems.

(a) The instrument should be such that it can be used in-situ in the field. This limits the instrument in terms of size for portability. Since a large amount of information on underground flow is accessable only in terms of communication through a borehole, a device that would go down such a cavity would be essential. Most exploratory holes in Mining & Civil Engineering are three inches in diameter therefore it was decided to build an instrument which could easily slide into a borehole that size.

(b) In view of the complex nature of seepage flow and unknown flow velocities it was decided to build an instrument which could be placed in a flow system and allowed to register automatically with the tracer concentration via a chart recorder. The main advantage being that a continuous record of the tracer concentration could be kept from the time of injection of the tracer. By integrating the curve under the concentration-time curve it is possible to calculate the percentage recovery of the tracer. In an anisotropic system the direction of flow is not parallel to the direction of the hydraulic gradient and therefore the seepage velocity can be grossly inaccurate if it is based on the transit time of a tracer front from one well to another without due regard to the anisotropy.

(c) The sensitivity and accuracy of the instrument should be such that it can detect minute quantities. If the instrument can measure quantities in the range of 1 part per 100 million tracing becomes an economic proposition. Vast aquifers can be thus contaminated; but not in such a way that the introduction of the dye can become a pollution hazard.

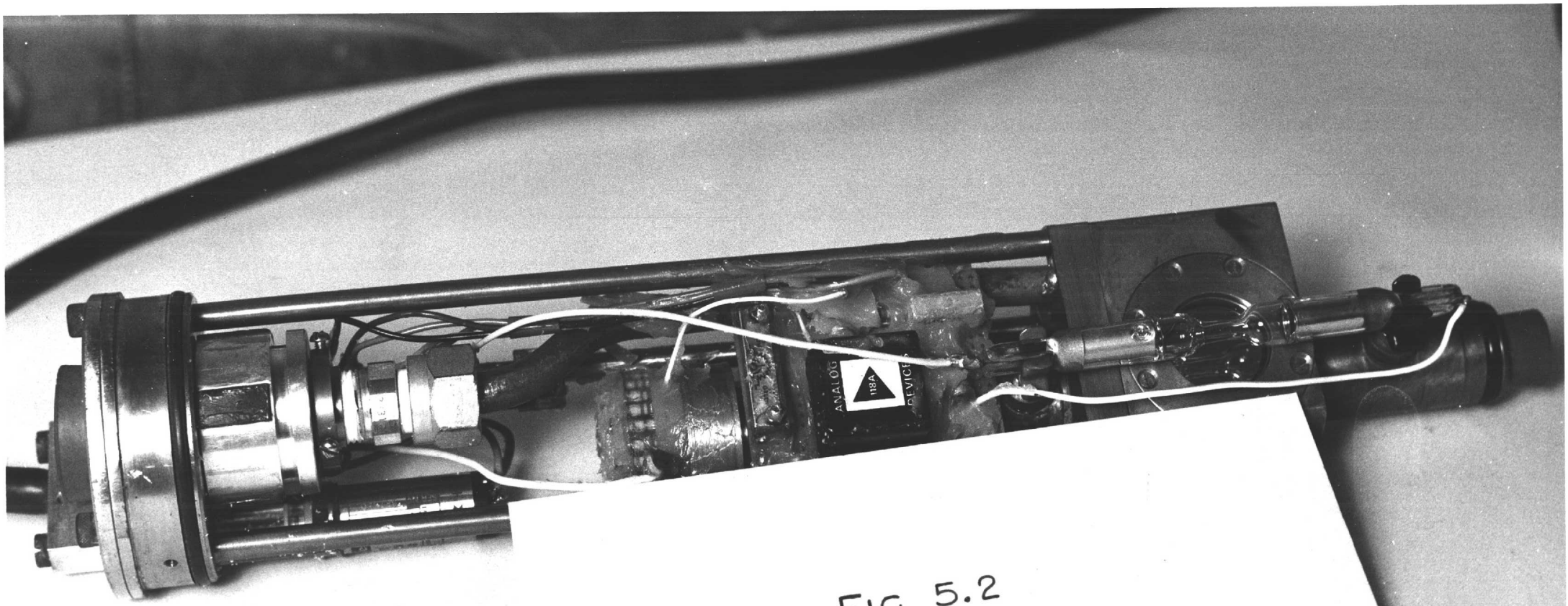


FIG 5.2

(d) The instrument should be such that it should be rugged. However, a combination of sensitivity, accuracy, portability and ruggedness is extremely difficult and this constituted a major part of the effort into the design of such a device.

(e) The tracers to be used are cheap and easily obtainable.

(f) There is little or no pollution hazard.

(g) The cost of the instrument within the scale of the Mining and Civil Engineering Industry.

5.2.1 ESSENTIAL CONCEPT OF THE BOREHOLE FLUORIMETER

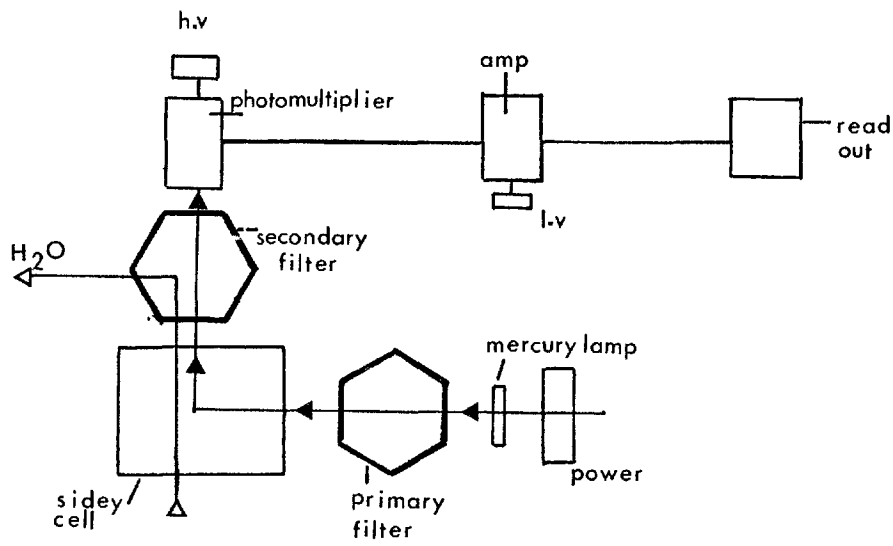


FIG 5-1

Fig.5.1 is a schematic diagram of the instrument. A low pressure mercury lamp provides the ultraviolet radiation required to cause fluorescence. The radiation passes through a primary filter (which maximises the excitation wavelength) into the sample cell which is continuously fed with "tagged water". The wavelength of the incident light is such that it causes fluorescence of the dye. The emission signal is passed through a secondary filter which maximises the emission wavelength and finally the signal is picked up by a photo-multiplier where the radiation is converted into an electrical voltage which is amplified and finally the output is displayed in digital or graphical form.

(A) Low pressure mercury lamp

This lamp was chosen for two reasons: (i) the majority of the output of the lamp was concentrated in the region of 253.1mm mercury line, (ii) the size of the lamp was small and it required a low voltage supply.

(B) Sample Cell

The errors caused by the sample cell can be enormous and are fully discussed by Hercules (54). The windows of the cell have to be such that they do not emit eluorescence. After extensive tests fused quartz windows were decided on and they had to be specially cut and polished for this particular application. The inside of the cell was painted matt black very carefully so as to avoid any internal reflections, so that the emission monochromator only sees the fluorescence and not the reflections off the walls. The right-angle bend design is used so that the emission monochrometer does not see the input source directly, since filters are never 100% efficient.

(c) Filters:

To a large degree the success of the system depends on the choice and efficiency of the filters. If possible absolutely no visible light should be allowed to enter the sample cell because this could easily be mistaken by the photomultiplier to be the fluorescence signal. Interference filters are about the best way of transmitting a narrow part of the waveband. The transmission efficiency of the particular filter used was 25% at 254mm. but not greater than 0.1% on the visible range. The secondary filter, an interference type maximised at 584mm. with a high degree of efficiency. The filter for this application has to be specially made owing to the constraints provided by the size of the instrument. These filters were chosen for Rhodamin (WT) as a tracer.

(d) Photomultiplier

A nine stage photomultiplier was chosen for its size of spectral response that would be encountered with Rhodamin and Fluorescence. The photomultiplier did however, require an expensive stable high voltage supply.

Further details of the equipment and design of electronic components is provided in the appendix. Also included are detail characteristics of the system without a tracer, e.g. electrical response to clear water, etc.

5.2.2 OPERATION OF THE BOREHOLE FLUOROMETER

Fig.5.2. is a close-up photograph of the inside of the Fluorometer. Water is sucked into the input end by a turbine pump, pushed into the sample and out through the top of the instrument. The instrument can be lowered on the reinforced cable into a borehole, lake, reservoir etc. The only requirement is that the instrument is well shielded from daylight as it would be if it were down a hole. A tracer such as Rhodamin is injected upstream of the instrument and monitoring begins as the controls are switched on. Fig.5.3.

5.2.3 LABORATORY TESTS

Laboratory tests were carried out on the probe prior to the use of tracers. This was done to assess the effectiveness of the sample cell in terms of being light proof and also the efficiency of the secondary filter was tested. The main advantage of a good light seal is that the photomultiplier can be used at maximum sensitivity without overloading it. This can be seen in Fig.5.3 where BH represents the output from the photomultiplier for a range of accelerating voltage for the case of clear water.

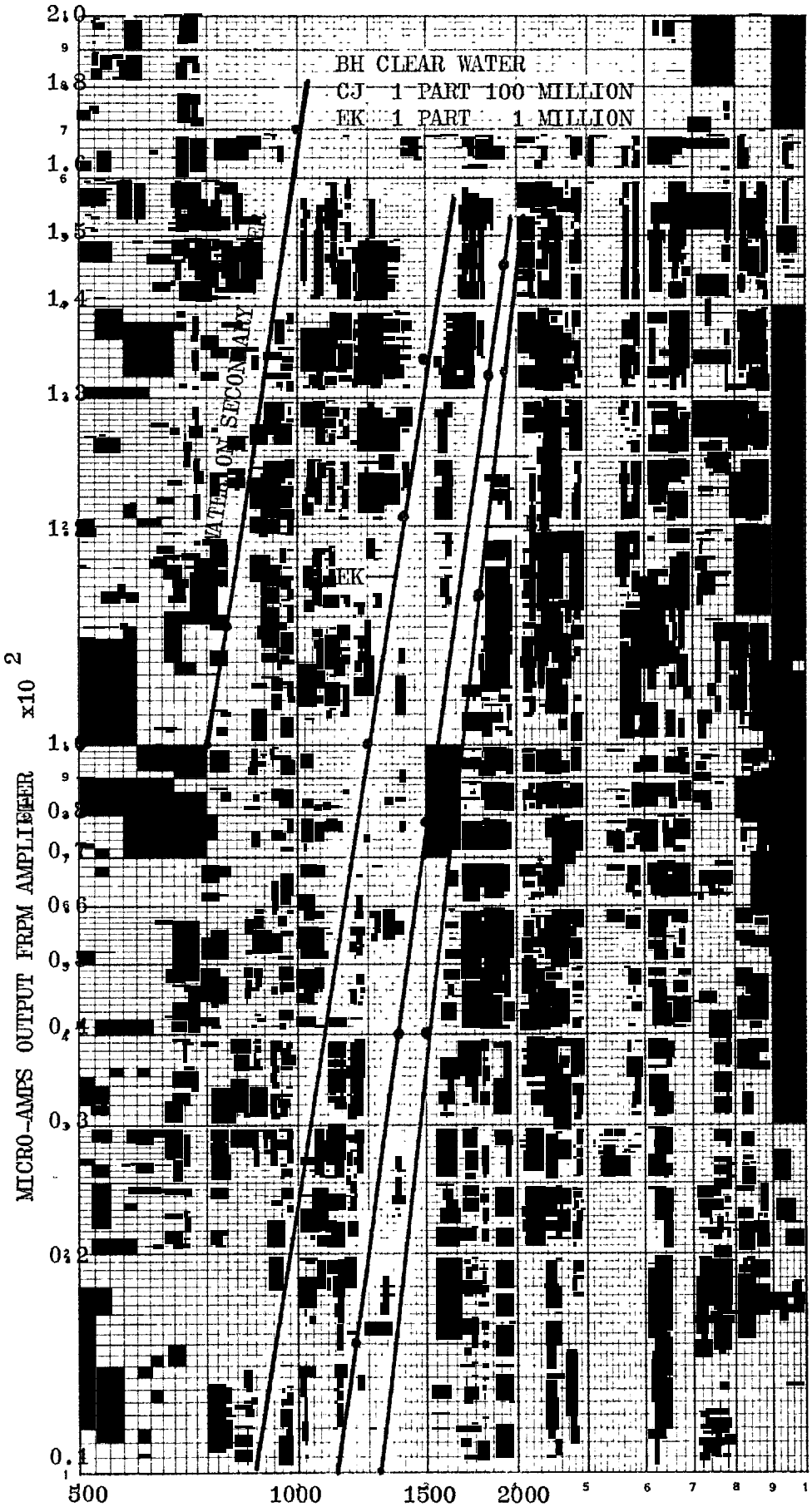


FIG 5.3

Log 2 Cycles x Cycle
Graph Data Ref. 921
WELL

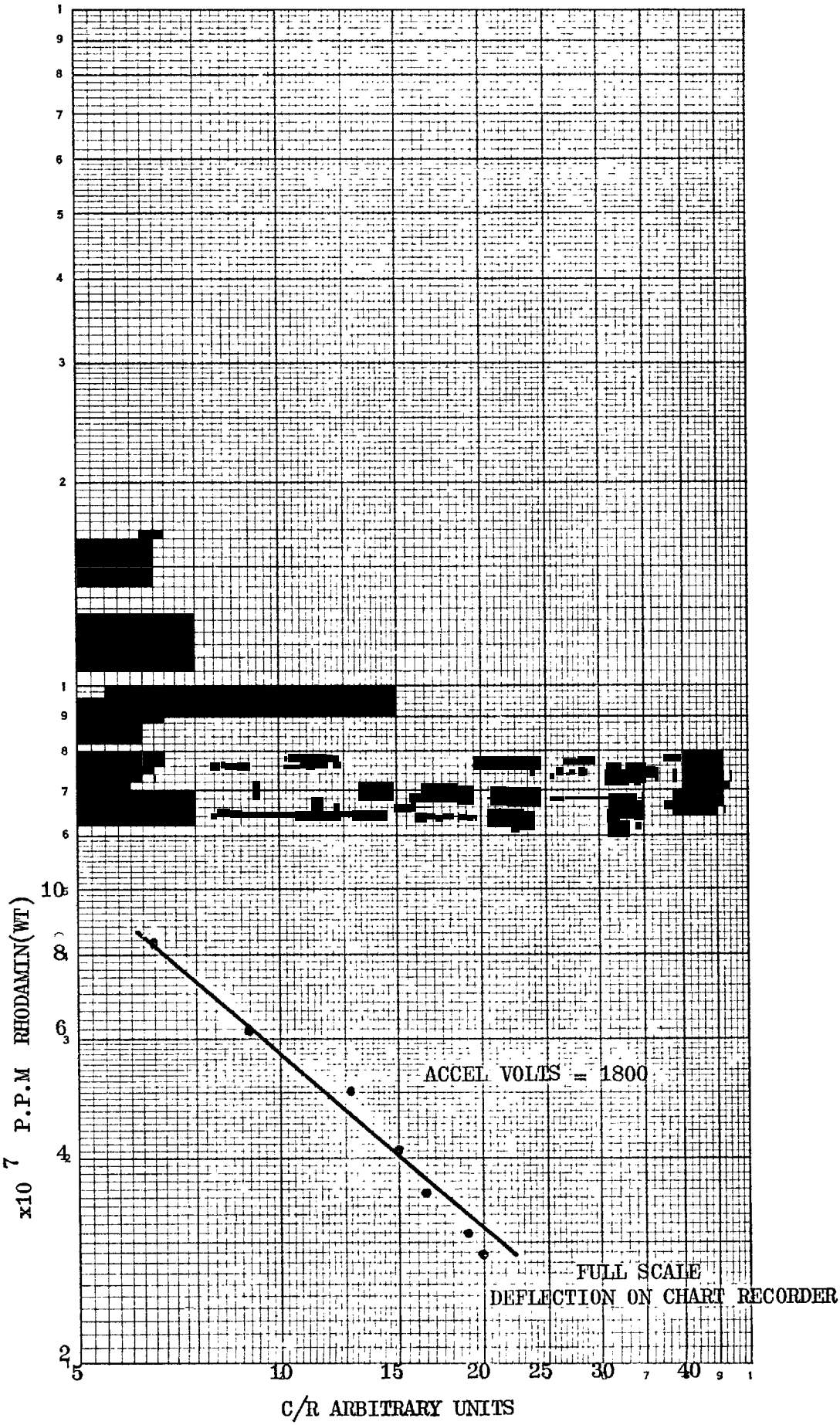


FIG 5.4

Log 2 Cycles x 1 Cycle
WELL Graph Data Ref. 5921

An output of 0.1 A at an accelerating voltage of 1300 volts indicating that the photomultiplier is being used at its peak sensitivity. Without the secondary filter the signal at low concentrations was very unstable and liable to drift with time. This drift could be association with the unstable light from the mercury lamp. However, the use of a secondary filter eliminated all the problems giving a clear set of points for a tracer concentration of 1 part in 100 million as indicated in Fig.5.3.

A large number of carefully controlled solutions were made with Rhodamin (WT) so that a calibration curve of the amplifier output could be made with concentration of the tracer in water. Fig.5.4. shows such a calibration for a 20% layout solution of Rhodamin. It is clear from the diagram that the instrument is very sensitive in picking up small changes in the tracer concentration and that the results are relatively free of drift.

5.3.0 FIELD TRIALS

Preliminary trials were carried out in Altwen to test the fluorometer under field conditions. In Chapter 2 the location of the boreholes is described in detail. Rhodamin (WT) was introduced into the inclined hole (Hole C) which is upstream of the vertical hole (Hole A). The borehole fluorometer was lowered down hole A and switched on prior to tracer injection so that it could settle down to a steady state. In the preliminary trials it was proposed that only the transit time of the tracer front from the time of injection to pickup would be used to calculate seepage velocity. This assumes that the tracer does not disperse and travels as a plug. As the Rhodamin (WT) solution was injected into the inclined hole the chart recorder was switched on. Fig.5.5. is an example of an early signal in three different tests prior to the dye entering the fluorometer. Fig.5.6 indicates the arrival of the tracer at the vertical hole.

Natural gradient from the inclined hole to the vertical hole=J=$^1/_{20}$

Transit time for dye
from inclined hole to vertical hole = 80 minutes.

$\therefore$ Seepage velocity assuming zero dispersion $= \frac{300 \times 12 \times 2.54}{80 \times 60} = 1.9$ cm/sec.

Assuming Darcy for low gradients
$V = K_J J$

V = seepage velocity

K_J= joint conductivity

$\therefore \quad \frac{1.9}{1/20} = 38$ cm/sec.

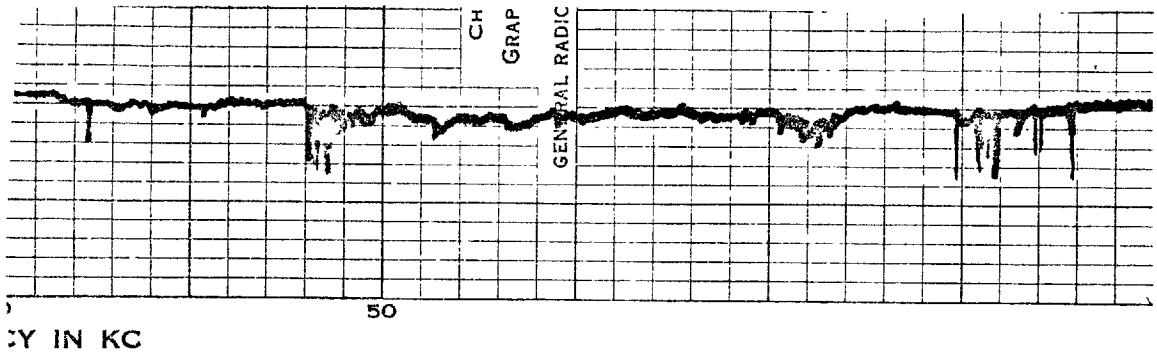


FIG 5-5

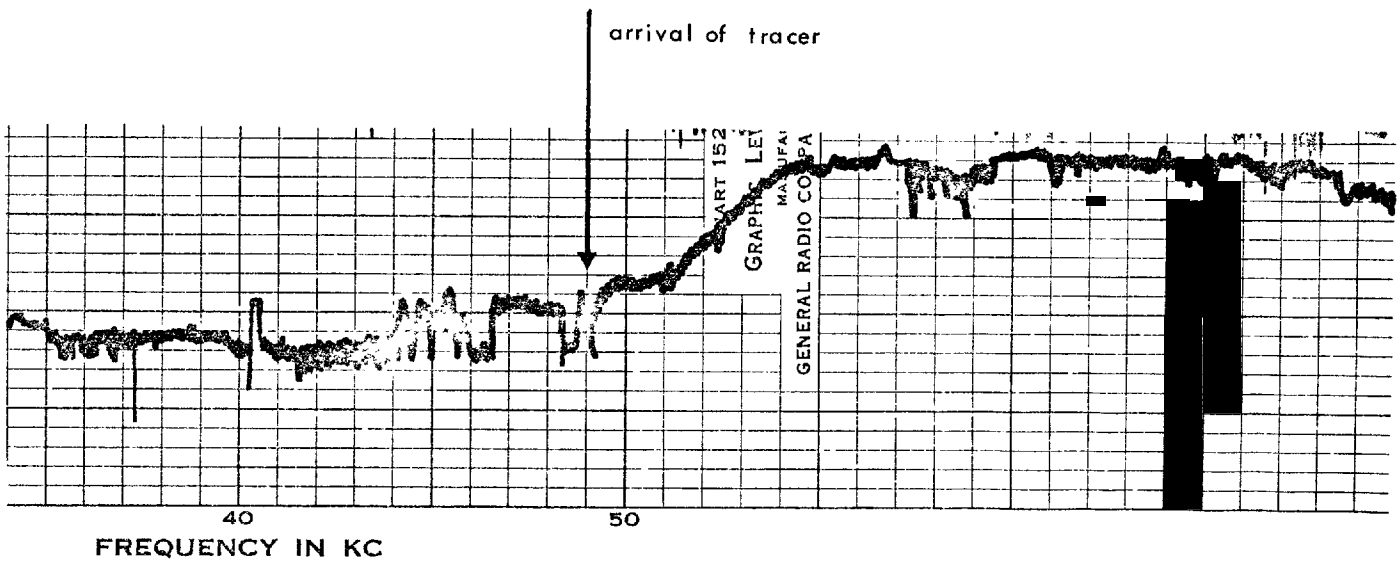


FIG 5-6

Assuming a parallel plate analogy for the horizontal bedding fractures

$$K_J = \frac{e^2 g}{12U}$$

the aperture of the fissure

$e = 0.74 \times 10^{-1}$ cm.

From pumping test data for the bottom section of the hole the value of eK_J to nearest order of magnitude =

10^{-2} $cm^2/sec.$

$\therefore$ $e = 5.2 \times 10^{-2}$ cm.

the two values are within the same order of magnitude indicating the test to be successful.

REFERENCES

REFERENCES

1 DUPUIT,J — Etudes theoriques et pratiques sur le movement des eaux dans les canaux decouverts et a transvers les terrains permeable. PARIS,DUNOD,1ST.ED.1848.

2 DARCY — Les fontaines publiques de la ville de Dijon. PARIS,DALMONT.

3 BOUSSINESQ — Essai sur la theorie de eaux courantes. MEMOIRES PRESENTE PAR DIVERS SAVANT A L'ACADEMIE DE SCIENCES,PARIS,VOL.23, P1-680.

4 IRMAY — Flow of liquids through cracked media. BULL.RES.COUN.ISRAEL,5A.NOL.JERUSALEM, P84.

5 BAKER — Flow in fissured formations. PROC.4TH PETROLEUM CONGRESS,ROME,1955.

6 POLUBARINORA KOCHINA — Theory of groundwater movement. UNIV.PRINCETON PRESS,1962.

7 SNOW — A parallel plate model of permeable fractured media. PH.D.THESIS.UNIV.CALIFORNIA,BERKELY, 1965.

8 LOUIS — A study of groundwater flow in jointed rock and its influence on the stability of rock masses. DOCTORAL THESIS.UNIV.KARLSRUHE,ENGLISH TRANS.IMPERIAL COLLEGE 1970.

9 SHARP — Fluid dlow through fissured media. PH.D.THESIS,IMPERIAL COLLEGE,LONDON UNIV.1970.

10 LOUIS MAINI — The determination of hydraulic parameters in jointed rock. ISRM.2ND SYMP.BELGRADE,1970.

11 MOSER — Borehole dilution method of measuring groundwater filtration velocity. INSTITUT FUR RADIOHYDROMETRIE,MUNICH, GSF-BERICHT R16. 1968.

12 CHILDS — The physical basis of soil water phenomena. WILEY INTERSCIENCE.

13 TROLLOPE, STARK, VOLKER — Complex flow through porous media. Research Bulletin No.C2. DEPT.OF ENGNG.UNIV.OF TOWNSVILLE,AUSTRALIA, MAY,1970.

14 BERNAIX — New laboratory methods of studying the mechanical properties of rocks. INT.J.ROCK MECH.MIN.SCI.VOL.6,N1,1969.

15 SNOW — Three-hole pressure test for anisotropic foundation permeability. FELMECHANIK UND INGENIEURGEOLOGIE,VOL.4, 1966.

16 FREEZE, WITHERSPOON — Theoretical analysis of regional groundwater flow. WATER RESOURCES RESEARCH,VOL.2,N4,FOURTH QUARTER,1966.

17 SOUTHWELL — Relaxation methods in theoretical physics. OXFORD UNIV.PRESS,248P,1966.

18 ZIENKIEWICZ — Solution of anisotropic seepage by finite elements. J.ASCE.FEB.1966.

19 STARK, VOLKER — Non linear flow through porous media, some theoretical aspects. R.B.NO.1.UNIV.TOWNSVILLE,AUSTRALIA,1967.

20 ASTM — Permeability and capillarity of soils. AMER.SOC.FOR TESTING MATERIALS.

21 NONVEILLER — Grouted cut off curtains in fissured rocks. ISRM 2ND SYMP.BELGRADE,1970.

22 TROTTER — The structure of the coal measures in the Pontardawe Ammanford area, South Wales. Q.J.G.S.NO.410,FEB.1947.

23 TERZAGIHL — Sources of error in joint surveys. GEOTECHNIQUE ICE.LONDON,VOL.15,1965.

24 PRICE — Fault and joint development in brittle and semibrittle rock. OXFORD,PERGAMON,1966.

25 TRAINER, EDDY — A periscope for the study of borehole walls and its use in groundwater studies in Niagara County, New York. U.S.G.S.PROF.PAPER 501D,1964.

26 TATE, ROBERTSON, GRAY — The hydrogeological investigation of fissure flow by borehole logging techniques. Q.J.ENG.GEO.VOL.2,1970.

27 KAZEMI — Pressure transient analysis of naturally fractured reservoirs with uniform distribution. S.P.E.JOURNAL,DEC.1969.

28 PICKETT, REYNOLDS — Evaluation of fractured reservoirs. S.P.E.JOURNAL,MARCH,1969.

29 IRMAY — Physical principles of water percolation and seepage. UNESCO PUBLICATION.

30 VAN POLLEN — Status of drill stem testing techniques and analysis. J.PET.TECH.APRIL,1961.

31 MCALISTER — A new system of tools for better control and interpretation of drill stem tests. J.PET.TECH.FEB.1965.

32 SABARLY — Les injections et drainages de pondation de barrages. GEOTECHNIQUE,18:229-249,1968.

33 SNOW — Fracture deformation and change of permeability and storage upon changes of fluid pressures. QUART.OF THE COLO.SCHOOL OF MINES,VOL. 63,NO.1,JAN.1968.

34 CUNDALL — The measurement and analysis of accelerations in rock slopes. PH.D.THESIS,IMPERIAL COLLEGE,LONDON,1971

35 BARTON — A model study of the behaviour of steep excavator slopes. PH.D.THESIS,IMPERIAL COLLEGE,LONDON,1971.

36 LOUIS — Hydraulic triple probe to determine the directional hydraulic conductivities of porous or jointed media. REPORT NO.D12,JUNE,1970,RM.PROJECT IMPERIAL COLLEGE,LONDON.

37 I.A.E.A. — Isotopes in hydrology. PROCEEDINGS OF A SYMP.IN VIENNA,1966, INTERNAT.ATOMIC ENERGY AGENCY.

38 CLAYTON SMITH — A comparison of radioisotope methods for river flow measurements, radioisotopes in hydrology. I.A.E.A.VIENNA,1964.

39 GRAY — Approximating well-to-fault distance from pressure build up tests. J.PET.TECH.JULY,1965.

40 POLLARD — Evaluation of acid treatments from pressure build up analysis. TRANS.AIME,1959,216.

41 WARREN ROOT — The behaviour of naturally fractured reservoirs. SOC.PET.ENG.J.SEPT.1963.

42 ODEH — Unsteady-state behaviour of naturally fractured reservoirs. SOC.PET.ENG.J.MARCH,1965.

43 SNOW — The frequency and apertures of fractures in rock. INTERNAT.J.ROCK MECH.MIN.SCI.VOL.7,JAN. 1970.

44 SERAFIM — Interstitial pressures on rock foundations of dams. J.OF SOILS AND FOUND.PROC.ASCE,SEPT.1965.

45 LOUIS — Hydraulic triple probe to determine the directional hydraulic conductivities of porous or jointed media. REPORT NO.D12,JUNE,1970,ROCK MECH.DEPT. IMPERIAL COLLEGE,LONDON.

46 MUSKAT — Flow of homogeneous fluids. EDWARDS 1937.

47 WEBSTER — Two-well tracer tests in fractured crystalline rock. USGS WATER SUPPLY,PAPER 1544-I.1970.

48 LEWIS KRIZ BURGY — Tracer dilution sampling technique to determine hydraulic conductivity of fractured rock. WATER RESOURCES RESEARCH,THIRD QUARTER,VOL.2, NO.3,1966.

49 STEPHENSON — Mathematical methods. LONGMANS.

50 RAMSAY — Folling and fracturing of rocks. MCGRAW HILL.

51 ZEMANEK CALDWELL — The borehole televiewer - a new logging concept for fracture location and other types of borehole inspection. J.PET.TECH.P72,1969.

52 TILBURN — Ph.d. Thesis in preparation. ROCK MECH.DEPT.IMPERIAL COLL.LONDON.

53 OGIL'VI FEDROVICH

54 HERCULES — Fluorescence and phosphorescence analysis 515. Principles and Applications. WILEY INTERSCIENCE,1966.

55 FEUERSTEIN SELLECK — Fluorescent tracers for dispersion measurements. J.SAN.ENG.DIV.ASCE 89,SA4:1-21,1963.

56 CONTE — Application of rhodamine B fluorescent dye to Davis Lake, REPORT TO OREGON STATE GAME COMMISSION, MAY 31ST,1961.

57 WATT — Development of the dye dilution method for measuring water yields from mountain watersheds. M.SC.THESIS,COLORADO STATE UNIV.FORT COLLINS,COLO.1965.

58 TERZAGHI — Stability of steep slopes on hard unweathered rock. GEOTECHNIQUE,VOL.12,NO.4,1962.

59 LONDE

ISRM,2ND SYMP.BELGRADE,1970.

60 HUITT — Fluid flow in simulated fractures. A.1.CH.E.JOURNAL,VOL.2,NO.2.

61 WILSON WITHERSPOON — An investigation of laminar flow in fractured porous rocks. PUBL.NO.70-6.DEPT.CIVIL ENNGN.UNIV.OF CALIFORNIA,BERKELY,1971.

62 LONDE — Recent developments in the design and construction of dams on deep aluvium, karst and other unfavourable formations. 1ST CONGRESS ON LARGE DAMS,1970.

63 AIHS-UNESCO — Hydrology of fractured rocks. PROC.OF THE DUBROVNIK SYMP.OCT.1965, IAHS-UNESCO.

64 WILKINSON — Fracturing in Spraberry reservoir, West Texas. BULL.AM.ASS.PET.GEOL.VOL.37,1953.

65 BIANCHI — Geology of the Manitou Springs, Cascade area, El Paso County with a study of the permeabilities of its crystalline rocks. MS.C.THESIS.COLORADO SCHOOL OF MINES, 1968.

66 FOOKES DENNESS — Observational studies on fissure patterns in cretaceous sediments of south east England. GEOTECHNIQUE,19,NO.4,1969.

67 RATS CHERNYASHOV — Statistical aspects of the problem on the permeability of the jointy rocks. AIHS-UNESCO SYMP.DUBROVNIK,1965.

68 FRANCIS — A textbook of fluid mechanics. EDWARD ARNOLL,1962.

69 BLAISDELL — Energy losses at pipe junctions. J.OF THE IRRIGATION AND DRAINAGE DIV. PROC.ASCE,SEPT.1967.

70 WITTKE — Three dimensional percolation of fissured rock. SLOPE STABILITY SYMP.JOHANNESBURG,1970.

71.CHARRON — Groundwater resources of Plum Conlee Area, Manitoba. GEOL.SURV.CAN.PAPER 60-22.

72.STIFF — The interpretation of Chemical Water Analysis by means of patterns. J.PETROL.TECH.VOL.3,OCT.

73.PIPER — A graphic procedure in the geochemical interpretation of water analysis. ANN.GEOPHYS.UNION TRANS.VOL.25.

74 SCHOELLER — Arid zone hydrology, recent developments. UNESCO. 1959.

75 SHARP — Personal communications.

76 ST. JOHN — Numerical and observational methods of determining the behaviour of rock slopes in open cast mines. PH.D. THESIS,IMPERIAL COLLEGE,LONDON.

APPENDIX

A simple program is included to show the influence of packer spacing on a Lugeon test in a fissured rock mass.This problem is discussed in section 3.3.2 part 2 of the thesis.

IMAX,JMAX refers to matrix size,i.e,IMAX=no of fissures in the vertical direction,JMAX=no of frac in the Horz Direction.

RX and RY are permeability in the X,Y direction.

For other symbols see section 3.3.2

This program is in Fortran 4 and is derived from Sharp(9)

```
      PROGRAM VERTBOR(INPUT,OUTPUT,TAPE5=INPUT,TAPE6=OUTPUT,TAPE27,
     1TAPE25)
C-------BOREHOLE TEST-----------------------------------------------
      LINEAR RELAXATION SOLUTION
      DIMENSION  H(50,50),RX(50,50),RY(50,50),QX(50,50),MY(5)
      DIMENSION KL(15)
      REAL MHY

C*********************INPUT**********************
C--------INITIAL POTENYIAL IS 10 EVERYWHERE EXCEPT B/H=0-------------

      READ(5,55)(IMAX,JMAX)
   55 FORMAT(2I4)
      WRITE(6,56)(IMAX,JMAX)
   56 FORMAT(2I4)

C*************SET INITIAL VALUES OF ARRAYS TO ZERO*****************

      DO 44 K=1,5
      MY(K)=0
   44 CONTINUE
      DO 45 M=1,15
      KL(M)=0
   45 CONTINUE
      DO 43 I=1,IMAX
      DO 43 J=1,JMAX
      H(I,J)=0.0
      RX(I,J)=0.0
      RY(I,J)=0.0
      QX(I,J)=0.0
   43 CONTINUE

C********* FOLLOWING DEFINE THE BOUNDRIES OF PROBLEM************

      KK=50
      NH=50
      NB=25
C*****************FREQUENCY OF JOINTS IN X,Y DIRECTION***************
      MX=50
      MY(1)=50
      MY(2)=25
      MY(3)=10
      MY(4)=5
      MY(5)=1
      DO 999 KL=45,48
      DO 900 K=1,5
      AY=MY(K)
C*************CONVERT ABOVE TO REAL NUMBERS**************
      AK=KK
      AH=NH
      AB=NB
      AX=MX

C************* GENERATE A JOINT SYSTEM************

      DO 19 I=1,IMAX
```

```
      DO 19 J=1,JMAX
      RX(I,J)=AW/AX
   19 CONTINUE
      DO 16 I=1,IMAX
      DO 19 J=1,JMAX
      RY(I,J)=AH/AY
   16 CONTINUE
C*************** UPPER AND LOWER BOUNDRY IMPERMEABLE ********************
      MP=IMAX-1
      DO 33 I=2,MP
      RY(I,2)=0.0
      RY(I,JMAX)=0.0
   33 CONTINUE

C*************** ZERO RESISTANCE IN Y DIRECTION IND B/H******************
      DO 12 J=1,NL
      RY(NB,J)=1000.0
   12 CONTINUE
      WRITE(6,701)((RY(I,J),I=1,25),J=1,JMAX)
  701  FORMAT(1H ,25F4.1)

C*****************GENERATE POTENTIAL GRID ******************
      DO 13 I=1,IMAX
      DO 13 J=1,JMAX
      H(I,J)=10.0
   13 CONTINUE
C*******POTENTIAL IN BOREHOLE ASSUMED TO BE ZERO ************************
      DO 34 J=1,NL
      H(NB,J)=0.0
   34 CONTINUE


C      PRELIMINARY 15 ITERATIONS $$

      N=0
      L=IMAX-1
      M=JMAX-1
  100 DO 10 J=2,M
      DO 10 I=2,L
      IF(H(I,J).EQ.0.0) GO TO 10
      H(I,J)=(RX(I,J)*H(I-1,J)+RX(I+1,J)*H(I+1,J)+RY(I,J)*H(I,J-1)+
     1RY(I,J+1)*H(I,J+1))/(RX(I,J)+RX(I+1,J)+RY(I,J)+RY(I,J+1))
   10 CONTINUE
      N=N+1
      IF(N.LT.15) GO TO 100
      IF(N.GT.15) GO TO 103


  103 N=0
  104 DO 11 J=2,M
      DO 11 I=2,L
C       COMPUTE EXCESS FLOW AT NODES $$$$$$$$$$$
      RX(I,J)=RX(I,J)
      RXX=RX(I+1,J)
      RY(I,J)=RY(I,J)
      RYY=RY(I,J+1)
      HX=H(I-1,J)-H(I,J)
      HXX=H(I+1,J)-H(I,J)
```

```
      RX=H(I,J-1)-H(I,J)
      RYY=H(I,J+1)-H(I,J)
      IF(H(I,J).EQ.0.0) GO TO 11
      QX(I,J)=RX(I,J)*RX+RXX*RXX+RY(I,J)*RY+RYY*RYY

      PHY=0.5

$$$$$$$$$$$$COMPUTE DIMINISHED FLOW$$$$$$$$$$$
      DIM=+PHY*QX(I,J)
      H(I,J)=(RX(I,J)*H(I-1,J)+RX(I+1,J)*H(I+1,J)+RY(I,J)*H(I,J-1)+RY(I,
     1J+1)*H(I,J+1)+DIM) /(RX(I,J)+RX(I+1,J)+RY(I,J)+RY(I,J+1))
  11 CONTINUE
      N=N+1
      IF(N.LT.75) GO TO 104
      WRITE(6,69) N
  69 FORMAT(15//)
      WRITE(6,63)((QX(I,J),I=1,25),J=1,JMAX)
  63 FORMAT(1H ,25F5.2)
      WRITE(6,702)
 702 FORMAT(*FINAL POTENTIAL DISTRIBUTION*)
      WRITE(6,905) NL
 905 FORMAT(I5//)
      WRITE(6,62)((H(I,J),I=1,25),J=1,JMAX)
  62 FORMAT(1H ,25F5.2)
 900 CONTINUE
 999 CONTINUE
      STOP
      END

FILER SPACE
```